Perturbation of chemo evasive mechanism of ex-vivo and in-vitro model of breast cancer stem cells: A molecular understanding for treatment failure cases of breast cancer

Thesis submitted for the degree of Doctor of Philosophy
(Department of Life science & Bio-technology)
Jadavpur University

By

Sourav Kumar Nandi

Index No. 80/19/Life Sc./26 of 2019

Registration No: SLSBT1108019 dated Sept.11, 2019

Department of Molecular Biology

Netaji Subhas Chandra Bose Cancer Research Institute

2023

Dedicated

To my Family, Supervisor and

Friends

CERTIFICATE FROM THE SUPERVISOR(S)

This is to certify that the thesis entitled "Perturbation of chemo evasive mechanism of ex-vivo and in vitro model of breast cancer stem cells: A molecular understanding for treatment failure cases of breast cancer" Submitted by Sri Sourav Kumar Nandi who got his name registered on 11th September 2019 for the award of Ph. D. (Science) Degree of Jadavpur University, is absolutely based upon his own work under the supervision of Dr. Rittwika Bhattacharya and that neither this thesis nor any part of it has been submitted for either any degree / diploma or any other academic award anywhere before.

Rittwika Bhattacharya

12 /05/23

Dr. Rittwika Bhattacharya
Scientist
Department of Molecular Biology
Netaji Subhas Chandra Bose
Cancer Research Institute
308 I Nayabad,
Kolkata-700094

(Signature of the Supervisor(s) date with official seal)

1

Details of the Thesis:

Index No. and Date of Registration: 80/19/Life Sc./26 registered on 02/09/2019

Title of the Thesis: Perturbation of chemo evasive mechanism of ex-vivo and in vitro model of breast cancer stem cells: A molecular understanding for treatment failure cases of breast cancer

Name, Designation and Affiliation of the Supervisor: Dr. Rittwika Bhattacharya, Scientist, Molecular Biology, Netaji Subhas Chandra Bose Cancer Hospital

E-mail ID of the Supervisor: molbiochem2021@gmail.com

List of Publications:

Research publications from Doctoral work:

1. Nandi SK, Chatterjee N, Roychowdhury T, et al. Kaempferol with Verapamil impeded panoramic chemoevasion pathways in breast cancer through ROS overproduction and disruption of lysosomal biogenesis. Phytomedicine. 2023;113:154689. doi:10.1016/j.phymed.2023.154689

2. Nandi SK, Roychowdhury T, Chattopadhyay S, et al. Deregulation of the CD44-NANOG-MDR1 associated chemoresistance pathways of breast cancer stem cells potentiates the anti-cancer effect of Kaempferol in synergism with Verapamil. Toxicol Appl Pharmacol. 2022;437:115887. doi:10.1016/j.taap.2022.115887

3. Nandi SK, Pradhan A, Das B, et al. Kaempferol attenuates viability of ex-vivo cultured post-NACT breast tumor explants through downregulation of p53 induced stemness, inflammation and apoptosis evasion pathways. Pathol Res Pract. 2022;237:154029. doi:10.1016/j.prp.2022.154029

4. Nandi, S.K., Bhattacharya, R., Roychowdhury, T., Roy, U.K., Chattopadhyay, S., & Mukhopadhyay, A. (2019). Ex-vivo drug sensitivity of primary breast cancer stem cell populations to potentiate therapeutic strategy for treatment resistant breast cancer. Annals of Oncology, 29(9), DOI: https://doi.org/10.1093/annonc/mdy428.012

Other publications during the period of Doctoral research:

1. Guchhait, K. C., Manna, T., Barai, M., Karmakar, M., Nandi, S. K., Jana, D., Dey, A., Panda, S., Raul, P., Patra, A., Bhattacharya, R., Chatterjee, S., Panda, A. K., & Ghosh, C. (2022). Antibiofilm and anticancer activities of unripe and ripe Azadirachta indica (neem) seed extracts. BMC complementary medicine and therapies, 22(1), 42. https://doi.org/10.1186/s12906-022-03513-4

2. Nandi SK, Basu S, Bhattacharjya A, et al. Interplay of gut microbiome, fatty acids, and the endocannabinoid system in regulating development, progression, immunomodulation, and chemoresistance of cancer. Nutrition. 2022;103-104:111787. doi:10.1016/j.nut.2022.111787

3. Basu, S., Banerjee, N., Nandi, S.K., Das, S., Parmar, K., & Mukhopadhyay, S. (2021). Deregulated molecular genetic pathways in urinary bladder cancer with the importance of molecular biomarkers in diagnosis and follow-up- A comprehensive and updated review. Journal of Clinical and Biomedical Sciences, 11(3), 96-111. DOI: 10.58739/jcbs/v11i3.2.

4. Rittwika Bhattacharyaa,1, Chinmay Kumar Pandab, Sourav K. Nandia,1, Ashis Mukhopadhyayc,1,∗ "An insight into metastasis: Random or evolving paradigms?" Pathology - Research and Practice 214 (2018) 1064–107

List of presentations in National/ International Conference:

1. ESMO (European Society of Molecular Biology), Asia, November 2018: "Ex-vivo drug sensitivity of primary breast cancer stems cell populations to potentiate therapeutic strategy for treatment resistant breast cancer" Annals of Oncology 29 (suppl_9) DOI: 10.1093/annonc/mdy428.012. Authors: Sourav Kumar Nandi , R. Bhattacharya , T. Roychowdhury, U.K. Roy , S. Chattopadhyay, A. Mukhopadhyay ; (Impact factor – 18.274)

2. National Science Congress, Punjab, 2019, for poster presentation: "Role of Kaempferol in attenuation of breast cancer stem cells: an insight into the molecular mechanism" Sourav Kumar Nandi , R. Bhattacharya , T. Roychowdhury , U.K. Roy , S. Chattopadhyay , A. Mukhopadhyay ;

3. 38th Annual conference of Indian association for cancer research (IACR) for poster presentation under the award category . Presenter: Mr Sourav Nandi, SRF, ICMR. Topic: "Kaempferol, in synergism with Verapamil, attenuates breast cancer stem cell survival through downregulation of iPSC markers and MDR1 expression"

4. International Conference on Chemistry for Human Development (ICCHD-2020), Organized by Professor Asima Chatterjee Foundation with University of Calcutta and Heritage Institute of Technology (9-11th Jan 2020), on : " Kaempferol, in synergism with Verapamil, attenuates breast cancer stem cell survival through downregulation cell surface Marker"

Statement of Originality

I, Sourav Kumar Nandi, registered for the degree of Doctor of Philosophy (Science) in the Department of Life Science & Biotechnology, Jadavpur University in 2019 do hereby declare that the thesis entitled "Perturbation of chemo evasive mechanism of ex-vivo and in vitro model of breast cancer stem cells: A molecular understanding for treatment failure cases of breast cancer" contains original research.

This thesis has been prepared following the existing academic rules and ethical conduct of Jadavpur University, and I declare that all sources used have been cited properly in the text.

As per the "Policy on Anti Plagiarism, Jadavpur University, 2019", I have maintained the similarity level below 10% for the thesis, and the similarity index is checked by the i-Thenticate software.

Signature of the Candidate: _____

Date:

Certified by the Supervisor: _____

(Signature with date and official seal)

Declaration

I do hereby declare that the thesis entitled **"Perturbation of chemo evasive mechanism of ex-vivo and in vitro model of breast cancer stem cells: A molecular understanding for treatment failure cases of breast cancer"** submitted by me for the degree of Doctor of Philosophy (Science) to Jadavpur University, is completely based on my own research work which was carried out under the supervision of **Dr. Rittwika Bhattacharya** at the **Department of Molecular Biology** of **Netaji Subhas Chandra Bose Cancer Hospital**. Neither this thesis nor any part of it has been submitted for either any degree/ diploma or any other academic award anywhere before. Furthermore, I have acknowledged all sources used and have cited these in the reference section accordingly.

Date: ………………..

(Sourav Kumar Nandi)

Acknowledgement

At the cutting edge, I would like to express my profound sense of gratitude to my guide and supervisor, Dr. Rittwika Bhattacharya, Senior Scientist at Netaji Subhash Chandra Bose Research Institute (NCRI) for her active guidance and tremendous support in my research study. Her patience, motivation, knowledge and encouragement have immensely helped me in the time of my research and writing of this thesis.

I wish to extend my sincere appreciation to Late Dr. Ashis Mukhopadhyay, Hemato-Oncologist at NCRI without whom the Research Department would not have seen its light at this institute. His presence, active participation, constructive criticism and constant encouragement have inspired me throughout the journey of my PhD.

I am immensely grateful to Dr. Soma Mukhopadhyay, Director at NCRI for her insight and valuable inputs that helped me carry out my research work successfully.

I am extremely thankful to Dr. Chinmoy Kumar Bose, Member of Central Drugs Standard Control Organization at NCRI for his belief and constant motivation in my research.

My heartfelt gratitude to Dr. Sudarshana Basu, Senior Scientist at NCRI for her support, constructive opinions and insightful discussions that have not only filled me with positive energy but immensely kept me motivated in this journey.

I would like to thank the entire Research team at NCRI: Scientists and professors, my fellow lab mates and juniors, including Varsha Mondal and Sumaiya Moiz for their constant support, cooperation and encouragement.

Special thanks to Dr. Amitava Dutta, Pathologist and his entire team at NCRI for providing me with all the tissue samples, reagents and clinicopathological details of the patients.

I would like to express my deepest appreciation to Dr. Samit Chattopadhyay, Ex-Director at the Indian Institute of Chemical Biology (IICB) and Professor at BITS-Pilani, Goa Campus for his support and collaboration.

I am highly grateful to Dr. Diptendra Kumar Sarkar, Professor at the Institute of Post-Graduate Medical Education and Research and his entire team for their insightful comments and suggestions.

I am grateful to everyone I have collaborated with; their assistance has helped me overcome all the troubleshooting that I encountered.

My earnest gratitude to Mr. Uttam Kumar Nandi, my Father, Mrs. Champa Nandi, my Mother, Purba Mondal, my elder sister and my entire family for everything that I have today. A mere thank you to them is not enough or justifiable in any sense.

Respectfully, I would like to acknowledge myself for all the good and bad days that I have been through. Every step of the way was a lesson towards this fruitful journey in the path of my life.

Last but not least, praises and thanks to the Almighty for all the experiences and the lessons that came with it in the form of blessings.

Contents

9

Abbreviations

2-NBDG	2-(N-(7-nitrobenz-2-oxa-1,3- diazol-4-yl)amino)-2-deoxyglucose
ABCB1	ATP Binding Cassette Subfamily B Member 1
ADME	Absorption, Distribution, Metabolism and Excretion
ADP	Adenosine Diphosphate
AJCC	American Joint Committee on Cancer
ALDH1	Aldehyde dehydrogenase 1
ANOVA	Analysis of Variance
ATCC	The American Type Culture Collection
ATP	Adenosine Triphosphate
ATP1B1	Na+/K+ ATPase gene
BBB	Blood-brain Barrier
BC	Breast Cancer
Bcl-2	B-cell lymphoma 2
BCSC	Breast Cancer Stem Cell
BL-1	Basal level subtype 1
BRCA	BReast CAncer gene
BSA	Bovine Serum Albumin
Ca^{2+}	Calcium ions
Caspase 3	Cysteine-dependent aspartate-directed proteases
CD44	Cluster of Differentiation 44
CDK1	Cyclin-dependent Kinase 1
cDNA	Complementary DNA
CI	Combination Index
CSC	Cancer Stem Cell
Ct	Cycle Threshold
DAPI	4',6-diamidino-2-phenylindole
DEPC	Diethyl pyrocarbonate
DFS	Disease-free Survival
DGIdb	Drug-Gene Interaction Database

DMEM	Dulbecco's Modified Eagle Medium
DMEM/F12	Dulbecco's Modified Eagle Medium/Nutrient Mixture F-12
DMSO	Dimethyl sulfoxide
DNMT3B	DNA (cytosine-5)-methyltransferase 3 beta
DOX	Doxorubicin
DPX	Dibutylphthalate Polystyrene Xylene
TFEB	Transcription Factor (EB)
EDTA	Ethylenediaminetetraacetic acid
EGF	Epidermal Growth Factor
EMT	Epithelial to Mesenchymal Transition
ER	Estrogen Receptor
F-2,6-BP	Fructose-2,6-bisphosphate
F6P	6-phosphofructose
FBS	Fetal bovine serum
FI	Fluorescence Intensity
FITC	Fluorescein isothiocyanate
G	Gemcitabine
GLUTs	Glucose Transporter
GSH	Reduced Glutathione
H&E	Hematoxylin and Eosin
H_2O_2	Hydrogen Peroxide
HA	Hyaluronan
HC	High glucose in control
h-DMEM	High-glucose Dulbecco's modified Eagle's medium
HER2	Human Epidermal Growth Factor Receptor 2
HG	High glucose in Gemcitabine
HIA	Human intestinal absorption
HIF1α	Hypoxia Inducible Factor1-α
HKV	High glucose in Kaempferol with Verapamil
HPLC	High-performance liquid chromatography
HRP	Horse Radish Peroxidase

IC	Inhibitory Concentration
ICC	Immunocytochemistry
IHC	Immunohistochemistry
IP	Immunoprecipitation
iPSC	induced Pluripotent Stem Cell
IV	Intravenous
JAK/STAT3	Janus kinase/signal transducers and activators of transcription
K	Kaempferol
K_i	Inhibition constant
KOH	Potassium Hydroxide
KV	Kaempferol with Verapamil
l –DMEM	Low-glucose Dulbecco's modified Eagle's medium
LC3-II	Microtubule-associated protein light chain 3-II
LG	Low Glucose Gemcitabine
MAPK	Mitogen-activated protein kinase
MCF-7	Michigan Cancer Foundation
MDA-MB-231	M.D. Anderson - Metastatic Breast 231
MDR1	Multidrug Resistance Mutation
MFE	Mammosphere Forming Efficiency
MFI	Mean Fluorescence Intensity
MKI67	Marker Of Proliferation Ki-67
mRNA	Messenger RNA
MRP1	Multidrug Resistance Protein 1
MTT	3-(4,5-Dimethylthiazol-2-yl)-2,5-Diphenyltetrazolium Bromide
Na_2HPO_4	Disodium phosphate
Na_2HPO_4	Potassium dihydrogen phosphate
NBT	Nitroblue Tetrazolium
NF-κB	Nuclear Factor Kappa B
NHE1	Na+/H+ exchanger membrane protein
NS	Non-significant
OCT4	Octamer-binding transcription factor 4

OS	Overall Survival
p62	Sequestosome 1 protein
PBS	Phosphate Buffered Saline
PCR	Polymerase Chain Reaction
PE	Phycoerythrin
PFKFB4	6-Phosphofructo-2-kinase/fructose-2,6-biphosphatase 4
P-gp	P-glycoprotein
PgR	Progesterone Receptor
pH	Potential of Hydrogen
pHe	extracellular pH
Pi	Inorganic Phosphate
PI3K/ AKT	Phosphoinositide-3-kinase–protein Kinase B
PIC	Protease Inhibitor Cocktail
PMA	Phorbol-12-Myristate-13-Acetate
p-NACT-TNBC	post-Neoadjuvant chemotherapy Triple Negative Breast Cancer
post-NACT	post-Neoadjuvant chemotherapy
PPI	Protein-protein Interaction
pVHL	Von Hippel Lindau protein
RCB	Residual Cancer Burden
RCSB PDB Bank	Research Collaboratory for Structural Bioinformatics Protein Data
RFS	Relapse-Free Survival
RIPA	Radioimmunoprecipitation
RNAi	RNA interference
ROS	Reactive Oxygen Species
RRID	Research Resource Identifiers
RT-qPCR	Real-Time Quantitative Reverse Transcription PCR
SD	Standard Deviation
SDS	Sodium Dodecyl Sulphate
SDS-PAGE	Sodium Dodecyl Sulfate Polyacrylamide Gel Electrophoresis
SEM	Standard Error of Mean

SIB	Swiss Institute of Bioinformatics
SOX2	SRY-Box Transcription Factor 2
STR	Short Tandem Repeats
STRING	Search Tool for the Retrieval of Interacting Genes/Proteins
TBS-T	Tris-buffered saline-Tween 20
TCGA	The Cancer Genome Atlas Program
TNBC	Triple Negative Breast Cancer
TNF-α	Tumor necrosis factor alpha
TNM	Tumour-node-metastasis
TPSA	Topological polar surface area
TSV	Tab-separated values
U	Untreated/Control
UICC	International Union against Cancer
V	Verapamil
WLOGP	log P method developed by Wildman and Crippen
XTT	Methoxynitrosulfophenyl-tetrazolium Carboxanilide
μM	Micromole

Abstract

The invincible role of Breast Cancer Stem Cells (BCSCs) in the development of chemoresistance is a well-known therapeutic challenge in the treatment of Breast Cancer (BC). Chemoevasion has a close association with stem cell renewal as well as several other compounding factors of the tumour microenvironment and the complexity of this mechanism is not fully characterized. Owing to their quiescent nature and comprehensive ability to repair DNA damage, chemotherapeutics that induce DNA damage (Gemcitabine, Carboplatin) cannot target BCSC. Several markers like SOX2, OCT4, NANOG as well as MDR1 and CD44 that contribute to pluripotency, stemness and chemo-evasive properties of BCSCs has been documented to be upregulated in BCSC. Previously, the role of Kaempferol, an aglycone flavonoid in attenuating epithelial-to-mesenchymal transition (EMT) in BCSCs has been established. The thesis work was done in three different study cohorts. In one set, Kaempferol alone was efficient in attenuating viability of post-NACT TNBC through downregulation of p53, MDR1, NANOG and upregulation of Caspase 3 and cleaved Caspase 3. In the second study cohort, Kaempferol (K) alone or in combination with Verapamil (V), an inhibitor of ATP driven proton pump, attenuated NANOG-CD44-MDR1 signalling cascade, that plays important role in chemoevasion. Both K and KV was found to induce DNA damage in tumour tissues but didn't show genotoxic effect to normal breast tissue, as evident by the expression of γH2AX in ex-vivo cultured adjacent breast tumour and normal tissues. In the third study cohort, we documented that KV, under low glucose condition attenuated a panoramic set of markers that play important role in chemoevasion, through tumour hypoxia, acidosis, drug efflux. KV, through ROS (Reactive Oxygen Species) overproduction, disrupted lysosomal biogenesis and lysosome-TFEB-Ca2+ signalling, one important attributor of chemoresistance. Also, an enhancement in the production of ROS after KV treatment resulted in autophagy-mediated cell death through the upregulation of LC3-II and p62 in low glucose conditions. In addition, the in-silico study validated the findings of the ex-vivo studies performed in this thesis with a parallel outcome. Earlier report stated Verapamil to be effective in depleting intracellular reduced glutathione and thus we hypothesized that KV would serve to enhance intracellular ROS overproduction in tumour cells to induce cell death and attenuate chemoevasion pathways.

In conclusion, the ex-vivo, in-vitro as well as in-silico studies revealed that the candidate drug combination KV could effectively target several pathways regulating chemoresistance stemness apoptosis phenomenon, that were not hitherto studied in the same experimental setup and thus may be endorsed for therapeutic purposes.

15

Introduction

Chemoresistance causes recurrence, metastasis, cancer dissemination and morbidity that impact the therapeutic strategies in breast cancer and thus an in-depth understanding of the mechanisms of chemoresistance is warranted for the better therapeutic outcome for patients. Chemoevasion pathways are responsible for chemoresistance in tumour. Breast cancer (BC) cells can activate a great variety of mechanisms to avoid the cytotoxic effects of drugs, involving a subpopulation of quiescent cells, the cancer stem cells. These cells decrease the influx or increase efflux of drugs, activate apoptosis-evading/survival pathways, or enhance DNA repair mechanisms. Previous evidence suggested that drug evasiveness can be intrinsic or acquired in these cells [**Nikolaou, Michail et al.2018**]. Since the chemo evasive mechanisms of breast cancer are mediated by multiple mechanisms, single or combined administration of chemotherapeutic drugs and other immunomodulating drugs can impart higher synergism and efficacy of treatment [**Ji, Xiwei et al. 2019**]. The predictive and prognostic markers can provide valuable evidence about the identification of BC patients that could benefit from chemotherapy treatments.

BC is the most frequent reason for cancer-related morbidity in women's health worldwide [**Harbeck, Nadia et al. 2019**]. BC is a complex heterogeneous disease, characterized according to the presence or absence of molecular biomarkers such as estrogen or progesterone receptors and human epidermal growth factor 2 (HER2) and based on their differential expression, has been classified into luminal A, luminal B, HER2 enriched and triple-negative breast cancer (TNBC) [**Yeo, Syn Kok, and Jun-Lin Guan. 2017**]. Additionally, Ki67 is a marker that is used for the evaluation of tumour proliferation and chemosensitivity and, also, has some prognostic value for certain molecular subtypes [**Yeo, Syn Kok, and Jun-Lin Guan 2017**]. TNBC tumours, owing to their least differentiation status show the most aggressive and metastatic behaviour, resulting in a shorter disease-free interval and survival time for patients [**Cardoso, F et al. 2019, DOI: Yang, Fang et al. 2017**]. TNBC show a robust response to chemotherapeutics initially but develops resistance earlier than other subtypes [**Yang, Fang et al. 2017**]. Earlier evidence has documented that residual cells of tumour which could be found during any stage or grade of cancer progression to be responsible for causing therapeutic resistance. These cells possess stem-like properties or functions associated with cancer stem cells (CSCs) [**Zheng, Hua-Chuan. 2017**]. Also, chemotherapy or radiotherapy treatments may endorse "stemness" in cancer cells, which may describe why effective therapeutics often fail to impart objective response to patients. Acquisition of stemness includes epithelial-

mesenchymal transition (EMT), in which epithelial cells are transformed into a mesenchymal phenotype characterized by increased capacities of migration, invasiveness, and resistance to apoptosis. EMT may also contribute to metastasis by driving the dissemination of mesenchymal CSCs to distant locations, whereupon the CSCs revert to an epithelial phenotype to support metastatic tumour growth **[Chang, Jenny C. 2016]**. Previous literature shows that CSCs also change in response to these dynamics, as an adaptive response for their survival in way of the constant change in the structure and anatomy of the tumour as cancer progresses **[Hatina, J. 2012]**.

Integral to the concept of tumour heterogeneity in cancer progression, CSCs, therefore, play an active role throughout the cancer progression as well as in therapy resistance by manipulating their intrinsic and extrinsic adaptation, favouring their growth and survival. Therefore, a better understanding of CSCs behaviours, which differs according to their nature consisting of the diverse stages or grade of cancer, is important to develop additional effective treatment strategies targeting the populations [**Ayob, Ain Zubaidah, and Thamil Selvee Ramasamy. 2018**]. Several different approaches to treatment aimed at overcoming the intrinsic resistance of CSCs to conventional therapies are currently being developed **[Chang, Jenny C. 2016]**. Contradictorily, conventional cancer treatments target the bulk of the tumour and are unable to target CSCs due to their high resistance nature, leading to metastasis and tumour recurrence. CSCs play a significant role in the chemo-evasiveness of breast cancer and resulting in relapse to a percentage of patients with breast cancer **[Pavlopoulou, Athanasia et al. 2016].**

Previous literature documented that CSCs escape chemotherapeutics through overexpression of various ATP binding cassette (ABC) transporters, including mainly P-glycoprotein (P-gp), a product of the MDR1 gene, that promote drug efflux; upregulation of Glutathione and glutathione metabolism enzymes; DNA repair mechanism; overexpression of DNA topoisomerase **[Perez, Edith A. 2009]**. The ATP-dependent efflux transporters like MDR (Multidrug Resistance) in cancer cells can actively transport a variety of substrates outside the cell membrane by the energy from ATP hydrolysis. An earlier study documented that P-gp, the protein product of the human multidrug resistance 1 gene (MDR1), is an important protein that plays a role indifferent chemoevasion mechanisms of breast cancer. One key player in stem cell determination is the tumour suppressor, p53, which decides cell fate through the initiation of DNA damage repair or induction of apoptosis. A functional mutation in p53 perturbs the homeostatic maintenance of cellular plasticity, the balance between stem cell renewal and differentiation **[Gao, Ling**

et al. 2013]. Mutation of TP53 also induces dedifferentiation of adult cells, through the upregulation of several pluripotent stem cell markers **[Gao, Ling et al. 2013]**. Several other less-characterized pathways concurrently maintain cancer stemness and chemoevasive phenotype. Aldehyde dehydrogenase 1 (ALDH1), which oxidises intracellular aldehydes for cellular detoxification, has been reported to be upregulated in CSCs in many kinds of cancers including breast cancer and thus accounts for the development of therapeutic resistance **[Croker, Alysha K, and Alison L Allan. 2012]**. Another cell surface glycoprotein stemness marker, CD44 is also highly upregulated in the cell surface of breast cancer stem cells **[Bourguignon, Lilly Y W et al. 2002]**. P-gp also associates with p53 in drug resistance process **[Gao, Ling et al. 2013]**. A previous study also indicated through a mice model that CSCs can promote drug efflux via DNA repair activity and up-regulation of anti-apoptotic markers **[Zhou, Zhi-Yong et al. 2016]**. Furthermore, a group of the literature demonstrated that a cluster of surface biomarkers such as EpCAM, BCl2, KI67, CD24, CD44, ALDH1 was involved in chemo evasion of CSCs **[Ji, Xiwei et al. 2019]**. Upregulation of pluripotent stem cell markers viz. NANOG, SOX2, OCT4 is other important mechanism of CSC renewal and thus such markers are termed induced pluripotent stem cell markers/iPSC). Expression of CD44 stoichiometrically upregulates NANOG expression, which, alongwith MDR1, induces pluripotency in stem cells during chemoresistance **[Chambers, Ian et al. 2003]**. The signalling of NANOG is controlled by the interactions of pluripotent stem cell markers such as SOX2, and OCT3/4) **[Rodda, David J et al. 2005]**. Cumulative evidence suggested that HA promotes the CD44-NANOG complex formation, leading to NANOG activation and stem cell marker expression. The complex also interacted with Stat-3 and activated its specific transcriptional activation, MDR1 gene expression, that play important role in tumour cell growth **[Bourguignon, Lilly Y W et al. 2008]**. Earlier evidence also suggested that the molecular mechanisms of chemo evasion also include glucose transporter pumps, oncogenes, acidosis, DNA repair, epithelial-mesenchymal transition (EMT) **[Brasseur, Kevin et al. 2017]**.

Apart from several pathways implicated in breast cancer drug resistance, the contribution of hypoxia-inducible factor-1α (HIF-1α) has increased attention recently**[Generali, Daniele et al. 2006]**.Hypoxia is upregulated in both primary and metastatic breast cancers **[Vaupel, P et al. 2001]**, leading to upregulation of HIF-1α in tumour tissue and is associated with poorer prognosis and drug resistance in such cells through intracellular reactive oxygen species **[Gilkes, Daniele M, and Gregg L Semenza. 2013]**. Earlier reports

suggested that the metastasis-promoting potential of HIF-1 assists to maintain an increasing population of BCSCs [**Philip, Beatrice et al. 2013**]. Upregulation of HIF-1α in BCSCs induces the expression of pluripotency factors such as NANOG, OCT4, and SOX2 in response to intra-tumour al hypoxia [**Lu, Haiquan et al. 2018**]. HIFs also mediate complex and bidirectional paracrine signalling between breast cancer cells (BCC) and mesenchymal stem cells (MSC) that stimulate breast metastasis. Moreover, earlier reports documented that HIF-1α controls cellular activities or functions for cell survival resulting that the resistance development to endocrine therapy as well as cytotoxic anti-cancer drugs [**McAleese, Courtney E et al. 2021**]. Few studies documented that in tumour the expression of MDR1 was regulated by HIF-1α[**Ding, Zhenyu et al. 2010**]. Besides, due to poor tumour vascularization, hypoxia is accompanied by glucose deficiency, which can independently activate HIF-1α as a survival mechanism in nutrient deprivation [**Nishimoto, Arata et al. 2014**]. Previous studies suggested that the upregulation of HIF-1α target genes encode proteins that promote tumour cell survival, immortalization, EMT or stem cell marker regulation in metastasis, and resistance to traditional treatment processes along with activation of various hallmarks of cancer such as angiogenesis, migration and invasion, pH regulation, and glucose metabolism [**Semenza, Gregg L. 2013; Keith, Brian et al. 2011**]. In context to the acidosis phenomenon, the increased rate of glycolysis leads to an acidic condition due to the increased levels of lactate and H+ ions that are actively efflux from tumour cells through the functions of many intracellular pH (pHi)-regulating proteins such as Na+/H+ exchanger 1 (NHE1) [**Shimoda, Larissa A et al. 2006**]. The pHi also regulated Na+/K+-ATPase, the encoding transmembrane protein of ATP1B1 gene, which induces an extracellular Na+ pool with the import of K+ and Ca2+ [**Granja, Sara et al. 2017**], using ATP as the driving force [**Zeino, Maen et al. 2015**]. Glucose transporters depend on this extracellular Na+ pool and thus glucose is imported into the tumour cells. Previous studies also reported that the Na+/K+-ATPase inhibitors controlled the expression of HIF-1α in cancer cells [**Zhang, Huafeng et al. 2008**]. Thus, markers that regulate tumour acidosis, cancer stemness, drug efflux and lysosome upregulation, function in a cooperative way to promote chemo evasive phenotype to the tumour s. Also, ROS production by chemotherapeutic drugs is one of the key mechanisms to control the growth of CSCs. However, different levels of ROS production determined the diverse role of ROS as a cellular toxic component or as a cellular signalling molecule or both. In high concentrations, ROS that exceed the cellular repair capacity can destroy cellular antioxidant mechanisms, impair cellular redox balance and cause damage to DNA,

protein, lipids and other cellular components. As a result, a high concentration of ROS will lead to cell death. While a low concentration of ROS may serve as a signalling molecule to activate cellular repair mechanisms and turn on cellular proliferation and apoptosis pathways. Interestingly, massive accumulation of ROS inhibits tumour growth in two different ways: (1) through blocking cancer cell proliferation by suppressing the proliferation signalling pathway, cell cycle, and the biosynthesis of nucleotides as well as ATP and (2) by inducing cancer cell death. Glutathione, that maintains cellular redox balance **[Massaro, Marika et al. 2002]**, is another important contributor of chemoresistance as it helps to quench free radicals generated during oxidative stress **[Traverso, Nicola et al. 2013].** Tumour cells through upregulation of lysosomes, induce autophagy in the damaged cells and thus can escape ROS-induced cytotoxicity. Previous studies have documented that ROS regulated EMT markers in cancer cells and promoted cancer cell invasion and metastasis **[Kim, Young Mee et al. 2020]**. Expression of MDR1 is controlled by the induction of antioxidant proteins (hemooxygenase-1, superoxide dismutase, catalase) **[Cui, Qingbin et al. 2018]**. Different category of ROS level is essential for chemoresistance through the upregulation of drug efflux against chemotherapy **[Hwang, In Tae et al. 2007]**. Besides, a high level of ROS production destabilizes lysosomal membranes through lipid peroxidation leading to its rupture **[Dielschneider, Rebecca F et al. 2017]**. Previous evidence confirmed, lysosomal sequestration of hydrophobic weak base drugs activates TFEB-mediated lysosomal biogenesis, resulting in an increased pool of lysosomes, capable of enhanced chemotherapeutic drug resistance that indicated lysosomes play an important role in chemoevasion due to their protonation in the acidic lumen of this organelle; thus, these sequestered drugs are unable to reach their target sites and therefore fail to exert their cytotoxic activity **[Zhitomirsky, Benny, and Yehuda G Assaraf. 2016]**. Previous studies also suggested that ROS-induced autophagy also requires dual roles of lysosomes in both signal transduction and lysosomal degradation **[Zhang, Xiaoli et al. 2016]**. Increased ROS is detoxified by superoxide dismutase, catalase, and peroxiredoxins. ROS has a role as a secondary messenger in signal transduction. Cancer cells induce fluctuations of redox homeostasis by variation of ROS-regulated machinery, leading to increased tumourogenesis and chemoresistance. Redox-mediated mechanisms of chemoresistance include endoplasmic reticulum stress-mediated autophagy, increased cell cycle progression, and increased rate of metastasis in cancer stem-like cells.

Based on molecular mechanisms of breast cancer progression, a group of scientists developed chemically synthesized anticancer drugs that have not significantly improved the frequency of survival rate in the past times. To overcome the obstacle, new strategies and novel chemoprevention agents were established through natural compounds from plant or plant-derived synthetic compounds to improve the treatment. The compounds regulate molecular pathways of breast cancer and cancer cell proliferation. Kaempferol, aglycone flavonoids in the form of glycoside, is a tetra hydroxy flavone in which the four hydroxy groups are positioned in 3,5,7-trihydroxy-2-(4-hydroxyphenyl)-4H-1-benzopyran-4-one and is detected in several plant parts, for example, seeds, leaves, fruits, flowers, and even vegetables like as edible plants (e.g., tea, broccoli, cabbage, kale, beans, endive, leek, tomato, strawberries, and grapes) and in plants or botanical products commonly used in traditional medicine (e.g., *Ginkgo biloba, Tilia spp, Equisetum spp, Moringa oleifera, Sophora japonica* and propolis). Kaempferol and its glycosylated derivatives have been shown to be cardioprotective, neuroprotective, anti-inflammatory, antidiabetic, antioxidant, antimicrobial, antitumour, and have anticancer activities **[Imran, Muhammad et al. 2019]**.

To overcome the obstacle of chemoresistance in cancer few groups of researchers used Verapamil, an L-type calcium channels inhibitor with picomolar affinity, which blocks P-gp protein expression in the micromolar range. Although, the previous study also suggested that. Verapamil showed a toxic effect at high concentrations. Early reports showed that Verapamil, through depletion of ATP, helps in increased rates of oxidative phosphorylation in drug-resistant cells eventually upregulating oxidative phosphorylation and increasing production of reactive oxygen species (e.g., O_2, H_2O_2). ROS overproduction and reductions in the anti-oxidant glutathione resulted in apoptosis in drug-resistant cell lines **[Callaghan, Richard et al. 2014]**.

Chemoresistance mechanisms in breast cancer is a current obstacle in treatment that is developed through the long-term consumption the chemotherapeutics drugs such as DNA methylation drugs such as 5-fluorouracil (5FU), Gemcitabine; taxanes (docetaxel, paclitaxel, and protein-bound paclitaxel), platinum agents (carboplatin, cisplatin) etc. The outcome of different kinds of anticancer drug treatment changes tumour proliferation and morphology. Moreover, in most treatment cases failure outcome of anticancer drugs impacts the overall survival frequency of breast cancer patients **[Rivera, Edgardo, and Henry Gomez. 2010]**. Chemoresistance due to the treatment with capecitabine, gemcitabine, vinorelbine, or albumin-bound paclitaxel, with capecitabine or the only single

drug administration, was documented through US Food and Drug Administration (FDA) **[Gradishar, William J et al. 2005]**. Besides, after administrated of taxane-based chemotherapeutics drugs, the outcome of response rates was about 32% to 75% with a time to progression of 6 to 10 months **[Cortes, Javier, and Jose Baselga. 2007]**. The response rates with anthracycline-based treatment diseases in 16% to 25%, and overall survival frequency is limited **[Degardin, M et al. 1994]**. Early reports suggested that chemoresistance may evolve tumourigenesis in the early phase of breast cancer, due to the onset of well-recognized genetic modulation **[Rivera, Edgardo, and Henry Gomez. 2010].** Except for this reason the chemoresistance also develops by modifications in drug pharmacodynamics and pharmacokinetics, error in metabolism, alteration of candidate drug targeting expression or function such as gene or protein expression and topoisomerase II/IV mutations, errors in apoptotic signalling pathways such as p53 mutation, and overexpression of P-gp protein **[Leonessa, F, and R Clarke. 2003]**. To repress the problems, significant compounds or agents with more long-term effectiveness and low toxicity are required that regulate drug resistance mechanisms and improve response rates of survival of breast cancer.

In recent years, various lines of research have been performed that aimed to bypass drug resistance and improve the sensitivity to chemotherapeutic agents in cancer cells. Various strategies, including RNA silencing, nano-preparations, co-administration of two or more strategies, novel cytotoxic agents and regulation of apoptosis, have been developed to overcome drug resistance in cancer cells. Although various attempts have been made to restore the sensitivity of existing chemotherapeutic drugs and overcome drug resistance to breast cancer, the effects are still unsatisfactory. The increasing knowledge of the resistance mechanisms and the improvement of therapeutic approaches will promote clinical outcomes and circumvent the problem of chemoresistance. In the present context, we aimed to study the role played by our candidate drug Kaempferol alone or in combination with an adjunct dosage of Verapamil on various chemoresistance pathways. Our study would endorse these candidate molecules as ideal candidates in aggressive breast tumours, for future therapeutic purposes.

Review of literature

Clinically, breast cancer is most prevalent cancer in women worldwide and the frequency of death rate is high. Current reports from the World Health Organisation documented that about 2.3 million were detected and near about 7.7 million alive with breast cancer according to global wise **[Mutebi, Miriam et al. 2020]**. Early reports suggested that the risk of breast cancer at a young age is greater than early age due to ionized radiation. This study also suggested that in the case of preeclampsia (related to low levels of pregnancy ER) during pregnancy, the offspring of mothers had a reduced amount of risk of breast cancer. The age factor of the mother during pregnancy is a vital key to breast cancer development among the offspring and mothers **[Michels, Karin B, and Fei Xue. 2006]**. Despite the short or long-term risks, chemotherapy or radiation therapy was an option for preventing the recurrence of patients with stage I-III breast cancer. A study exhibited an increase in lactate concentrations as the grade of breast carcinomas progressed from well-differentiated, slow-growing grade I to poorly differentiated, rapidly growing grade III tumours **[Cheung, Sai Man et al. 2020]**. Even though, several risk factors such as hormone regulation, food habits, alcohol consumption, lifestyle, reproduction factors, etc, are associated with breast cancer **[Michels, Karin B, and Fei Xue. 2006]**. Among them, reproduction factors are robustly associated with ER. Depending on receptors breast cancer is characterised by two major groups such as TNBC and non-TNBC **[Muley, Helena et al. 2020]**. In TNBC, about 25% of cases are invasive breast cancer that is generally aggressive along with high grades in young patients **[Haffty, Bruce G et al. 2006]**. Based on the molecular classification, breast cancer is classified into five major subtypes such as luminal A /B, HER2-enriched, basal, and normal-like patients **[Haffty, Bruce G et al. 2006].** In the TNBC subtype, about 80% of cases are the basal-like subtype that is the most aggressive in nature along with maximum population content of breast cancer stem cells (BSCSs) that is characterized through BCSC biomarkers such as CD44+/CD24−and ALDH1+ **[Croker, Alysha K, and Alison L Allan. 2012]**. These markers are also associated with the chemoresistance pathway **[Ji, Xiwei et al. 2019]**. Furthermore, a group of the literature demonstrated that a cluster of surface biomarkers such as EpCAM, BCl2, KI67, CD24, CD44, ALDH1 was involved in chemo evasion of CSCs **[Ji, Xiwei et al. 2019].**

Mechanisms of chemoresistance: A previous study also indicated through a mice model that CSCs can promote drug efflux via DNA repair activity and up-regulation of anti-apoptotic markers **[Zhou, Zhi-Yong et al. 2016]**. Moreover, collected shreds of evidence

documented that high CD44+/CD24- ratio and ALDH1+ were conserved during metastasis. The indication also demonstrated that ALDH hi/CD44+ cells displayed enhanced metastatic characters in vitro or in vivo relative to ALDH low/CD44-cells in TNBC, resulting ALDH hi/CD44+cells surviving chemotherapy/radiotherapy relative to ALDH low/CD44- cells **[Croker, Alysha K, and Alison L Allan. 2012]**. CSCs are generally defined by the expression of surface markers related to stem cells, such as CD326, CD44, CD24, and side population cells by which they can be isolated and enriched in vitro and in vivo, although no single marker can be used to define the CSC populations **[Beck, Benjamin, and Cédric Blanpain. 2013]**. Hyaluronan (HA) interacts with CD44 which belongs to a family of multifunctional transmembrane glycoproteins expressed in breast tissue **[Iida, N, and L Y Bourguignon. 1995]**. CD44 could be expressed in a diversity of isoforms through alternative splicing of variant exons of CD44 into an extracellular membrane-proximal site **[Screaton, G R et al. 1992]**. The expression of CD44 variant (CD44v) isoforms has been revealed to be closely associated with tumour progression and chemoresistance phenomenon **[Bourguignon, Lilly Y W et al. 2014]**. Earlier evidence suggested that CD44 is expressed not only in tumour stem cells but also in normal cells **[Al-Hajj, Muhammad et al. 2003]**. Previously reported that CD44 interacts with P-gp to promote cell migration and the invasion of breast tumour cells **[Miletti-González, Karl E et al. 2005]**. However, the transcriptional factor(s) of CD44 was correlated with stem cell markers such as NANOG which was a transcription factor involved in the self-renewal and maintenance of pluripotency in stem cells during chemoresistance phenomenon **[Chambers, Ian et al. 2003]**. The signalling of NANOG is controlled by the interactions of pluripotent stem cell markers such as SOX2, and OCT3/4) **[Rodda, David J et al. 2005]**. Cumulative evidence suggested that HA promotes the CD44-Nanog complex formation, leading to NANOG activation and stem cell marker expression. The complex also interacted with Stat-3 and activated its specific transcriptional activation, MDR1gene expression, in tumour cell growth **[Bourguignon, Lilly Y W et al. 2008]**. Cumulative evidence also suggested that the molecular mechanisms of chemo evasion also include glucose transporter pumps, oncogenes, acidosis, DNA repair, and epithelial-mesenchymal transition (EMT) **[Brasseur, Kevin et al. 2017]**.

HIF-1α stability is also controlled through pyruvate and lactate. Since, lactate can be transformed to pyruvate via lactate dehydrogenase, resulting the accumulation of intracellular lactate will also stabilise HIF-1α **[Nagao, Ayako et al. 2019]**. Interestingly, a similar association is seen with HIF-1α expression **[Campbell, Elizabeth J et al. 2019]**.

The HIF-1α is regulated via both hypoxia-dependent and hypoxia-independent pathways. However, the different subtypes show markedly different levels of HIF-1α expression. An experimental model of 900 breast cancer patients observed significant changes in HIF-1α expression between Luminal A tumour s (46% positive), HER2-positive tumour s (69% positive), and basal tumour s (85% positive) **[Bane, A L et al. 2014]**. A previous study documented that ROS can upregulate the expression of HIF1 under different environments and other evidence also suggested that ROS can regulate the expression of P-gp **[Jung, Seung-Nam et al. 2008, Chen, Jianfang et al. 2014]**. Besides, wild-type p53 is usually downregulated with high expression of P-gp, a mechanism with is transcriptionally regulated. Interestingly, mutant p53 is still capable of interacting with TATA-binding protein but is unable to repress MDR1 transcription and leads to PgP activation **[Kanagasabai, Ragu et al. 2011]**. An earlier study has shown that the NF-kappaB (NF-κB) signalling plays a significant role in regulating ROS-mediated P-gp expression. This study also reported that the upregulation of P-gp occurs via NF-κB activation **[Wartenberg, Maria et al. 2003]**. Collective documents suggest that nuclear factor-kappa B (NF-κB) and HIF-1 link inflammatory signalling to hypoxia NF-κB and HIF-1 link inflammatory signalling to hypoxia.NF-κB and HIF-1 coordinated the activation of oncogene promoters such as BCL2 **[Zong, W X et al. 1999]**. Moreover, a large body of experiments documented that, HIF-1αis also involved in p53 expression in tumour cell survival. This study indicated that p53 accumulates to a relevant degree only under drastic conditions of oxygen reduction through regulation of HIF-1α expression and acidosis **[Schmid, Tobias et al. 2004]**.

ROS have been identified as signalling molecules in various pathways regulating both cell survival and cell death. Autophagy, a self-digestion process that degrades intracellular structures in response to stress, such as nutrient starvation, is also involved in both cell survival and cell death. Alterations in both ROS and autophagy regulation contribute to cancer initiation and progression, and both are targets for developing therapies to induce cell death selectively in cancer cells. Previous literature reported that ROS generation also induces autophagy, including nutrient starvation, mitochondrial toxins, hypoxia, and oxidative stress **[Azad, Meghan B et al. 2009]**. It is usually known, ROS induce autophagy and that autophagy, in turn, serves to survive under oxidative damage **[Azad, Meghan B et al. 2009]**. Redox regulation of tumour markers by moderate levels of ROS was observed in several signalling pathways, including autophagy which was a catabolic pathway for the degradation of intracellular proteins and organelles through the lysosome **[Finkel, Toren.**

2003]. Increasing ROS levels, either endogenously or exogenously, induce lysosomal Ca2+ release, triggering TFEB nuclear translocation to enhance autophagy **[Zhang, Xiaoli et al. 2016]**. These reports also indicated that TFEB promotes autophagy by inducing the biogenesis and function of both lysosomes and phagophores (the precursors to autophagosomes), facilitating the degradation of autophagic substrates. During the formation of autophagosomes, LC3 is lipidated, and thisLC3-phospholipid conjugate (LC3-II) is localized on autophagosomes and autolysosomes. If the lysosomal degradation ofLC3-II is slower than the formation of autophagosomes during autophagy, the cellular level of LC3-II reflects activation of autophagy **[Tanida, Isei et al. 2005]**. Another widely used marker for autophagic flux is the autophagy receptor sequestosome 1 (SQSTM1or p62) which physically links autophagic cargo to the autophagic membrane **[Larsen, Kenneth Bowitz et al. 2010]**. LC3 expression correlated with p62 markers during autophagy. The autophagosome then fuses with the lysosome to form the autolysosome, where the breakdown of the autophagosome vesicle and its contents occurs. The ubiquitin-associated protein p62, which binds to LC3, is also used to monitor autophagic flux. During autophagy, cytosolic LC3-1 is conjugated to phosphatidylethanolamine to form LC3-II; LC3-II is then incorporated into the autophagosomal membrane **[Tanida, Isei et al. 2008]**. Previous studies demonstrated that the role of$O_2^{(-)}$ in the ROS production process, was the induction of autophagy which was suggested under conditions of prolonged starvation/glucose deprivation or low glucose conditions **[Chen, Y et al. 2009]**. In the study, the researchers conclude that $O_2^{(-)}$ is the major ROS radical for autophagy during prolonged starvation of glucose.

In the transformation of cancer cells from normal tissue, cells reprogramme ordinary metabolic functions to enable rapid growth potential. Otto Warburg reported the high rates of glycolysis in cancer cells even in aerobic conditions change through a mechanism by which cancer cells have adapted for rapid proliferation. As a result of this transformed metabolism, cancer cells use large amounts of glucose and generate high amounts of lactate. Glucose metabolism through glycolysis contributes to ATP synthesis and provides intermediates for other biosynthetic processes. Thus, cancer cells are dependent on high rates of glucose uptake and metabolism for survival **[Zhuang, Yongxian et al. 2014]**. Increased uptake of glucose by these cells is due to the overexpression of glucose transporters (GLUTs). BC treatment with the reduction of glucose supply in cancer is called starvation therapy which can inhibit tumour growth by reducing the carbohydrate supply or by inhibiting glycolysis. Recent studies demonstrated that high glucose (HG) increased cell proliferation and growth, and when

glucose is lowered, the chemotherapeutic drugs show more effective cytotoxic properties to cancer cells. In low glucose (LG) conditions ranging from 0 to 5 mM, cytotoxic drugs are effective in breast cancer cell lines MCF7, MDA-MB-231 and SKBR3 where MDA-MB-231 and SKBR3 were shown resistant in normal and HG medium **[Zhuang, Yongxian et al. 2014]**. Previous literature also suggested that the large numbers of chemoresistant cells in cancer cells after conventional treatment, while these resistant cells proliferate more slowly in glucose-deficient environments, thus decreasing the proportion of drug-resistant cells in the drug-surviving cells, which in turn reduces cancer drug resistance **[Wang, Chenglong et al. 2020]**. Chemoresistant cells showed higher ATPase vitality and oxidative phosphorylation, indicating that chemoresistant cells have higher energy requirements, which means that chemoresistant cells are more dependent on glucose. To know if the concentration of glucose in the cell culture medium had a significant effect on the cell viability of chemoresistant cells, the chemoresistant/chemosensitive cells were cultured in media containing different concentrations of glucose **[Wang, Chenglong et al. 2020]**. The study also documented that the LG concentration effectively decreased the proportion of chemoresistant cells in the mixed cell population, demonstrating that starvation therapy can reverse cancer resistance.

Chemotherapeutic resistance mostly develops with long-term drug treatment exposure. Gemcitabine, (2′, 2′-difluoro deoxycytidine) is a difluorinated analogue of deoxycytidine, a pyrimidine analogue that inhibits DNA synthesis. Mechanisms of Gemcitabine resistance in breast cancer are still unknown **[Zheng, Chunning et al. 2013]**. As a single agent, 20-40% response rate to Gemcitabine is known but several previous reports suggested that after long time treatment of chemotherapy, the chemoresistance develops **[Motoi, Fuyuhiko. 2021]**. Other reports of different types of cancer, documented the expression of a few markers such as CD44 **[Hong, Sung Pil et al. 2009]**, NF-KB, PI3K/AKT, MAPK, HIP1-α, ABC transporter family proteins and NANOG that are directly or indirectly related Gemcitabine resistance phenomenon **[Jia, Yanfei, and Jingwu Xie. 2015]**. Previous reports also documented, tumours with high levels of expression of CD44s are more invasive and rapidly become resistant to Gemcitabine and ABC transporter inhibitor Verapamil re-sensitized the resistant cells to Gemcitabine in a dose-dependent manner and RNA interference of CD44 inhibited the clonogenic activity of resistant cells **[Hong, Sung Pil et al. 2009]**. Recent evidence has supported the link of Gemcitabine resistance and EMT with stem cell phenotype to CD44 high-expressing cells **[Quint, Karl et al. 2012; Samulitis, Betty K et al. 2015]**. The CD44 interacts with P-gp to promote cell migration or the invasion of breast tumour cells and CD44-NANOG complex formation with the help

of SOX2 and OCT4, leads to NANOG activation and embryonic stem cell marker expression in chemotherapeutic drug resistance phenomenon [**Bourguignon, Lilly Y W et al. 2008**]. More importantly, inhibition of HIF-1α in Gemcitabine-resistant cells caused the partial reversal of EMT phenotype, suggesting that HIF-1α was critically involved in the Gemcitabine-resistant-mediated EMT mediated pathway [**Wang, Rui et al. 2014**]. Mechanically, HIF-1α induces glucose uptake and lactate accumulation and lowers intracellular ATP concentrations [**Xi, Yun et al. 2020**]. The Na+/H+ exchanger (NHE1) plays a crucial role in cancer cell proliferation and metastasis. However, the mechanism underlying chemotherapeutic resistance in cancer cells has not been completely elucidated. Earlier reports suggested that the effect of NHE1 on resistance to the chemotherapy drug doxorubicin (DOX) was also investigated [**Chen, Qi et al. 2019**]. Na/K-ATPase has been studied as a target for cancer treatment that promoted triggers several cell-signalling pathways, resulting in the proliferation, differentiation and promotion of autophagy or apoptosis [**Themistocleous, Sophia C et al. 2021**].

To resolve the problems in anticancer therapy, several research groups documented plant-based natural compounds or plant-derived synthetic compounds. Previously reported, bioflavonoids-based anticancer studies show more effectiveness in vitro/ in vivo models [**Kim, Seung-Hee, and Kyung-Chul Choi. 2013**]. Kaempferol, a yellow colour bioflavonoid, show antioxidant properties and anti-inflammatory activity that leads to potential anticancer treatment through preventing cell migration and invasion, inhibiting MMP-2 protein, downregulating AKT phosphorylation, and increasing the focal adhesion kinase (FAK) activity in renal cell carcinoma [**Kim, Seung-Hee, and Kyung-Chul Choi. 2013; Hung, Tung-Wei et al. 2017**]. Moreover, the induction of pro-apoptotic or apoptotic factors such as p53, Caspase- 3/8/9 and anti-apoptotic factors such as BCL2, cyclin-dependent kinase 1 were controlled through Kaempferol [**Zhu, Li, and Lijun Xue. 2019**]. Interestingly, Kaempferol shows an inhibitory effect in cell migration and invasion stages through the downregulation of RhoA and stimulation of Rac1 markers in breast cancer [**Li, Shoushan et al. 2017**]. Also, Kaempferol inhibits the mitogen-activated protein kinase (MAPK) signalling pathway that upregulates cell adhesion, migration, and invasion phenomenon [**Li, Chenglin et al. 2015**]. The previous study documented, the important oncogenic markers (RAS, SRC and HIF1α) promoted glycolysis by activating glucose transporter genes and helping in glucose uptake for tumour cell proliferation [**Furuta, Eiji et al. 2010**]. The increased rate of the glycolysis process produces a large rate of lactate that facilitated the acidification process in cancer cells and apoptosis and chemoresistance

through the p53-mediated pathway. To maintain acidosis and intracellular pH, cancer cells pump out H+-ion by utilizing a Na+/H+ pump or by monocarboxylate transporter which transports H+ with lactate **[Furuta, Eiji et al. 2010].** The increased glycolytic metabolism ultimately originates an increase in lactate release by cancer cells, causing a tumour al acidic microenvironment, originating an increased invasion and suppression of anticancer immune response. In the MCF-7 cell line, Kaempferol regulated the glucose transporter system (GLUTs) in mRNA levels and inhibits the uptake of (3)H-deoxy-d-glucose ((3)H-DG) facilitated lactate cellular that help in the accumulation process of extracellular lactate accumulation **[Azevedo, Cláudia et al. 2015]**.

The earlier study documented that with the Verapamil combination, the anticancer effect of any compounds was enhanced along with the induction chemosensitizers in vitro/vivo model of lung cancer **[Wang, Haolu et al. 2013]**. Co-encapsulated Verapamil and Doxorubicin (DOX) with nanoparticles against drug resistance provided a significant outcome in ovarian cancer **[Zheng, Weiping et al. 2018]**. Besides, another study reported that co-treatment with Verapamil-chemotherapeutic agents (Cisplatin) decreased MDR1 gene transcription **[Wang J, Wang H, Zhao L, et al. 2010]**. Moreover, Verapamil decreased the Ca2+ ions and also regulate ROS production **[Verma, Nisha et al. 2021]**.

Objectives

Hypothesis: Kaempferol alone or in combination with Verapamil, could attenuate different kinds of pathways associated with chemo evasion in breast cancer

Aim of the study

- ➢ Study the antiproliferative effect of Kaempferol with Verapamil in vitro and ex-vivo BCSC models with their role on pathways regulating chemo-evasion and expression of stemness markers.
- ➢ Toxicology study of Kaempferol alone and Kaempferol with Verapamil
- ➢ Efficacy of Kaempferol with Verapamil on lysosomal biogenesis based chemoevasion pathways under low glucose and high glucose condition
- ➢ Effect of Kaempferol with Verapamil on the expression of genes associated with hypoxia, glucose uptake, tumour acidosis, and the key regulators of chemoevasion with apoptosis.

Summary of work designed:
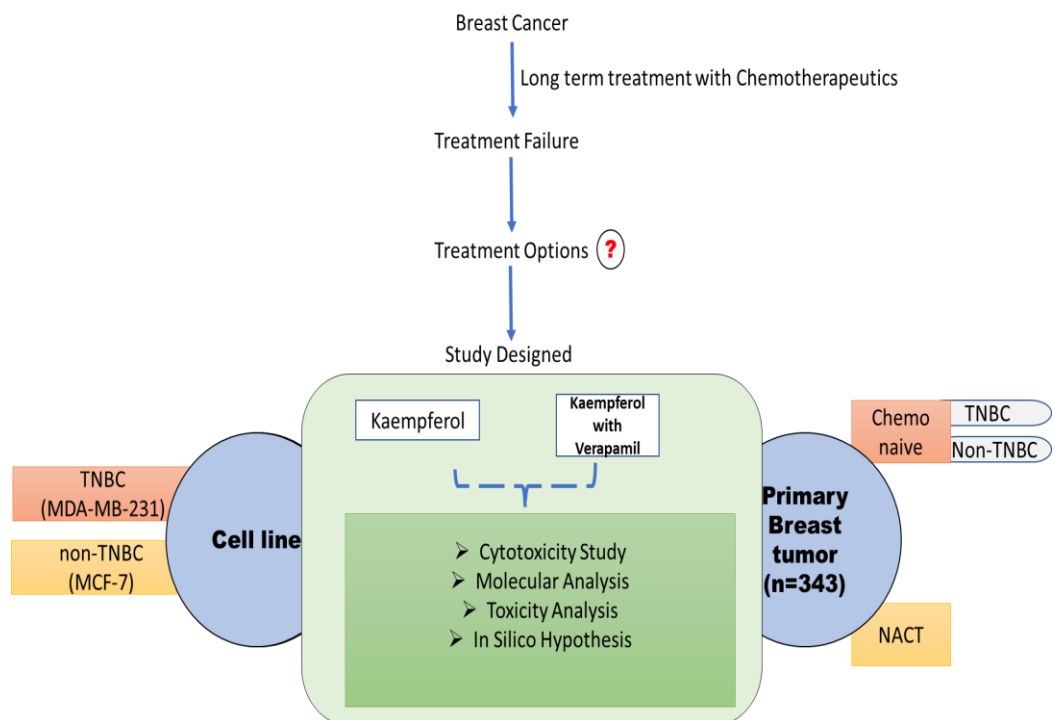
Figure 1: Design of the investigation

Chapter 1

Title: Study the antiproliferative effect of Kaempferol in vitro and ex-vivo BCSC models with their role on pathways regulating chemo-evasion and expression of stemness markers

Background

Breast cancer stem cells (BCSC) are a distinct niche of cancer cells in tumours, that confer aggressiveness and chemo evasive phenotype to the resident tumour. The process of chemoevasion occurs in close association with stem cell renewal through several complex cascades of events. DNA-damaging drugs such as Gemcitabine cannot target BCSC as the cells are mostly quiescent and have fully functional DNA repair genes. Earlier reports documented the role of Kaempferol in attenuating and reducing stemness markers in cancer. In the present context, we tried to study the effect of Kaempferol on widely known markers that regulate chemoevasion, stemness and apoptosis escape, in p-NACT TNBC. The residual cancer burden is considered an indispensable qualifier of residual disease. In our study cohort, a significant percentage of patients with high grade and high residual cancer burden (RCB) scores, showed upregulated nuclear p53 expression with downregulated expression of Caspase 3. Altered p53 expression could unleash stem cell renewal, proliferation and apoptosis evasion and we found robust expression of several candidate proteins regulating these processes in such tumour explants.

Introduction

Chemoevasion is an ominous challenge in treating aggressive breast tumours. Irrespective of subtypes, chemoevasion is initiated with the upregulation of stem cell renewal and a diverse array of networks that results in disease progression. Triple-negative breast cancer (TNBC), which comprises hormone receptor-negative undifferentiated subpopulations of breast cancer, is more amenable to developing early resistance to chemotherapy, involving various signalling networks **[Nedeljković, Milica, and Ana Damjanović. 2019]**. Early reports suggested that molecular profiling of TNBC would provide therapeutic benefits from neoadjuvant chemotherapy (NACT) **[Jiang, Yi-Zhou et al. 2019]**. The tumour suppressor, p53 is considered one important gatekeeper that regulates cell cycle progression and decides cell fate through the initiation of DNA damage repair or induction of apoptosis. The homeostasis of cellular plasticity, the balance between stem cell renewal and differentiation is disrupted when p53 is functionally mutated **[Spike, Benjamin T, and Geoffrey M Wahl. 2011]**. It was also revealed that TP53 mutation also induces dedifferentiation of adult cells, through upregulation of several pluripotent stem cell markers **[Spike, Benjamin T, and Geoffrey M Wahl. 2011]**. Apart from the canonical pathways leading to cancer stem cell renewal, several other less-characterized pathways concurrently maintain cancer stemness and chemoevasive phenotype. Aldehyde dehydrogenase 1 (ALDH1), which oxidises intracellular aldehydes with the aim of cellular detoxification, has been reported to be upregulated in CSCs in many kinds of cancers including breast cancer and thus accounts for the development of therapeutic resistance **[Tomita, Hiroyuki et al. 2016]**. CD44, a cell surface glycoprotein adhesive molecule is highly expressed in the cell surface of breast cancer stem cells **[Senbanjo, Linda T, and Meenakshi A Chellaiah. 2017]**.

In our erstwhile study **[Nandi, Sourav Kumar et al. 2022]**, we observed robust antiproliferative efficacy of Kaempferol on breast cancer stem cell populations, through downregulation of pluripotent stem cell markers (SOX2, OCT4, NANOG), MDR1 and CD44 **[Nandi, Sourav Kumar et al. 2022; Nandi, Sourav Kumar et al. 2018].** Herein, we wanted to check the efficacy of Kaempferol on tumour explants, obtained from NACT recipient TNBC patients. Our present study revealed that Kaempferol attenuated the expression of induced pluripotent stem cell markers (NANOG, CD44, and ALDH1) as well as MDR1, CD44+/ CD24- and CD44+/CD326+, downregulated the expression of pro-survival markers BCL-2, Ki-67, NF-kB and upregulated Caspase 3 expression. STRING pathway analysis and co-expression analysis revealed the mutual association of these

candidate proteins and suggested the probable antiproliferative mechanism of Kaempferol in such p-NACT-TNBC. The cumulative information of the prognostic markers upregulated in chemotolerant TNBC and their attenuation upon Kaempferol treatment could provide insights on developing treatment strategies.

Materials and Methods

Reagents: All chemicals were achieved from Sigma Aldrich (St. Louis, MO, USA) excluded boric acid (Sisco Research Laboratories, Mumbai, and Maharashtra, India), Disodium phosphate (Na_2HPO_4), ethanol, Potassium dihydrogen phosphate (KH_2PO_4), sodium dodecyl sulphate (Merck, India), CD44, CD24, CD326 and BD Cycletest™ Plus DNA Kit (BD Biosciences, San Jose, CA, USA). All reagents of primary tumour cell culture and breast cancer cell line culture were collected from Gibco, Thermo Fisher Scientific – US. For RNA-related experiments, Diethyl pyrocarbonate (DEPC) was acquired from Invitrogen, Carlsbad, CA, USA. All antibodies were obtained from Abcam, Cambridge, United Kingdom.

Ethics clearance: Fresh human (female) p-NACT-TNBC tumours were obtained from breast cancer patients with approved informed consent that underwent surgery at Netaji Subhas Chandra Bose Cancer Hospital (NSCBCRI). Standards methods were implemented through the relevant guidelines and regulations Ethics Committee. The project was approved by the ICMR and by the Ethics Committee of NSCBCRI (EC/ NSCBCRI/01/2021).

Tumour collection: For this study, we collected the female breast tumour (n=271) of patients who were pathologically identified as p-NACT-TNBC and received medicinal surgery for the treatment of breast cancer at Netaji Subhas Chandra Bose Cancer Hospital during the period 2016–2021. All included patients were also classified in respect of TNBC subtype (basal-like 1, basal-like 2, immunomodulatory and mesenchymal-like) (Table 1). To observe the regulation of p53 and Caspase-3, tumour samples (n=67) were randomly collected from the above tumour pool. For the second set of experiments, another pool of tumour samples (n=38) was obtained for explant culture and targeted markers analysis upon candidate drug treatment. Among the set of tumour samples (n=38) a minor subset of tumour samples (n=17) was used for immunohistochemistry to measure the effect of Kaempferol on tumour cell viability. The regulation of MDR1, NANOG, Caspase 3, and Cleaved Caspase 3 alongwith p53 protein markers that maintained stemness and chemoresistance phenomenon was studied in a major group of patients (n = 5).

All related informed consents of involved patients were obtained from the pathologist of the hospital division. The follow-up of targeted patients was achieved. The histological information of tissue samples was investigated by the clinical pathologist as previously maintained authorized protocol **[Makki, Jaafar. 2015]**. Subtype status for breast cancer

such as ER/PR/HER2 was also identified according to International Union against Cancer (UICC) and American Joint Committee on Cancer (AJCC) tumour-node-metastasis (TNM)

Age	Basal Like -1 (n=69)	Basal Like -2 (n=66)	Immunomodulatory (n=64)	Mesenchymal-like (n=72)	p- values
Median	39	42	47	52.5	0.006
Stage					
1	38 %	33.26%	15.33%	42%	0.005
2	31 %	27.8 %	34.3 %	27.5%	0.0001
3	21 %	26.2 %	47.9 %	18%	0.0001
4	5.8 %	10 .5 %	42. 6 %	6%	0.0001
Bilateral Carcinoma	1.9 %	1.2%	1.4 %	1.3%	0.05
Nuclear Grade					
1	6.3 %	1.3%	3.1 %	3.6%	0.0001
2	57 %	42.9%	28.5 %	18%	0.0001
3	11.5 %	53.3%	66.6 %	26%	0.0001
Ki-67 Mean Range	38 %	46.7%	59 %	36%	0.0023
Histological grade					
1	7.5 %	3.6%	2.5 %	4.1%	0.0001
2	52.3 %	33.8%	26.5 %	39%	0.0001
3	14.4 %	57.5%	63.5 %	43%	0.0001
Adjuvant Chemotherapy	78.8 %	82.5 %	92 %	71%	0.0017
Adjuvant Radiation therapy	48.5 %	58 %	72 %	63%	0.0001
Histology	DC, IDC	DC, IDC, INFDC	DC	IDC, AC	

Table 1: Study of the clinicopathological profile of post-NACT breast cancer patients. (n=271)

staging. The clinicopathological analysis of the included patients were illustrated in Table 1. The feedback of chemotherapy treatment was justified by an oncologist and morphologically verified by a clinical pathologist. In our experiment, all p-NACT-TNBC patients were included, and no one of the patients were related to the clinical trial.

Immunohistochemical analysis of p53 and Caspase 3 in different grades of p-NACT-TNBC: The expression of p53 and Caspase 3 protein markers were studied through the earlier approved immunohistochemical method in low-grade (I/II) and high-grade (III/IV) tumour in TNBC **[Nandi, Sourav Kumar et al. 2022]**. For histological examination, the H&E [1% alcoholic] staining was performed as an earlier established method **[Nandi, Sourav Kumar et al. 2022]**. Immunohistochemical evaluation of ER (1:200), PR (1:200), HER2 (1:200) was carried out through earlier conventional methods **[Kooistra, A et al. 1995]**.

Databases and bioinformatics tools: The protein expression level of p53 and Caspase3 together with the iPSC markers such as NANOG, ALDH1, CD44 and EMT markers such as MDR1, NF-kappaB, BCL2 were retrieved from TCGA-TNBC database, (http://ualcan.path.uab.edu/). The protein-protein interactions (PPI) were evaluated through the online STRING database (version 11.0). First, our candidate oncological markers were placed and the minimum interaction score was kept to the highest confidence (score 0.900). The retrieval of Interacting Genes (STRING, http://string.embl.de/) was finalized, evaluated and expatriate TSV format and employed to figure out the PPI networks. In addition, we applied DGIdb (http://www.dgidb.org), a valuable database that flows charge-free services for investigating the confirmation of drug-gene interactions, to analyze the potential candidate targets of Kaempferol

Cytotoxicity Assay: MTT assay of our candidate drugs were completed previously maintained methods **[Arunasree et al., 2010]**, IC-50 concentration of Kaempferol in ex-vivo for breast tumour explant cultures were maintained at 224.51 µM] The IC50 doses of Carboplatin were fixed in ex-vivo and in-vitro experiments from a dose-dependent survival of cells to Carboplatin (23.74 ± 4.67 µM) (Fig. 3 A). The cytotoxic assay was validated with IC-50 concentration, which is the dose mandatory to diminish the transmission density of treated cells by 50% as compared with the respective control (untreated cells). Tumour explants were cultured for 48 hrs with the following treatment conditions, viz. untreated, with Kaempferol, with Carboplatin, both at their IC-50 concentration i.e., 224.51 µM and 23.74µM respectively.

Target gene	Primer	Oligonucleotide Sequence 5' - 3'
NANOG	Forward	CCGGTCAAGAAACAGAAGA
	Reverse	CTGCGTCACACCATTGCTA
SOX2	Forward	CAAGACGCTCATGAAGAAGGATAA
	Reverse	TCATGCTGTAGCTGCCGTT
ALDH1	Forward	TGTTAGCTGATGCCGACTTG
	Reverse	TTCTTAGCCCGCTCAACACT
MDR1	Forward	CACGTGGTTGGAAGCTAACC
	Reverse	GAAGG CCAGAGCATAAGATGC
B-ACTIN	Forward	ACCAACTGGGACGATATGGAGAAGA
	Reverse	TACGACCAGAGGCATACAGGGACAA

Table 2: Primer pairs for quantitative real-time PCR analysis of gene expression.

Tumour explant culture: culture of tumour tissue obtained from a biopsy or surgical specimen: For the experiment of explants culture, all tumour tissue samples (n = 38) were acquired under sterile condition, washed and disintegrated into ~10 mm segments with a surgical knife. Tumour-derived explants were cultured in DMEM/F-12 complete medium added with 10% FBS, 5 μg/ml insulin, 500 ng/ml hydrocortisone, 10 ng/ml EGF, 1% penicilicin/streptomycin,50 μg/ml Gentamicin, 2.5 μg/ml Amphotericin B antibiotics in at 37°C in 5% CO_2/air.

Gene expression analysis by PCR: mRNA isolation upon the treatment of candidate drugs treated p-NACT-TNBC tumour (n = 38) explants was performed utilizing Trizol reagent **[Baelde, H J et al. 2001]**. cDNA was prepared from 10 μg of total RNA through our earlier recognized procedure **[Nandi, Sourav Kumar et al. 2022]**. The expression of candidate markers was analysed through a semiquantitative (Semiq) PCR from the cDNA with the 10 picomolar each of the gene-specific primers in Table S1. Semiq RT-PCR and SYBR Green-based qRT-PCR were performed in triplicates reaction in StepOne™ Real-TimePCR System (Applied Biosystems). The relative expression of the gene was studied depending on the comparative Ct values process **[Jackson, D P et al. 1990]**.

Hematoxylin and Eosin (H&E) staining, Immunohistochemical analysis to classify stemness, proliferation or apoptosis evasion: H&E staining (Fig. S1) was conducted following earlier well-known procedure for p-NACT-TNBC (n = 17) after candidate drug treatment for 48 h. After the termination of candidate drug treatment, paraffin-embedded tissue blocks were developed and 3 μM sections were taken for histological and

immunohistochemical experiments. For the histological assay, the H&E [1% alcoholic] staining was confirmed as an earlier defined technique **[Kooistra, A et al. 1995]**. In immunohistochemistry experiments, the expression of candidate targeted proteins regulating stemness, proliferation and apoptosis escape (p53, KI-67, CD44, NF-kappaB, ALDH1, NANOG, MDR1, BCL2) were analysed through our earlier methods **[Nandi, Sourav Kumar et al. 2022]**. The expression of Caspase 3 was also studied.

Protein immunoblot analysis to evaluate the levels of stemness and chemoresistance markers in response to experimental treatments: Following explant culture (n = 5), upon candidate drug treatment with IC-50 concentration for 48 h, tissue explants were sonicated for cell lysis and protein concentrations of the study groups (untreated, Carboplatin, Kaempferol) were measured through Bradford protein estimation methods **[Nandi, Sourav Kumar et al. 2022]**. A fixed amount (30 μg) of protein from each treatment panel was loaded in each lane of a 10% SDS-PAGE gel and transferred to nitrocellulose membranes. The membranes were washed with TBS-T (5% milk in Tris-buffered saline-Tween 20), blocked with 5% skimmed milk and treated with targeted specific primary antibodies like Anti-NANOG (Abcam Ca # ab109250, RRID: AB_10863442), Anti-MDR1(Santa Cruz Ca # sc-13131, RRID: AB_626990), Anti-p53 (Cell SignalingTechnology#2527), Anti-Caspase3(Cell Signalling Technology #9662), Anti-Cleaved-Caspase3(Cell Signalling Technology#9664) (1:1000dilution). TBS-T washed-off membranes were incubated with horse radishperoxidase-conjugated monoclonal secondary antibody (dilution: 1: 10,000; GeneTex Cat# GTX14122, RRID: AB_373069). The membranes were washed and after incubation with chemiluminescence substrate, were pictured by Chemi Doc Imaging System, Bio-Rad.

Evaluation of CD44 and CD326 expression as potential targets for improving chemo efficacy in TNBC: The expression status of CD44 (FITC- conjugated), CD24 (PE-conjugated), CD326 (APC-conjugated) in Kaempferol (224.51 μM and) and Carboplatin (23.74 μM) treated MDA-MB-231 cells, were measured through flow cytometry **[Li, Wenzhe et al. 2018]**. Momentarily, 1×10^6 cells were allowed to grow under the treatment of candidate drugs with IC-50 concentration for 48hrs and were incubated with CD44, CD24, CD326 antibodies with required dilution for 1 h. Cells were washed off and re-suspended in sheath buffers and measured through a flow cytometer. Untreated cells were treated with proper isotype PE-, FITC- and APC-conjugated antibodies. Cellular debris was left out from the investigation based on low forward light scatter.

Significance testing: The IC-50 (experiment data were exposed as means and SD from triplet individual findings) calculation of our candidate drugs were measured from the cell viability curve through GraphPad Prism® 8 software. All samples were analysed in triplicate. For RNA-related studies, Student's Z test is applied to determine the significance. Student's t-test and two-way ANOVA were applied to define the significance of the candidate protein marker's expression. Statistical tests were examined significantly at probability value, $p \leq 0.05$. For 95% confidence in all statistics, a p-value of $\leq 0.05$was considered statistically significant. All of above the experiments were done without important loss of statistical power.

Results

Clinicopathological profiles of patients based on TNBC subtypes: It was found patients with immunomodulatory (n = 64) or Mesenchymal-like (n = 72) displayed significantly poor survival than patients with basal like-1 (n = 69) or basal like-2 (n = 66) TNBC tumours. The H&E staining of p-NACT-TNBC tumour samples (Fig. 2A – 2C), with immunohistochemically confirmed ER/PR/ HER2 negative (Fig. 2D – 2F) expression were shown with microscopic images in Fig. 2A-C; 2D-F.
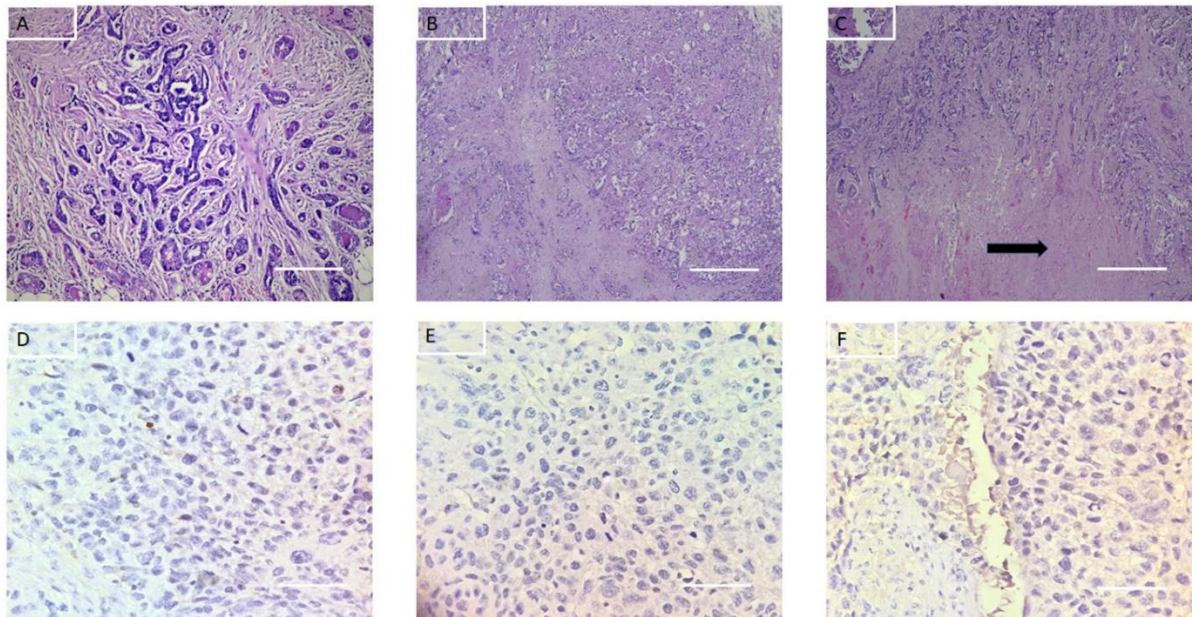
Figure 2: Microscopic appearance of triple-negative breast cancers exhibiting clinical progressive disease following NACT treatment: (A): Tumour cells arranged in tubules with intervening fibrous stroma; H&E; magnification 40X (B): Tumour cells forming abortive tubules with areas of necrosis; H&E; magnification 40X (C): Tumour cells with desmoplastic reaction and a large area of infarction (arrow); H&E; magnification 40X Hormone receptor expression: (D): Negative for estrogen receptor (ER) (E): Negative for progesterone receptor (PR) HER2 status: (F): Negative for human epidermal growth factor receptor 2 (HER2)

The association amongst survival of low grade (I/II) (Fig. 3A) and high grade (III/IV) (Fig. 3B) was analysed and represented with Kaplan–Meier survival plots (Fig. 3). Progression-free survival for the p-NACT-TNBC group was significantly increased in low grade (I/II) tumour samples than in high grade (III/IV) when compared with pre-therapeutic tissue samples. The consequence of disease-free (Fig. 3C) and overall survival curve (Fig. 3D) was studied. The 5-year survival disease-free survival and overall survival possibility were

plotted respectively for the whole experimental group of patients.
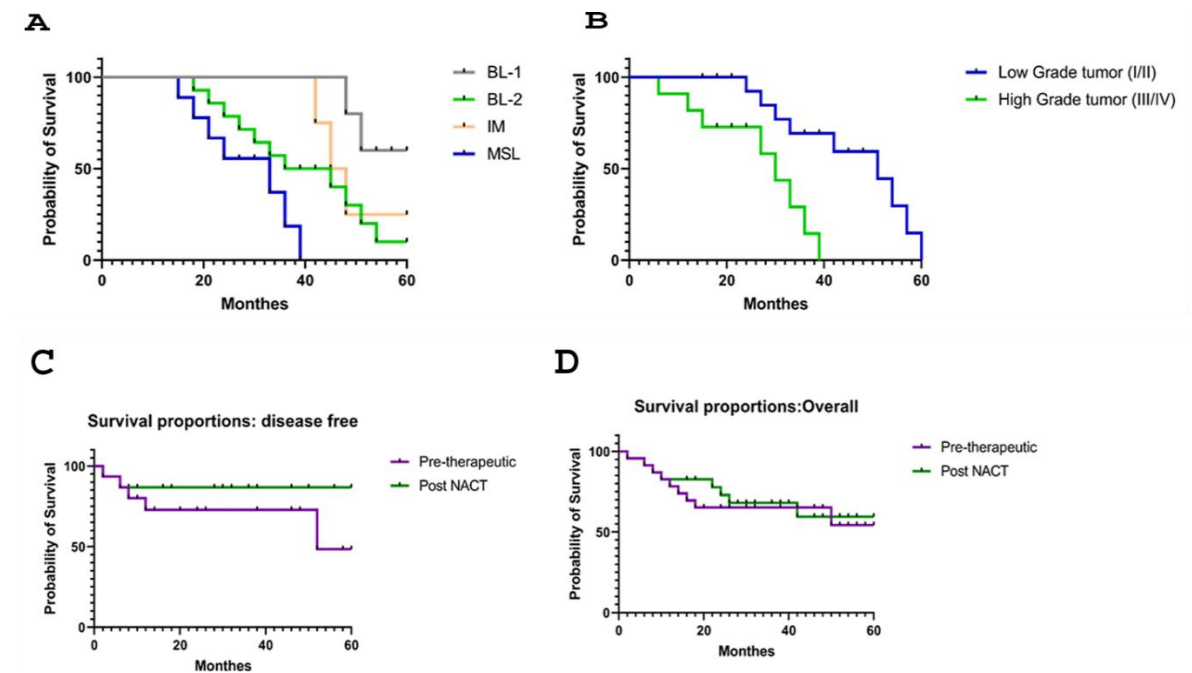
*Figure 3: Relapse-free survivals (RFS) of Random breast cancer and TNBC in with pre therapeutic vs post-NACT treated patients according to each TNM (tumour–node–metastasis) stage before and after chemo therapy. (A) RFS of the patients with grade I/II, (**** p < 0.0001), (B) RFS of the patients with grade III/IV, (*** p < 0.01), (C) RFS (**** p < 0.0001), (D) overall survival of the patients(**** p < 0.0001), (E)progression free survival of BL-1, BL-2, IM, and ml (****p < 0.0001), Abbreviation Basal Like 1:(BL-1), Basal Like 2:(BL-2), Immunomodulatory: (IM), and Mesenchymal-like (ML).*

In the subset of pre-therapeutic patients, there was a relapse earlier than in the p-NACT-TNBC group of sets. No significant change was observed in the overall survival study.

Expression profiling of p53 and Caspase 3 or its association: TCGA database (primary breast tumour sample, n = 1097 vs normal tissue sample, n = 114) revealed that the expression of p53 (Fig. 4 A) and Caspase 3 (Fig 4B) proteins were greater in breast tumours than the normal tumour sample. The activation of Caspase3 indicates apoptosis and consequent cell death. Although, p53 gene expression is upregulated and the stimulation of caspase3 could not trigger apoptosis limiting the efficacy of chemotherapy that shows anti-tumour potency through the p53 wild-type context [**Thottassery, J V et al. 1997**]. In this study, a trend of low p53 expression with high Caspase 3 expression in low-grade tumour samples and high nuclear p53 expression with low Caspase 3 expression was observed in high-grade tumours (Fig. 4C-D, Table 3). The TCGA database for p53 and Caspase 3 expression in different stages (Fig. 5A, 5B) and different nodal metastatic status

42

(Fig. 5C, 5D) were analysed, which showed the expression of p53 was increased in higher
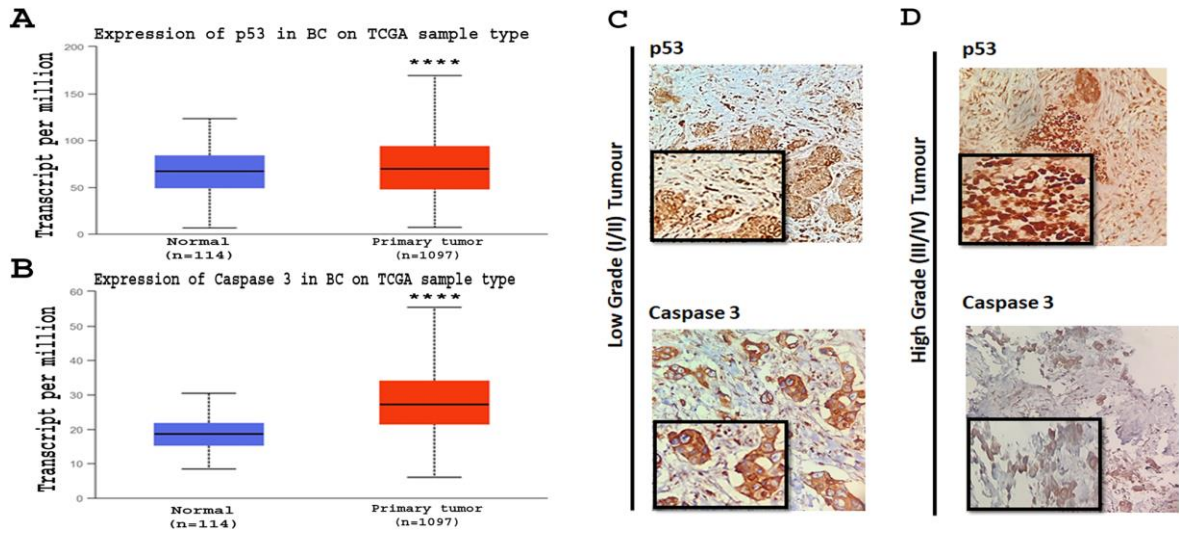
Figure 4: Association of p53 and caspase 3 expression in several grades of post-NACT-TNBC tumour (A) Differential expression analysis of p53 in TCGA normal and TNBC tumour samples (B) expression of caspase 3 in normal and tumour from TCGA samples (C) expression of p53 and caspase 3 in low grade tumour (I/II) and expression of p53 and caspase 3 in high grade tumour (III/IV).
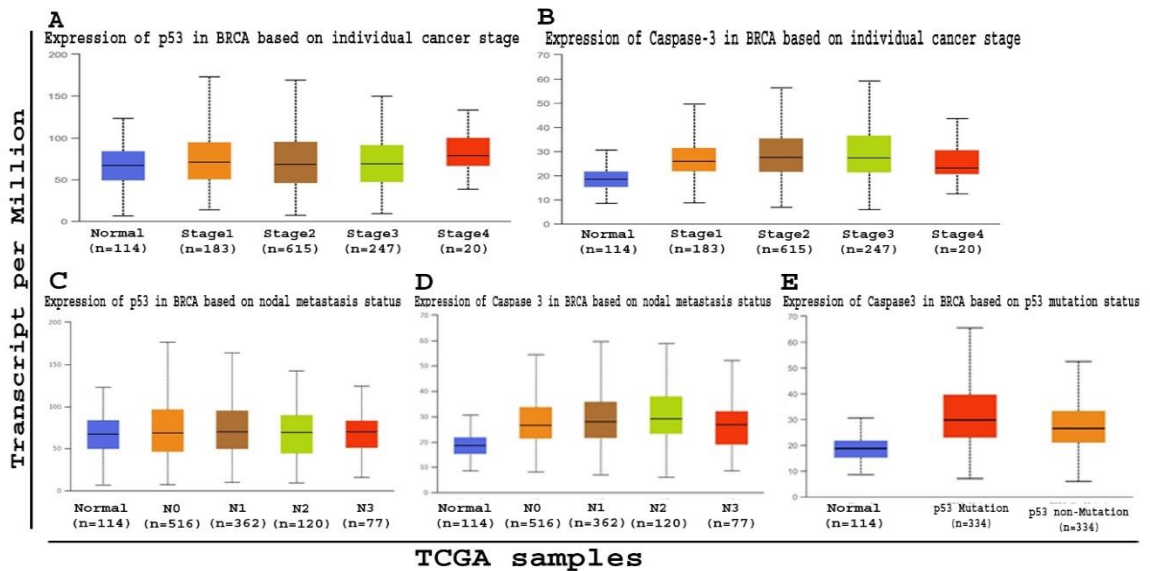
Figure 5: Differential expression of p53 and caspase 3 in TNBC. A study of the RNA abundance (measured in transcripts per million) of ten human p53 and caspase 3 genes in normal and TNBC samples from The Cancer Genome Atlas (TCGA). The regulation of p53 in diverse stages (A) and on the basis of node status (C). The expression of caspase 3 in different stages (B) and on the basis of node status (D) and based on TP53 mutation.

stages (III/IV) (Fig. 4D) and high nodal metastatic status. In contrast, the expression of Caspase 3 was high in lower stage (I/II) (Fig. 4C) and low nodal metastatic status (Fig. 5C, 5D), that indicated the expression of p53 was increased in higher grade. Moreover, the relation between the Caspase 3 expressions with mutated p53 status was confirmed by the TCGA-BRCA database. In this study, we observed that the expression of Caspase 3 was decreased in p53 mutation as compared with non-mutant p53 (Fig. 5E). In the initial part of our study, we analysed the expression of p53 and Caspase-3 in breast cancer through IHC analysis n = 62) (Table 3) on a subset of p-NACT-TNBC patients to confirm the TCGA data analysed.

	Total Number (n)	Caspase 3 (%)	P-53 (%)	p-value
Tumour Size (cm)				
≤ 2	28	26.58 (±0.16)	89.2	0.001
>2	34	17.84 (±0.12)	76.43	0.0001
Histological grade				
1	17	58.9	6.33	0.005
2	21	43.4	17.8	0.0001
3	24	31.6	52.33	0.0001
Histological type				
Ductal	56	36.9	48.29	0.0001
Lobular	6	24.33	81.37	0.0001
Nodes				
Positive	48	57.46	16.29	0.0001
Negative	14	23.11	67.77	0.0001
Adjuvant Chemotherapy	36	26.38 (±4.28)	81.24	0.0017
Adjuvant Radiation therapy	62	42.35 (±3.10)	61.41	0.0001

Table 3: Correlation between protein expression of caspase 3 and p53 in breast cancer.

In our study, we showed the induction of high nuclear p53 expression in high-grade (III/IV) tumour samples than the low-grade (I/II) (Fig. 4C) and increased expression of Caspase-3 was also found in the low-grade (I/II) tumour than the high grade (III/IV) tumours (Fig. 4D). All related statistical experiments were completed in Table 3.

Association between Kaempferol and changes in proliferation kinetics and gene expression profiles in post-NACT-TNBC patients: A significant diminution of cell

viability was detected in a dose-dependent aspect in p-NACT-TNBC tumour-derived cells upon the treatment (48hrs) with several doses of Kaempferol (Fig. 6B) and Carboplatin
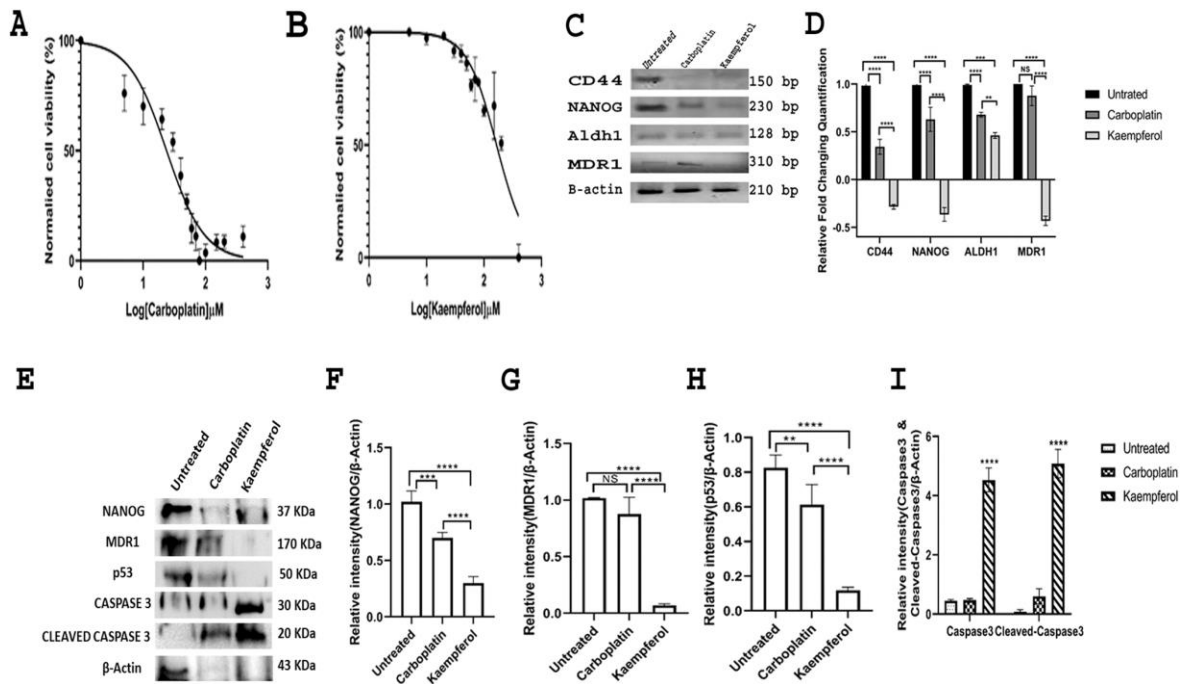
Figure 6: Cell proliferation assay in ex-vivo cultured primary post-NACT-TNBC tumour cells. (A): Carboplatin, (B): Kaempferol, IC-50 dosage was analysed. Semi qRT-PCR (C) and qRT-PCR (D) analysis of gene in post-NACT-TNBC tumour. Relative gene expression fold changes were normalized to β-Actin and compared to untreated cells, were presented as bar graphs (F-I). The treatment groups included: U: Control; C: carboplatin; K: Kaempferol. Immunoblot analysis to check the fold change of expression of iPSC, chemoresistance and apoptosis markers in p-NACT-TNBC patients under various treatment conditions (48 h) (E). U: Control; C: Carboplatin; and K: Kaempferol.

(Fig. 6A). The IC50 concentration of the Kaempferol treated in p-NACT-TNBC tumour-derived cells was $205.7 \pm 6.67 \, \mu M$ and Carboplatin was $23.74 \pm 4.67 \, \mu M$.

RNA expression profiling of candidate markers associated with cellular plasticity: Expression of CD44, NANOG, MDR1, and ALDH1 were evaluated in individual treatment groups (Untreated, Carboplatin, Kaempferol) and normalized in respect of β- ACTIN (Fig. 6C-D). In the Kaempferol-treated sample, a lower expression of NANOG was detected (Fig. 6C). Other findings from qRT-PCR data, Kaempferol was more effective than Carboplatin in downregulating the expression of *CD44, NANOG, ALDH1, MDR1* (Fig. 6D). In *ALDH1* expression panel, Kaempferol treatment was more significant than carboplatin whereas in *MDR1* expression panel, the carboplatin treatment group was not

significant (NS). The finest significant changes in both drug treatment sets were found in *CD44* and *NANOG*.

Western blot assay: In the experiment of western blot, Kaempferol downregulated p53, iPSC markers and chemoresistance markers such as NANOG and MDR1 with upregulation of cleaved caspase 3 (Fig. 6E) compared to the untreated group. Relative fold changes of the expression of the candidate proteins were normalized with respect to the housekeeping gene (β-Actin) (Fig. 6F–I). Another finding from the outcome of immunoblotting, no significant changes occurred in the expression of MDR1 and p53 markers compare to untreated upon Carboplatin treatment (Fig. 6F–I), while Kaempferol regulated the expression of targeted oncogenic markers. The outcome signified that Kaempferol showed a significant downregulation of targeted proteins in p-NACT TNBC.

Protein-protein interaction and Co-expression analysis: According to certain information, mutant p53 accelerated stemness and upregulates MDR1 expression of other anti-apoptotic genes regulation such as KI-67, CD44, NF- kappaB, ALDH1, NANOG, and BCL2, and arrested cell cycle ensuring chemotolerance in breast cancer patients through NF- kappaB associated p53 pathway.
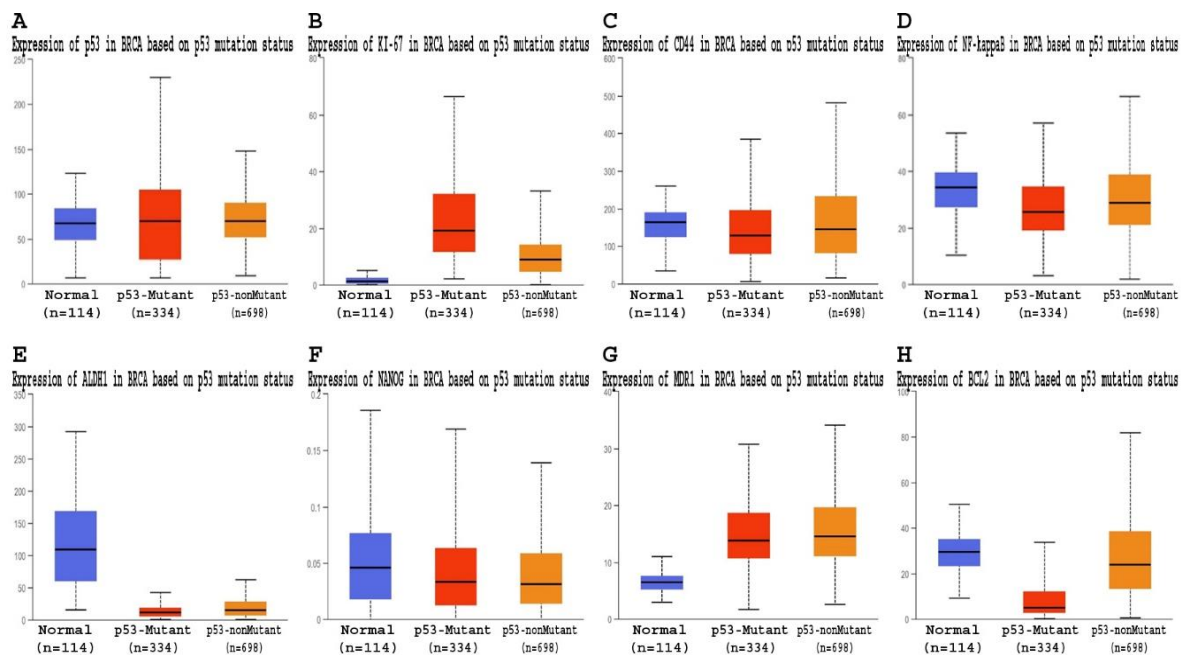
Figure 7: Transcriptomic analysis of p53 (A), KI-67 (B), CD44 (C), NF-κB (D), ALDH1 (E), NANOG (F), MDR1 (G), and BCL2 (H) expression in normal and TNBC samples from The Cancer Genome Atlas (TCGA) dataset, stratified by p53 mutation status.

The expression of targeted markers (transcript per million) responsible for bypassing chemotherapeutic agents in a p53 mutated background from the TCGA database, viz. p53 (Fig. 7A), KI—67 (Fig. 7B), CD44 (Fig. 7C), NF- kappaB (Fig. 7D), ALDH1 p53 (Fig. 7E), NANOG (Fig. 7F), MDR1 (Fig. 7G), BCL2 (figure 7H) and Caspase 3 (Fig. 4E) are shown. The results also indicated that the mutant p53 is overexpressed in aggressive tumours but was incapable to stimulate apoptosis in such tumours. Though, the molecular mechanism behind these correlations is not properly implied. In our study, we analysed protein-protein interactions of genes regulated by mutant p53 through the STRING database. The data showed the potential function and metabolic networks (Fig. 8) regulated by mutant p53.

Pathways	Color code	False discovery rate
Regulation of intrinsic apoptosis signaling pathway by p53		0.0028
Intrinsic apoptosis signaling pathway		0.0294
Regulation of response to DNA damage stimuli		0.0448
Drug resistance		0.0232
Negative regulation of metabolic process		0.0351
Regulation of cell proliferation		9.08e-08
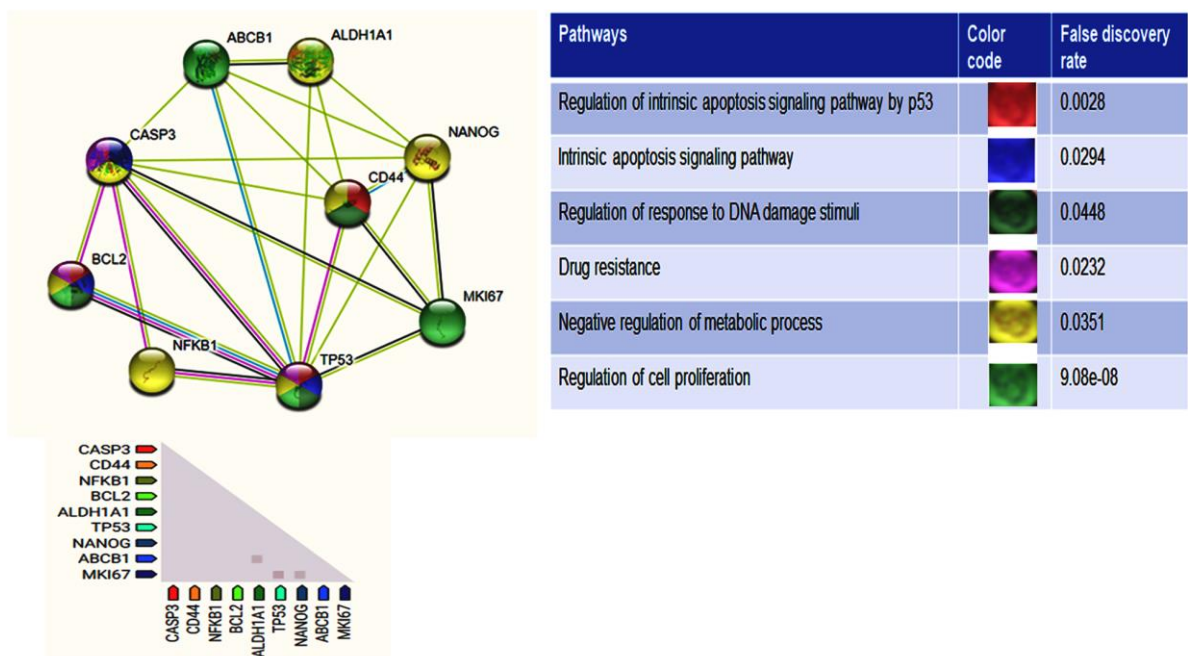
Figure 8: Pathway and functional analysis of genes associated with p53, including MDR1, ALDH1, NANOG, CD44, KI-67, TP53, NFKB1, BCL2, and CASP3, using the STRING database.

The outcome of the PPI network displayed the association of metastatic and anti-apoptotic networks related to p53 mutation. Co-expression of candidate oncological markers (Fig. 8) was found. The uppermost co-expression was found amongst KI67 and p53, which is consistent with our earlier determinations where the expression of KI67 was increased in p53 mutant tumour tissue with reference to normal tissue and p53 nonmutant tissue (Fig. 7). Co-expression was also found between p53 and KI-67, CD44, NF- kappaB, ALDH1,

NANOG, MDR1, and BCL2. Several other interactions between CD44 and NF- kappaB, NANOG, MDR1, and ALDH1were detected. In Fig. 8, the square pointer displayed the interaction.

IHC examination of candidate proteins regulated by mutant p53 in TCGA samples: To analyse the impact of targeted chemotherapeutical drugs upon ex-vivo culture primary tumour tissue, we checked in different p-NACT-TNBC tumour sample. The H&E staining of the p-NACT-TNBC tumour sample upon Kaempferol treatment was studied and observed cell death (Fig. 9A – 9C). In all these tumours, both Carboplatin and Kaempferol induced cell death in these explants. Treatment with Kaempferol also indicated the downregulation
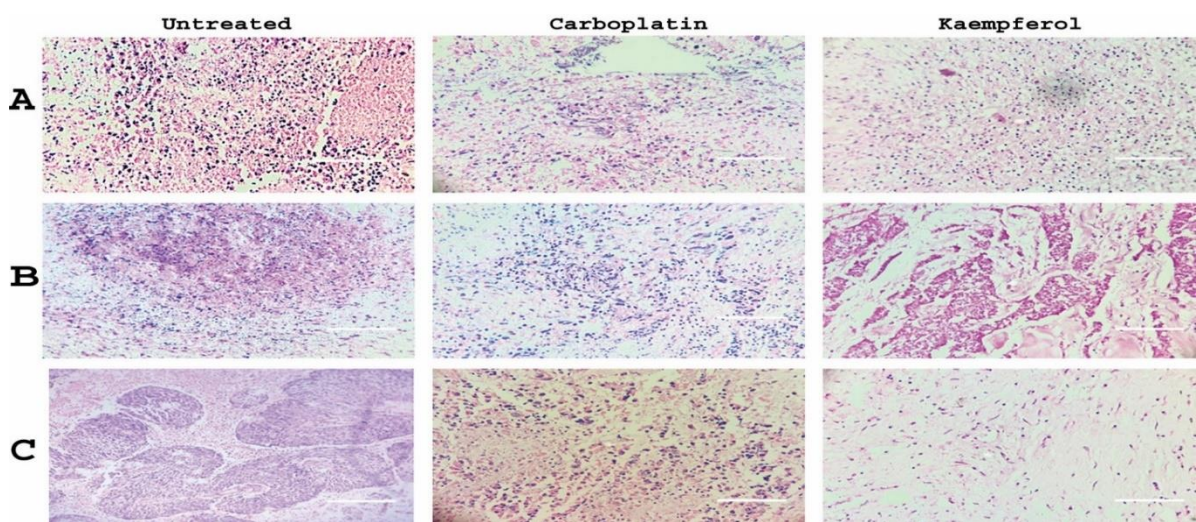
Figure 9: Histological examination of post-NCT-TNBC tumours using H&E staining after candidate drug treatments. (A) Tumour cells arranged in tubular structures with fibrous stroma; H&E; 40X, (B): Tubular tumour structures that are abortive with foci of necrosis; H&E; 40X, (C): Tumour cells in a desmoplastic stroma

of p53 (Fig. 10A), KI—67 (Fig. 10B), CD44 (Fig. 10C), NF- kappaB (Fig. 10D), ALDH1 (Fig. 10E), NANOG (Fig. 10F), MDR1 (Fig. 10G), and BCL2 (Fig. 10H), whereas the expression of Caspase 3 (Fig. 10H) was upregulated in these groups. In the Carboplatin treated group, the expression of targeted markers did not indicate any significant changes with respect to the untreated group, apart from the expression of NANOG, p53 and Caspase 3 markers.
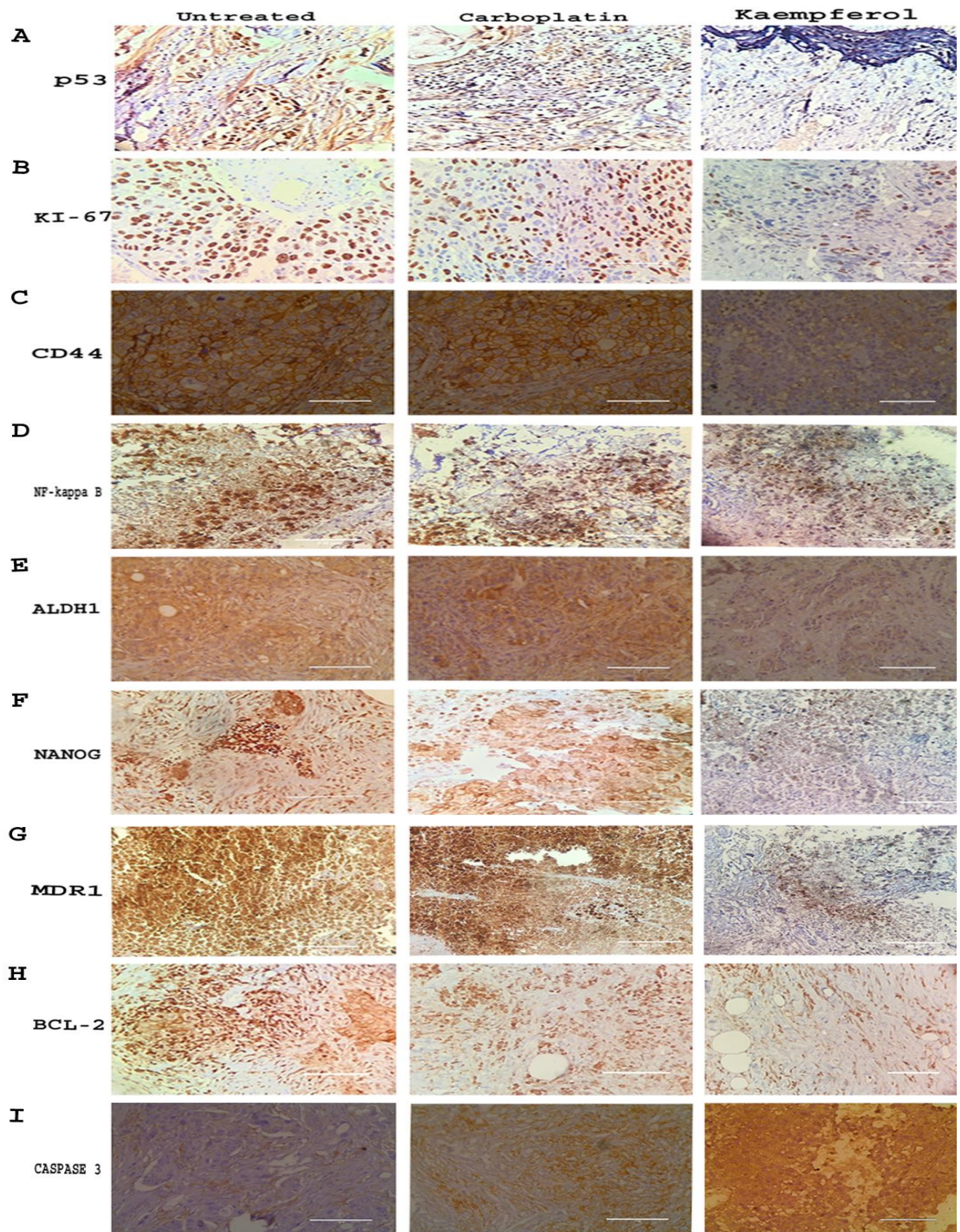
Figure 10: IHC assessment of proliferation markers in tumour samples treated with p53 inhibitor (A), KI—67 (B), CD44 (C), NF- kappaB(D), ALDH1 (E), NANOG (F), MDR1 (G), and BCL2 (H) in explant culture. Outcome are shown as mean ± SEM. Values are statistically significant at *P < 0.05. Magnification: 40X.

In the Fig. 10F, we found that the expression of NANOG is reduced upon candidate drug treatment where Kaempferol showed more effectiveness than Carboplatin. In Kaempferol

treatment, the expression of Caspase 3 was increased with respect to Carboplatin. From the analysis of this study, we documented the expression status of these targeted markers that can be exploited for the evaluation of the treatment response of chemo-tolerant breast TNBC and recommend a new strategy for molecular-based targeted therapies in advance of clinical trials.

Experimental verification of Kaempferol and the Investigation of CD44 and CD326 as cancer stem cell indicators in cell line: The efficacy of Carboplatin (Fig. 11A) and
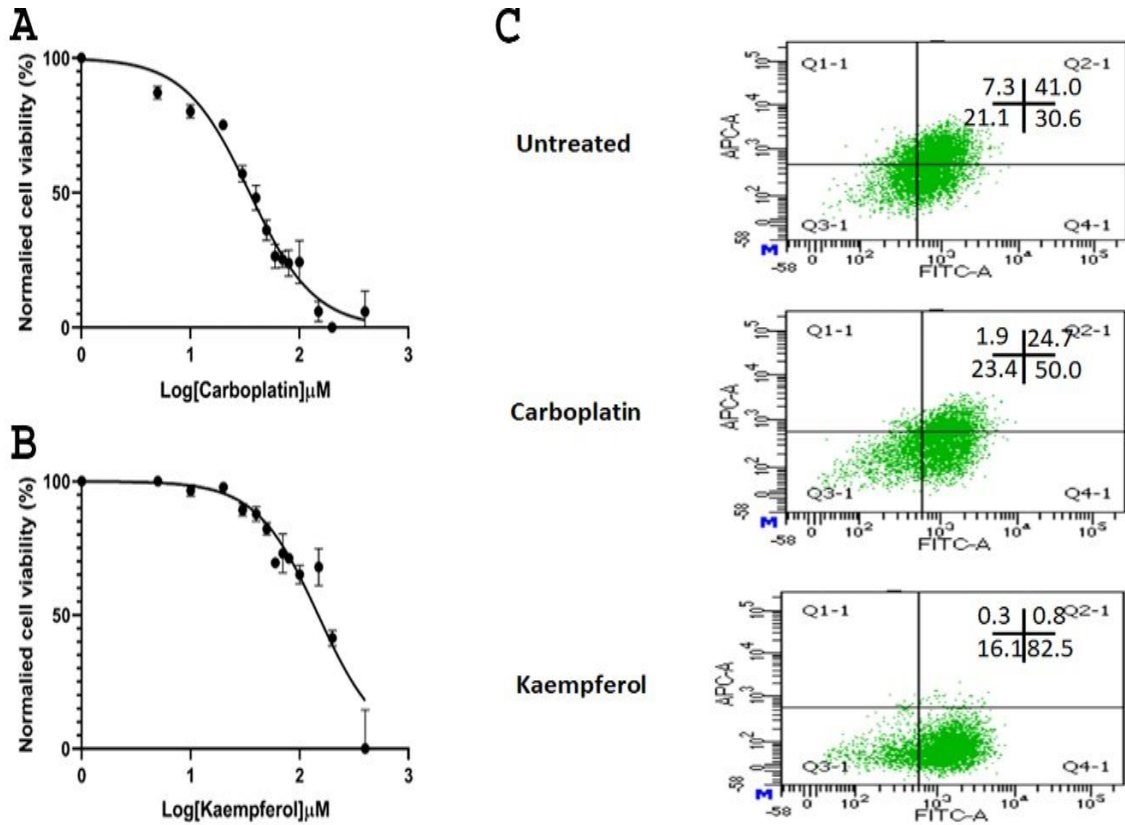
Figure 11: Cell proliferation assay (48-hour) in MDA-MB-231 cell line treated with (A) Carboplatin (B) Kaempferol. Expression analysis of CD44 (FITC conjugated) / EpCAM (APC conjugated) in MDA-MB-231 cells treated with candidate drug (C) such as untreated, carboplatin, Kaempferol respectively

Kaempferol (Fig. 11B) drug on MDA-MB-231 cell line were analysed through CD44/CD24 (Fig. 12A) and CD326/CD24 (Fig. 12B) markers. The outcome of this experiment revealed that the population of CD44 +, CD24- cells and CD326 +, CD24- cells
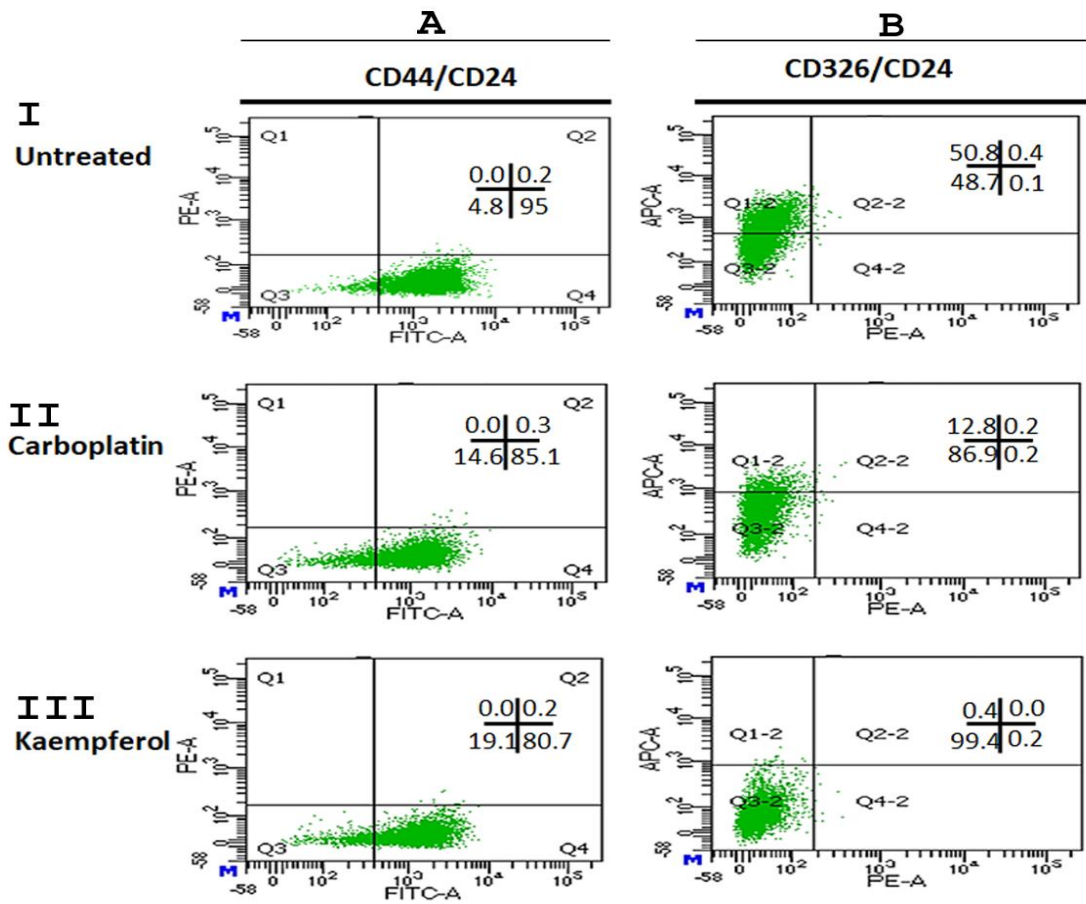
Figure12. Immunophenotyping of MDA-MB-231 Upon treatment of (A) Carboplatin (B)Kaempferol for 48 hrs.

were reduced by about 18.33% (Fig. 12 AIII) and 50.57% (Fig. 12 BIII) in the 48 hrs treatment of Kaempferol with compared to the untreated panel whereas, in Carboplatin treatment group, the same populations diminished almost 17% (Fig. 12 AII) and 38.67% (Fig. 12 BII) individually. The efficacy of couple drugs were also examined for CD326/CD44 population (Fig. 11) whereas Kaempferol decreased 40.2% cells in comparison to the Untreated group.

Discussion

The network of chemo tolerance and resulting therapeutics evasion technique is intrinsically complicated mechanisms. With the long-time treatment of chemotherapy, it becomes even more important to determine the status of oncological markers that control stemness, proliferation, chemoevasion, proliferation and apoptosis mechanisms of tumour. Mutated p53, the guardian of the genome, shows a high nuclear expression profile, that plays an important role in the upregulation of stem cell renewal, uninhibited cell proliferation and chemo-tolerance in breast cancer development **[Thottassery, J V et al. 1997]**. Wild-type p53 is an important regulator of the cell cycle that promotes either apoptosis or DNA damage repair **[Chen, Jiandong. 2016]** following a cell cycle arrest. Mutant p53 is related to the upregulating of integral oncogenic markers **[Alvarado-Ortiz, Eduardo et al. 2021]** that leads to chemo-tolerance mechanisms. The absence of a p53 maker in fibroblasts is also associated with therapeutics bypass networks in the p53 based xenograft model **[Liu, Qing et al. 2020]**. Residual Cancer Burden (RCB) index, which includes residual tumour thickness, the ratio of cellularity, lymph node positivity, tumour histology and grade is an essential predictor of progression-free survival. Still, apart from these limits, the determination of prognostic markers determining overall disease prognosis is studied as vital markers at the molecular oncological level. Our study hypothesized that the inverse correlation of p53 and Caspase 3 expression in high-grade tumour samples with high RCB index to be attributed to the tissue-specific expression of p53 on targeted markers regulating stem cell renewal, proliferation, chemo resistance and apoptosis evasion. Overexpression of MDR1 marker, an ATP-dependent efflux pump could lead to the tolerance to drugs by pumping off the drugs from cells. A transient transfection study documented that NF-kappaB, MDR1 promoters are also influenced by the p53 mutation network **[Spike, Benjamin T, and Geoffrey M Wahl. 2011]**. Furthermore, the inactivation of NF-κB was reported to be associated with the downregulation of BCL-2 and resultant in Caspase-3 activation that increased apoptosis activity **[Chuthapisith, Suebwong et al. 2010]**. Our study also documented the correlation between Ki-67 expression, histopathological grading and BCL-2 expression by various molecular markers that were associated with high/low p53 status, and elevated levels of BCL-2 expression **[Chuthapisith, Suebwong et al. 2010]**. Moreover, BC patients with high Ki-67/BCL2 and mutated p53 are predicted to be at major risk of survival in comparison with the TNBC patients with lower expression of BCL2 in our study **[Chuthapisith, Suebwong et al. 2010].** Earlier studies documented that through numerous mechanisms, in chemo tolerant

52

breast cancer cell line, the expression of ALDH1, (cellular detoxification protein) and CD44 (the transducer of microenvironmental signals) are upregulated [**Li, Wenzhe et al. 2018; Bourguignon, Lilly Y W et al. 2012**]. Furthermore, another study suggested that the interaction between Hyaluronan (HA) and CD44 induces the association with MDR1, which promotes chemo evasion [**Bourguignon, Lilly Y W et al. 2012**]. Trock and associated collaborators accepted that breast cancer expressing MDR1 were three times more responsible for chemotherapy failure than patients with poor survival with MDR1 negative expression [**Trock, B J et al. 1997**]. In this study, we also observed up regulation of NANOG, ALDH1, CD44, MDR1 in ex-vivo cultured breast tumour explants that got decreased upon treatment with Kaempferol.

An earlier study demonstrated that the mutant p53 marker, which is usually expressed in aggressive and chemo-tolerant tumours cell, might impede the potential of pro-Caspase-3 to be proteolytically activated by Caspase-9, resulting in inhibition of Apaf-1 expression, the cell-death effector and downstream target of caspase-9, as noticed in metastatic melanomas [**Brentnall, Matthew et al. 2013**]. Furthermore, resistance to apoptotic stimuli has been documented in the MCF-7 cell line that lacked expression of Caspase-3 as the outcome of a 47 bp deletion in exon 3 of the CASP3 gene [**Devarajan, Eswaran et al. 2002**]. In our study, we hypothesized that the high nuclear expression of mutant p53 in pre-treated high-grade tumours, inhibited the expression of Caspase 3, thus stimulating apoptosis evading which also leading chemo tolerance networking (Fig. 3, Fig. 5). The outcome indicated the loss of Caspase 3 expression that may have rendered the breast cancer cells insensitive to chemotherapeutics and radiation-based therapeutics. However, drug evasion mechanisms of TNBC cells can also occur through over expression of the caspase 3 markers [**Devarajan, Eswaran et al. 2002**]. It is also predicted that mutant p53 associate with MDR1 resulting in up regulated MDR1 gene expression. NANOG expression is also associated with NF kappaB, involved in a NANOG-CD44-MDR1 pathway, to stimulate chemo tolerance and consistent stemness [**Chuthapisith, Suebwong et al. 2010**]. We assumed that wild-type p53 regulates endogenous MDR1 gene expression and that the effect of loss of functional p53 on the spectrum of drug sensitivity is, in part, determined by its selective tissue-specific effects on MDR1.

The impact of flavonoids in the inhibition and care of breast cancer has earlier been documented [**Nandi, Sourav Kumar et al. 2022; Imran, Muhammad et al. 2019**]. Kaempferol, an aglycone flavonoid is a tetrahydroxy flavonein that the quadruplet hydroxy groups are observed at 3, 5, 7, and 4 positions. Earlier, Kaempferol and its derivatives have

been documented as anti-cancer agents and the oncogenic-related pathway was not extensively studied. A previous report identified the quantity consumption in a day of Kaempferol (14.97 mg) and pursued a plasma concentration of 16.69 ng/ml [**Nandi, Sourav Kumar et al. 2022**]. The previous report suggested, Kaempferol halts cancer cell progression through G2/M dependent cell-cycle arrest, downregulates the expression of phosphoinositide 3-kinase (PI3K)/protein kinase B(AKT) network and halts the production of reactive oxygen species (ROS) by its groups at C3, C5, and C4, an oxo group at C4, and a double bond at C2-C3 linked in cancer developments. ROS at moderate level promotes malignant cell growth [**Nandi, Sourav Kumar et al. 2022**]. In our prior study, we documented the expression of γH2AX in explants of breast tumour and not in adjacent normal tissues, upon the treatment of Kaempferol [**Nandi, Sourav Kumar et al. 2022**]. From the experimental data, we concluded the reduction of stemness, cell growth and apoptosis evasiveness markers and increased the expression of Caspase-3 marker in p-NACT-TNBC showed the robustness of Kaempferol in inducing apoptosis. The robustness was not found in Carboplatin treatment groups. Previous documentation suggested that ALDH1 and CD44 positive patients had the worst prognosis which was related to worse tumour differentiation, lymph node metastasis, diminished overall and disease-free survival and enhanced tumourigenesis [**Tomita, Hiroyuki et al. 2016**]. Furthermore, Ki-67, a non-histone nuclear protein has been determined as an independent prognostic marker of proliferation in breast cancer. Induction of the expression of Ki-67 has been documented to be associated with tumour size, high histological grade, lymph node interest, poor DFS and OS in breast cancer. An earlier report also demonstrated that the frequency of high expression of Ki-67 showed correlation with p53 mutation was more elevated that is the main origin of more invasive tumour and higher frequency of metastasis in breast cancer [**DOI: 10.1371/journal.pone.0172324**]. This study found that the expression of Ki-67 was decreased upon the treatment of Kaempferol.

In MCF- 7 cell line, the CD44 + /CD24- and Epithelial-mesenchymal transition (EMT) marker such as ALDH1 has led to a vital function in chemo tolerance and malignancy [**Li, Wenzhe et al. 2018; Guttilla, I K et al. 2012**]. Moreover, in CD44 + and ALDH1+ tumours, the upregulation of NANOG is identified [**Chuthapisith, Suebwong et al. 2010**]. The results indicated that both CD44+ and ALDH1+ increased the survival rate of tumours through self-renewal of the stem cell. Several indications in cell lines demonstrated that cell surface markers i.e., CD44 + /CD24- and CD44 + /CD326 in TNBC are related to the upregulation of EMT markers that leads the metastasis [**Zou, Weiyan et al. 2020**].

54

To assure the effectiveness of Kaempferol, the analysis of cancer stem cell markers (CD44 and CD326) in the MDA-MB-231 cell line and the expression of targeted markers were studied and compared with the effect of Carboplatin in this experiment. Prior reports revealed that EMT markers of MCF-7 cells induced the CD44 + /CD24 - mesenchymal phenotype sub-population **[Guttilla, I K et al. 2012]**. To address this prospect, we utilized FACS analysis to determine the proportion of CD44 + /CD24- and CD326 + /CD24- cells under the candidate drug treatment. Our studies showed that Kaempferol decreased the expression of the EMT marker, CD44 + / CD326 + marker in the tumour cells ($p < 0.05$) more effectively than the Carboplatin administered cells. Early reports showed that Kaempferol arrested the cell cycle at the G2/M stage through the downregulation of CDK1 in triple-negative breast cancer cells **[Zhu, Li, and Lijun Xue. 2019]**. Similar findings were obtained by our team in chemo tolerant primary breast tumour cells which are collected from NACT tumours **[Nandi, Sourav Kumar et al. 2022]**. EMT markers and iPSC markers represent a vital role in the induction of breast cancer. Renewal of the expression of EMT markers in breast cancer leads to survival of such cells in chemotherapeutic treatment, resulting chemo resistance **[Huang, Jing et al. 2015].** In our study, we observed that Kaempferol (IC- 50) decreased the expression of ALDH1, and NANOG markers that activated the tumour cells through downregulating MDR1 gene. The immunoblotting study also shows an associated induction of NANOG, MDR1 markers in tumour with increased expression of p53 markers and cleaved Caspase 3 expression. The downregulation of stemness and chemo resistance markers (NANOG and MDR1) with the association of Caspase 3 and cleaved Caspase 3 upregulation upon Kaempferol treatment documented the capability to activate apoptosis in the cultured primary breast tumour explants.

The DGIdb (http://www.dgidb.org) results supported the NF-kappa B and NANOG markers to be the target of the Kaempferol drug. The correlated malignant marker of p-NACT-TNBC was confirmed through the TCGA database and STRING study and validated through immunohistochemistry analyses which revealed that Kaempferol downregulates the p53, NF-kappaB, ALDH1, CD44, NANOG, MDR1, KI-67 and BCL2 expression. Moreover, we analysed a PPI network through the STRING database, which indicated that all targeted markers are associated with the p53 pathway. Higher association and co-expression between p53 and KI67 were analysed which is uniform in our experimental outcome. p53 has mostly controlled functions such as intrinsic apoptosis

pathway, DNA damage response, drug resistance and regulation, metabolic progression, and cell survival.

In our study, we demonstrated Kaempferol induced apoptosis in breast tumours. The pharmacokinetics and pharmacodynamics properties of Kaempferol were documented in our earlier reports **[Nandi, Sourav Kumar et al. 2022]**. Earlier studies documented that MDR1 plays an important role in chemotolerance **[van der Kuip, Heiko et al. 2006]**. In view of this, we also developed the monitoring of biomarkers in the explant platform to analyse the effect of the drug. Carboplatin was powerful in attenuating the survival of tumour cells but has fewer effects on oncogenic markers contributing to cancer stemness properties. A previous study of oncology suggesting that at high dosages Carboplatin administration might be utilised in first-line chemotherapy treatment of TNBC patients **[Perez, E A et al. 2000].** Until now, Carboplatin is applicable as a medication for cancer. Carboplatin is impeded in DNA repair, to control and ultimately destroy cancer cells. The induction of the DNA repair process is one important characteristic in platinum-resistance cells. Apart from TNBC subtypes, only the BL1 subtype with BRCA1 mutation is developed for Carboplatin treatment and can achieve resistance by different mechanisms **[Bhattacharya, Rittwika et al. 2017].** Our study showed the p53 independent Caspase 3 stimulation with our candidate drug.

To summarize, a wide number of preclinical speculative analyses have definite the mechanisms of Kaempferol in the prevention and treatment of chemo-tolerance breast cancer. But there is a lack of in-depth understanding of Kaempferol. Moreover, the explants are representatives of the unique tumour microenvironment and an ideal system to check the therapeutic efficacy of a drug. The technology is low-cost, rapid, and achievable within an integrated cancer translational research setting. The insights from these data would help in the improvisation of therapeutic strategies for p-NACT breast tumours.

Chapter 2

<u>Title:</u> Study of the anti-cancer effect of Kaempferol in synergism with Verapamil in deregulation of the CD44-NANOG-MDR1 associated chemoresistance pathways of breast cancer stem cells

Background

Chemoresistance is a perpetual therapeutic challenge for metastatic breast cancer. A prior study demonstrated that breast cancer stem cells (BCSC) acquire resistance through induction of stemness property and increased expression of pluripotent chemo-evasion markers such as SOX2, OCT4, NANOG, MDR1 and CD44, during long-term anticancer treatments with chemotherapeutics agents. Previous evidence documented the inhibition effect of Kaempferol in BCSC proliferation occurs through the reduction of epithelial-mesenchymal transition marker expression. Hypothetically we designed the network that is associated with chemo-resistance and might approached by Kaempferol (K), alone or coupled with Verapamil (V), which is a blocker of MDR1 marker. We utilized K with a couple of V, in several studies to identify the inhibitory effect on BCSC. Individually K or KV diminished pH-dependent mammosphere development in primary BCSC and MDA-MB-231 cells. Gene and protein (immunocytochemistry, western blot) expression of targeted markers such as SOX2, OCT4, NANOG, MDR1 and CD44 were achieved in the ex-vivo grown primary BCSC and MDA-MB-231 cell line upon the treatment of candidate drugs. Immunoprecipitation study and cell cycle determination were performed in the MDA-MB-231 cell line. Both drugs (K, KV) were not only anti-propagative but also reduced the targeted markers expressed in gene or protein levels of both experiment models, along with more strong effectiveness in KV treated panel than K. Moreover, our candidate drug increased G2/M-dependent cell cycle arrest and disrupted the interconnection of CD44 with NANOG also MDR1 in MDA-MB-231. In explant tissue of the primary breast tumour but not in adjacent normal tissue of the breast, both candidate drugs (K, KV) increased the expression of γH2AX protein. Thus, our candidate drugs are effective in attenuating BCSC survival.

Introduction

The chemo-resistance phenomenon has been closely associated with stem cell regeneration, a process that is not fully interpreted. The appearance of the earliest progress of chemo-resistance is specifically found in triple-negative breast cancers (TNBCs), the most heterogeneous and undifferentiated subset among breast cancer, characterized by the absence of estrogen receptor (ER), the progesterone receptor (PgR) and deficiency of overexpression/gene amplification of human epidermal growth factor receptor 2 (HER2) markers. Hence, treatment options of these targeting hormone receptors are very poor for TNBC patients **[Anders, Carey K, and Lisa A Carey. 2009]**. Moreover, chemo-resistance mechanisms are not only the entitlement of TNBC, but also the non-TNBC such as ER/PR+/HER2+, ER/PR-/HER2+ or ER/PR+/HER2- breast tumours developed chemo-resistance in long-term chemotherapeutic treatment **[Brandão, M et al. 2019]**.

In aggressive-metastatic breast tumours, the expression of several induced pluripotent stem cell markers/iPSC such as NANOG, SOX2, OCT4 are evidently up regulated to promote the stemness and drug resistance property, throughout a feed-back loop pathway **[Jeter, Collene R et al. 2015]**. One critical attribute of chemo-resistance is overexpression of P – glycoprotein (Pgp) protein, the product of the *MDR* genome **[Miletti-González, Karl E et al. 2005]**, that associated with the expression of stem cell markers to regulate chemo-resistance mechanisms. The previous study **[Chen, Y N et al. 1990]** in a human female breast cancer cell line, demonstrated that Verapamil, a calcium channel blocker, could be effective in blocking P-gp function **[McDevitt, Christopher A, and Richard Callaghan. 2007]**.

BCSCs are an individual niche of cancer stem cells in tumours that are slow-growing but contribute to the aggressiveness and chemo-resistance property of the resident tumour. Collective documents demonstrated that excluding iPSC markers, MDR1 and CD44 also promoted the proliferation of BCSCs **[Bourguignon, Lilly Y W et al. 2002]**. In this study, we revealed the capability of our candidate drug, Kaempferol alone or in combination with Verapamil in diminishing the survival rate of BCSC and the effect on the targeted markers maintaining chemo-resistance and stemness properties.

Kaempferol, a bio-flavonoid, show numerous pharmacological effects, as well as an anticancer effect **[Kim, Seung-Hee, and Kyung-Chul Choi. 2013]**. Earlier reports documented that Kaempferol, abundant in tea, grapes, berries, and cruciferous vegetables, play a role as an effective anti-tumour proliferative agent of BCSCs through the reduction

of EMT markers **[Liang, S-Q et al. 2015]**. We assumed that Kaempferol singly or in combination with Verapamil **[Callaghan, Richard et al. 2014]** could predictably diminish the progression of BCSCs.

To tackle the problem of chemotherapy resistance network in ex-vivo / in vitro model of breast cancer stem cells (BCSC), it was crucial to investigate the impact of our experimental medications on the viability of BCSC. Our current investigation unveiled that Kaempferol, either alone or in combination with Verapamil, diminished the RNA and protein expression of pluripotency markers (NANOG, SOX2, and OCT4) as well as MDR1 and CD44 in BCSCs, specifically in MDA-MB-231 cell line and primary cells derived from breast tumours. Moreover, the drug combinations disrupted the activation network of the CD44-NANOG-MDR1 feedback loop, revealing a potential mechanism by which the drug combination attenuates cell viability and impedes the acquisition of chemoresistance in BCSCs, highlighting their significant pharmacological significance.

Methods

Cell culture assay: The breast cancer cell line MDA-MB-231 enriched with stem cells (obtained from AddexBio; ATCC; Cat# CRL-12532, RRID: CVCL_0062) was obtained from the National Centre for Cell Science (NCCS) in Pune, Maharashtra, India. The MDA-MB-231 cells (Holliday, D. L et al., 2011) were seeded at 37°C in a humidified environment containing 5% CO_2, using DMEM/F-12 (Gibco) medium supplemented with 10% fetal bovine serum (FBS, Thermo Fisher Scientific, India), 5 µg/ml insulin (Himedia), 500 ng/ml hydrocortisone (Sigma-Aldrich), and 10 ng/ml EGF (Sigma, St. Louis, MO) **[Baker, Emma K et al. 2005].** The potentiality of the cultured cells was analyzed utilizing the Trypan Blue dye exclusion method with a conventional hemocytometer counting chamber, as earlier detailed **[Morten, Brianna C et al. 2016].**

Ex-vivo culture of tumour cells: The evaluation of patients with histopathologically verified primary breast tumours, who were taken in Neoadjuvant chemotherapy (NACT) treatment (Table 4), was picked as the cohort for this investigation.

Age (year)	Position of tumour (side)	Type	Grade	Tumour Size (cm.3)	TNM Status
1. 39	Left side	TNBC	3	17x15x6	$T_3N_0M_X$
2. 47	Right side	ER+/PR+/HER2-	4	12x10x4	$T_2N_xM_X$
3. 37	Left side	TNBC	3	16x15x6	$T_3N_1M_X$
4. 43	Right side	ER+/PR-/HER2-	2	17x17x5.3	$T_2N_2M_X$
5. 32	Left side	TNBC	3	7x6x5	$T_1N_2M_X$
6. 47	Left side	ER-/PR-/HER2+	4	17x17x7	$T_2N_3M_X$
7. 34	Left side	TNBC	3	17x16x10	$T_3N_2M_X$
8. 41	Left side	ER+/PR-/HER2+	4	16x13x4	$T_3N_0M_X$
9. 35	Right side	TNBC	4	14x12x3	$T_4N_0M_X$
10. 52	Right side	ER+/PR+/HER2+	4	16x16x4	$T_3N_1M_X$
11. 24	Right side	TNBC	3	13x10x5	$T_3N_1M_X$
12. 31	Right side	TNBC	4	16x16x5	$T_3N_2M_X$
13. 42	Right side	ER+/PR+/HER2-	2	20x18x4	$T_4N_2M_X$
14. 53	Left side	ER-/PR-/HER2+	3	14x13x4	$T_2N_0M_X$
15. 38	Right side	TNBC	4	19x18x6	$T_4N_0M_X$
16. 25	Right side	TNBC	3	14.5x13x4	$T_3N_1M_X$
17. 37	Right side	TNBC	3	13x13x8	$T_3N_0M_X$
18. 35	Left side	ER-/PR-/HER2+	4	11x9x5	$T_{4b}N_0M_X$
19. 39	Left side	TNBC	3	16x15x7	$T_3N_1M_X$
20. 40	Right side	ER+/PR-/HER2-	2	18x18x7	$T_2N_0M_X$
21. 35	Left side	TNBC	4	20x20x8	$T_4N_1M_X$
22. 36	Right side	TNBC	4	17x15x6	$T_4N_0M_X$
23. 48	Right side	ER+/PR+/HER2-	3	14x14x5	$T_2N_0M_X$
24. 69	Left side	ER+/PR+/HER2+	2	9x17x3	$T_2N_0M_X$

25. 50	Left side	ER+/PR-/HER2-	3	17x16x4.6	$T_3N_0M_X$
26. 39	Left side	TNBC	4	21x19.5x3	$T_4N_0M_X$
27. 57	Right side	TNBC	2	16x17x6	$T_2N_0M_X$
28. 63	Right side	TNBC	1	13x11x9	$T_1N_1M_X$
29. 45	Right side	TNBC	2	11x1.5x8	$T_2N_1M_X$
30. 55	Left side	TNBC	2	4x12x7.5	$T_2N_1M_X$
31. 37	Left side	ER+/PR+/HER2+	2	17.5x14x5	$T_4N_1M_X$
32. 70	Right side	TNBC	1	16x13x8	$T_2N_1M_X$
33. 30	Left side	TNBC	3	8x3.2x3	$T_2N_0M_X$
34. 36	Left side	ER+/PR-/HER2-	1	5.3x4x5	$T_2N_0M_X$

Table 4: TNBC patient characteristics including age, gender, race, and TNM status.

	TNBC	NON - TNBC
Age		
Early (≤40)	15	2
Late (≥ 40)	5	12
p-value	0.0012 *	
Grade		
High (III/IV)	15	8
Low (I/II)	5	6
p-value	0.4684	
Stage		
High (III/IV)	15	7
Low (I/II)	5	7
p-value	0.2562	

Table 5: Evaluation of TNBC and non-TNBC subtypes in relation to clinicopathological factors, including age, grade, and stage, using two-tailed Fisher's exact test with p-value ≤ 0.05.

A total of 34 primary tumour samples from female patients were incorporated into this study. Breast cancer patients with unknown subtypes, male breast cancer, and patients enlisted in clinical trials were left out. All involved patients submitted written consent for the utilization of tumour samples for research purposes, and the study was authorized by

the Ethics Committee of Netaji Subhash Chandra Bose Cancer Research Institutional Review Board (approval No. ECS/NCRI/08/2012). Freshly resected female primary tumour samples (n=34) were randomly collected from the hospital section of Netaji Subhas Chandra Bose Cancer Research Institute. Tumour margins were measured by a clinical pathologist as early designated, and tumours were categorized according to International Union against Cancer (UICC) and American Joint Committee on Cancer (AJCC) criteria. Tumour -node-metastasis (TNM) staging, as well as tumour subtype, were obtained from the pathologist (Table 4). The clinicopathological history of the patients is categorized in Table 5. All patient samples were obtained in sterile containers with 1X Phosphate-buffered saline (PBS). The tumour was minced into 1 mm pieces with a scalpel. The minced pieces were further treated with collagenase type IV and hyaluronidase solution (Sigma-Aldrich), and incubated at 37°C in a 5% CO2 incubator, to obtain a single-cell suspension. The digested tissue slurry was filtered through a 40μm sterile cell strainer, transferred to sterile conical tubes filled with PBS, and centrifuged at $700 \times g$ for 5 min. The supernatant was disposed of, and the pellet was resuspended with 0.25% trypsin/EDTA solution (Sigma-Aldrich), and Dispase/DNase solution (Himedia) in DMEM/F-12 medium with supplements, and kept at 37°C. After centrifugation at $700 \times g$ for 5 min, the pellet was resuspended in haemolysis buffer solution and incubated at 37°C for 5 minutes, centrifuged at $700 \times g$ for 5 min, and washed with PBS twice. The pellet was resuspended appropriately in DMEM/F-12 complete medium (DMEM/F-12 with 10% FBS, 5 μg/ml insulin, 500 ng/ml hydrocortisone, 10 ng/ml EGF, 1% penicillin/streptomycin (Sigma-Aldrich), 50μg/ml Gentamicin (Sigma-Aldrich), 2.5μg/ml Amphotericin B (Sigma-Aldrich) antibiotics), and cells were allowed to grow **[Jiao, Xuanmao et al. 2016].**

Analysis of the response of ex-vivo and in-vitro cell models to mono- and combination therapies: To investigate the impact of a combination of drugs on ex-vivo culture from tumour-derived cells and in-vitro culture with MDA-MB-231 cell line, the evaluation of combination index (CI) is a suitable technique to resolve the optimal dosage of each drug to achieve a synergistic effect, as earlier reported **[Zhao, Liang et al. 2004, Cao, Nuo et al. 2011].**

The efficient concentration (e.g., IC-50) of the drug-positive control Gemcitabine (G), as well as candidate drugs Kaempferol (K) and Verapamil (V), were analysed with established protocols of MTT (ABCAM) **[Arunasree, K M. 2010]** and XTT (ABCAM) **[Kuo, Po-Lin et al. 2005]** assays in MDA-MB-231 cell line and ex-vivo grown primary breast tumour cells, respectively. XTT assay was carried out for ex-vivo primary tumour-derived cells

(n=12). The mean value of each single drug, i.e., G, K, and V, was outlined in a two-dimensional coordinate plot, and the drug concentration that increased by 50% cell death (IC-50) was determined.

To investigate the combinational system, MTT/XTT study was carried out using different concentrations of Kaempferol along with a fixed concentration of Verapamil (5 µM). The nature of the interaction between the two drugs, Kaempferol and Verapamil, was evaluated using CI analysis, as previously described **[Ashton, John C. 2015, Chou, Ting-Chao. 2010].** Based on CI index calculations, for subsequent studies involving the combination of Kaempferol and Verapamil, both drugs were used at low concentrations (Kaempferol at 104.8 µM, corresponding to its IC-15 value, and Verapamil at 5 µM, corresponding to its IC-5 value) to induce synergism. Additionally, for Verapamil alone treatment, a dosage of 5 µM was utilized.

Impact of pH-modulating drugs on tumour sphere formation assay: MDA-MB-231 cell line and primary breast tumour cells (1000 cells/cm^2) were seeded in 6 well ultra-low attachment plates in serum-free non-adherent mammosphere culture media supplemented with B27 (Invitrogen), following established protocols **[Reynolds, C Patrick, and Barry J Maurer. 2005; Shaw, Frances L et al. 2012; Grimshaw, Matthew J et al. 2008].** Secondary mammospheres (2°) **[Rota, Lauren M et al. 2012]** were formed by disaggregating the primary mammospheres and culturing the same number of cells in new 6 well plates. For primary breast tumours (n=6), cells were allowed to grow for 14 days until visible mammospheres were formed. For both cell lines and ex vivo grown primary tumours, five sets of treatment groups were prepared, including untreated (U), Gemcitabine (G) treated, Kaempferol (K) treated, Verapamil (V) treated, and Kaempferol with Verapamil (KV) treated. For each group, experiments were performed in triplicates to enable statistical power analysis calculations under different treatment conditions, with a statistical significance value of p≤0.05. Drug treatments were carried out in 2° mammospheres using the appropriate concentrations, i.e., IC-20 for G (100 µM; as 50% cell death was not attained), IC-50 for K (224.51 µM), IC-5 for V (5 µM), and IC-50 for KV (K: 104.8 µM; V: 5 µM) as per CI index. The number of mammospheres was enumerated by two independent investigators who were blinded to the treatment conditions. The effectiveness of mammosphere formation under various treatment conditions (Mammosphere Forming Efficiency) was graphically represented. Drug resistance, metastasis, and cell-to-cell adhesion are known to be influenced by alterations

in tumour cell pH, which play a crucial role in regulating tumour sphere development **[Silva, Ariosto S et al. 2009]**.

Equation-1: Following drug treatment in 2° Mammospheres, the extracellular pH (pHe) was quantified using a method described by **[Prescott, D M et al. 1993]** and calculated using the following equation 2 **[Boyer, M J et al. 1993].**

$$pHe = pKa + \log\{(C_B - C_A) / (C_T - C_B)\}$$

where C_B represents the pH of the drug, C_A is the mean value of pH before drug treatment at the acidic endpoint observation, and C_T is the mean value of pH after drug treatment at the alkaline endpoint observation. The dissociation constant (pKa) values for Gemcitabine (G), Kaempferol (K), and Verapamil (V) were obtained from Drug Bank (1.89), **[Herrero-Martínez, José M et al. 2005]** (7.96), and **[Zhang, S et al. 1999]** (8.92), respectively. The pKa value for Kaempferol with Verapamil (KV) was calculated using a previous method described by **[Critchfield, F.E. and Johnson, J.B. 1959]**. Prior to each study, the electrodes were calibrated using buffered solutions with pH values of 6.0, 7.0, 8.0, and 11.0.

Flow cytometry study: Cell cycle analysis, based on the incorporation of Propidium Iodide into DNA, was conducted using the BD Cycletest™ Plus DNA Kit, following the manufacturer's instructions. MDA-MB-231 cell line, at a concentration of 1×10^5 cells per ml seeded overnight in a 25 cm^2 flask, was treated with candidate drug concentrations as described previously. Cell cycle distribution of nuclear DNA was analyzed by flow cytometry (BD Biosciences) using the analyzer and BD FACS Diva v8.0.1 software, as reported by **[Choi, Eun Jeong, and Woong Shick Ahn. 2008].**

Quantitative gene expression analysis: RNA extraction of candidate drug-treated cells in both cell line and ex-vivo cultured primary breast tumour cells (n=12) was performed using TRI Reagent® (Sigma-Aldrich) reagent, following the manufacturer's protocol. cDNA was synthesized from total RNA using the Verso cDNA Synthesis Kit (Thermo Fisher), as per the manufacturer's instructions. Semi-quantitative real-time PCR and RT-qPCR using Power SYBR Green master mix (Thermo Fisher) were conducted with gene-specific primers (Table 6).

Gene abbreviation	Transcription ID of Gene Bank	Location & Band	Pseudogene	Primers	Sequence	Annealing Temperature	Length of Primer
SOX2	ENSG00000181449	Chromosome 3: 181.71 – 181.71 Mb & 3q26.33	+	S	F: 5′ CAAGACGCTCATGAAGAAGGATAA -3' R: 5′- TCA TGC TGT AGC TGC CGT T -3'	52 °C	173bp
OCT4	ENSG00000204531	Chromosome 6: 31.16 – 31.18 Mb & 6p21.31	+	S	F: 5′- TCC CAG GAC ATC AAA GCT C -3' R: 5′- CAC TTC TGC AGC AAG G -3'	52 °C	215bp
NANOG	ENST00000526286.1	Chromosome12: 7.79 – 7.8 Mb &12p13.31	+	D	F: 5′- CCG GTC AAG AAA CAG AAG A -3' R: 5′- CTG CGT CAC ACC ATT GCT A -3'	53 °C	228bp
MDR1	ENSG00000085563	Chromosome 7:7.79 - 9.84 Mb & 7p21.12	-	D	F: 5′- AAGCTAACCCTTGTGATTTTGG -3' R: 5′- TTTCTTTTGTCCTCCAAATGCA -3'	50 °C	317bp
CD44	ENST00000278385.10	Chromosome 11: 35.14 – 35.23 Mb&11p13	-	S	F: 5′- CTGCAGGTATGGGTTCAT AG -3' R: 5′- ATATGTGTCATACTGGGAGGTA -3'	60 °C	124bp

| β - Actin | ENSG0000016 6710 | Chrom osome 15: 44.71 – 44.72 Mb& 15q21. 1 | - | S | F: 5′- ACCAACT GGGACGA TATGGAG AAGA -3' R: 5′- TACGACC AGAGGCA TACAGGG ACAA -3′ | 52 °C | 193bp |

Table 6: Primer design for gene expression analysis by reverse transcription PCR

PCR products were analyzed using 2.0% agarose gel electrophoresis. RT-qPCR amplifications were performed in triplicates for each gene, and the Ct values were calculated **[Ghadimi, B Michael et al. 2005].** The fold change in the expression of candidate genes was calculated after normalization with the corresponding Ct values of β-Actin, following an established protocol **[Silver, Nicholas et al. 2006].**

Fluorescence imaging and confocal microscopy analysis of candidate protein expression in ex vivo tumour explants subjected to drug treatment: To investigate the impact of drug treatment on the expression and co-localization of candidate genes, fresh primary breast tumour tissue explants (n = 8) were sectioned into approximately $2.5\times2.5\times2.5$ mm^3 size and cultured for 48 hours in DMEM/F-12 complete medium (DMEM/F-12 50/50 medium with 10% FBS, 1% penicillin/streptomycin (Sigma-Aldrich), 50 μg/ml Gentamicin (Sigma-Aldrich), 2.5 μg/ml Amphotericin B (Sigma-Aldrich)) in a 6-well dish, following the protocol by **[Karekla, Ellie et al. 2017]**. Different experimental drug treatments, as mentioned above, were applied during the 48-hour culture period. After the treatment, the explant specimens were embedded in paraffin blocks, and 5 μm sections were collected for immunofluorescence detection of candidate proteins using an established protocol (ABCAM).

Validation of protein expression and subcellular localization of SOX2, OCT4, NANOG, CD44, and MDR1 was conducted through immunofluorescence staining and confocal microscopy in MDA-MB-231 cells. Cells were seeded at a concentration of 1×10^4 per well in 6-well plates and treated with drugs when they reached 60% confluence. After 48 hours of drug treatment, immunocytochemistry was performed following an established protocol (ABCAM) as described by **Bockhorn, Jessica et al. 2013**.

67

For immunofluorescence experiments with the cell line, cells were fixed with 4% paraformaldehyde, permeabilized, and blocked. Primary antibodies against SOX2 (Abcam Cat# ab79351, RRID:AB_10710406), OCT4 (Thermo Fisher Scientific Cat# MA5-31458, RRID:AB_2787090), NANOG (Abcam Cat# ab109250, RRID:AB_10863442 and Santa Cruz Cat# sc-293121, RRID:AB_2665475), CD44 (Abcam Cat# ab51037, RRID:AB_868936), and MDR1 (Santa Cruz Cat# sc-13131, RRID:AB_626990) or Phospho-Histone H2AX (Ser139) or γH2AX (Cell Signaling Technology Cat#9718) were incubated at a 1:200 dilution overnight. Cells were then washed and treated with fluorescent-conjugated secondary antibodies (Alexa Fluor 488 conjugated Goat Anti-Rabbit IgG, Abcam Cat# ab97048, and Alexa Fluor 647 conjugated Goat Anti-Mouse IgG, Abcam Cat# ab150115), and mounted on slides with ProlongGold antifade reagent containing DAPI (Invitrogen). The slides were visualized using an Olympus Fluoview confocal microscope with a 60X objective.

Immunoblot and co-IP analyses to assess the expression and interaction of target proteins in response to experimental drug treatments: MDA-MB-231 cells at a seeding concentration of 1×10^5 cells/flask, upon treatment with different compounds in the aforementioned concentrations for 48hrs, were homogenised and protein concentrations of the different drug-treated cells were estimated using Bradford protein assay **[Bradford, M M. 1976].** 30μg of protein from each treatment group was loaded in each lane of a 12% SDS-PAGE gel and transferred to nitrocellulose membranes. The membranes were washed with TBS-T (5% milk in Tris-buffered saline-Tween 20), blocked with 5% skimmed milk and treated with specific primary antibodies (1:1000 dilution). TBST washed membranes were incubated with horseradish peroxidase-conjugated monoclonal secondary antibody (dilution: 1: 10,000; GeneTex Cat# GTX14122, RRID: AB_373069). The membranes were washed and after incubation with a chemiluminescence substrate, were visualized by ChemiDoc Imaging System.

For co-immunoprecipitation, MDA-MB-231 cells were plated in 100mm dishes and cultured in DMEM media supplemented with 1% antibiotic-antimycotic at 37°C in a CO_2 incubator with 5% CO_2. When the cells reached 70% confluency, they were subjected to overnight serum starvation. The next day, fresh media containing 2% FBS and 1mg/ml of hyaluronic acid were added, along with the following treatments: DMSO control, Kaempferol alone, and Kaempferol in combination with Verapamil. After 48 hours of treatment, the cells were harvested for co-immunoprecipitation (IP). Briefly, the cells were lysed using RIPA lysis buffer containing 1X PIC cocktail and centrifuged at 12,000 rpm

for 20 minutes at 4°C. The supernatant was collected in a fresh tube, and pre-clearing was performed using 20μl of BSA-blocked protein A/G beads for 1 hour at 4°C on a rotation platform at 6 rpm. After centrifugation at 1500 rpm for 5 minutes, the supernatant was collected in fresh 1.5ml Eppendorf tubes. Protein concentration was estimated using the Bradford protein assay, and 35μg of lysate was used for each co-immunoprecipitation (IP) and Isotype control IgG pair. Additionally, 5% input samples were prepared for each experiment, boiled with 5X SDS loading dye, and stored at -20°C until further use. For each co-immunoprecipitation (IP) and isotype control, 3μg of rabbit anti-CD44 antibody (Abcam Cat# ab51037) and 3μg of normal rabbit IgG were added to the lysates, respectively.

Tubes were subjected to overnight rotation at 6 revolutions per minute (r.p.m) at 4°C. The following day, 30μl of BSA-blocked protein A/G beads were added to each tube and rotated for 4 hours at 4°C. After centrifugation, the supernatant was discarded and the beads were washed thrice with RIPA lysis buffer containing 1X PIC. Subsequently, 40μl of 2X SDS dye was added to each tube and vortexed for 5 minutes at room temperature. Samples were then heated at 95°C for 5 minutes, followed by centrifugation at 12,000 rpm for 20 minutes at 4°C. Supernatants were collected in fresh tubes, and Western blotting was performed. Blots were probed with anti-mouse/rabbit CD44, anti-mouse NANOG and mouse anti-MDR1 antibodies (Santa Cruz Ca # sc-13131), followed by incubation with goat anti-mouse HRP (GeneTex Cat# GTX14122) conjugated secondary antibody (Sigma). Images were captured using the Biorad Chemidoc system **[Rust, Steven et al. 2013].**

Evaluation of the genotoxic effects of candidate drugs in primary breast tumour and normal tissue explants: To investigate the genotoxic impact of our candidate drug formulations in primary breast tumour and adjacent normal breast tissue, explant (n=4) cultures of breast tumour and adjacent normal tissues were exposed to our candidate drug systems as detailed previously, for 48 hours. The expression of phosphorylated H2AX on serine 139 (gamma-H2AX) was assessed through immunocytochemistry, following the protocol mentioned earlier.

Statistical study: One-way analysis of variance (ANOVA) using GraphPad Prism version 8 (GraphPad Prism, RRID:SCR_002798) was employed to determine the mean fluorescent intensity and Pearson correlation coefficient of immunofluorescence staining and confocal microscopic analyses. Two-way ANOVA, also using GraphPad Prism, was utilized to evaluate the percentage distribution of cells in the cell cycle. Student's t-test was employed

to determine the effect of treatment on mammosphere formation (diameter of mammospheres) and the significance of RNA and protein expressions in the five treatment groups, as well as in immunoprecipitation analysis. Fisher's exact test with two-tailed statistics was used to correlate different clinicopathological parameters with tumour subtypes. Two-way ANOVA was also used to quantify the normalized fold change of expression of candidate proteins with respect to untreated controls. A p-value of ≤ 0.05 was considered statistically significant for all statistical analyses, with a confidence level of 95%. It should be noted that all experiments were conducted without any significant loss of statistical power.

Results

Cytotoxicity assay: The cytotoxic study was analysed with a nonlinear regression to
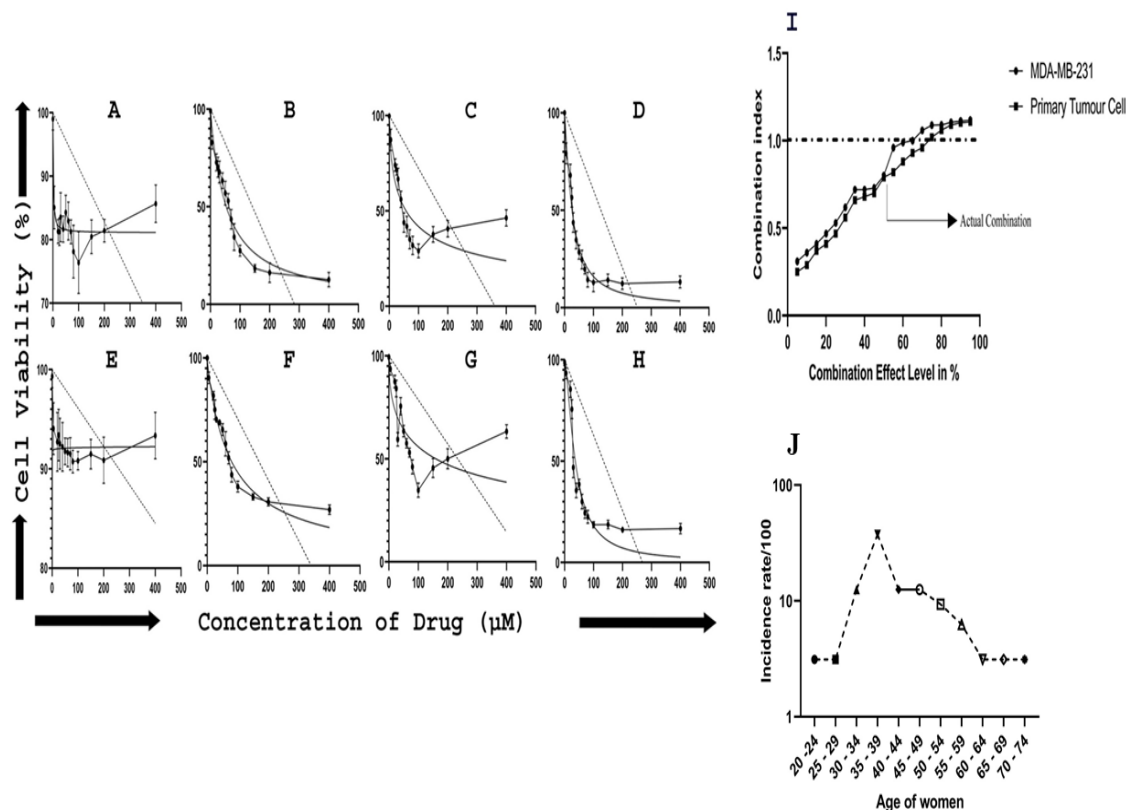
Figure 13: A nonlinear regression-based cell viability assay was performed in MDA-MB-231 and ex-vivo cultured primary breast tumour cells to evaluate the effect of candidate drugs. The drugs evaluated were Gemcitabine (A & E), Kaempferol (B & F), Verapamil (C & G), and the combination of Kaempferol with Verapamil (D & H). The IC-50 dose was calculated for each treatment condition in both cell types, and the data were analysed using both nonlinear (bar line) and linear (dot line) regressions. The mean values (dots) and ± SD (bars) were plotted, and the best-fitted regressed lines (nonlinear plots) were determined. Additionally, the combination index (CI) of Kaempferol with Verapamil was analysed in both MDA-MB-231 and primary tumour derived cells. CI values less than, equal to, or greater than 1 represent synergy, additivity, or antagonism, respectively. The dosages corresponding to a CI index of 0.7 for KV treatment were selected for further studies. Furthermore, an age-incidence curve of breast cancer (log-log plot) was generated using data from NCRI hospital (supplementary Table 4) (Fig. 13J).

achieve a more optimal fit curve (Fig. 13). We conducted MTT or XTT cell survival experiments using single drugs K and V in MDA-MB-231 cells and primary breast tumour -derived cells of BCSC, similarly. The nonlinear survival curves were observed in MDA-MB-231 cells (upper panel of Fig. 13; A-D) and primary tumour cells (lower panel of Fig.

71

13; E-H) when treated with single drug K and V, with IC-50 mean value approximately 224.51 µM, 170.6 µM respectively. Verapamil was included to inhibit the drug efflux pumps and not as an antiproliferative drug. The concentration of about 5 µM of V (IC-5) was utilized for single as well as for combination treatment. (Fig. 13 C, G). G treatment did not attain a 50% inhibitory effect, for comprehensive comparisons in our study, the quantity of G was utilized as 100 µM (≥20% inhibitory effect) (Fig. 13 A, E). For combinational system, Kaempferol was used at a much lower dosage (104.8µM in MDA-MB-231 and 109.9 µM in primary BCSC respectively, estimated corresponding to its IC-15 value) indicating the robust effectiveness in combination with Verapamil (5 µM, IC – 5 value). The CI index of the KV combination drug was analysed and the CI index value of the combination which displayed a 50% inhibitory effect, was 0.7 (Fig. 13 I) in together cell line and ex-vivo grown primary breast tumour cells.

Baseline features and clinical outcomes of individuals: This reflective study of BC patients (n=34) with a median follow-up of 36 months was taken for evaluation of adding gemcitabine as a positive control of the chemotherapeutic drug. In Figure 13J, the Breast cancer incidence ratio was raised with age through the reproductive with a median age of about 37.5 years and then a gradual increase after the age of 50 years (n=34). As per details of patients, the maximum number of patients had invasive breast carcinoma with nothing special type inflammatory breast cancer along with predomination grade 3/4 tumours (77 %). In Table 5, the outcome of clinicopathological correlations, displayed a significant correlation between the early age of onset and triple-negative breast cancer (TNBC) but the significant outcome between grade and stages was missing.

Mammosphere assay with drug-induced pH alterations: Mammosphere development from MDA-MB-231 (Fig. 14 A) cell line and primary breast tumour derived cell (figure 14D) was completed through the determination of Mammosphere Forming Efficacy (MFE) (Fig. 14 B, C and Figure 14 E, F). In the following model such as *in-vitro* grown MDA-MB-231 and ex-vivo grown primary tumours, the external acidic pH got neutralised and possibly blocked the uptake efficiency of weak-base chemotherapeutic agents, Gemcitabine, and developed drug resistance. The mean value of pH*e* in MDA-MB-231 and

primary tumour derived cells were determined from Mathematical expression (equation-1) and the value were, U: 6.7 ± 0.01, and 6.2 ± 0.01; G: 6.82 ± 0.01 and 6.5 ± 0.01; K: 11.8 ± 0.01 and 9.6 ± 0.01; V: 7.1 ± 0.01 and 5.3 ± 0.01; KV: 11.3 ± 0.01 and 10.62 ± 0.01 correspondingly
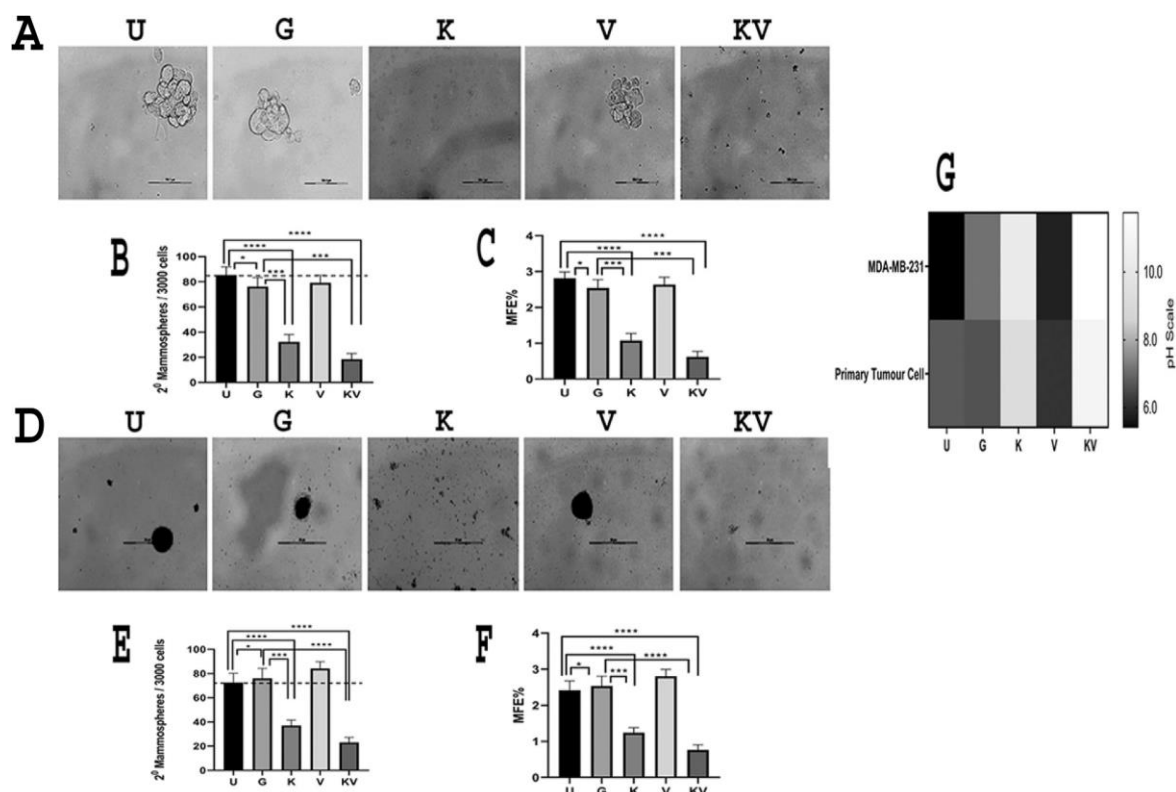
Figure 14: Mammosphere generation in MDA-MB-231 cells (A) and primary breast tumour cells (D) under different drug treatment conditions: U: untreated (Control), G: Gemcitabine, K: Kaempferol, V: Verapamil, KV: Kaempferol with Verapamil. The IC-50 dose resulting in a 50% inhibitory effect was calculated. The percentage of mammosphere and MFE was quantified concerning an inoculum of 3000 cells in the MDA-MB-231 cell line (B, C) and primary breast tumour-derived cells (E, F). Significance was analyzed using Student's t-test, where ***p < 0.01 and **** < 0.0001. The extracellular pH changes in the 2∘ mammosphere after drug treatment (48 h) were shown in the heat map in Fig. 2G, with the upper panel for MDA-MB-231 and the lower panel for primary tumour-derived cells. U: untreated (Control), G: Gemcitabine, K: Kaempferol, V: Verapamil, KV: Kaempferol with Verapamil.

(Fig. 14 G). Hence, the pH*e* was proposed as complicating factor for reducing the effectiveness of Gemcitabine however Kaempferol alone or coupled with Verapamil treatment had a significant impact in diminishing tumour sphere formation. The significant effect on diminishing tumour sphere formation upon the treatment of single Verapamil could not be observed.

Cell cycle assessment: Upon candidate drug treatments, the cell cycle experiment is MDA-
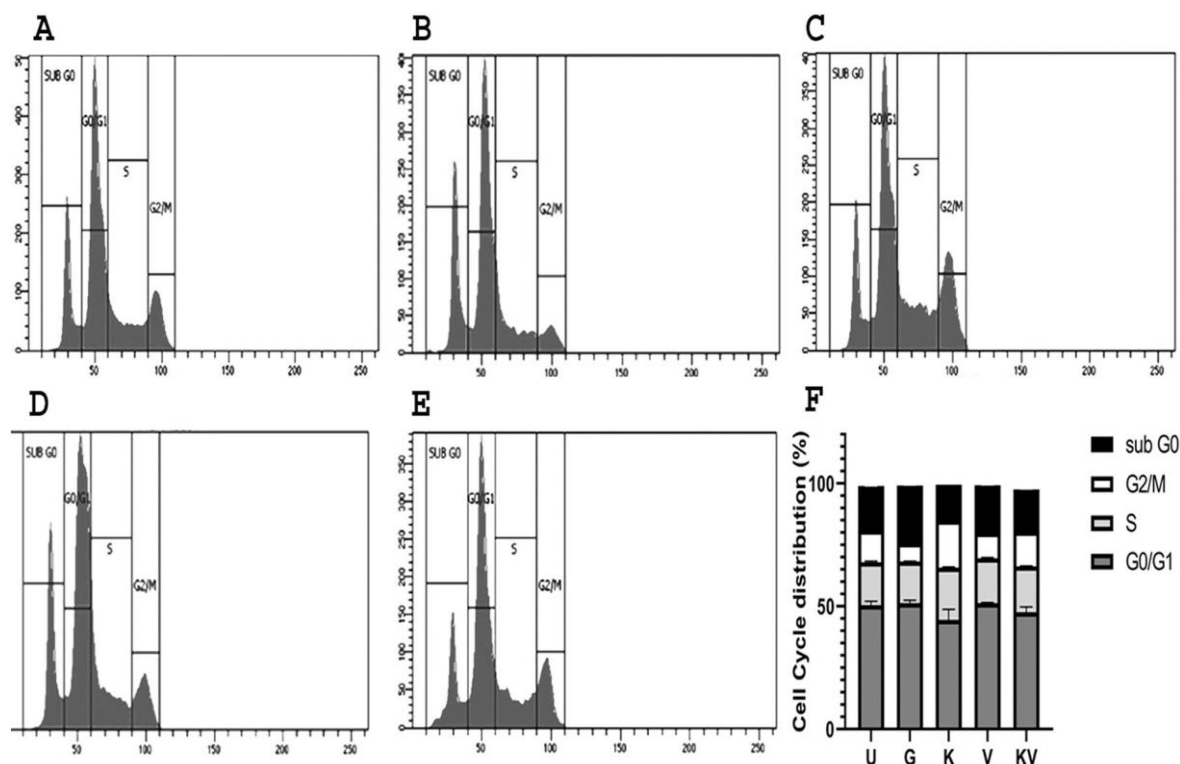
Figure 15: Cell cycle analysis was performed by staining cells with propidium iodide (PI) followed by flow cytometry. Asynchronized MDA-MB-231 cells were treated under different experimental conditions (48 h): A: Control; B: Gemcitabine; C: Kaempferol, D: Verapamil, E: Kaempferol with Verapamil. The relative distribution of total DNA in different phases of the cell cycle (G0/G1, S, G2/M) was determined and quantified. Statistical analysis was performed using two-way ANOVA, and the results showed that treatment with Kaempferol and Kaempferol with Verapamil resulted in significant G2/M cell cycle arrest compared to control (p-value ≤ 0.05).

MB-231 displayed that in Gemcitabine treatment, the apoptosis was induced (approximately 5%) evaluated to untreated cells as well as it had no inconsequential outcome on G0/G1, S or G2/M phase compared to the control (Fig. 15 A - F). The outcome of Kaempferol was increased by about 4% in the S phase and about 5% in the G2/M phase with associated reduction of G0/G1 phase population, signifying that K impedes both DNA replication along with the gateway of mitosis, influencing cell cycle arrest (Fig. 15 C). Kaempferol with Verapamil also exhibited synergism of increasing the S phase and G2/M phase (Fig. 15 E). In Gemcitabine and Verapamil single treatment, the cell cycle progression was not altered (Fig. 15 B and D). Cell cycle distribution demonstrated a

significant diminution of fold change in Kaempferol alone or in combination with the Verapamil treatment set.

The RNA expression of candidate genes in cultured breast tumour cells was attenuated by Kaempferol alone and in combination with Verapamil: Gene expression of *SOX2, OCT4, NANOG, MDR1, CD44* and housekeeping control marker *β-Actin* **[Livak,**
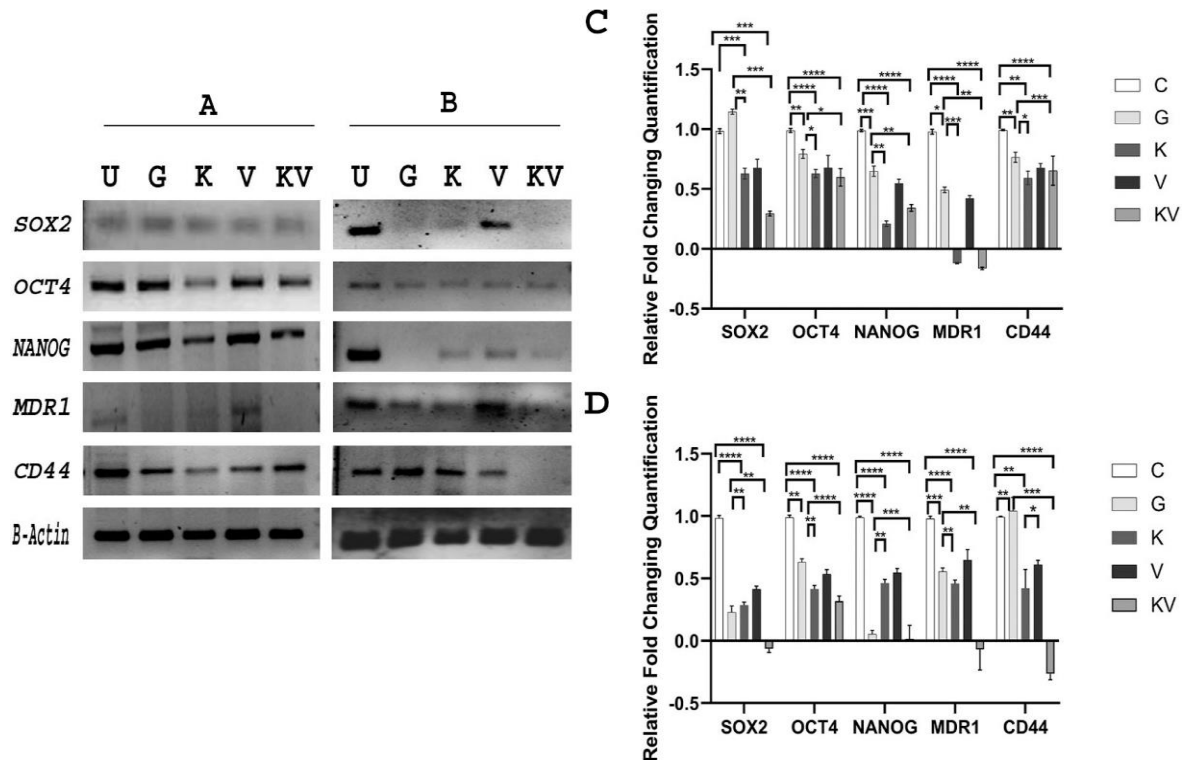
Figure 16: Semiquantitative (A, B) and quantitative real-time PCR (C, D) were used to assess the expression levels of candidate genes, including SOX2, NANOG1, OCT4, MDR1, and CD44, that are upregulated in breast cancer stem cell line MDA-MB-231 (A, C) and cultured primary breast cancer (B, D). The β-Actin gene was used as an endogenous control for both semiquantitative and quantitative real-time PCR. The different treatment groups in the semiquantitative PCR include U: untreated control, G: Gemcitabine, K: Kaempferol, V: Verapamil, and KV: Kaempferol with Verapamil. In the quantitative PCR, the bars indicate the relative fold change in gene expression normalized to the β-Actin gene and relative to the corresponding untreated cells. Statistical significance was determined using Student's t-test, where *p < 0.0332, **p < 0.0021, ***p < 0.0002, and ****p < 0.0001.

K J, and T D Schmittgen. 2001; Schmittgen, Thomas D, and Kenneth J Livak. 2008]; were quantitated through semi-RT-PCR and q-RT-PCR, upon candidate drug treatment in MDA-MB-231 and primary breast tumour cells. For MDA-MB-231 K and KV reduced the expression of *CD44, OCT4, NANOG* and *MDR1* although an insignificant outcome was shown in the expression of *SOX2* (Fig. 16A, C). In primary tumour-derived cells, KV

treatment displayed strong effectiveness than K treatment in the downregulation of *SOX2, OCT4, NANOG, MDR1* and *CD44* (Fig. 16B, D). It was observed that the expression of *CD44* was increased upon Gemcitabine treatment in ex-vivo has grown primary tumour s derived cells (Fig. 16 B, D). The relative fold change value of candidate genes displayed noticeable outcomes in K and KV treatment groups of together MDA-MB-231 and ex-vivo grown primary breast tumour-derived cells (Fig.16 B, D). The Independent t-test was utilized to analyse the quantifiable discrepancy in fold change of all treatment sets and the significant differences were represented in Fig 16.

Immunofluorescence examination of primary explant cultures: In primary tumour
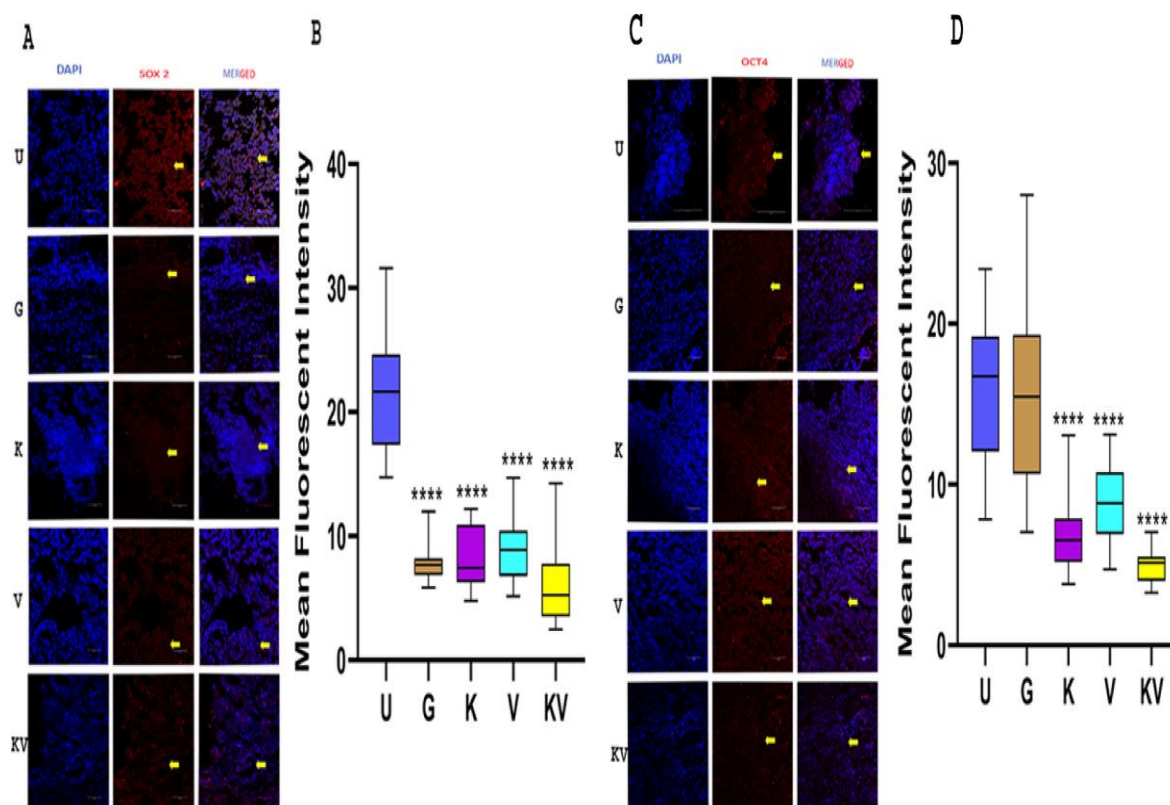
Figure 17: Fluorescence-based immunocytochemical localization of SOX2 (A) and OCT4 (C) proteins was performed in primary breast tumour cells subjected to different treatment conditions (48 h). The scale bar used was 10 µM. The various treatment groups examined were U: Control; G: Gemcitabine; K: Kaempferol; V: Verapamil; KV: Kaempferol with Verapamil. The mean fluorescent intensity of SOX2 (B) and OCT4 (D) was quantified and analysed for statistical significance using One-way ANOVA, where ***p < 0.0002 and ****p < 0.0001.
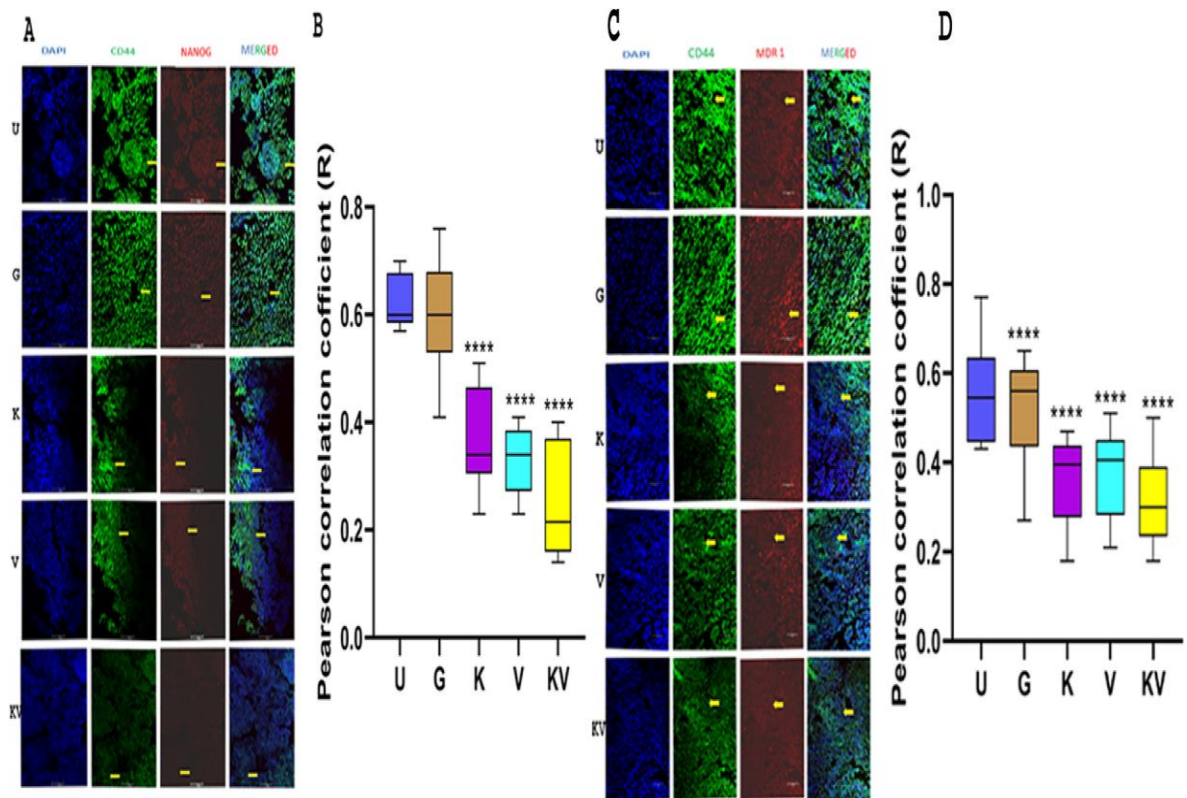
*Figure 18: The co-localization of CD44-NANOG (A) and CD44-MDR1 (C) was reduced under the treatment of Kaempferol (K) and Kaempferol with Verapamil (KV). The explant culture was imaged with a magnification of 20×, and the scale bar was 100 µM. The different treatment groups included: U: Control; G: Gemcitabine; K: Kaempferol; V: Verapamil; KV: Kaempferol with Verapamil. The Pearson correlation coefficient (R) of CD44 and NANOG co-localization was analyzed in Fig. B, and the correlation coefficient of CD44 and MDR1 co-localization was analyzed in Fig. D. One-way ANOVA was used for statistical analysis, and the significance level was set at ***p < 0.0002 and ****p < 0.0001.*

explant culture, expression of SOX2 and MFI analysis (Fig. 17 A, B) as well as OCT4 (Fig. 17 C, D) were decreased under K and KV treatment sets. The co-localizations of NANOG - CD44 (Fig. 18 A) as well as MDR1 - CD44 (Figure 18 C) were attenuated in K and KV treatment panels that determined an expected role in the treatment of breast cancer through interrupting CD44-NANOG-MDR1 associated pathway. Pearson's-correlation-coefficient (R) exhibited a significant diminution of co-localization of CD44-NANOG and CD44-MDR1 individually (Fig. 18B, 18D).

Immunocytochemical examination in the MDA-MB-231 cellular model: It was noticed that Kaempferol alone or in combination with Verapamil impeded the proliferation of tumour cells and reduced SOX2, OCT4, NANOG, MDR1 and CD44 expression, however

upon the individual treatment of Gemcitabine or Verapamil, no significant changes on the expression status of these markers were observed.
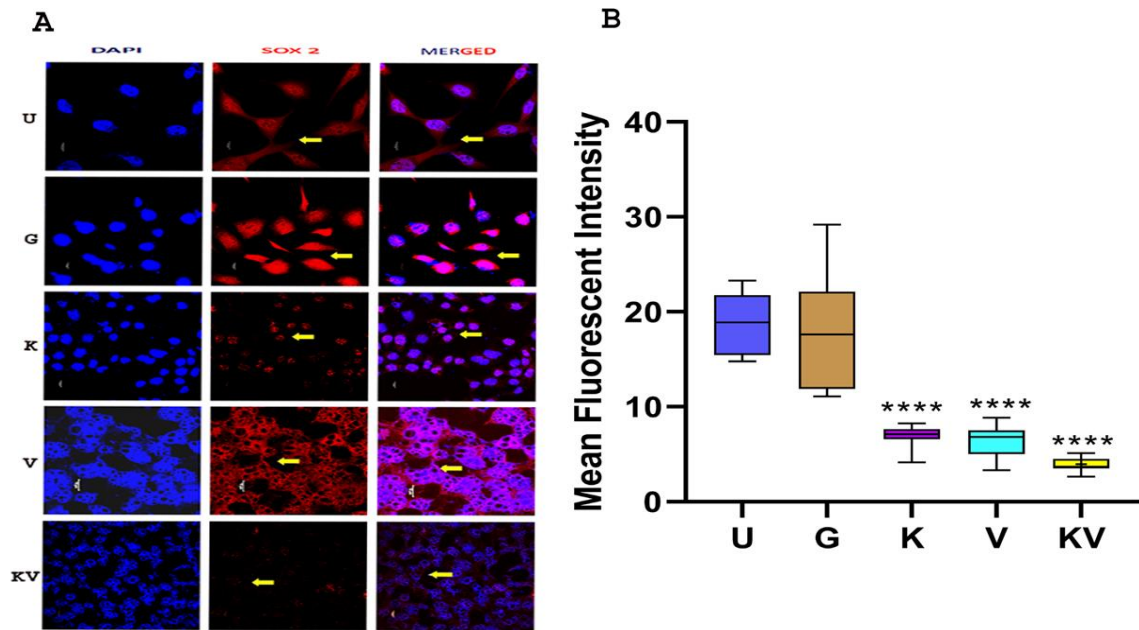
*Figure 19: Fluorescence-based immunocytochemical localization of SOX2 protein (A) was performed in MDA-MB-231 cell line under different treatment conditions (48 hours): U - control, G - Gemcitabine, K - Kaempferol, V - Verapamil, KV - Kaempferol with Verapamil. The scale bar for the images is 10 μm. Mean fluorescent intensity (F) of SOX2 protein (B) in MDA-MB-231 cells was analyzed. One-way ANOVA was employed to determine the statistical significance of the results, with ***p < 0.0002 and ****p < 0.0001 being considered significant.*
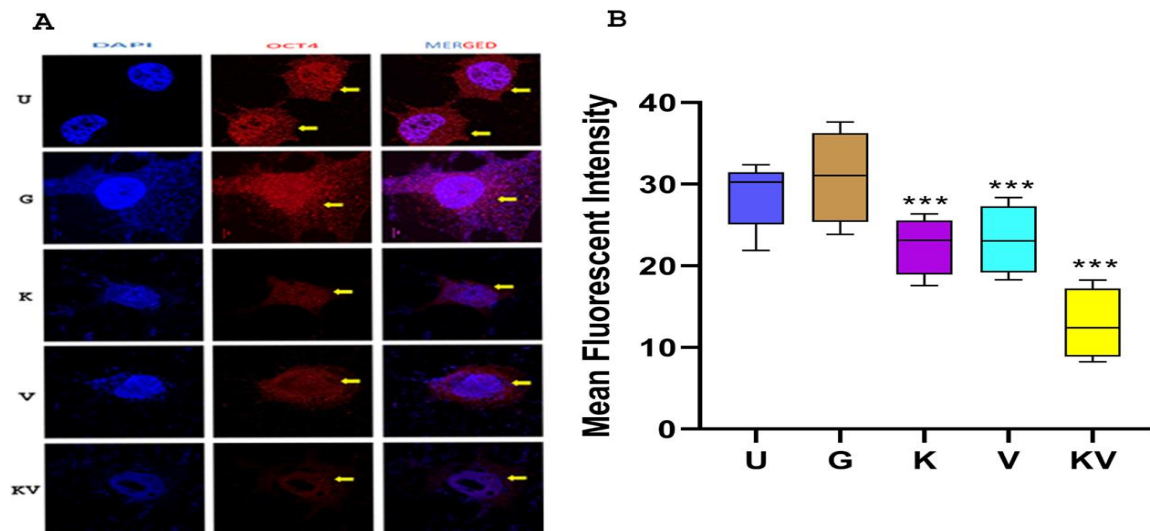
*Figure 20: Immunocytochemical analysis to localize the OCT4 protein in the MDA-MB-231 cell line under different treatment conditions (48hrs). The scale bar 10μM, and the treatment groups included U: Control, G: Gemcitabine, K: Kaempferol, V: Verapamil, KV: Kaempferol with Verapamil. The mean fluorescent intensity (F) of OCT4 was quantified in panel B. One-way ANOVA was employed to determine statistical significance, where ***p < 0.0002 and ****p < 0.0001.*
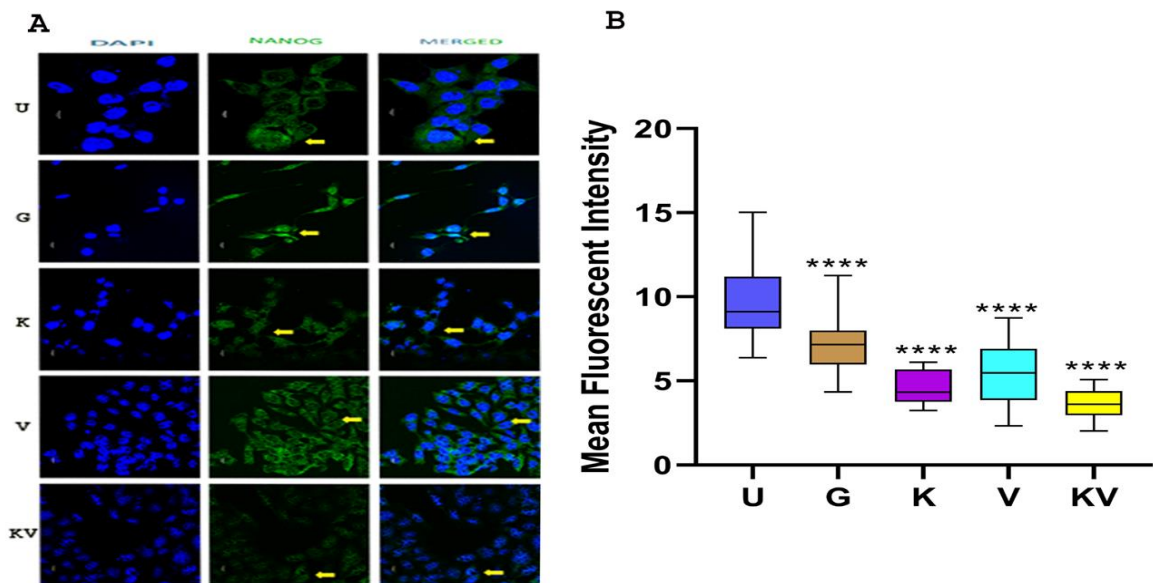
*Figure 21: Immunocytochemical mapping of NANOG (A) protein in MDA-MB-231 cell line was performed under diverse treatment (48hrs.) regimes. The treatments included U: Control, G: Gemcitabine, K: Kaempferol, V: Verapamil, and KV: Kaempferol with Verapamil. Mean fluorescent intensity (F) of NANOG (B) was determined and analyzed in MDA-MB-231 cells. Statistical significance was evaluated using One-way ANOVA, and the results indicated significant differences with ***p < 0.0002 and ****p < 0.0001.*
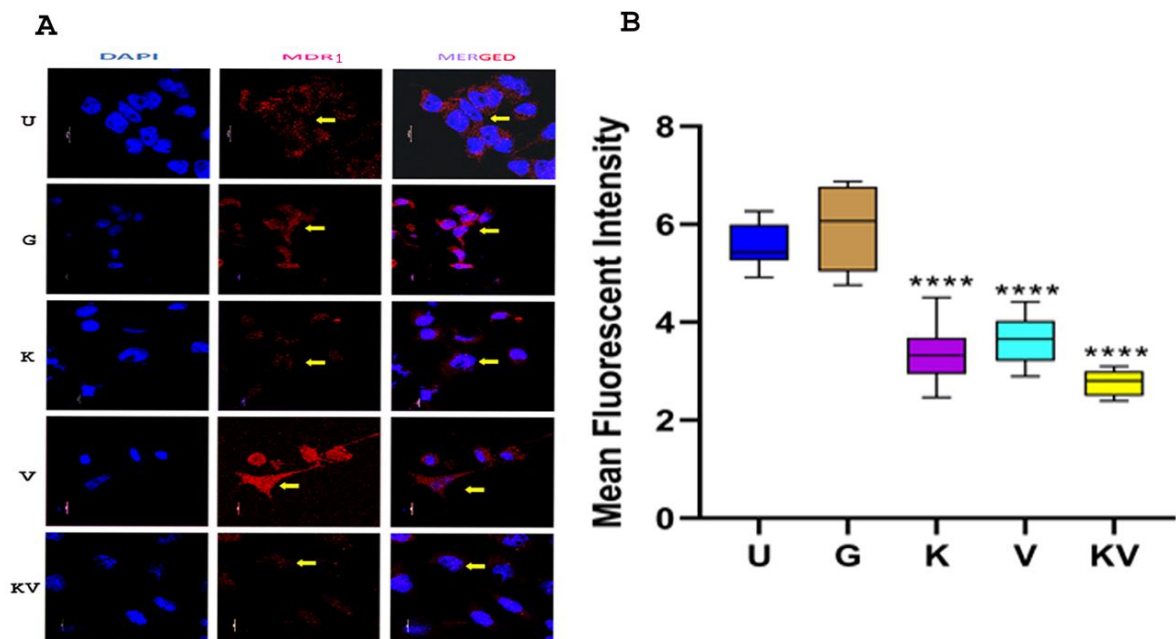
*Figure 22: Immunocytochemical localization of MDR1 (A), protein in MDA-MB-231 cell line in different treatment (48hrs.) conditions. Scale bar: 10μM. The different treatment groups included: U: Control; G: Gemcitabine; K: Kaempferol; V: Verapamil; KV: Kaempferol with Verapamil. Mean fluorescent intensity (F) of MDR1 (B), in MDA-MB-231 cells was analyzed. One-way ANOVA was used for statistical significance, where ***p < 0.0002 and ****p < 0.0001.*

79
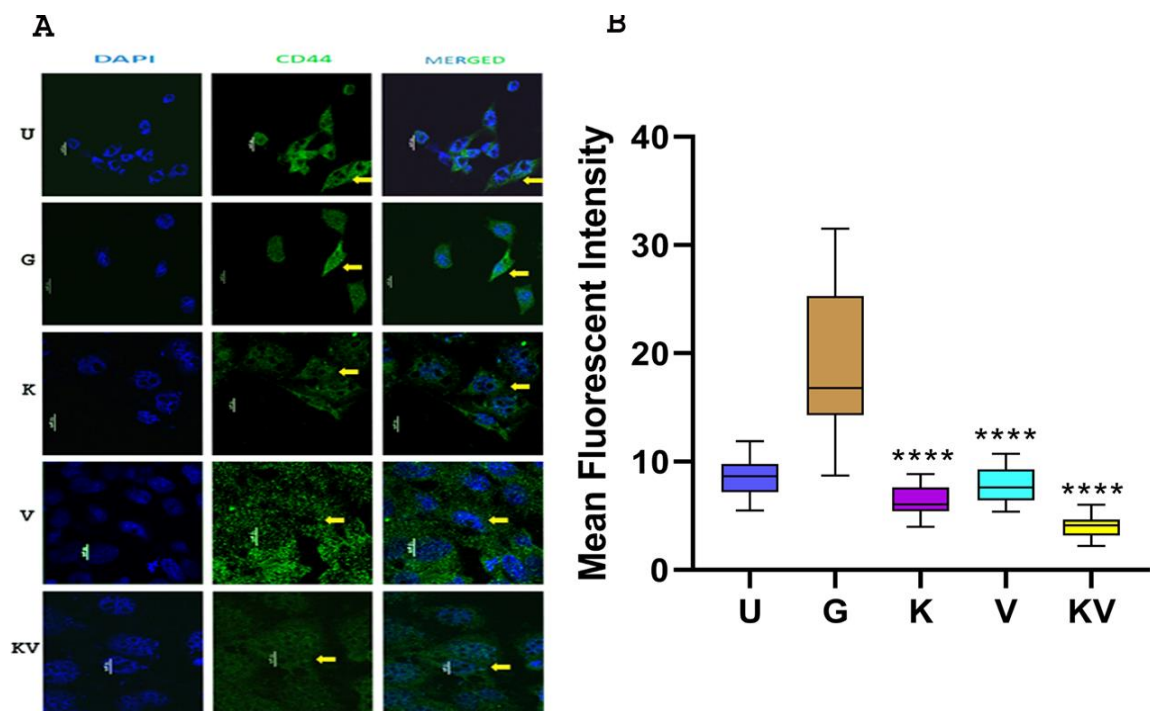
Figure 23: Immunocytochemical localization of CD44 (A), a transmembrane glycoprotein, in MDA-MB-231 breast cancer cell line was examined under different treatment (48hrs.) conditions. The scale bar used was 10µM. The different treatment groups applied were U: Control; G: Gemcitabine; K: Kaempferol; V: Verapamil; KV: Kaempferol in combination with Verapamil. Mean fluorescent intensity (F) of CD44 (B) was analyzed. Statistical analysis was performed using One way ANOVA, and the results were considered significant at ***p < 0.0002 or ****p< 0.0001

In MDA-MB-231 (Fig. 19A, 20A, 21A, 22A, 23A) was observed. Mean fluorescence intensity (MFI) value (Fig. 19B, 20B, 21B, 22B, 23B) displayed a significant reduction of candidate proteins expression in the K and KV treatment set. In the control set and individual treatment of Gemcitabine or Verapamil treatment set, the expression of candidate targeted markers was exhibited in both nuclear and cytoplasmic however in only Kaempferol treatment set and in Kaempferol with Verapamil treatment set, the expression of the candidate proteins were inadequate, marked with dots and disseminated cytoplasmic. Apart from the expression of the NANOG protein, Gemcitabine could not complete any significant fold change compared with the expression of other candidate proteins (Fig. 21B).

Fluorescence intensity (FI) was analysed through the application of ImageJ with a developed method, illustrated by Iinuma S, et al. **[Iinuma, S et al. 1994]**. The outcome of

mean FI (MFI) in each cell was evaluated from Five distinct zones and the context of FI in the cell-free area was excluded.

Immunoblotting and Immunoprecipitation assay: The single-use Kaempferol and combination with Verapamil decreased the expression of the targeted candidate iPSC protein marker such as SOX2, OCT4, NANOG, MDR1 or CD44 and determined from distinct western blot (Fig. 24 A) with individual densitometric
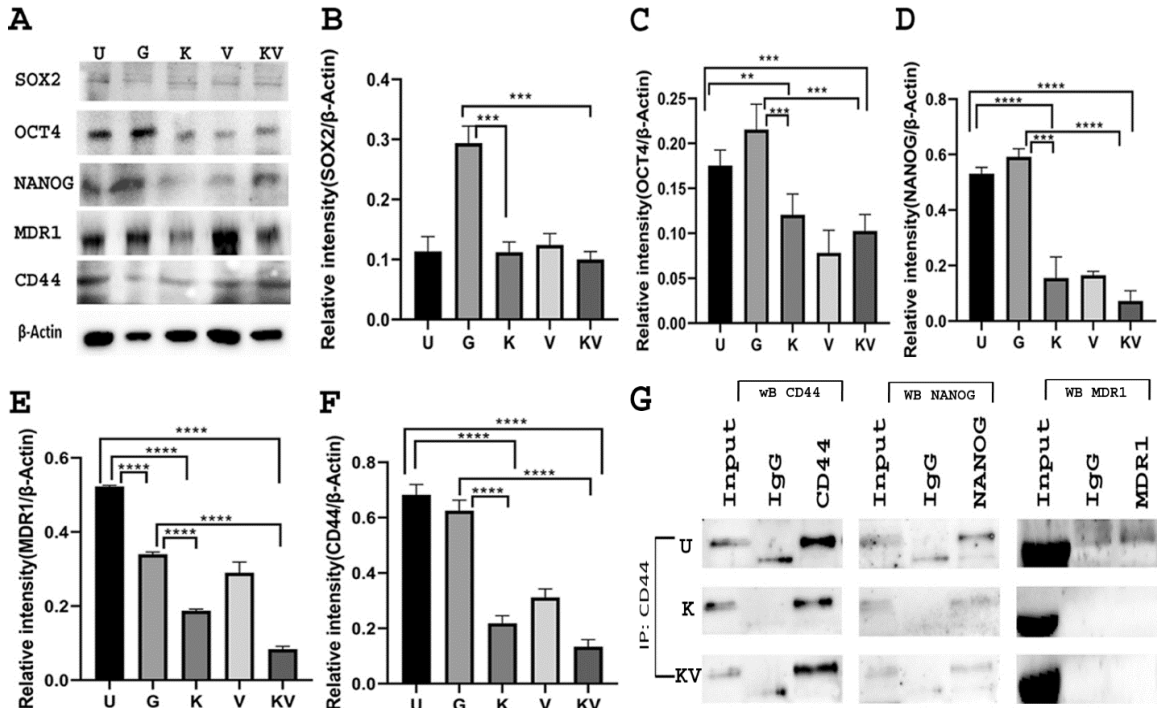
Figure 24: Western blot analysis was conducted to determine the fold change in the expression of candidate pluripotency markers in the MDA-MB-231 cell line under various treatment conditions (48 h) (A). The treatments included U: Control, G: Gemcitabine, K: Kaempferol, V: Verapamil, and KV: Kaempferol and Verapamil. The fold change in expression of candidate genes was normalized to the expression of β-Actin (B-F). Co-immunoprecipitation analysis was also performed in the MDA-MB-231 cell line (G) under different treatment conditions including untreated, K, and KV treatment, with CD44 serving as the bait. Results showed that in both K and KV treatment, the co-localization of NANOG with CD44 as well as MDR1 with CD44 was reduced. U: Control, K: Kaempferol, KV: Kaempferol and Verapamil. The co-immunoprecipitation data for each candidate protein was quantified and plotted after normalization with their corresponding untreated controls (Fig. 7H). The significance was correlated using Student's t-test and Two way ANOVA, where *p < 0.0332, **p < 0.0021, ***p < 0.0002, and ****p < 0.0001.

evaluation of the relative-fold-change-expression normalized to β-Actin expression **[Khan, Shafqat A et al. 2014]** (Fig. 24 B - F). Remarkably, Gemcitabine could not complete any reduction in the fold-changing expression of the targeted proteins with respect to control

(Fig. 24 B - F). The outcome revealed that Kaempferol alone or along with Verapamil increased significant downregulation of candidate proteins reportedly upregulated in breast cancer stem cells. Co-immunoprecipition using CD44 as bait showed that both K and KV diminished expression of CD44 as well as NANOG and MDR1, the interacting partners of CD44. NANOG -CD44 and MDR1- CD44 was impeded in K or KV treatment set (Fig. 24 G), implying disruption of the CD44 with NANOG and CD44 with MDR1 (Fig. 24 G) pathway. The outcome of two-way ANOVA displayed a significant diminution of fold changing in alone Kaempferol or a couple of Verapamil treatment set (Fig. 24 I).

Assessment of genotoxic impact of investigational drug regimens on explants of primary breast tumour and adjacent normal tissues: K increased the expression of
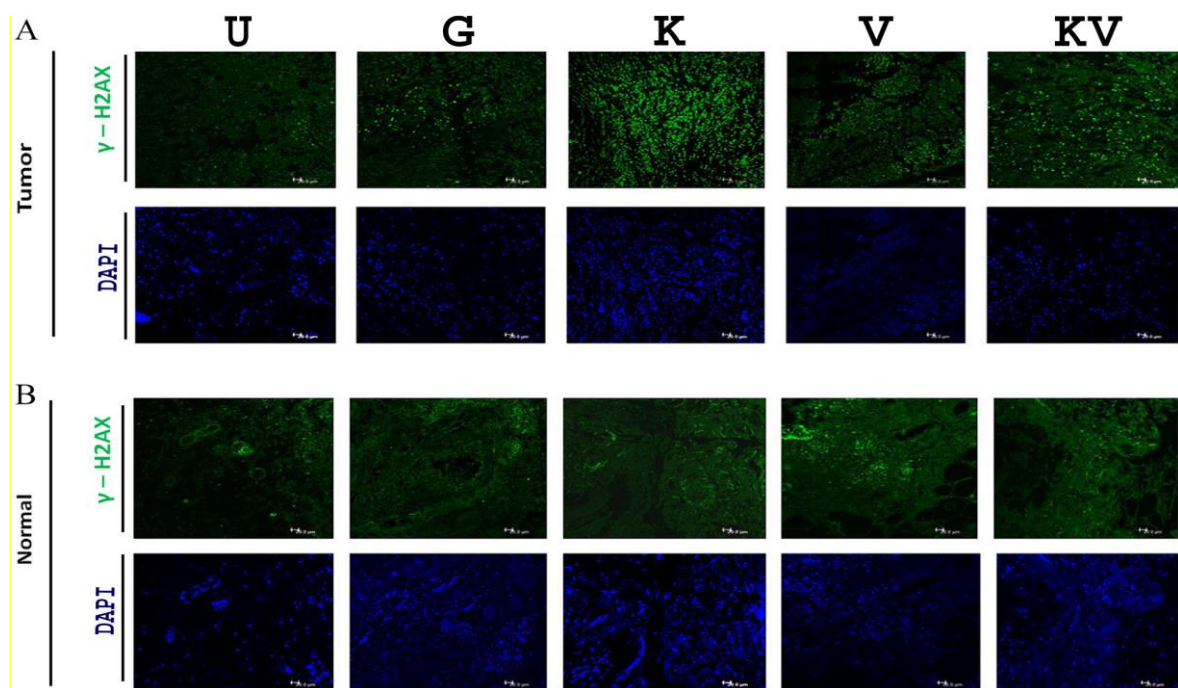
Figure 25: Measurement of genotoxicity induced by our candidate drug systems in primary breast tumours and their paired normal tissues (n=4), through immunofluorescence-based assessment of phosphorylated histone H2AX on serine 139 (gamma-H2AX) expression. Panel A illustrates gamma-H2AX expression in tumor explant cultures treated with different conditions including U: untreated; G: Gemcitabine; K: Kaempferol; V: Verapamil; KV: Kaempferol with Verapamil. Panel B depicts gamma-H2AX expression in adjacent normal tissue explants grown under similar treatment conditions. Our figure graphical abstract summarizes the molecular mechanisms of Kaempferol (K) and its combination with Verapamil (KV) with respect to Gemcitabine (G) in ex vivo/in vitro breast cancer, targeting the CD44-NANOG-MDR1 network.

γH2AX (Ser-139 phosphorylated H2AX) in primary tumour resulted in a significant increase in γH2AX expression in ex-vivo cultured adjacent breast normal tissues. (Fig. 25). This suggests that the administered dosages of our candidate drugs did not induce significant genotoxic effects in normal breast tissues, as evidenced by the lack of significant upregulation of γH2AX expression in ex-vivo cultured adjacent breast normal tissues.

Discussion

Chemo-resistance, a well-known attribute of cancer stem cells, is a multifaceted process that involves intricate pathways that are not yet comprehensively characterized. A previous study demonstrated that induced pluripotent stem cells (iPSCs) are abundantly displayed in aggressive and metastatic tumours. **[Cabarcas, Stephanie M et al. 2011].** Based on several corroborating data, we proposed that the iPSC markers could confer upon chemoresistance interrelated network utilizing a mechanism that implicates MDR1, CD44, NANOG, SOX2 and OCT4 markers.

Earlier investigations revealed that P-gp, an ATP-dependent transmembrane protein encoded by the MDR1 gene, is extensively expressed in cancer stem cells and plays a pivotal role in the efflux of chemotherapeutic agents **[Moitra, Karobi. 2015].** A previous study also documented that the upregulated MDR1 gene is associated with CD44 and NANOG markers **[Bourguignon, Lilly Y W et al. 2008]** in chemo-evasion pathway. Preliminary studies proposed a potential implication of Kaempferol in CSCs proliferation by reduction of the EMT marker expression **[Tièche, Colin Charles et al. 2019].** The impressive anti-cancer potential of Kaempferol, along with its minimal toxicity to normal cells, provides solid support for its application as a therapeutic agent **[Imran, Muhammad et al. 2019; Ren, Jie et al. 2019]**.

The present study was conducted to analyse the effect of Kaempferol on the expression of the candidate genes involved in perpetual stemness and chemoresistance. As Verapamil a blocking agent of ATP-based proton pump was shown to impede P-gp **[Lerner-Marmarosh, N et al. 1999; Welker, E et al. 1995]** and low dosage (5µM) of Verapamil was also subjected to Kaempferol, to displayed their effect on chemoresistance pathway, stemness and survival of breast cancer.

The evolution of mammospheres formation and its culture from MDA-MB-231 cell lines and primary breast tumours (NACT) derived cells remains an ongoing obstacle to several researchers **[Zhang, Fengchun et al. 2011]** nevertheless, it is a suitable model to determine the anticancer effect of candidate drugs and chemoresistance pathway. Tumour acidosis impart a selective role in the progression of cancer and resistance to treatment **[Gillies, Robert J et al. 2012]**. Acidic conditions of pHe promote the invasion and metastasis process of cancer cells by heterogeneous mechanisms **[Gatenby, R A et al. 2007]**, and also induce the generation of a cancer stem cell **phenotype [Martinez-Outschoorn, Ubaldo E et al. 2011]**. The acidic pHe enhanced the malignancy process by promoting OCT4, CD44

84

and NANOG markers expression expression [Hjelmeland, A B et al. 2011] and altered the human mesenchymal stem cells to tumour cells [Rattigan, Yanique I et al. 2012]. In our current exploration, the efficacy of our candidate drug-based system was significantly collated on disruption of tumour sphere formation associated with pH dependence in vitro or ex vivo model, regardless of tumour grade or volume and pH*e*.

To formulate the molecular cascade of Kaempferol enhancing response, the expression of *SOX2, OCT4, NANOG, MDR1, and CD44* genes was performed in the MDA-MB-231 cell line and primary tumour-derived mammosphere culture. Only Kaempferol or along with Verapamil displayed effectiveness in downregulating the expression of the targeted proteins markers in ex-vivo and in-vitro models, in contrast to which exhibited a minimal impact on BCSCs.

Our investigation uncovered that the expression of iPSC markers such as NANOG, SOX2, and OCT4 is increased in primary BCSCs. Also, the expression of NANOG, CD44 and MDR1 was persistently elevated in both the MDA-MB-231 cell line and tumour-derived cells. In the MDA-MB-231 cell line, the outcome of immunoblot results indicated the expression of SOX2 was minimal during the expression of NANOG, MDR1, CD44 and OCT4 were remarkable and utilizing the combination drug, the expression of targeted markers was decreased. In addition to Verapamil, the effectiveness of Kaempferol was even more effective as its IC-50 dosage was achieved at a significantly lower level. As a result of the incorporation of Verapamil, in our study, the KV combination was exhibited to be stronger than K, as exhibited through mammosphere formation, and relative fold change of candidate markers.

NANOG plays a role as a transcription factor, regulates the self-regeneration process and controls the pluripotency in embryonic stem cells, and has been demonstrated in numerous tumour cells [Chambers, Ian et al. 2003]. The activation of NANOG emerges in a feedback-loop mechanism in BCSC. In association with OCT4, NANOG maintained the transcription factor SOX2 for regulating the pluripotency of BCSCs. NANOG promoted the expression of SOX2 and OCT4, in turn, depends on upregulated CD44-MDR1 framework. The intrinsic mechanism of chemo-evasiveness by these factors is complicated. The candidate drug system revealed that the synergistic effect of the drugs was more impactful than only Kaempferol treatment, in diminishing the expression of the candidate proteins, as analysed through immunoblotting and immunoprecipitation. The outcome of the RT-PCR results documented that the anti-stemness effect of KV treatment

resulted in a diminution of expression of MDR1, CD44, NANOG, OCT4, and SOX2 markers.

Bourguignon and allied team revealed that the association of CD44 with extracellular Hyaluronic acid triggers CD44 and NANOG co-relation and correspondingly initiates the activation of MDR1 markers during tumour development process, and chemo-resistance in several carcinoma cells **[Bourguignon, Lilly Y W et al. 2002]**. Earlier studies have confirmed that the interaction between hyaluronic acid and CD44 promotes the binding of NANOG to CD44, which subsequently initiates the activation of proteins involved in regulating stem cell functions **[Chanmee, Theerawut et al. 2015]**. For the first time, the outcome of an immunoprecipitation experiment utilizing CD44 as bait displayed that only Kaempferol or in combination, with Verapamil, diminished Hyaluronic acid promoted CD44 upregulation and also CD44 induced transactivation and membrane translocation of NANOG as well as MDR1. This was confirmed in an observational report on the co-localization of CD44 with NANOG and CD44 with MDR1 in the primary breast tumour explant culture model, upon candidate drug treatment conditions.

The outcome of the immunocytochemical study exhibited that Kaempferol with Verapamil combination led to disruption of the cellular-cytoskeleton, and low localized expression of the candidate proteins viz. SOX2, OCT4, NANOG, MDR1 and CD44.

Moreover, we also validated that both K and KV increased G2/M phage cell cycle arrest in the MDA-MB-231 cell line, suggesting the effectiveness of our drug system in potentially causing DNA damage, which subsequently led to the activation of G2/M checkpoints. This was correspondingly confirmed in our presented study where we identified that only K and KV increased overexpression of γH2AX in primary breast tumour explant tissue but not in adjoining normal tissues of the breast. This study revealed that only K and KV with IC-50 dosage could be validated as drugs for therapeutic purposes.

The combination of Gemcitabine and Carboplatin is extensively utilized in NACT treatment for breast cancer patients in India, and we selected Gemcitabine as our control drug system. Previous research has demonstrated that the emergence of resistance to Gemcitabine therapy occurs in nearly all patients, possibly via the activation of CD44 **[Gillies, Robert J et al. 2012; Dorman, Stephanie N et al. 2016].** Based on the outcome of the present study, we assumed, Gemcitabine had a non-significant effect on did not show
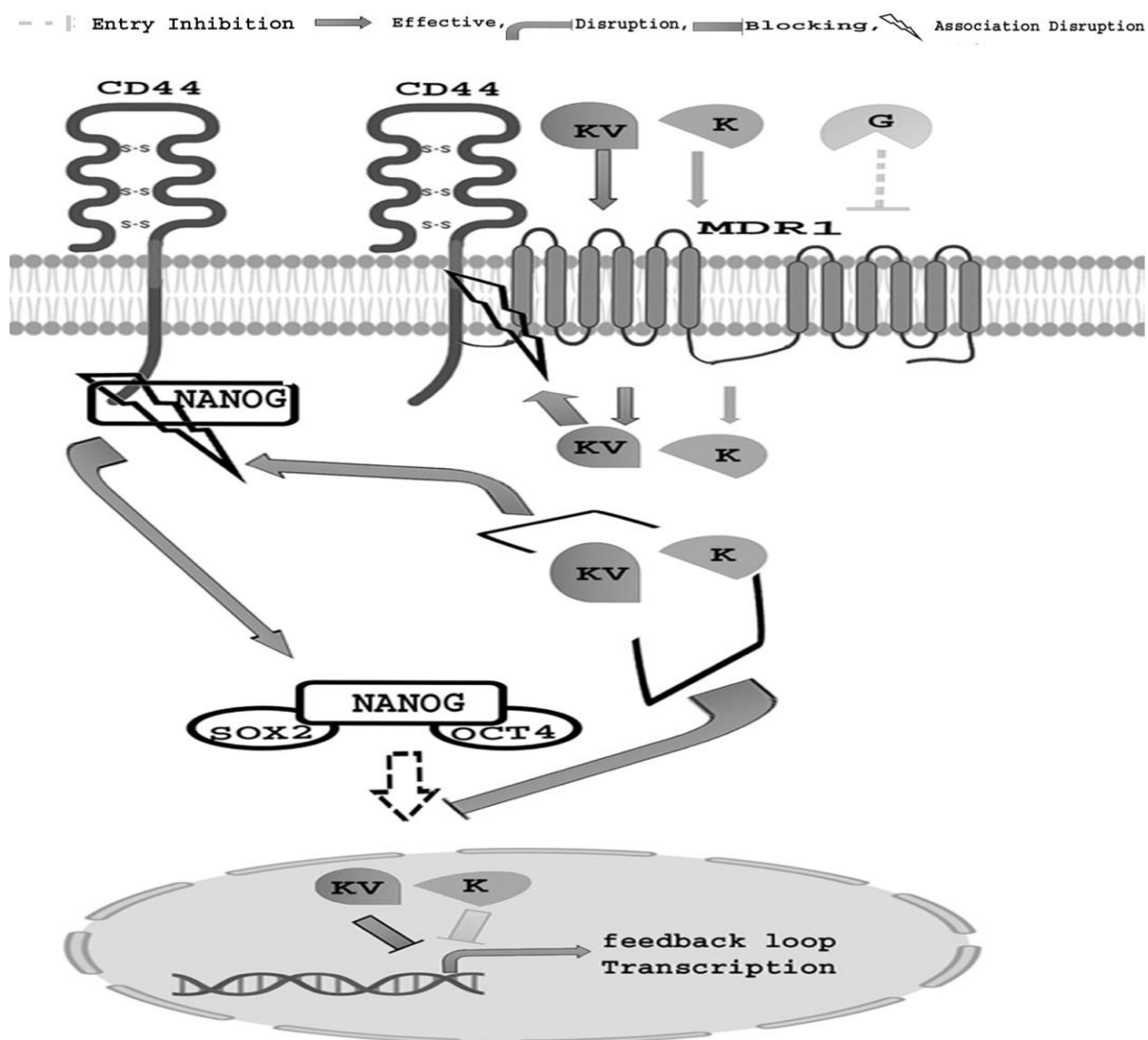
Figure 26: Kaempferol alone and Kaempferol with Verapamil targeting CD44-MDR1-NANOG network

any effectiveness as an anti-cancer drug. Our analysis demonstrated that our candidate drug system could mitigate Gemcitabine treatment failure breast tumour progression. Earlier report of **Barve, Avantika et al. 2009** exhibited that after IV administration of Kaempferol, the plasma concentration period was increased with a terminal half-life value of 3-4 hours while the oral administration displayed poor bio-availability (2%) due to their comprehensive and fast glucuronidation and other alterations in the gut and in the liver. Through intestinal-conjugation enzymes, the incorporated Kaempferol endures metabolic alteration to synthesize the glucuronides and sulfate-conjugates forms in the liver **[Yodogawa, Shinya et al. 2003]** and small intestine **[Crespy, Vanessa et al. 2003]**. Prior evidence documented that derivatization of Kaempferol could increase its effectiveness,

anywhere Kaempferol-3-O-α-arabino-furanoside was studied to be more robust than Kaempferol-3-O-rhamnoside in diminishing viability of diverse cancer cell lines **[Diantini, Ajeng et al. 2012]**. In our study, we utilized HPLC-purified Kaempferol (Sigma-Aldrich) and assume that derivatization of our candidate drugs for upcoming therapeutic application through the intravenous route would not only increase their bio-availability but improve their therapeutic potential for aggressive breast cancers. Pharmacodynamically, Kaempferol imparted an anti-proliferative effect by various mechanisms such as interference with TNF-α-induced mitogen-activated protein kinase (MAPK) activation **[Ren, Jie et al. 2019]**, activation of JAK/STAT3, PI3K/AKT and NF-κB etc **[Riahi-Chebbi, Ichrak et al. 2019]**. Kaempferol was also documented to downregulate DNMT3B expression, thus affecting DNA methylation patterns in bladder cancer **[Qiu, Wei et al. 2017]**.

Pharmacokinetics of Verapamil disclosed that the drug is almost 90.2% consumed when administrated orally, while its bioavailability is much lower (10-35%) due to its rapid metabolic process.

Remarkably, aside from its inhibiting influence on P-gP **[Welker, E et al. 1995]**, Verapamil also reduces intracellular GSH in cells by overexpressing MRP1, thereby imparting anti-proliferative outcome on tumour cells **[Lorendeau, Doriane et al. 2014]**. Thus, both K or KV drugs can decrease the proliferation rate of aggressive tumours. Moreover, our investigation demonstrated their synergistic outcome in impeding BCSC cell viability through inhibiting transcription. We endorse that to overcome the chemo-resistance pathway of cancer cells to Gemcitabine, our drug system is the best way to regulate the CD44 –NANOG-MDR1 (Fig. 26) in BCSCs.

Chapter 3

Title: **Synergistic ex vivo and in silico anti-cancerous efficacy of Kaempferol with Verapamil targeting lysosome-Ca2+-TFEB pathway under low glucose: a panoramic interference with chemo-evasion, tumour stemness & acidosis, through ROS mediated autophagy induced cell death**

Background

Reactive-oxygen species (ROS) at Low levels increased cell survival by lysosome-triggered autophagy induction. Glucose stress stimulated acidosis, hypoxia, and ROS, and also upregulated the expression of markers associated with stemness of cancer and multi-drug resistance. Moreover, the upregulation of lysosome is speculated to be one of the critical points for the proliferation of cells under ROS-stimulated stress. Reports documented that, the induction of the Lysosome-TFEB-Ca2+ network has led a vital role in the induction of chemoresistance and survival of cancerous cells. Based on our earlier findings as well as previous studies, we hypothesized, our drug combination would effectively downregulate the chemo-evasion markers that regulate tumour stemness or acidosis process, hypoxia, drug efflux or lysosome-TFEB-Ca2+ network. Expression levels of targeted genes and proteins, as well as measurements of ROS production and calcium ion (Ca2+) concentrations, were quantified in ex vivo models subjected to modified glucose conditions followed by the treatment with KV. Furthermore, computational strategies were employed to propose the mechanism of action of the drug combination. RT-PCR, IHC/ICC, immunoblotting and molecular docking methods were applied in this investigation. The over-production of ROS through our candidate drugs, KV, reduced the chemo-resistance, and tumour-acidosis markers in addition to ATP1B1 that reduced lysosomal dysfunction with diminution of Ca2+ ion release through downregulation of TFEB expression under low-glucose condition. An aberrant result was identified in high-glucose conditions. We also detected KV increased the over-production of ROS hence promoting autophagy-dependent cell death by increasing the expression of LC-3-II and p-62 in low-glucose conditions. The ex-vivo experiment was also validated with in-silico experiments that showed similar finding. Our ex vivo or in silico experiments unveiled that our drug combination KV, could efficiently attenuated multiple network-controlling chemo-resistance, that were not previously investigated using the same experimental design and thus may be recommended for therapeutic applications.

Introduction

Reactive oxygen species (ROS) are evaluated as a crucial predictor not only of the onset of cancer but also of its advancement and apoptosis, thereby serving a dual function in the survival of malignant cells **[Zhang, Xiaoli et al. 2016]**. Initial research has pinpointed that upon exposure to oxidative stress, lysosomes activate and upregulate TFEB which upon nuclear translocation, along with the subsequent release of calcium ions (Ca2+), that enhanced autophagy, ultimately helps cellular survival by scavenging extracellular ROS **[Zhang, Xiaoli et al. 2016]**. Numerous cancer treatments, therefore, aim to enhance ROS production, although their precise cellular fate and underlying mechanism of action remain to be investigated.

In our prior investigation, we detected a potent anti-proliferative effect of a drug combination of Kaempferol and Verapamil (KV) against breast cancer (BC) stem cells **[Nandi, Sourav Kumar et al. 2022]**. Drawing on previous research that established Verapamil's effectiveness in expelling intracellular reduced Glutathione **[Lorendeau, Doriane et al. 2017]**, we postulated that the KV drug combination may interfere with the signalling cascades that inhibit proliferation and chemoresistance in breast cancer by promoting elevated ROS production.

Tumour cells are known to be capable of surviving in moderate levels of ROS as compared to normal cells due to the upregulation of hypoxia-inducible factor 1-alpha (HIF1α) **[Jung, Seung-Nam et al. 2008].** HIF1α, in turn, contributes to the over-expression of Na+/H+ exchanger 1 (NHE1), a type of membrane protein that regulates the pH balance of the extracellular environment in tumours **[Holthouser, Kristine A et al. 2010; Stock, Christian, and Stine Falsig Pedersen. 2017].** NHE1 upregulation co-operatively increased Na+/K+ ATPase (Gene name, ATP1B1) markers expression, the key controller that maintains the overall cellular membrane potential **[Holthouser, Kristine A et al. 2010]**. In normal cells, HIF1α controls the expression of sodium-potassium-ATPase, through Von-Hippel-Lindau protein (VHLp) **[Zhou, Qiao et al. 2008]**, in cancer cells, due to the ROS induced stabilization of HIF1α, as well as inactivation of VHLp, this process is perturbed. This perturbation of homeostasis leads to a favourable outcome for tumour progression. Moreover, hypoxic conditions were found to increase HIF1-α levels and promote the transcription of several key markers, including certain membrane proteins involved in glucose transport (GLUTs) **[Calvert, John W et al. 2006]**. Hence, an optimal level of ROS sustains a conducive intracellular environment for facilitating neoplastic

proliferation and chemoresistance [**Liou, Geou-Yarh, and Peter Storz. 2010**]. However, excessive and disproportionate production of ROS can be deleterious to cancer cells and result in their death. During the process of malignant transformation, cells increase the expression of their normal glucose transport system to promote their invasive capacity [**Calvert, John W et al. 2006**]. However, the mechanism of glucose uptake upregulation was not well explained in the context of drug cytotoxicity studies, as high glucose levels alone can stimulate proliferation pathways in cancer cells [**Nandi, Sourav Kumar et al. 2022**].

In general, we revealed the efficacy of KV under low or high glucose stress, on the expression of targeted markers viz. HIF1α, GLUT2, NANOG, MDR1, CD44, ATP1B1, and NHE1 regulated tumour acidosis phenomenon, hypoxia and chemo-evasion. We elucidated that, KV impedes with lysosome-Ca2+-TFEB network-associated chemo-resistance through autophagy and autophagy-induced cell death. We also simulated a molecular model of the interactome of these candidate genes that are expressed under glucose stress, in the presence of our candidate drug KV. Our data showed that our candidate drug system KV had robust antiproliferative efficacy through downregulation of the aforementioned candidate genes regulating tumour acidosis, hypoxia and chemoevasion, perturbation of lysosome-Ca2+-TFEB mediated autophagic survival and upregulation of cell death under low glucose condition, indicating the therapeutic potential of the candidate drug combination under low glucose condition. The novelty of this unique study is the surprising result that a synergistic combination of Kaempferol (anti-cancerous concentration) and Verapamil (adjunct dosage) in the chosen concentration inhibits cancerous cells through a complex signalling pathway under low glucose, downregulating all these markers of chemoresistance and indirectly through increasing ROS production, finally leading to autophagy induced cell death, unlike several other class of inhibitors which act by decreasing the ROS level or reducing overall oxidative stress of the cellular environment.

Materials and methods

Materials: All chemical compounds were procured from Sigma Aldrich (located in St. Louis, Missouri, United States), with the exception of tris-Cl obtained from Himedia and sodium dodecyl sulfate obtained from Merck India. All essential components required for the culture of tumour cells and breast cancer cell lines were obtained from Gibco, a division of Thermo Fisher Scientific in the United States. The BC cell lines, including MDA-MB-231 and MCF-7, were sourced from NCCS in Pune and are reported to have a validated STR profile as per ATCC guidelines.

Tumour collection: Thirty-eight (n=38) primary breast tumour s were collected from the hospital wing of NCRI (Netaji Subhas Chandra Bose Cancer Research Institute), and their respective subtypes were confirmed through immunohistochemistry (IHC) analysis (Table 7). Additionally, normal tissues from these patients were also collected for this study. Tumour boundaries were identified by an onco-pathologist and classified according to internationally recognized guidelines, such as UICC (International Union Against Cancer) and AJCC (American Joint Committee on Cancer). Patients with unknown types of breast cancer, male breast cancer patients, and those with clinical trial-related breast cancer were excluded from this study.

S.N	Type	Grade	Tumour Size (cm.^{3})	TNM Status
1.	TNBC	3	16x15x6	$T_3N_0M_X$
2.	TNBC	4	12x10x4	$T_2N_xM_X$
3.	TNBC	3	16x15x6	$T_3N_1M_X$
4.	TNBC	2	17x12x5.3	$T_2N_2M_X$
5.	TNBC	3	7x1.6x5	$T_1N_2M_X$
6.	ER-/PR-/HER2+	4	17x11x7	$T_2N_3M_X$
7.	TNBC	3	17x16x2	$T_3N_2M_X$
8.	TNBC	4	16x13x4	$T_3N_0M_X$
9.	TNBC	4	14x12x3	$T_4N_0M_X$
10.	TNBC	4	16x16x4	$T_3N_1M_X$
11.	TNBC	3	13x10x5	$T_3N_1M_X$
12.	TNBC	4	16x16x5	$T_3N_2M_X$
13.	ER+/PR+/HER2-	2	20x18x4	$T_4N_2M_X$
14.	ER-/PR-/HER2+	3	14x13x4	$T_2N_0M_X$
15.	TNBC	4	19x18x6	$T_4N_0M_X$
16.	TNBC	3	14.5x13x4	$T_3N_1M_X$
17.	TNBC	3	13x13x8	$T_3N_0M_X$
18.	TNBC	4	11x9x5	$T_{4b}N_0M_X$
19.	TNBC	3	16x15x7	$T_3N_1M_X$
20.	TNBC	2	18x18x7	$T_2N_0M_X$
21.	TNBC	4	20x20x8	$T_4N_1M_X$
22.	TNBC	4	17x15x6	$T_4N_0M_X$

23.	ER+/PR+/HER2-	3	14x14x5	$T_2N_0M_X$
24.	ER+/PR+/HER2+	2	9x17x3	$T_2N_0M_X$
25.	TNBC	3	17x16x4.6	$T_3N_0M_X$
26.	TNBC	4	21x19.5x3	$T_4N_0M_X$
27.	TNBC	2	16x17x6	$T_2N_0M_X$
28.	TNBC	1	13x11x9	$T_1N_1M_X$
29.	TNBC	2	11x1.5x8	$T_2N_1M_X$
30.	TNBC	2	4x12x7.5	$T_2N_1M_X$
31.	TNBC	2	17.5x14x5	$T_4N_1M_X$
32.	TNBC	1	16x13x8	$T_2N_1M_X$
33.	TNBC	3	8x3.2x3	$T_2N_0M_X$
34.	ER+/PR-/HER2-	1	5.3x4x5	$T_2N_0M_X$
35.	TNBC	3	12.5x11x1.2	$T_3N_1M_X$
36.	TNBC	2	7.5x10x3	$T_2N_0M_X$
37.	TNBC	3	8.5x9x1.55	$T_2N_1M_X$
38.	TNBC	3	13.5x8x4.5	$T_2N_2M_X$

Table 7: Data providing additional details regarding the medical history of patients with triple negative breast cancer (TNBC), including the status of the tumour, lymph node involvement, and metastasis according to the TNM classification system.

All patients included in this study provided a signed consent form for the use of their tumour samples in research investigations, and the research proposal was approved by the Ethics Committee of the Netaji Subhash Chandra Bose Cancer Research Institutional Review Board (EC approval No. ECS/NCRI/08/2012, with extended approval under EC/NSCBCRI/01/2021).

Cell culture assay: The BC cell lines MDA-MB-231 (TNBC cell line) and MCF-7 were cultured afresh using l-DMEM (Catalogue No: 11054001, Gibco) and h-DMEM (Catalogue No: 11960592, Gibco), supplemented with appropriate additives, in a humidified 5% CO_2 chamber. Both cell lines were sustained in l-DMEM or h-DMEM media until to achieve 80% confluence and treatment with the combination of Kaempferol along with Verapamil (KV) that earlier had shown 50% inhibitory effect (K: 104.81 μM; V: 5 μM for MDA-MB-231 and K: 103.15 μM, V: 5μM in MCF-7 based on CI-index) in following l-DMEM or h-DMEM panel, in line with our previous investigation **[Nandi, Sourav Kumar et al. 2022]** in cell line model. In ex vivo experiments (primary tumour drive cell culture) we utilized the synergistic concentration at IC-50 dose of K (109.9 μM) and Verapamil at IC-5 value (5 μM) where prior experiments showed the lowest rates of survival outcome (about 5%) **[Nandi, Sourav Kumar et al. 2022]** and conducted a new cytotoxicity assay with TNBC patient samples and documented the outcome again (Fig. 27). Gemcitabine (G) was included as a positive experimental control at 101 μM

concentration, whereas 50% cell death was not found. In our experiment, we labelled the candidate drug-treated panel for l-DMEM as LC (low glucose control), LG (low glucose
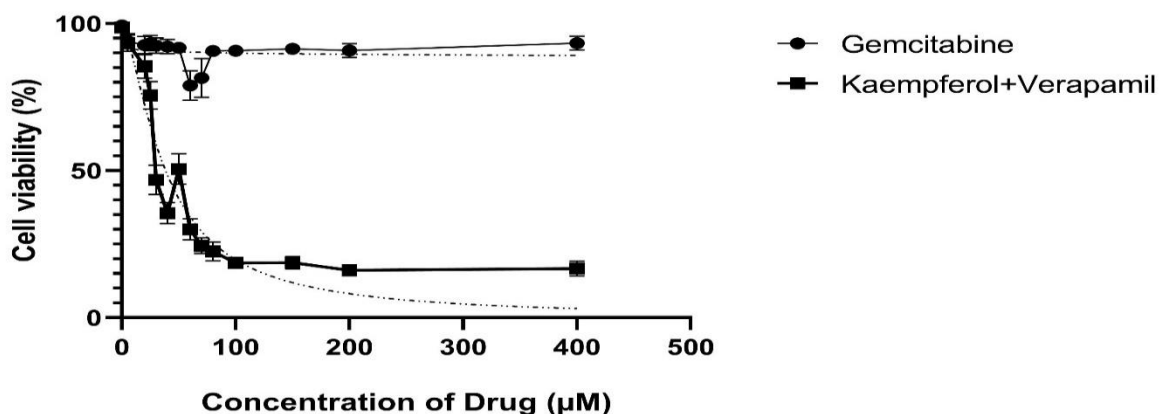
Figure 27: XTT assay showing the efficacy of Kaempferol and Verapamil, with respect to positive control Gemcitabine in patient derived tumor cells.

in Gemcitabine), and LKV (low glucose in Kaempferol with verapamil), and for h-DMEM as HC (high glucose control), HG (high glucose in Gemcitabine), and HKV (high glucose in Kaempferol with verapamil).

Explant culture assay: A portion of the tumour and corresponding normal tissue were collected for chemoresistance gene expression analysis without candidate drug treatment. To evaluate the impact of the candidate drug on gene expression in both l-DMEM and h-DMEM culture conditions, recently obtained breast tumour tissue sections (n=12) were cut into ~2.3 × 2.1 × 2.5 mm³ pieces and incubated in similar treatment conditions using l-DMEM and h-DMEM, as per **Nandi, Sourav Kumar et al. 2022**. Following treatment, one part of the tissue was placed in a Trizol reagent to determine the candidate gene expression, while the remaining portion was prepared as a paraffin block for immunocytochemistry analysis. All tissues were collected as explants within 12 hours of receipt from the onco-pathological check-up.

Gene expression of candidate markers: In accordance with the established protocol, both cell lines and explants were cultured in complete l-DMEM and h-DMEM media and treated with the predetermined dose of KV for 48 hours, as described in our previous study **[Nandi, Sourav Kumar et al. 2022]**. RNA was extracted from untreated tissue (n=21) using the established protocol **[Nandi, Sourav Kumar et al. 2022]** and analyzed spectrophotometrically. Primers for specific target genes and reference genes were

Gene abbreviation	Sequence	Annealing Temperature	Length of Primer
SOX2	F: 5′-CAAGACGCTCATGAAGAAGGATAA -3' R: 5′- TCA TGC TGT AGC TGC CGT T -3'	52 °C	173bp
OCT4	F: 5′- TCC CAG GAC ATC AAA GCT C -3' R: 5′- CAC TTC TGC AGC AAG G -3'	52 °C	215bp
NANOG	F: 5′- CCG GTC AAG AAA CAG AAG A -3' R: 5′- CTG CGT CAC ACC ATT GCT A -3'	53 °C	228bp
MDR1	F: 5′- AAGCTAACCCTTGTGATTTTGG -3′ R: 5′- TTTCTTTTGTCCTCCAAATGCA -3'	50 °C	317bp
CD44	F: 5′- CTGCAGGTATGGGTTCAT AG -3' R: 5′- ATATGTGTCATACTGGGAGGTA -3'	60 °C	124bp
NHE1	F: 5'- AGA ACT GGA CCT TCG TCA TCA -3' R: 5'- CAT AGG CGA TGA TGA ACT GGT C -3'	55 °C	138bp
ATP1B1	F: 5'- GTC TTT CTT CAT CCT TTC TCT CAT CC -3' F: 5'- CCA CTC TGA TTC TCT GTC GTA TCA-3'	61 °C	310bp
HIF1-α	F: 5'- CAT CAG TTG CCA CTT CCA CAT AAT -3' R: 5'- ATC TGT GCT TTC ATG TCA TCT TCA -3'	56 °C	140bp
GLUT2	F: 5'- ATG AAC TGC CCA CAA TCT CAT ACT CAA -3' R: 5'- CAA GAG AGC TCC AAC TAA TGA CAG AAT GTT -3	60 °C	230bp
β-Actin	F: F: 5' TACAATGAGCTCCGTGTGGC 3' 5'- CCA GAA TCC ATC ACG ATG CCT G -3'	59 °C	198bp

Table 8: In gene evaluated study, Primers for transcripts of the gene are designed.
Primers used for cDNA expression analysis of breast cancer markers and the control

designed using IDT's Oligo Analyzer Tools (Table 8). Fold change in RNA expression was determined by qRT-PCR and normalized to the Ct value of β-Actin, following our standardized protocol **[Nandi, Sourav Kumar et al. 2022]**. All experiments were conducted in triplicate.

Auto-analyser-based Ion analysis: We conducted an analysis of Ca2+ ion levels in both l-DMEM and h-DMEM media in all treated and untreated samples, including normal tissue, using an auto-analyzer (Roch Cobas C 311) with slight modifications to a previous protocol **[Altunok, İbrahim et al. 2019]**. A total of 12 consecutive tissue samples were cultured and treated with candidate drugs in this study as per our earlier protocol **[Nandi, Sourav Kumar et al. 2022]**. Cells were harvested and separated by a 10-minute spin at 2000 rpm, with the supernatant collected. Blank complete media was used as a reaction control. The auto-analyzer was calibrated at 24-hour intervals according to the manufacturer's instructions for the experiment.

Study of ROS: TNBC cells (2.23×10^5) were cultured in complete l-DMEM and h-DMEM media and allowed to adhere to gelatin-coated coverslips placed in a non-adherent six-well cell culture plate. Following 48 h of treatment with the candidate drug at its IC-50 concentration in different glucose media panels, the cells were treated with 0.1% NBT (Nitroblue-Tetrazolium) with PMA (-phorbol-12-myristate-13-acetate) with slight modifications to the previously established protocol **[Esfandiari, Navid et al. 2003]**. Negative control cells were placed in NBT with PMA on coverslips. After a few minutes, cells were washed with warm 1X PBS and fixed with 4% paraformaldehyde for 10-15 mins or counterstained with a 1% solution of Safranin O **[Javvaji, Pradeep K et al. 2020]**. Following mounting of the coverslips with DPX, both ROS-positive cells (blue colour) and ROS-negative cells (red colour) were counted in at least three microscopic fields under a bright-field microscope.

For the colourimetric NBT assay, cells isolated from primary tumours (n=8) were cultured using a previously established protocol **[Choi, Hyung Sim et al. 2006]**. Cells ($1X10^3$) were cultured and treated with candidate drugs at IC50 concentration. The above-described procedure was followed in this assay without fixation and counterstaining. To remove extracellular Y-NBT completely, the cells were resuspended in methanol. To release the deposited NBT in cells, 120 mL of 2M KOH was used to degrade the cell membrane, and 140 mL of DMSO was added to dissolve the blue-coloured formazan by shaking for 10 minutes. The solution was then transferred to another plate, and absorbance was measured at 620 nm.

Western blot study: To validate the impact of candidate drugs on the expression of targeted gene products (SOX2, OCT4, NANOG, MDR1, CD44, GLUT2, HIF1-α) in both low and high glucose conditions, we employed an immunoblotting technique with slight modifications from a previously established protocol **[Nandi, Sourav Kumar et al. 2022]**. The protein expressions were normalized against β-Actin expression in their respective sets **[Nandi, Sourav Kumar et al. 2022]**.

Confocal immunofluorescence imaging of selected protein markers: TNBC cells ($1X10^6$) were cultured in l-DMEM and h-DMEM and allowed to adhere to coverslips, following a previously described protocol **[Nandi, Sourav Kumar et al. 2022]**. After 48 hours of treatment with candidate drugs at their IC50 concentration in different glucose media panels, the expression and sub-cellular localization of gene-targeted proteins, such as SOX2, OCT4, NANOG, MDR1, CD44, GLUT2, TFEB, HIF1-α, NHE1,

Na+/K+/ATPase, LC3-II, and p62, were analyzed using the established protocol of immunocytochemistry (ICC) **[Nandi, Sourav Kumar et al. 2022]**. The cells were fixed with 4% paraformaldehyde, permeabilized with 0.025% Triton-X-100 in PBS for 10 minutes, and blocked with 3% BSA. They were then incubated overnight with the respective primary antibodies, including anti-SOX2 antibody (Abcam Cat # ab79351), anti-OCT4 antibody (Thermo Fisher Scientific Cat # MA5-31458), anti-NANOG antibody (Abcam Cat # ab109250), anti-MDR1 antibody (Santa Cruz Cat # sc-13131), anti-CD44 antibody (Abcam Cat # ab51037), anti-GLUT2 antibody (Abcam Cat # ab54460), anti-TFEB antibody (Abcam Cat # ab267351), anti-HIF1-α antibody (Cell Signalling Technology #79233), anti-NHE1 antibody (Abcam Cat # ab67314), anti-Na+/K+/ATPase antibody (Cell Signalling Technology #23565), anti-LC3-II antibody (Abcam Cat # ab192890), and anti-p62 antibody (Cell Signalling Technology # 88588), at a 1:200 dilution. The cells were washed and then incubated with fluorescent-conjugated secondary antibodies, including Alexa Fluor 488 conjugated Goat Anti-Rabbit IgG (Abcam Cat # ab97048) and Alexa Fluor 647 conjugated Goat Anti-Mouse IgG (Abcam Cat # ab150115), at a 1:500 dilution. The experimental slides were mounted with ProlongGold antifade reagent containing DAPI (Abcam Cat # ab104139). The protein expressions were analyzed by immunofluorescence microscopy.

To investigate the expression of the candidate proteins in the explant cultures under the aforementioned glucose conditions, human breast tissue sections embedded in paraffin were deparaffinized and gradually rehydrated using a previously established protocol **[Nandi, Sourav Kumar et al. 2022]**. Antigen retrieval was performed using Tris-EDTA buffer (pH 9), as per the aforementioned protocol. Immunocytochemistry (ICC) was carried out using primary and secondary antibodies conjugated with fluorescence. All experimental slides were mounted with DAPI-containing ProlongGold antifade. All reactions were performed in triplicate.

LysoTracker red (L 7528, Thermo Fisher) was utilized to detect viable cells with intact lysosomes in both the cell line and explant culture. The Mean Fluorescence Intensity (MFI) of LysoTracker™ probes was calculated from all tumour samples (n=38) to determine lysosome expression. Images were captured with an Olympus Fluo-view confocal microscope using a 60X objective and analyzed using Image J software.

Identification of Glucose uptake: Confocal microscopy imaging was performed on experimental sets assessing the uptake of 2-NBDG (2-(N-(7-nitrobenz-2-oxa-1,3-diazol-4-

yl) amino)-2-deoxyglucose) via GLUT2 receptor in MDA-MB-231 cell lines under treatment conditions (U: Untreated, G: Gemcitabine, KV: Kaempferol + Verapamil) using previously established IC-50 concentrations. The assay was conducted using modified methods as described by **Rajaram, Narasimhan et al. 2013**. Cells were incubated with 2-NBDG for 20 minutes, and the uptake in the presence of GLUT2 protein (Abcam Cat# ab234440) was determined using the above-mentioned immunocytochemistry protocol. The co-localization of 2-NBDG and GLUT2 was analyzed using statistical parameters, such as Pearson correlation coefficient. An Olympus Fluo-view confocal microscope with a 60X objective was used to obtain images, which were extracted using Image J software.

In silico analysis: We conducted an in-silico investigation of the two compounds in addition to ex vivo anti-cancer studies on breast cancer cell lines to evaluate their efficacy against malignant cells and to decipher the pathways they regulate to inhibit cancer. Computational methods were used to analyze physicochemical and drug-like properties, pharmacokinetic parameters, toxicity, biological activities, and gene expression changes induced by the compounds, with Gemcitabine serving as the reference drug. These in-silico studies were carried out using a variety of free databases, web resources, and software tools. Furthermore, we employed molecular docking to evaluate the interaction of these compounds with the targets of our ex vivo experiments, as these results can provide critical data for drug utilization in physiological systems.

The ligands used in this study were retrieved from PubChem (https://pubchem.ncbi.nlm.nih.gov/), while the receptors were obtained from RCSB PDB (www.wwpdb.org) **[Berman, Helen et al. 2003]**. Physico-chemical, drug-likeness, and basic pharmacokinetic parameters of the ligands were evaluated using the Swiss-ADME server, a freely distributed online portal for such assessments provided by the Swiss Institute of Bioinformatics (SIB) **[Daina, Antoine, and Vincent Zoete. 2016]**. Target prediction was performed using the Swiss Target server, also provided by SIB (www.swisstargetprediction.ch) **[Daina, Antoine, and Vincent Zoete. 2016]**. Molecular docking analysis was carried out using the PyRx software, which processed and prepared the macromolecular structures of the ligands and receptors for the in-silico interaction analysis.

Statistical study: The MFI was calculated using one-way ANOVA (GraphPad Prism 8, RRID: SCR_002798). The software was used to perform the student's t-test for analyzing the gene and protein experimental outcomes in the six treatment groups. A p-value of ≤0.05 was considered statistically significant for a 95% confidence level. All the studies were completed without any significant loss of statistical power.

Results

ROS detection and linked signalling cascade of NANOG-CD44-MDR1-ATPase: ROS production is a significant hallmark of cancer. However, an excessive amount of ROS can contribute cancer cell apoptosis or senescence through oxidative stress. ROS signalling can initiate both autophagy induction and lysosome biogenesis. Using confocal microscopy, we observed an increased fluorescence of LysoTracker red in tumour cells (Fig. 28A), suggesting that intact lysosomal biogenesis mechanisms play a vital role in their survival prior to the administration of our candidate drug. The Mean Fluorescence Intensity (MFI) value of LysoTracker™ for all tumours in the patient (n=38) cohort (n=38) was (54.9008 ±1.215) (Fig. 28B) recorded. The lysosome also engages in interactions with other organelles through the calcium ions (Ca2+). The concentration of intracellular
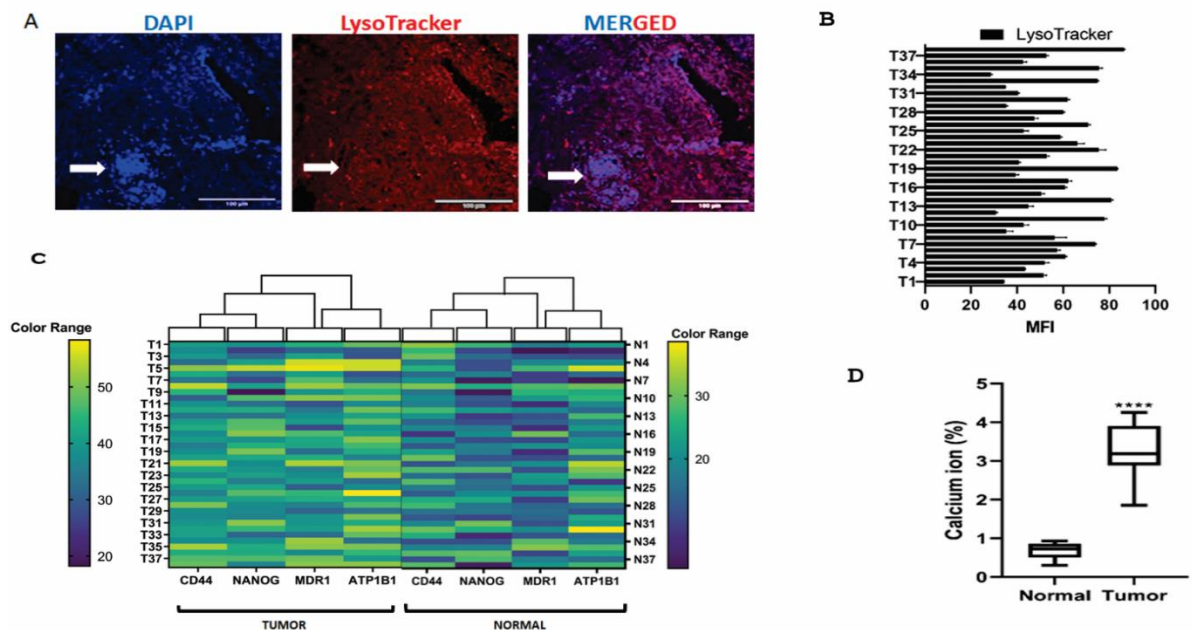
Figure 28: Hypothesis on the induction of chemoresistance markers might be contributed by lysosomalCa2+ based ROS signalling in tumour. (A) Fluorescence-based immunohistochemical localization of Lysosome. (B) Index of Mean Fluorescence Intensity (MFI) of LysoTracker™ probesin tumour samples (n=38). (C) Expression of chemoresistance marker in together tumour (n=38) and respective normal (n=38) sample. (D) Estimation of Calcium ion in normal and tumour sample. Student's t-test was used to correlate the significance where *p <0.0332 **p <0.0021 ***p <0.0002 **** <0.0001.

Ca2+ in the extracted tumour tissue was determined at about 3.231% (±0.785%) as compare to normal tissues with 1.1% (±0.101%) (Fig. 28D). To know the association a heatmap was generated to examine the relationship between lysosomal Ca2+-based ROS signalling and chemoresistance markers. The expression levels of NANOG, CD44, MDR1, and ATPase genes were compared in 38 breast tumour samples and various normal tissues

(Fig. 28 C). The cycle threshold (Ct) values of these genes were significantly upregulated in tumour samples, along with the upregulation of lysosomes. Therefore, we infer that the upregulation of chemoresistance genes might be associated with lysosomal Ca2+-based ROS signalling, which promotes lysosomal upregulation and tumour cell survival (Fig. 28).

Measurement of ROS levels and analysis of expression of candidate genes upon treatment with Kaempferol in combination with Verapamil in breast cancer: The correlation between the detection and quantification of intracellular ROS production based on NBT staining and the previous results of lysosomal expression analysis was assessed. After 48 hours of treatment with a candidate drug on the MDA-MB-231 cell line, intracellular ROS was detected in both l-DMEM and h-DMEM media panels. No formazan precipitate was observed in the control set, while the Gemcitabine-treated panel showed a few reddish-blue darkly as an indicator of uncontrolled free radical production in the examined MDA-MB-231 cell line (Fig. 29 A). In the KV treatment group the l-DMEM panel produced more ROS than the h-DMEM panel in the MDA-MB-231 cell line. No significant difference in ROS production was observed in the Gemcitabine and KV-treated panel of the h-DMEM. In this assay, the NBT reaction exhibited oxidative activity in the cell cytoplasm as a source of free radical production and colored cells darkly as an indicator of uncontrolled free radical production in the examined MDA-MB-231 cell line. The intracellular level ROS (% of NBT stained area) in MDA-MB-231 did not vary significantly among LC (11.9 ± 0.35%) or LG (13.3 ± 2.07%) (Fig. 29 A, B). Remarkably (p < 0.0001) maximal level of intracellular ROS (96.5 ± 2.56%) was observed in LKV group however in h-DMEM panel, the ROS production of HC (18.6 ± 0.26%), HG (10.35 ± 0.42%) and HKV (21.38 ± 0.33%) was not significant (Fig. 29B). To confirm the assay, a colourimetric NBT test was also conducted, which showed a significant increase in the OD value of dissolved NBT in the LKV group of both MDA-MB-231 (Fig. 30A) and primary tumour cells (Fig. 29 C), compared to the LG and HG treatment panels. During this treatment, a significant reduction in intracellular Ca2+ ions was observed (1.92 ±0.24) (Fig. 30B) in the LKV treatment panel. The gene expression of *SOX2, OCT4, NANOG, MDR1, CD44, ATP1B1, NHE1, HIF1-α, GLUT2* and housekeeping control gene *β-Actin* were studied utilising semi qRT-PCR and q-RT-PCR, after treatment with candidate drugs in both l-DMEM and h-DMEM panels, in MDA-MB-231, MCF-7, and primary breast tumour derived cells. In MDA-MB-231(Fig. 29D and 29F) and primary tumour cells (Fig. 29E and 29G), in the l-DMEM panel, KV treatment resulted in a reduction of candidate gene expression, while in the h-DMEM panel, no significant differences were observed
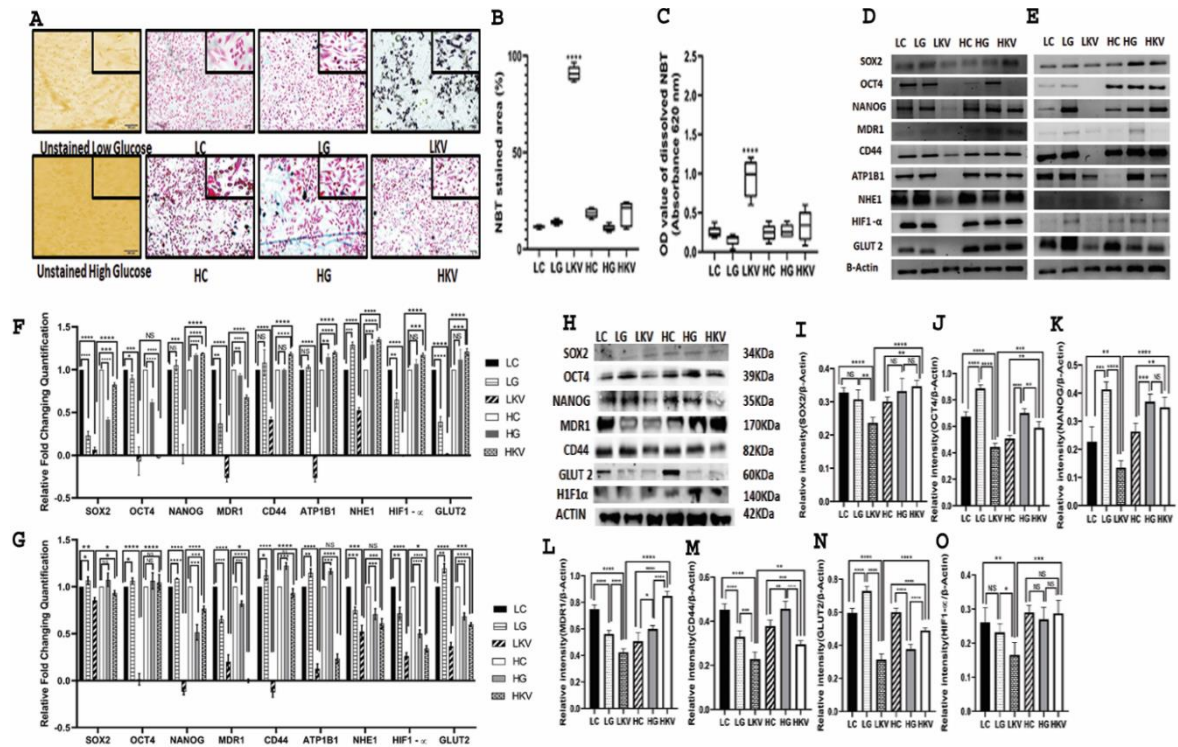
Figure 29: Impact of Kaempferol with verapamil in expression of ROS production and chemo-evasion mechanisms. (A) ROS production was evaluated in MDA-MB-231 cells, with the upper panel showing the low glucose treated group and the lower panel showing the high glucose treated group. (B) The NBT stain area was estimated in MDA-MB-231 cells under various treatment conditions (48 h). (C) ROS production was estimated in primary tumour cells under similar treatment conditions (48 h). (D, E) Semiquantitative and (F, G) quantitative RT-PCR were performed to determine the expression status of candidate genes including SOX2, OCT4, NANOG1, MDR1, CD44, ATP1B1, NHE1, HIF1-α, and GLUT2, which were upregulated in (D, F) MDA-MB-231 and (E, G) primary tumour, respectively. The β-Actin gene was used as the endogenous control for both semiquantitative and quantitative RT-PCR under identical treatment groups (48 h). (H) Western blot analysis was conducted to investigate the fold change of expression of candidate markers in MDA-MB-231 cell line under various treatment conditions (48 h). The fold change of expression of candidate genes was normalized to the expression of (I–O) β-Actin. The significance was correlated using Student's t-test and Two-way ANOVA, where *p <0.0332 **p <0.0021 ***p <0.0002 **** <0.0001. Different treatment groups indicated in the above experiment include Low glucose control (LC), Low glucose Gemcitabine (LG), Low glucose Kaempferol with verapamil (LKV), High glucose control (HC), High glucose Gemcitabine (HG), and High glucose Kaempferol with verapamil (HKV).
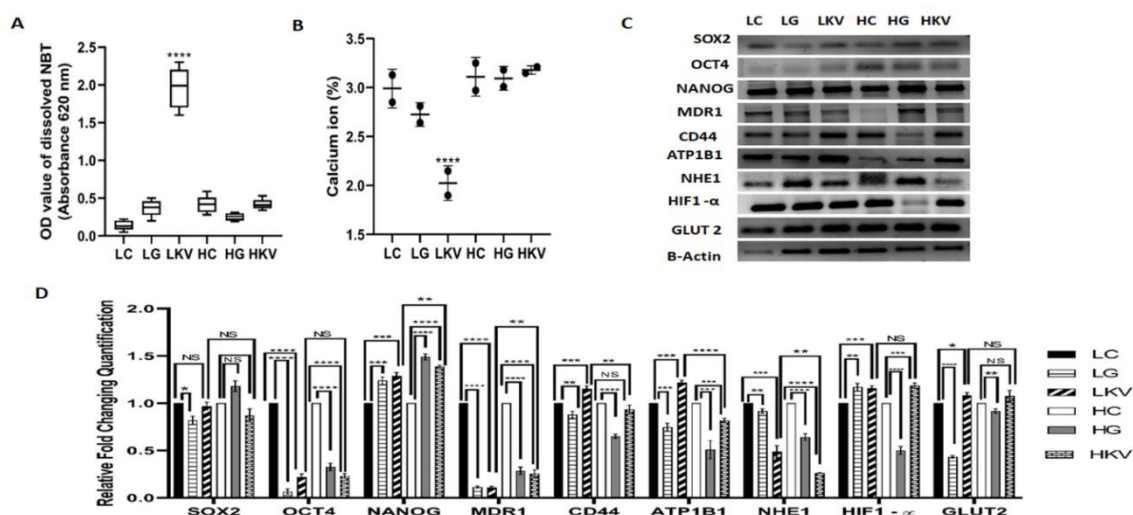
Figure 30: The impact of Kaempferol combined with verapamil on the expression of ROS production and chemo-evasion mechanisms was investigated. (A) ROS production was assessed in MDA-MB-231 cells under similar treatment conditions (48 h). (B) Changes in calcium ion levels were analyzed in primary tumours under similar treatment conditions. (C, D) Semiquantitative and quantitative RT-PCR were performed to evaluate the expression of candidate genes including SOX2, OCT4, NANOG1, MDR1, CD44, ATP1B1, NHE1, HIF1-α, GLUT2, which were upregulated in MCF-7 cells. β-Actin gene was used as an endogenous control for both semiquantitative and quantitative RT-PCR under identical treatment groups (48 h). Significance was analyzed using Student's t-test and Two-way ANOVA, where *p <0.0332, **p <0.0021, ***p <0.0002, and ****<0.0001. The different treatment groups tested included Low glucose control (LC), Low glucose Gemcitabine (LG), Low glucose Kaempferol with verapamil (LKV), High glucose control (HC), High glucose Gemcitabine (HG), and High glucose Kaempferol with verapamil (HKV).

among the various treatment groups. In MCF-7 cells, abnormal results (Fig. 30C, 30D) were observed. In this cell line, in the l-DMEM panel, the KV treatment showed a lower reduction in the expression of SOX2 and MDR1 genes (Fig. 29D and 29F), while there was no significant change in the expression of the HIF1-α gene. The KV treatment was found to be inefficient in attenuating the expression of the HIF1-α gene in both l-DMEM and h-DMEM panels. It was interesting to note that the downregulation of chemo resistance genes, such as CD44, NANOG, MDR1, and ATP1B1, along with other markers in the l-DMEM panel in the KV treatment group in MDA-MB-231 cell line resulted in increased ROS production, as shown in Fig. 29.

Immunoblotting assay: After examining the gene expression and their involvement in ROS production, we validated the candidate protein expression. KV treatment caused

significant changes in the expression levels of crucial chemo-resistance proteins such as CD44, NANOG, and MDR1, as well as related proteins including SOX2, OCT4, HIF1-α, and GLUT2, as shown by specific western blotting (Fig. 29H) and densitometric analysis of the relative fold change of candidate proteins that were normalized to β-Actin (Fig. 29I–O). Moreover, the treatment of Gemcitabine (LG/HG) in both l-DMEM and h-DMEM panels did not result in any significant diminution in relative fold changing of the candidate proteins expression in respect of control (LC/HC) in Fig 29. The outcome indicated, KV increased a significant reduction of candidate proteins expression that extremely increased the chemo-resistance associated aspects in breast cancer. In this experiment, KV show significant effectiveness in the l-DMEM panel while, in the h-DMEM panel, the outcomes were aberrant or indeterminate. Specifically, in the HKV treatment set, SOX2 (Fig. 29 I), MDR1 (Fig. 29 L), GLUT2 (Fig. 29 N), and HIF1-α (Fig. 29 O) were upregulated, and OCT4 (Fig. 29 J), NANOG (Fig. 29 K), and CD44 (Fig. 29 M) were downregulated compared to the Gemcitabine-treated set (HG). In contrast, the LKV treatment set showed a significant reduction in candidate gene expressions compared to the HKV treatment set. This was confirmed by specific western blotting (Fig. 29 H) and densitometric analysis of the relative fold change of candidate proteins, which were normalized to β-Actin.

Immunocytochemical analysis of chemoresistance proteins: Upon comparison with the LC treatment set, it was observed that LKV treatment significantly inhibited tumour cell growth and reduced the expression of candidate markers such as CD44 (Fig. 31A, 31E), NANOG (Fig. 31B, 31F), MDR1 (Fig. 31C, 31G), and Na+/K+/ATPase (Fig. 31D, 31H). However, treatment with LG did not have any significant effect on the expression status of candidate markers in tumour samples and MDA-MB-231 cells (Fig. 32A, 32B, 32C, and 32D). In the h-DMEM panel, HKV treatment resulted in the upregulation of candidate protein expression. The MFI determination of tumour samples targeted breast cancer patients (Fig. 31E, 31F, 31G and 31H) and MDA-MB-231 cell line (Fig. 32E, 32F, 32G and 32H) displayed a significant reduction of targeted proteins expression in LKV treatment. The targeted markers upon HG treatment were significantly increased. In Gemcitabine treatment, the significant fold change of the candidate proteins expression was not observed excluding NANOG protein expression (Fig. 31B and 32B). Fluorescence intensity (FI) was measured using the ImageJ software as previously reported (Nandi et al, 2022). Mean fluorescence intensity (MFI) values were calculated from five different areas and the background FI of the cell-free area was subtracted. Statistical analysis was performed to determine the significance of MFI values in different treatment groups.
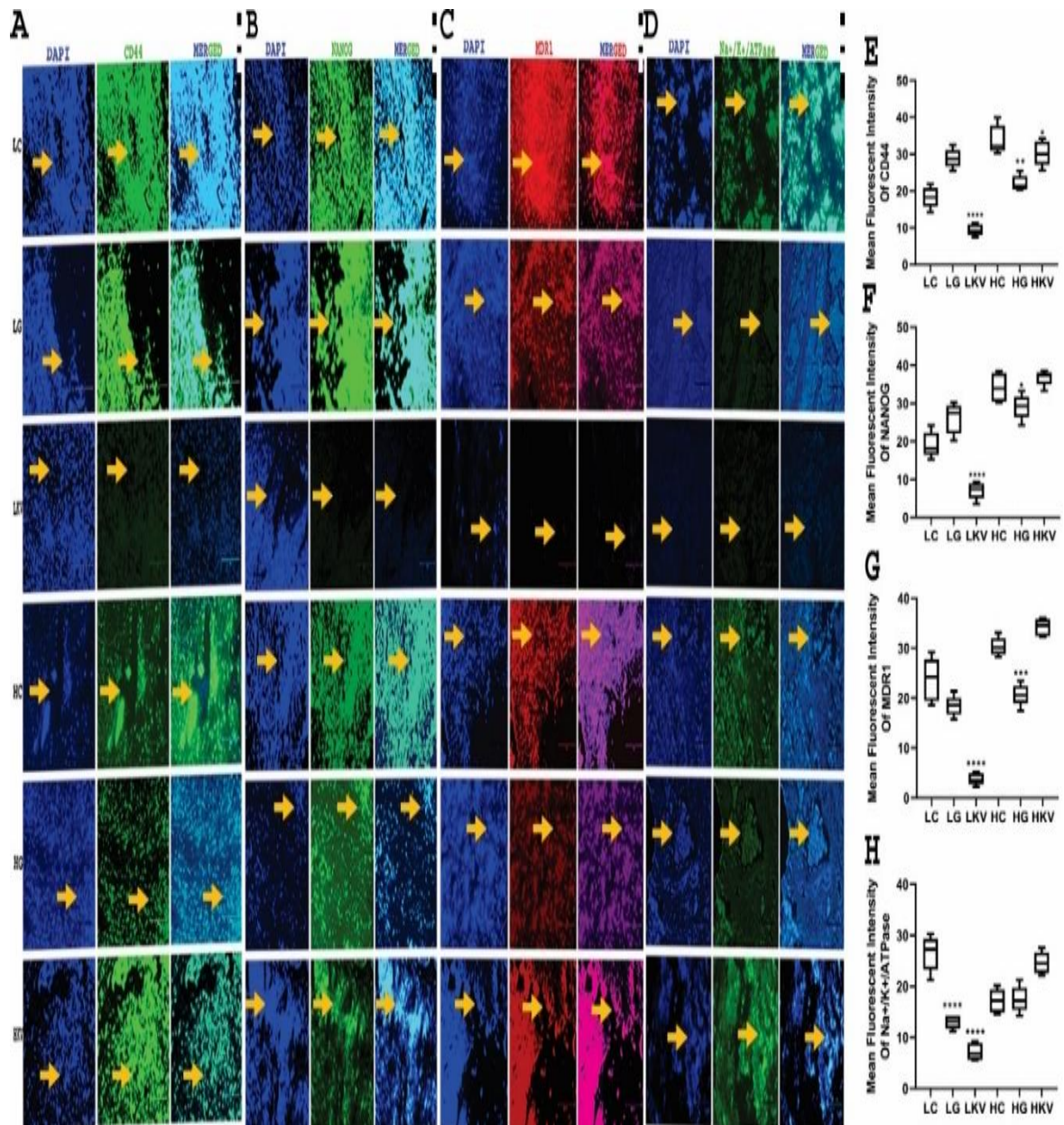
Figure 31: Immunofluorescence microscopy was performed to assess the expression of chemoresistance marker after drug treatment. Fluorescence-based immunohistochemical localization of (A) CD44, (B) NANOG, (C) MDR1, and (D) Na+/K+/ATPase protein was observed in primary tumour cells under different treatment conditions (48 h.). The scale bar represents 150μM. Mean fluorescence intensity of (E) CD44, (F) NANOG, (G) MDR1, and (H) Na+/K+/ATPase were quantified. The various treatment groups included Low glucose control (LC), Low glucose Gemcitabine (LG), Low glucose Kaempferol with verapamil (LKV), High glucose control (HC), High glucose Gemcitabine (HG), and High glucose Kaempferol with verapamil (HKV). Statistical significance was determined using one-way ANOVA, where ***p < 0.0002 and ****p < 0.0001.

Impact of Kaempferol and Verapamil on glucose transport: In both primary tumours,
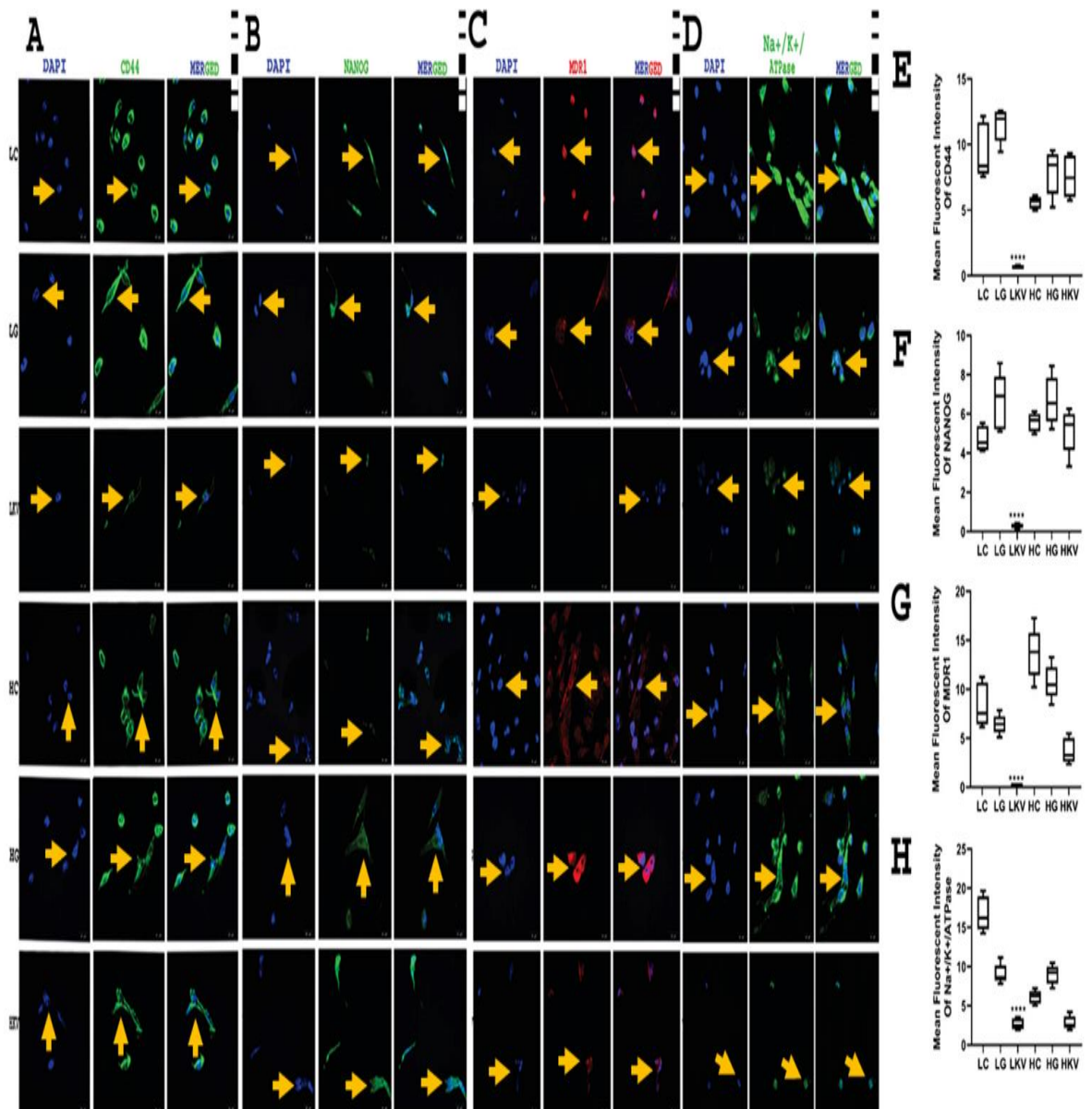
Figure 32: Exploration of chemoresistance markers expression using immunofluorescence microscopy after drug treatment exposure. Fluorescence-based immunohistochemical localization of (A) CD44, (B) NANOG, (C) MDR1 and (D) Na+/K+/ATPase proteins in MDA-MD-231 under different treatment conditions (48 h). Scale bar: 150 μM. Mean fluorescence intensity of (E) CD44, (F) NANOG, (G) MDR1, and (H) Na+/K+/ATPase. The different treatment groups used were Low glucose control (LC), Low glucose Gemcitabine (LG), Low glucose Kaempferol with verapamil (LKV), High glucose control (HC), High glucose Gemcitabine (HG), and High glucose Kaempferol with verapamil (HKV). One-way ANOVA was used for statistical analysis with ***p <0.0002 and ****p <0.0001 as significant levels.
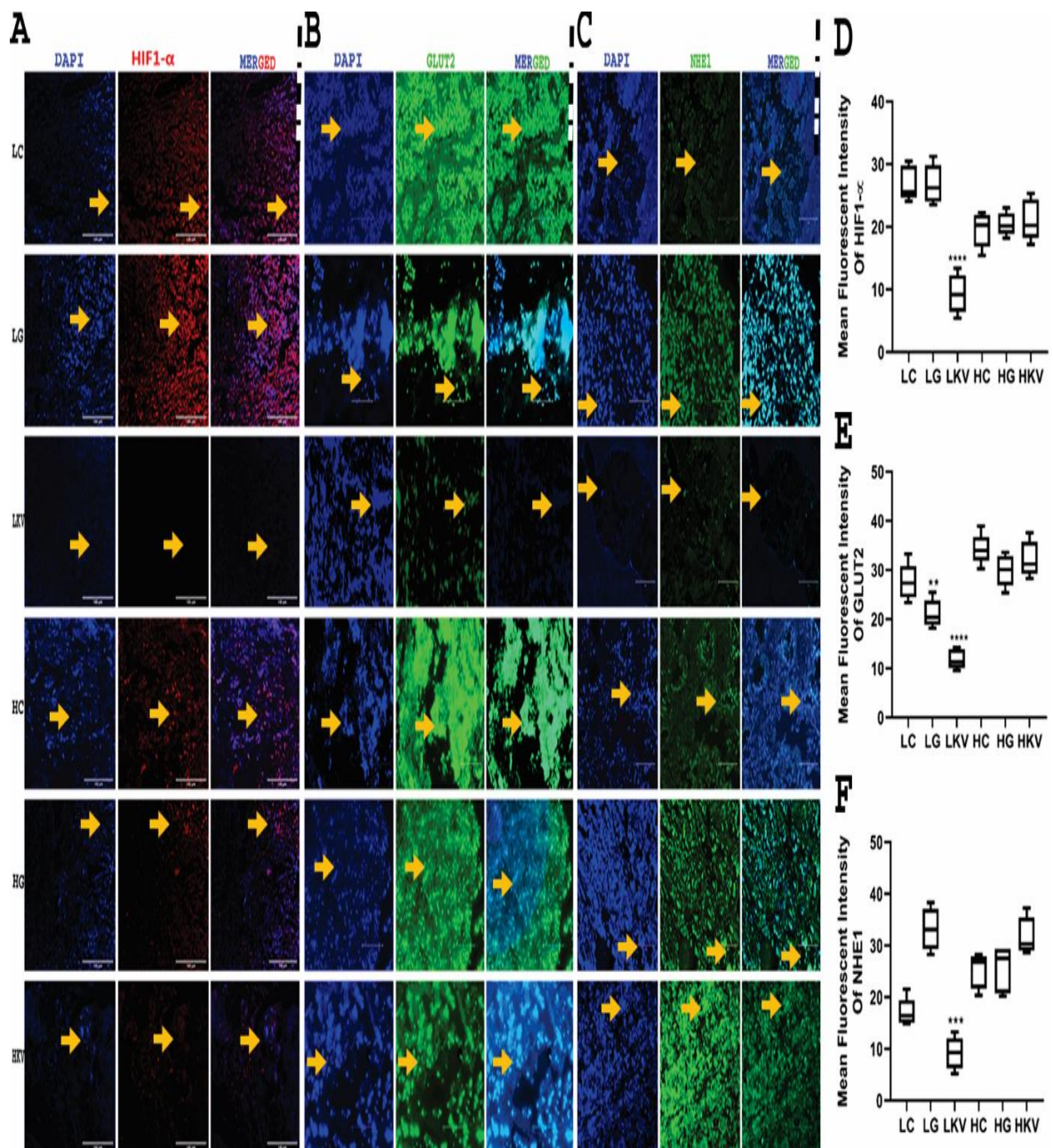
Figure 33: Assessment of hypoxia and glucose transporter-based acidosis marker expression following treatment with Kaempferol and Verapamil in response to low and high glucose. Fluorescence-based immunohistochemical localization of (A) HIF1-α, (B) GLUT2, and (C) NHE1 protein in primary tumour cells after treatment with candidate drugs (48 h) under different glucose conditions. Scale bar: 150μM. Mean fluorescent intensity of (D) HIF1-α, (E) GLUT2, and (F) NHE1. The different treatment groups included: Low glucose control (LC), Low glucose Gemcitabine (LG), Low glucose Kaempferol with Verapamil (LKV), High glucose control (HC), High glucose Gemcitabine (HG), and High glucose Kaempferol with Verapamil (HKV). Statistical significance was determined using one-way ANOVA, with ***p < 0.0002 and ****p < 0.0001.
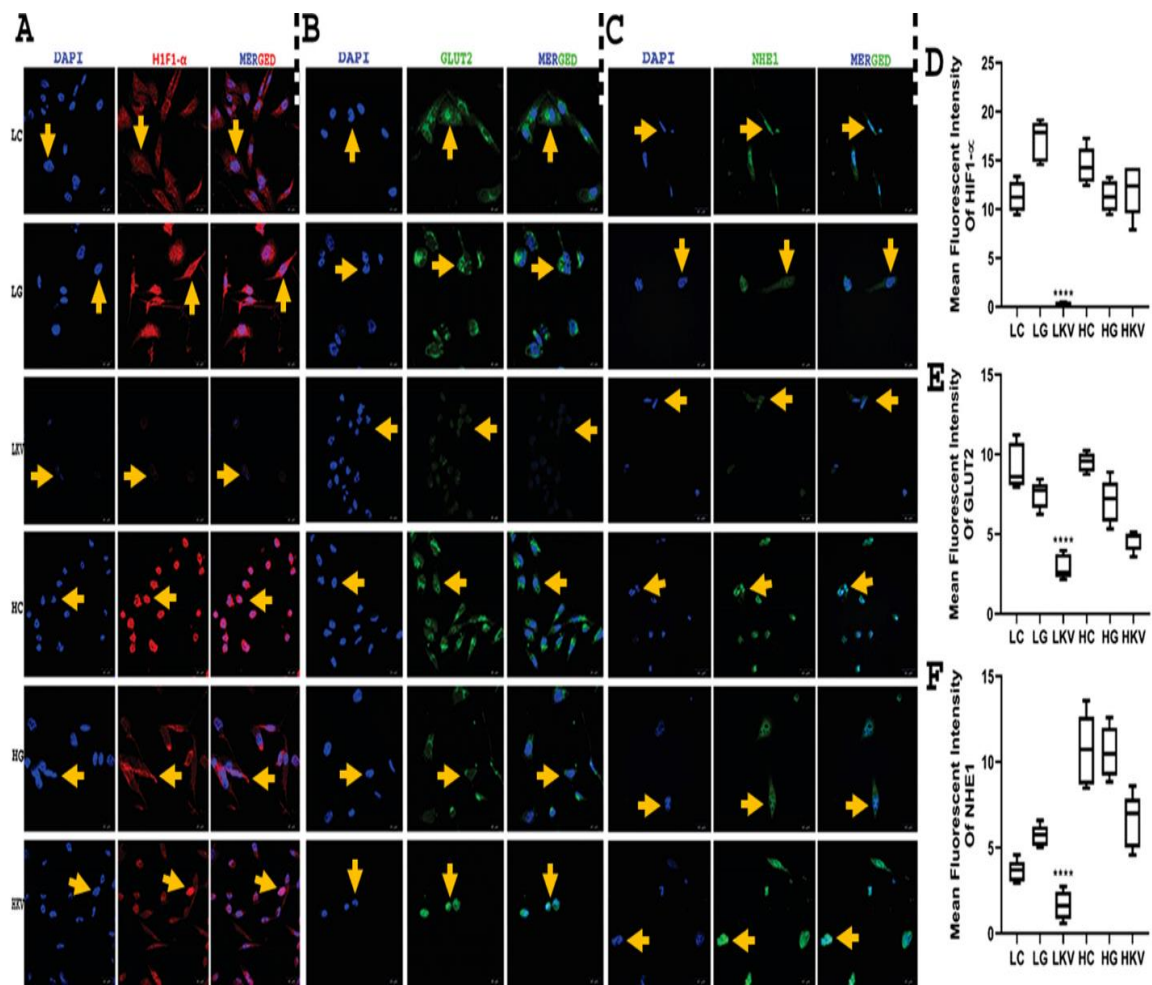
Figure 34: The impact of hypoxia and glucose transporter-mediated acidosis in response to Kaempferol and verapamil treatment under low and high glucose conditions was evaluated. Fluorescence-based immunohistochemical analysis of HIF1-α, GLUT2, and NHE1 protein expression was performed in MDA-MB-231 cells treated with different regimens for 48 hours. The mean fluorescent intensity of HIF1-α, GLUT2, and NHE1 was quantified. Treatment groups included low glucose control (LC), low glucose Gemcitabine (LG), low glucose Kaempferol with Verapamil (LKV), high glucose control (HC), high glucose Gemcitabine (HG), and high glucose Kaempferol with verapamil (HKV). Statistical analysis was performed using one-way ANOVA with ***p <0.0002 and **** p <0.0001 indicating significance. The scale bar in the images represents 150μM.

LKV treatment resulted in the downregulation of HIF-1α (Fig. 33A, 33D) dependent NHE1 (Fig. 33C, 33F), which was demonstrated to be crucial for sustaining high levels of ROS production. In contrast, in the HKV set, both proteins were also downregulated compared to the control. Similar outcomes were observed in MDA-MB-231, where the HIF-1α (Fig. 34A, 34D) dependent NHE1 (Fig. 34C, 34F) showed comparable results. Remarkably, the outcomes indicated that, the effectiveness of LKV was found to be superior to that of the HKV set (Fig. 34D, 34F) in both primary tumour (Fig. 34) and MDA-MB-231 (Fig. 34). Moreover, the reduction of GLUT2 markers was observed in the primary tumour (Fig. 33B,

33E) and MDA-MB-231 (Fig. 34B, 34E). indicated the low cellular proliferation in the LKV treatment group. Here, for validation of the investigation, the 2-NBDG treatment was
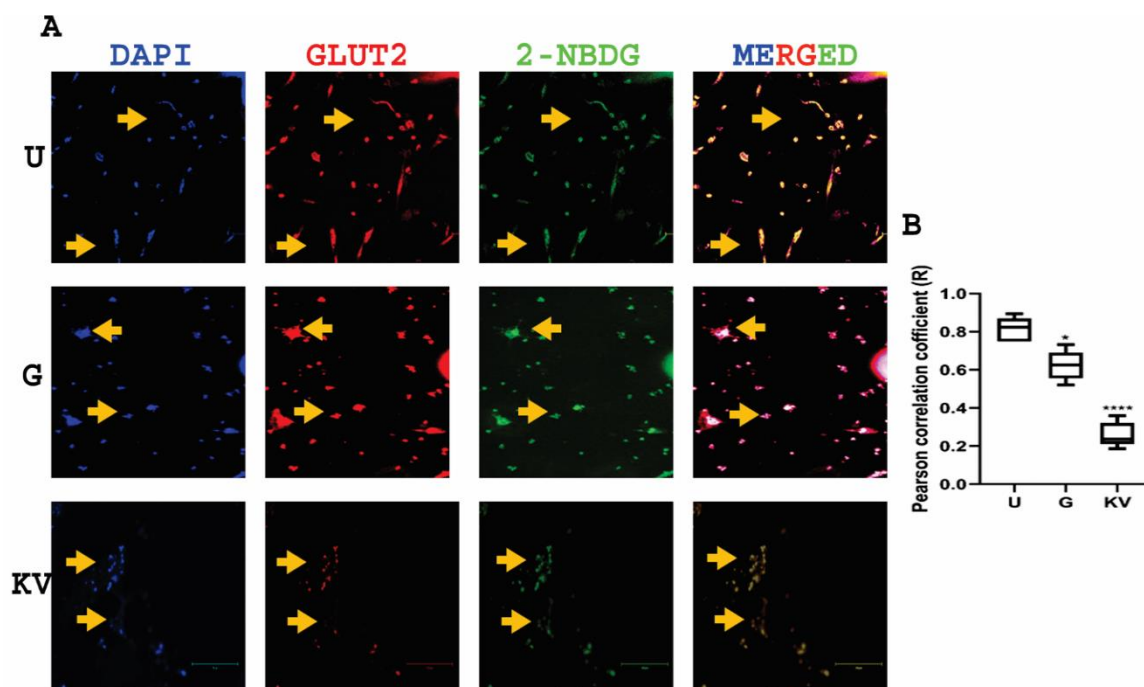
*Figure 35: Effect of candidate drug treatment on GLUT2 expression and fluorescent glucose uptake. Co-localization analysis of (A) GLUT2 and 2-NBDG in primary tumor cells under different treatment conditions (48 h). Scale bar: 150 µM. (B) Pearson correlation coefficient (R) of GLUT2 and 2-NBDG co-localization was determined. Treatment groups were as follows: control (C), Gemcitabine (G), Kaempferol with verapamil (KV). Statistical significance was determined using one-way ANOVA with ***p <0.0002 and ****p <0.0001.*

in MDA-MB-231 and then observed the glucose uptake with the GLUT2 receptor. After 48h candidate drug treatment, the experimental MDA-MB-231 cells were determined by confocal microscopy with MFI sessions (Fig. 35A, 35B). The findings of the investigation revealed that both MDA-MB-231 and tumour samples showed more glucose uptake in the KV treatment than control or Gemcitabine treatment set. Moreover, the expression of HIF-1α and NHE1 was decreased in this treatment condition (LKV) with respect to control or Gemcitabine treatment.

ROS in the lysosomal response to treatment with Kaempferol and Verapamil: In prolongation with our previous study, we aimed to investigate the substantial alteration in the expression of lysosomes in both treatment groups of the tumour sample (Fig. 36A) and MDA-MB-231 (Fig. 37A). In comparison to the control (LC) in the l-DMEM panel of both

samples, it was observed that in LKV panel a downregulation of lysosomal expression was observed, whereas treatment with Gemcitabine in both l-DMEM and h-DMEM panels did
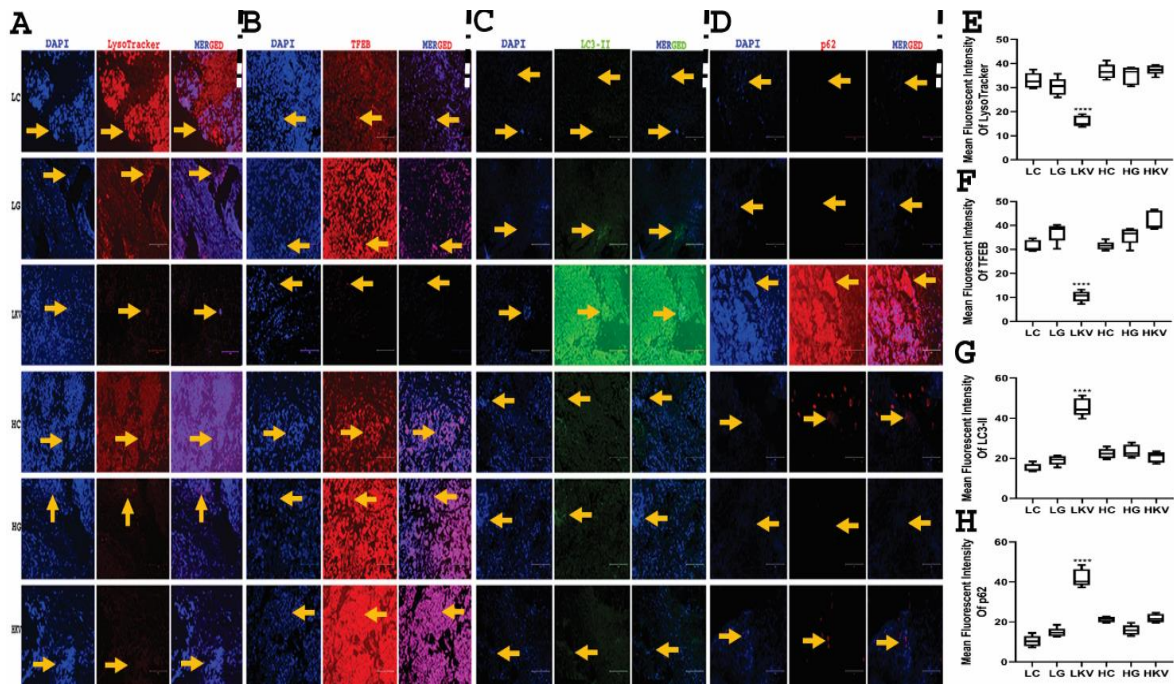
Figure 36: Disruption of lysosomal function and transcription factor EB (TFEB) activation regulate autophagy-mediated cell death in the treatment of Kaempferol with Verapamil under low and high glucose conditions. Fluorescence-based immunohistochemical analysis was performed to localize lysosomes (A), TFEB (B), LC3-II (C), and p62 protein (D) in primary tumours after treatment for 48 hours under different conditions. The mean fluorescent intensity of LysoTracker™ probes (E), TFEB (F), LC3-II (G), and p62 (H) was also measured. The treatment groups included Low glucose control (LC), Low glucose Gemcitabine (LG), Low glucose Kaempferol with Verapamil (LKV), High glucose control (HC), High glucose Gemcitabine (HG), and High glucose Kaempferol with Verapamil (HKV). Statistical analysis was performed using one-way ANOVA and the results showed a significant difference with ***p <0.0002 or **** p <0.0001.

not have a significant effect on the expression of lysosomes. MFI index of tumour sample (Fig. 36E) and MDA-MB-231 (Fig. 37E) exhibited a significant reduction of lysosome in the LKV treatment panel whereas no significant deviations were detected in the h-DMEM panel of the experiment model. In the LKV treatment panel, we observed that TFEB expression was also decreased in tumour samples (Fig. 36B, 36F) and MDA-MB-231 (Fig. 37B, 37F). In Figure 6 as well as Figure S5, we observed that the KV drug represses the lysosomal-Ca2$^+$ expression that stimulated ROS production however, Gemcitabine (G) did not show any vital role. In the LKV treatment set, we observed autophagy-mediated cell

death by the reduction of autophagy-associated proteins expression viz. LC3II (Protein-light-chain-3) (Fig. 36C, 36G) and p62 (sequestosome1) (Fig. 36D, 36H) in both primary tumour and MDA-MB-231 (Fig. 37C, 37G) and (Fig. 37D, 37H) respectively.
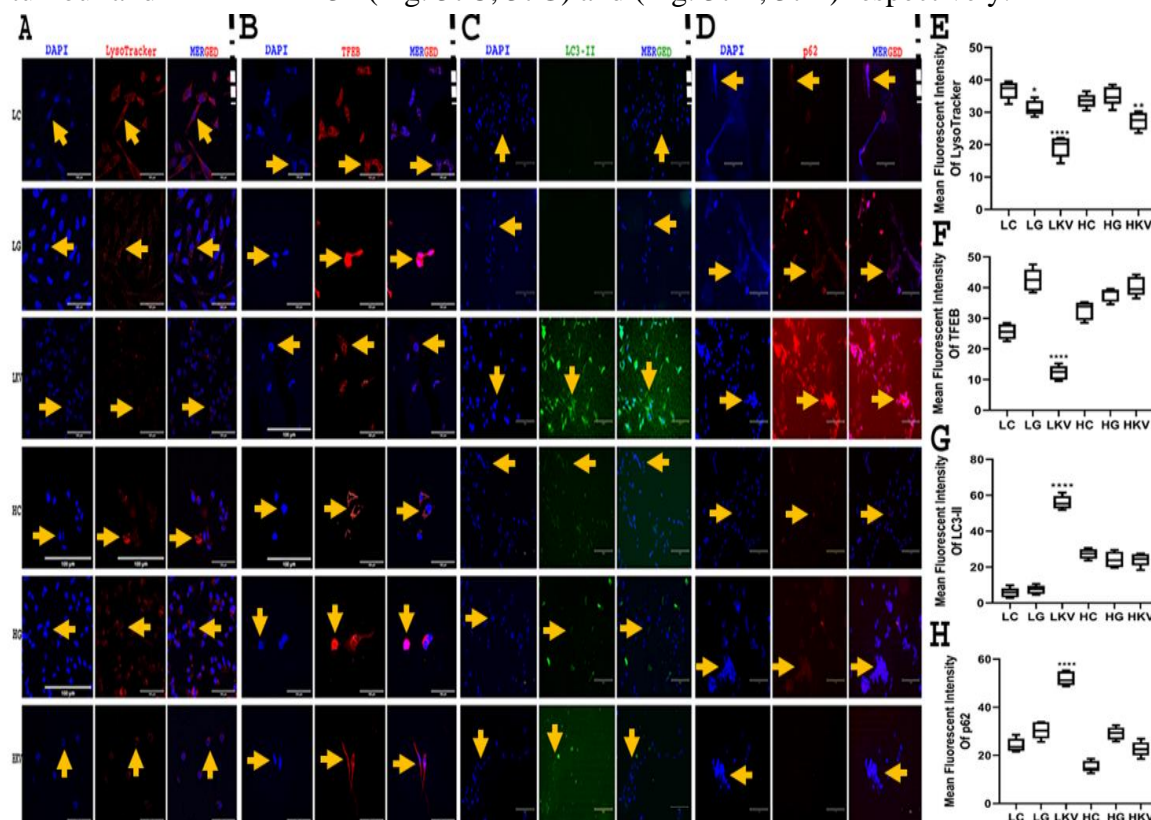
Figure 37: The treatment of Kaempferol with verapamil disrupts lysosomes and regulates transcription factor EB (TFEB), leading to autophagy-mediated cell death in response to both low and high glucose conditions. Immunohistochemical analysis using fluorescence-based methods was performed to localize lysosome, TFEB, LC3-II, and p62 protein in MDA-MB-231 cells under different treatment conditions (48 h). Mean fluorescent intensity of LysoTracker™ probes, TFEB, LC3-II, and p62 were measured, and the treatment groups included Low glucose control (LC), Low glucose Gemcitabine (LG), Low glucose Kaempferol with verapamil (LKV), High glucose control (HC), High glucose Gemcitabine (HG), and High glucose Kaempferol with verapamil (HKV). Statistical analysis was performed using one-way ANOVA, and the results showed significant differences with ***p <0.0002 and **** p <0.0001.

Morphologically, autophagy-mediated cell death depended on the autophagic markers, extensive cytoplasmic vacuolization with lysosomal degradation was observed in LKV-treated tumour tissue (Fig. 27) or MDA-MB-231 cells (Fig. 37), while no significant upregulation was observed in HKV-treated cells. In both l-DMEM and h-DMEM panels, Gemcitabine treatment (LG/HG) showed no significant difference compared to the control (LC/HC).

In silico study

Structure retrieval of ligands and receptors: Our previous study has revealed the combination of Kaempferol and Verapamil shows more effect than only Kaempferol in cancerous cell lines. The chemical structures of the flavonoid, drug, and Gemcitabine (control) are depicted in Fig. 38 (Fig. 38A, 38B, and 38C). The receptors' chemical structure is provided in the supplementary materials (Fig. 39).

Figure 38: A, B, and C. Ligand structures: Kaempferol, Verapamil and Gemcitabine respectively. D, F, and H. Physico-chemical properties of Kaempferol, Verapamil and Gemcitabine respectively. E, G, and I. Boiled egg representation of Kaempferol, Verapamil and Gemcitabine respectively. J, K, and L. predicted cellular targets of Kaempferol, Verapamil and Gemcitabine respectively.

Figure 39: Structure of Receptors retrieved from RCSB PDB.

Drug-likeness, Physico-chemical property and pharmacokinetics of Ligands: The physico-chemical and drug-like characteristics of the three selected ligands are illustrated using the bio-radar of the SWISS-ADME webserver. The outcome exhibited that the high degree of unsaturation in the molecule of Kaempferol renders it unsuitable as a fully viable drug molecule. (Fig. 38D.) i.e. the proportion of carbon atoms in the sp3 hybridized state (C-sp3 fraction) is below 0.25 (0.00). The drug compound Verapamil was found to have a limited drug-like character, as indicated by the radar plot, with a flexibility score of 13 which falls outside the optimal range (Fig. 38F) of 1-9. On the contrary, the drug Gemcitabine exhibited complete adherence to the biological radar (Fig. 38H), implying its potential as a full-fledged drug that can be readily made bioavailable compared to the preceding ligands. Nevertheless, the combined impact of these ligands within the biological system may differ. Although they lack optimal drug-likeness characteristics, they remain effective as anti-cancer agents while efficiently complying with Lipinski's rule. Further details regarding their physicochemical properties, solubility, and drug-likeness parameters are presented in Table 9.

114

Ligand	Physicochemical Properties	Lipophilicity and Water Solubility	Pharmacokinetics	Drug Likeness & Medicinal Chemistry
Kaempferol	Molecular weight 286.24 g/mol No. heavy atoms 21 No. arom. heavy atoms 16 Fraction Csp3 0.00 No. rotatable bonds 1 Num. H-bond acceptors 6 No. H-bond donors 4 Molar Refractivity 76.01 TPSA 111.13 Å	Log Po/w (iLOGP) 1.70 Log Po/w (XLOGP3) 1.90 Log Po/w (WLOGP) 2.28 Log Po/w (MLOGP) 0.03 Log Po/w (SILICOS-IT) 2.03 Consensus Log Po/w 1.58 Log S (ESOL) -3.31 Solubility 1.40e-01 mg/ml; 4.90e-04 mol/l Class Soluble Log S (Ali) -3.86 Solubility 3.98e-02 mg/ml; 1.39e-04 mol/l Class Soluble Log S (SILICOS-IT) 3.82 Solubility 4.29e-02 mg/ml; 1.50e-04 mol/l Class Soluble	GI absorption High BBB permeant No P-gp substrate No CYP1A2 inhibitor Yes CYP2C19 inhibitor No CYP2C9 inhibitor No CYP2D6 inhibitor Yes CYP3A4 inhibitor Yes Log Kp (skin permeation) -6.70 cm/s	Lipinski Yes Ghose Yes Veber Yes Egan Yes Muegge Yes Bioavailability Score 0.55 Synthetic accessibility 3.14
Verapamil	Molecular weight 263.20 g/mol No. heavy atoms 18 Num. arom. heavy atoms 6 Fraction Csp3 0.56 Num. rotatable bonds 2 Num. H-bond acceptors 7 Num. H-bond donors 3 Molar Refractivity 54.83 TPSA 110.60 Å²	Log Po/w (iLOGP) 4.50 Log Po/w (XLOGP3) 3.79 Log Po/w (WLOGP) 5.09 Log Po/w (MLOGP) 2.96 Log Po/w (SILICOS-IT) 5.89 Consensus Log Po/w 4.45 Log S (ESOL) -4.46 Solubility 1.59e-02 mg/ml; 3.49e-05 mol/l	GI absorption High BBB permeant Yes P-gp substrate Yes CYP1A2 inhibitor No CYP2C19 inhibitor No CYP2C9 inhibitor No CYP2D6 inhibitor Yes CYP3A4 inhibitor Yes	Lipinski Yes; Ghose No; Veber No; Egan Yes Muegge Yes Bioavailability Score 0.55 Synthetic accessibility 3.75

| | | Class Moderately soluble
Log S (Ali) -4.83
Solubility 6.77e-03 mg/ml; 1.49e-05 mol/l
Class Moderately soluble
Log S (SILICOS-IT) 8.00
Solubility 4.54e-06 mg/ml; 9.98e-09 mol/l
Class Poorly soluble | Log Kp (skin permeation) -6.38 cm/s | |
| Gemcitabine | Molecular weight 263.20 g/mol
No. heavy atoms 18
Num. arom. heavy atoms 6
Fraction Csp3 0.56
Num. rotatable bonds 2
Num. H-bond acceptors 7
Num. H-bond donors 3
Molar Refractivity 54.83
TPSA 110.60 Å² | Log Po/w (SILICOS-IT) -0.94
Consensus Log Po/w -0.72

Log S (ESOL) -0.67
Solubility: 5.67e+01 mg/ml ; 2.15e-01 mol/l
Class Very soluble
Log S (Ali) -0.36
Solubility 1.15e+02 mg/ml; 4.38e-01 mol/l
Class Very soluble
Log S (SILICOS-IT) -0.34
Solubility 1.21e+02 mg/ml ; 4.59e-01 mol/l
Class Soluble | P-gp substrate No
CYP1A2 inhibitor No
CYP2C19 inhibitor No
CYP2C9 inhibitor No
CYP2D6 inhibitor No
CYP3A4 inhibitor No
Log Kp (skin permeation) -8.94 cm/s | Muegge Yes
Bioavailability Score 0.55
Synthetic accessibility

3.71 |

Table 9: Evaluation of pharmacokinetic, physicochemical, and drug-likeness properties of ligands using the SWISS-ADME web server
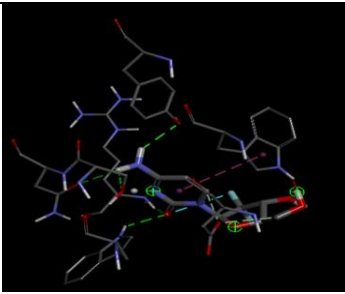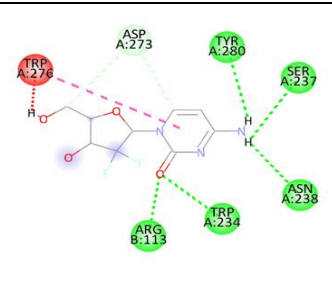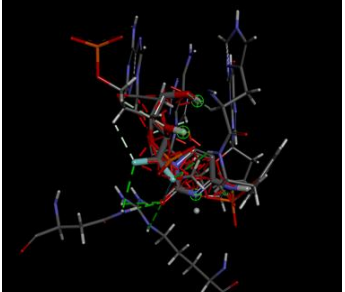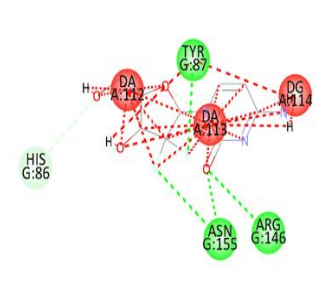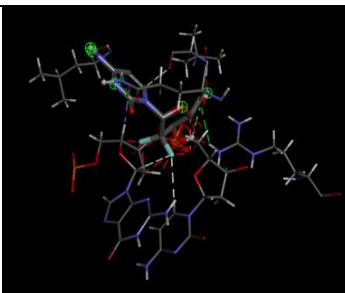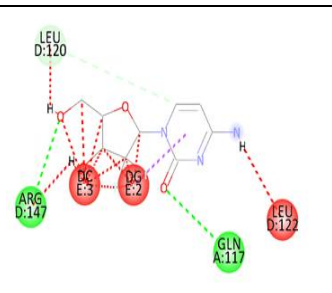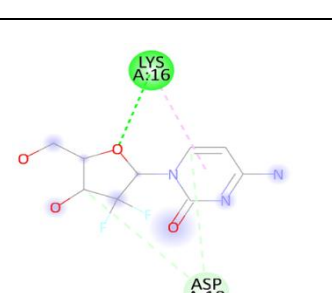
The BOILED-Egg method is capable of predicting two essential ADME parameters, namely, passive gastrointestinal absorption (HIA) and brain access (BBB) of ligands, while also taking into account active efflux from the central nervous system or the gastrointestinal lumen. This outcome is determined solely by two physicochemical descriptors, specifically, WLOGP and TPSA, which are indicative of lipophilicity and polar surface area, respectively. Kaempferol falls in the white portion have highly possible HIA incorporation and least likely BBB penetration in addition to not being a substrate of the P-glycoprotein receptor (Fig. 39E.), is nearly identical to Gemcitabine (Fig. 39I.), while

116

Verapamil falsehood in the inner yolk portion with a high likelihood of BBB permeation and also actively pumps out by P-gp (Fig. 38G).
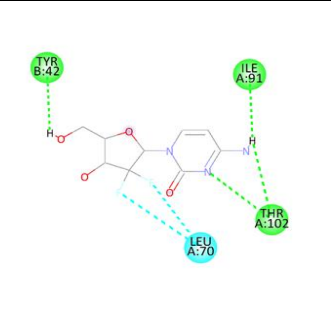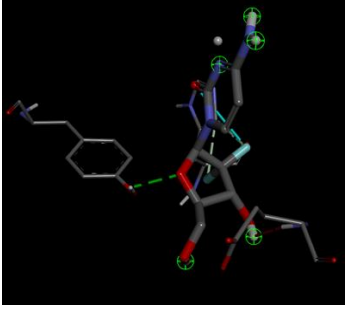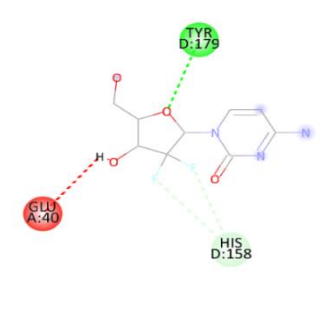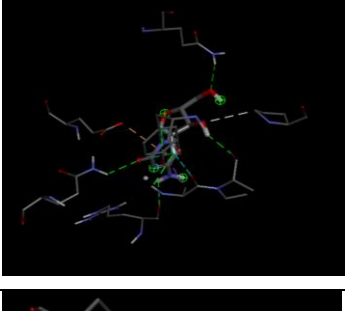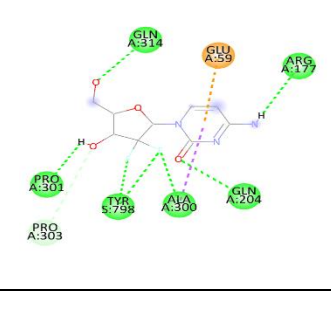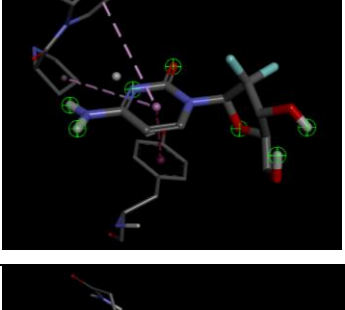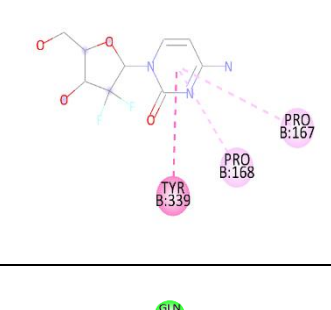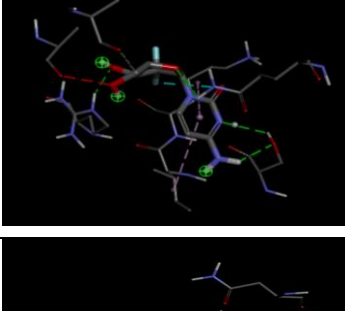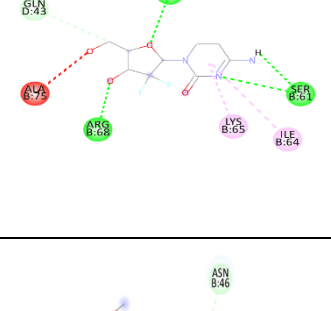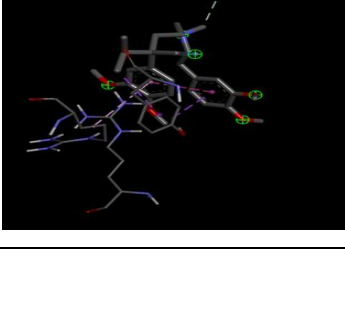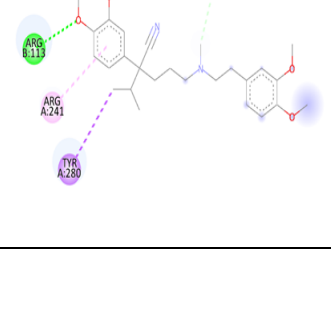
Target prediction: To predict the most likely targets of our ligands or bioactive molecules, we employed the Swiss Target, which predicts the macromolecular targets (human proteins) of our ligands. According to Swiss-Target analysis, Kaempferol shows high activity against enzyme targets followed by kinase receptors. The next class of potential targets includes oxidoreductase, G-protein coupled receptors, and lyase receptors. The least affected group of proteins consists of proteases, phosphatases, transcription factors, and transporter proteins (Fig. 39J). On the contrary, the Verapamil drug exhibits the highest activity against G-Protein coupled receptors followed by kinase receptors. The Lyase protein, voltage-gated ion channels, and transporter proteins are also potential targets that can be targeted for biological activities. Cytosolic proteins, active transporters, and membrane receptors are the least likely targets of this ligand (Fig. 38K). The biological activity of Gemcitabine reveals that it has the highest affinity for enzymatic receptors, followed by the Lyase and Protease group of proteins. Oxidoreductase and Transferase class of enzymes are also putative targets, whereas GPCR receptors, Ligand-gated ion channels, and electrochemical receptors are the least affected ones (Fig. 38L).
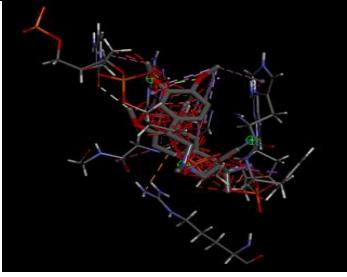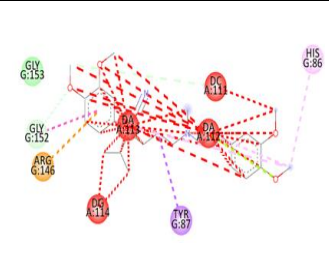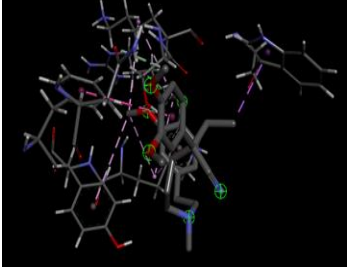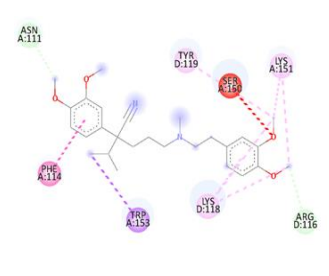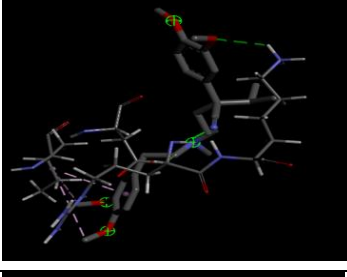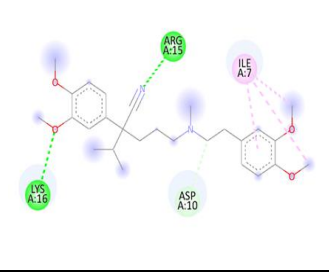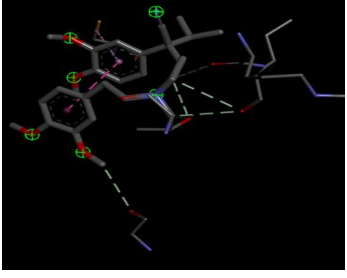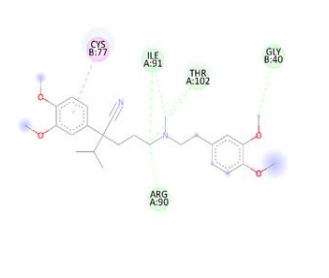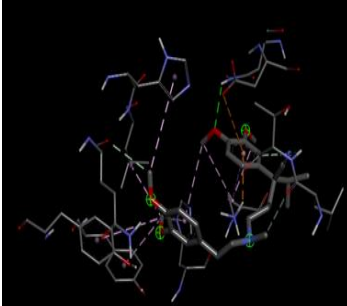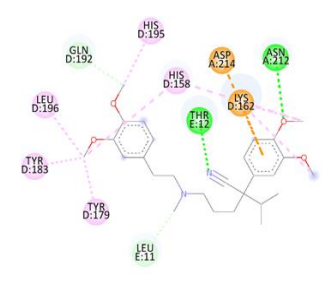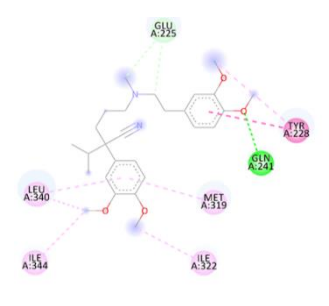
Molecular docking studies: Molecular docking was conducted to analyze the binding interactions between the selected ligands and the receptor proteins investigated in our ex vivo experiments. Kaempferol exhibited the maximum binding effect to NHE1, a plasma membrane ion anti-port transporter along with a binding affinity of -8.2 kcal/mol. These protein markers play vital role to maintain an acidic microenvironment in cells and consequently, the induction of Lysosome expression promoted ROS activity finally triggering autophagy-induced cell death. The other targeted markers, namely TFEB, LC3-II, NANOG, and CD44, exhibited notable binding affinities, with each of them displaying a high affinity of more than -7.0 kcal/mol. TFEB is a well-established transcription factor that participates in the development of lysosome induced autophagy, and LC3-II activates autophagy in response to starvation. The two additional chemoresistance markers are also positively related, with the former playing a significant part in stem cells and the latter performing an immunological function and maintaining an acidic environment. MDR1 exhibited the minimum binding with about -4.7 kcal/mol score which might conclude, the regulation of the Pg-P receptor was not controlled by totally Kaempferol. Verapamil also displayed the maximum binding to NHE1 (-7.6 kcal/mol), followed by TFEB (-7.6 kcal/mol) almost similar to the former ligand. NANOG and LC3-II, showed lower binding
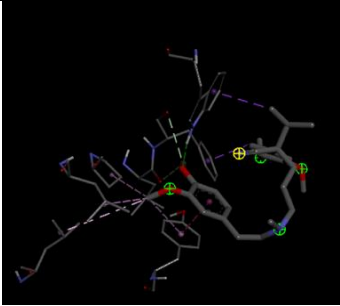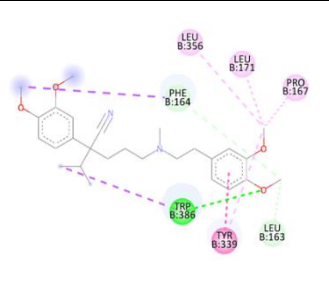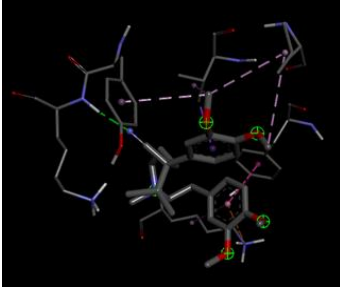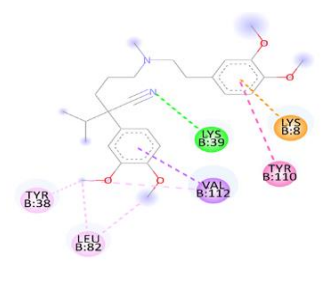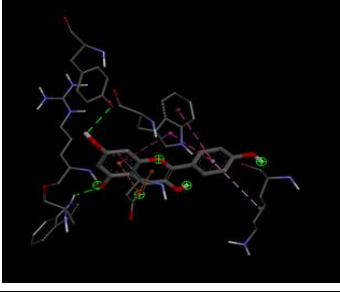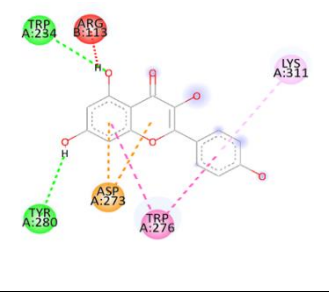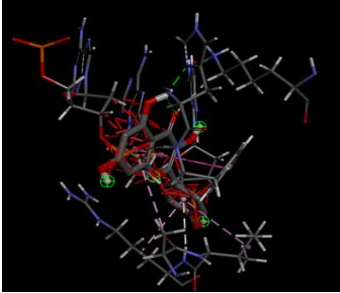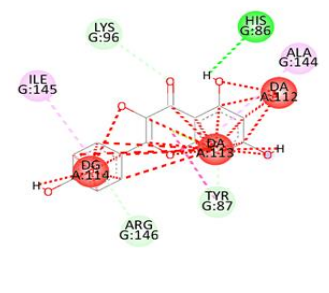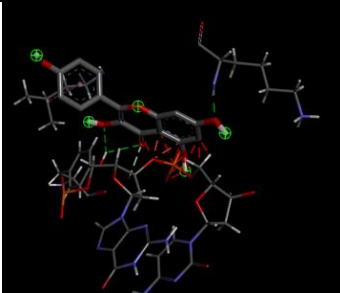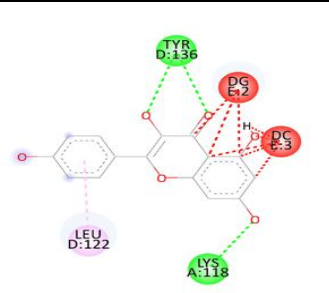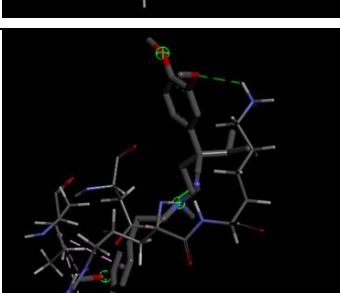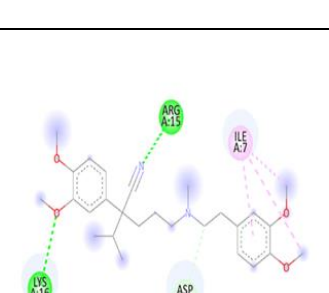
to this drug having docking scores of -6.1 and -5.6 kcal/mol respectively. SOX2 and OCT4 transcription which play important roles in development and self-renewal, stem cell plasticity is at the lower ends with binding around -5.0 kcal/mol. The combination of KV may upregulate the function of MDR1 thereby increasing $Ca2+$ ions as well as lysosomes, increasing the anti-cancerous activity of the ligand combination manifold. Gemcitabine showed bindings in an almost similar range with LC3-II showing the highest (-6.9) which is much lower than the top-most receptor binders of previous ligands and then NHE1 (-6.8 kcal/mol) (Table 10).
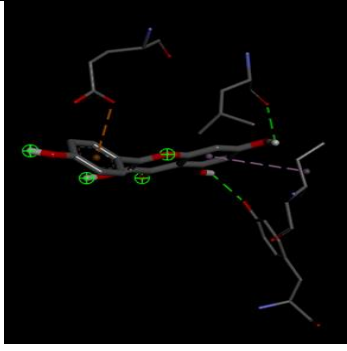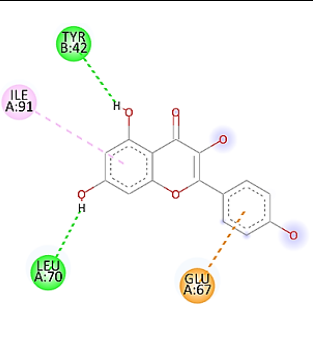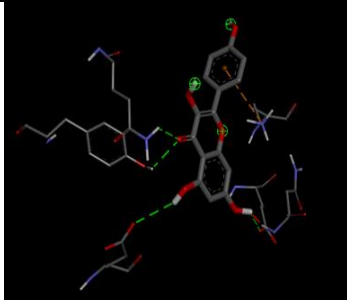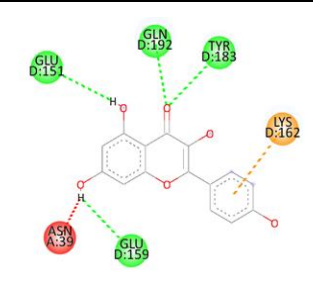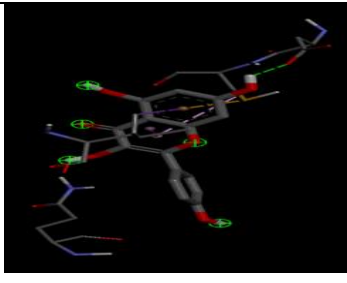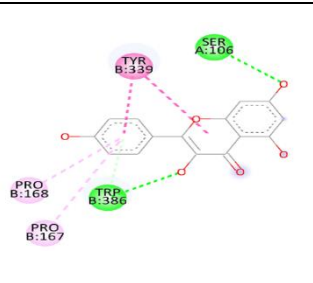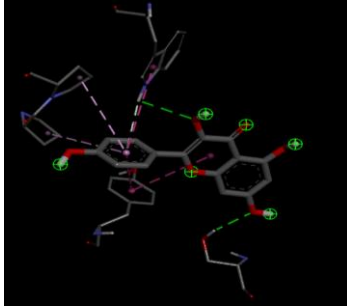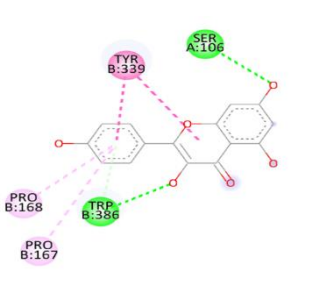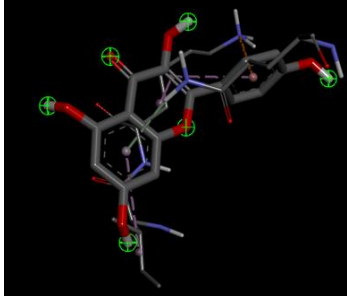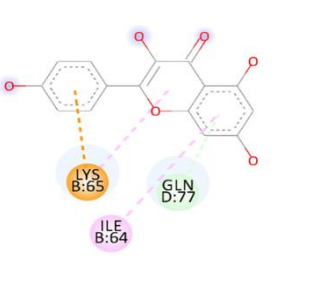
Ligand	Receptor	3D interaction	2D interaction	Binding energy	Inhibition /dissociation constant (Ki)
Gemcitabine	SOX2(6WX9)			**-5.6 ± 0.05**	**0.997743**
	OCT4 (5KRB)			**-6.1 ± 0.06**	**0.997543**
	NANOG(4RBO)			**-6.1 ± 0.063**	**0.997543**
	MDR1 (6COV)			**-4.3 ± 0.052**	**0.998267**

	CD44 (1UUH)			-6.6 ± 0.083	0.997341
	TFEB (6A5S)			-6.4 ± 0.072	0.997421
	HIF1A (1H2K)			-5.4 ± 0.061	0.997823
	NHE1 (7DSW)			-6.8 ± 0.052	0.997260
	LC3-II (5XAC)			-6.9 ± 0.068	0.997220
Verapamil	SOX2(6WX9)			-4.8 ± 0.052	0.998065

OCT4 (5KRB)			**-4.9 ± 0.059**	**0.998025**
NANOG(4 RBO)			**-6.1 ± 0.066**	**0.997543**
MDR1 (6COV)			**-5.2 ± 0.058**	**0.997907**
CD44 (1UUH)			**-5.7 ± 0.044**	**0.997703**
TFEB (6A5S)			**-7.4 ± 0.051**	**0.997019**
HIF1A (1H2K)			**-5.5 ± 0.056**	**0.997836**

120

	Target	3D	2D	Binding energy	Correlation

	NHE1 (7DSW)			**-7.6 ± 0.069**	**0.996938**
	LC3-II (5XAC)			**-5.8 ± 0.086**	**0.997666**
Kaempferol	SOX2 (6WX9)			**-6.4 ± 0.091**	**0.997421**
	OCT4 (5KRB)			**-7.0 ± 0.11**	**0.997180**
	NANOG(4RBO)			**-7.3 ± 0.096**	**0.997060**
	MDR1 (6COV)			**-4.7 ± 0.075**	**0.998105**

121

CD44 (1UUH)			**-6.9 ± 0.095**	**0.997220**
TFEB (6A5S)			**-7.5 ± 0.078**	**0.996979**
HIF1A (1H2K)			**-6.5 ± 0.097**	**0.997381**
NHE1 (7DSW)			**-8.2 ± 0.099**	**0.9966797**
LC3-II (5XAC)			**-7.8 ± 0.11**	**0.996858**

Table 10: Molecular Docking-based computational analysis of ligand-receptor interactions. The results include 3D and 2D interaction maps of the ligand-receptor complexes, with identified interacting residues and binding affinities. The most favourable interactions are highlighted in red in the table.

122

Likewise, the binding strength can be compared using the inhibition constant (Ki), which indicates the degree of inhibition of an enzyme by a ligand. The lower the Ki value, the higher the binding affinity between the receptor and ligand. While there wasn't a significant numerical difference in the values, the differences in enzyme chemistry are noticeable. The value of Ki diversified between 0.998267 (G-MDR1) and 0.9966797 (K-NHE1). Within the range of favourable binding affinity determined (i.e., around 0.996) through in silico analysis, we identified three complexes such as K-NHE1, K-TFEB and K-LC3-II. Given the outcomes, it can be firmly concluded that Kaempferol is the most potent drug among all the compounds evaluated in this study. In addition, when comparing the amino acid residues involved in receptor binding or the active residues of the binding pocket, significant differences have been observed among the ligands. In SOX2, Gemcitabine or Kaempferol appeared to be bound to a similar pocket however not Verapamil, despite all of them binding to a single common amino acid residue, LYS B113, there were differences in the hydrogen bonds formed between the ligands and the receptor. Similarly, a similar pattern was observed in OCT4 where ARG G146 was identified as the common amino acid. However, in the case of NANOG, no such common amino acids were observed in the binding pockets. On the other hand, the MDR1 receptor exhibited a distinct trend as all the ligands were found to be bound to the same binding pocket with significant similarity in terms of amino acids and bonding. CD44 exhibited dissimilar remains While Gemcitabine or Kaempferol displayed similar affinity for binding pocket. TFEB also exposed dissimilar amino acids in binding pockets and these markers bind to different pockets. In the case of NHE1, Gemcitabine and Kaempferol binds to a highly similar active site of the receptor, as evidenced by the shared amino acid residues, unlike Verapamil. The amino acid Proline (B167) is conserved among all three complexes, and each of the ligands appears to interact close to this target. The association of the HIF1 α receptor with Gemcitabine and Kaempferol exhibited numerous bindings remains likeness demonstrating that they are observed to bind to the identical binding pocket. Several amino acid residues are shared between the ligands for LCS-II, indicating that they bind to the same binding pocket. However, in the case of V, there are no shared residues. While the other one is significantly dissimilar in terms of binding amino acids. In general, it can be deduced that the ligands Gemcitabine and Kaempferol demonstrate striking similarities in terms of receptor binding, implying that they exert comparable effects or act via comparable mechanisms in biological systems. Verapamil on the other hand is radically different and enhances the mode of action of Kaempferol.

Discussion

ROS-mediated regulation of autophagy plays a dual role in inducing both uncontrolled cell proliferation as well as apoptotic cell death, thereby acting as promising targets for novel anti-cancerous therapy. The survival of cancer cells under ROS-induced stress conditions is maintained by lysosomal activity **[Zhang, Xiaoli et al. 2016]**. Studies have reported enhancement in the activity of lysosomes under cellular stress, mediated by autophagic cell death as compared to mitochondrial activity **[Zhang, Xiaoli et al. 2016]**. During oncogenic transformation, an increase in the number and volume of lysosome up-regulates lysosomal enzymes that play a critical role in cancer growth, metastasis, and multidrug resistance (MDR). P-glycoprotein (Pgp), a product of the MDR1 gene that is expressed in the intracellular organelles is known to confer drug resistance **[Schneider, Lina S et al. 2015]**. A limited study shows an elevation in the level of Ca2+ ion as one of the factors responsible for PgP overexpression in tumour cells **[Nygren, P et al. 1991]**. Ca2+ signalling initiates upon stimulation of the cell through the entry of extracellular Ca2+ and its discharge from the intracellular stores. Apart from Endoplasmic Reticulum, the lysosome acts as a significant intracellular Ca2+ store that is responsible for the regulation of various cellular processes **[Settembre, Carmine et al. 2013]**. In Fig. 28, we observed an increase in the expression of lysosomal Ca2+ in tumours with respect to normal along with the upregulation of chemo-resistant markers such as CD44, NANOG, MDR1 and ATP1B1.

Several studies have reported development of chemo resistance in patients after long-term treatment with chemotherapeutic drugs **[Liou, Geou-Yarh, and Peter Storz. 2010]**. The ambiguous and explicit relationship of several markers such as CD44, NF-KB, PI3K/AKT, MAPK, HIF1α, ABC transporter family proteins and NANOG with resistance to Gemcitabine has been discussed in a variety of cancers **[Jia, Yanfei, and Jingwu Xie. 2015]**. Previous reports have shown that tumours with overexpressed CD44 is more invasive and tend to become resistant to Gemcitabine. Verapamil, an inhibitor of ABC transporter resensitizes the resistant cells to Gemcitabine whereas, RNAi of CD44 represses the clonogenic properties of the resistant cells **[Jia, Yanfei, and Jingwu Xie. 2015]**. It has been reported that CD44 in association with P-gp induces cell migration or invasion of BC tumour cells **[Miletti-González, Karl E et al. 2005]**. Moreover, the CD44-NANOG complex together with the help of pluripotent markers like SOX2 and OCT4 leads to the activation of NANOG and expression of embryonic stem cell markers, important in chemotherapeutic drug resistance **[Bourguignon, Lilly Y W et al. 2008]**. An upregulation of HIF-1α in Gemcitabine-treated resistant cells has been reported. Also, its inhibition in

the same triggers partial reversal in the phenomenon of EMT phenotype [**Jia, Yanfei, and Jingwu Xie. 2015**]. Furthermore, the association of HIF-1α with Warburg's effect contributes to an increase in the expression of glucose transporter as well as lactate accumulation [**Jia, Yanfei, and Jingwu Xie. 2015**]. Additionally, the Na+/H+ pump (NHE1) is known to play a vital role in the survival of cancer cells. Studies have proclaimed that increase in the expression of NHE1 causes resistance to chemotherapeutic drugs like doxorubicin (DOX) [**Chen, Qi et al. 2019**]. Besides, Na/K-ATPase is another relevant marker that stimulates the activation of various oncogenic signalling pathways and plays a vital role in the elevation of stress-elicited cellular pathways like autophagy and apoptosis [**Themistocleous, Sophia C et al. 2021**]. However, an underlying mechanism of how these chemo-resistant markers are linked to one another has not yet been reported.

The expression of chemoresistance markers in different cell lines and mice models has been extensively studied, but previous research has not examined these gene signatures in ex-vivo breast cancer models. Additionally, no prior studies have compared the expression of all these chemoresistance genes under both low and high glucose conditions. Our study is unique in that we observed the effects of our drug combination, KV, on markers that regulate chemoevasion, tumour stemness, acidosis, and lysosome upregulation, all of which are critically associated with chemoresistance (as shown in Fig. 40). We used Gemcitabine as our standard positive control drug, given that it is a mainstream treatment for metastatic breast cancer and patients often develop early resistance to it after a short period.

Drawing on prior research on the antagonistic impact of Verapamil on multidrug efflux transporters, we selected it as a supplementary drug in our previous investigation and observed that co-administration of Kaempferol with Verapamil augments its efficacy as an anti-cancer agent. Another significant function of Verapamil falls in its potency to expel reduced Glutathione with a multidrug efflux pump [**Settembre, Carmine et al. 2013**], for which addition of Verapamil to Kaempferol, generates heightened oxidative stress in the tumour cells of our study. Kaempferol alone can induce the generation of reactive oxygen species (ROS), specifically superoxide anion (O2•-), in cancer cells [**Sharma, Vivek et al. 2007**] and has been reported to exhibit anti-inflammatory effects in tumours [**Sharma, Vivek et al. 2007**]. In our investigation, the synergistic combination of drugs like KV arrested the cellular antioxidant scavenging phenomenon that was observed in the NBT experiment. Furthermore, the combined drugs show effect on reduction the expression of

HIF1α, NHE1, MDR1 etc. that lead vital role in chemo evasion depending oxidative stress phenomenon.

Autophagy is modulated by ROS, such as superoxide anion ($O_2^{\bullet-}$) and hydrogen peroxide (H_2O_2). In our investigation, the KV increased autophagy-dependent cell death and promoted ROS overproduction under low glucose condition. By utilizing NBT assay, we observed that $O_2^{\bullet-}$ was specifically induced under low glucose conditions. Furthermore, **Zhang, Xiaoli et al. 2016** reported that the viability of cells was significantly increased with the addition of the autophagy inhibitor 3-methyladenine in Verapamil treatment, indicating that Verapamil-induced autophagy may contribute to its cytotoxicity. In our investigation, the treatment with KV also resulted in the generation of ROS, which led to oxidative stress and was also found to initiate autophagy.

It has been proposed that increased expression of glucose transporters may play a crucial role in sustaining the growth of cancer cells **[Vishvakarma, Naveen Kumar et al. 2013]**. Various medical conditions can elevate blood glucose levels, resulting in decreased effectiveness of chemotherapy and imparting resistance to tumours **[Vishvakarma, Naveen Kumar et al. 2013]**. In preclinical investigations, the culture media is typically maintained at a glucose concentration of approximately 17.5 mM, with extracellular levels of around 10 mM **[Zhang, Xiaoli et al. 2016]**. In our study, we found the effectiveness of the candidate drug combination (KV) in low (5.55 mM) and high extracellular glucose (25 mM) concentrations. The outcome indicated that KV displays effectiveness under low glucose conditions. In our previous investigation, we reported that KV treatment led to robust γH2AX expression in cancerous cells, but not in non-malignant breast tissue (Nandi et al.2022). In our current experiment, in low glucose conditions, KV exhibited strong efficacy in the reduction of the stemness properties and downregulation of the chemo evasion markers such as NANOG, SOX2, OCT4, MDR-1, CD44, Na+-K+ ATPase, however, KV exhibited aberrant results in high glucose panel.

Autophagy has a crucial role in lysosomal Ca2+-dependent scavenging of ROS in cancer. Previous studies have suggested that sequestration of lysosomotropic drugs promotes Ca2+ release into the cytoplasm, resulting in calcineurin stimulation, chelation of cytosolic Ca2+, and translocation of TFEB into the nucleus **[Zhitomirsky, Benny et al. 2018]**. In our investigation, the LKV panel showed decreased levels of intracellular Ca2+ and lysosomal expression compared to the untreated group. From our experiment, we pointed out that

downregulation of TFEB, in treatment with KV in low glucose condition decreased the lysosomal Ca2+ related chemo-resistance.

Extensive research has demonstrated that the upregulation of ion channels can impede the proliferation of tumours and metastatic activity in several types of cancer cell lines **[Holthouser, Kristine A et al. 2010]**. Previous investigations have reported a 35% increase in breast cancer incidence associated with the use of cardiac glycosides, although it remains unclear whether Na/K-ATPase and GLUTs have a direct causal relationship with breast cancer development **[Holthouser, Kristine A et al. 2010]**. Interestingly, normal and tumour cells display differential uptake of glucose via GLUTs, which is associated with the Na/K-ATPase pump and facilitated by the presence of ATP and Ca2+ ions. Further studies have postulated a correlation between ion channels and the Warburg effect, hypoxia, and the involvement of the Na+/K+ pump in hypoxia generated by the acidic pH mechanism of tumours. The deleterious consequences of Na+/K+ ATPase and the excessive production of ROS may elucidate the phenomenon of oncogene-induced cellular senescence **[Holthouser, Kristine A et al. 2010]**. In our previous research research **[Nandi, Sourav Kumar et al. 2022]**, we investigated the potential of KV to modify the acidic pH environment of tumour cells. Herein, we observed that Na+/K+ATPase were reduced upon KV treatment in low glucose panel along with the reduction of Ca^{2+} however in identical circumstances, ROS was significantly upregulated and excessively generated.

The Na+/K+ ATPase is an active antiporter that expels Na+ ions outside the cell, creating a gradient that drives Na+ and glucose reabsorption **[Holthouser, Kristine A et al. 2010]**. Similarly, Na+/K+ exchangers such as NHE1 maintain tumour acidosis by exchanging H+ ions for Na+ ions. Previous studies have shown that hypoxia promotes acidosis through HIF-1α-mediated upregulation of NHE1. Tumour acidosis is closely associated with hypoxia **[Calvert, John W et al. 2006]**, and hypoxia-induced acidosis increases the expression of proteases that remodel the extracellular matrix. In our experiment, the expression of NHE1 was also decreased in LKV treatment panel in both MDA-MB-231 cells and primary tumour tissue. In LKV treatment conditions, the expression of Na+/K+-ATPase protein was found to be decreased, in addition to its suppressive effect on lysosomal Ca2+-related resistance to chemotherapy via TFEB in our study, whereas in HKV treatment, all of these pathways showed abnormal regulation, and the treatment with KV did not affect these corresponding markers of resistance to chemotherapy. Therefore,

127

it can be postulated that extracellular glucose substantially impedes the anti-proliferative effectiveness of KV treatment.

Overexpression of GLUTs has been linked to the induction of carcinogenesis and tumour aggressiveness **[Holthouser, Kristine A et al. 2010]**. In hexose, uptake assays, MCF-7 and MDA-468 cells were found to regulate the GLUT2 glucose transporter, which is expressed in both normal breast tissue and breast tumour tissue **[Zamora-León, S P et al. 1996]**. Previous studies have suggested that CD44 plays a role in the regulation of glucose metabolism in metabolic tissues **[Weng, Xiong et al. 2022].** While CD44's involvement in stem cell self-proliferation and differentiation is well-established, its role in glucose metabolism remains poorly understood. Furthermore, Ca^{2+} influx has been shown to regulate the proteolytic activity of the CD44 ectodomain from the membrane. CD44 overexpression also increases lactate dehydrogenase expression, promoting lactate glycolysis through HIF-1α in breast cancer cells **[Gao, Ruifang et al. 2018]**. Earlier research has indicated that PFKFB4, a bi-functional enzyme, can catalyze the conversion of 6-phosphofructose (F6P) to fructose-2,6-biphosphate (F-2,6-BP) during glycolysis. Moreover, it has been found that CD44 enhances glycolysis by elevating the expression of PFKFB4 **[Gao, Ruifang et al. 2018]**. Further studies have suggested that HIF-1α can control the function of GLUTs **[Calvert, John W et al. 2006]**. In our experiment, the expression of both *HIF-1α* and *GLUT2* was decreased in LKV conditions. The outcome of HIF1α protein expression was decreased in l-DMEM while increased in h-DMEM. In our experiment, the reduction of glucose uptake by GLUT-2 was observed utilizing 2-NBDG, a fluorescent glucose analogue, in the immune-cytochemical co-localization study of the MDA-MB-231 cell line.

Prior findings have demonstrated that in neoplastic cells, elevated glucose levels **[Holthouser, Kristine A et al. 2010]** and reactive oxygen species (ROS) promote the stabilization of hypoxia-inducible factor-1 alpha (HIF-1α) **[Jung, Seung-Nam et al. 2008]**, thereby promoting their aggressive phenotype. In our study, we observed that upon KV treatment, HIF-1α expression was found to be reduced along with an increase in the production of ROS levels, which ultimately led to cell death under low glucose conditions. An initial investigation demonstrated that the knockdown of HIF-1α in cells led to the induction of lysosomal degradation and the development of autophagosomes, along with the promotion of the expression of autophagy-related proteins LC3-II and p62 **[Huang, Jinling et al. 2019]**. Lysosomal impairment can lead to the release of proteolytic enzymes into the cytosol, inducing apoptosis. Prolonged activation of the autophagy-lysosomal

system can lead to cell death by autophagy, as demonstrated by previous studies [**Linder, Benedikt, and Donat Kögel. 2019**]. In our experiment, the expression of autophagy markers such as LC3-II and p62 were increased upon KV treatment conditions in low glucose conditions. From our findings, based on our hypothesis, it is plausible that in tumours where Na+/K+ ATPase is upregulated, the combination of elevated extracellular glucose and Na+ ions leads to the cooperative activation of glucose transporters such as GLUT2 and the Na+/H+ antiporter NHE1, both of which are Na+-dependent. This process, in turn, sustains extracellular acidosis. The outcome of the western blot experiment also showed that the expression of HIF1α is also reduced and thus, numerous molecular oncogenic networks are inhibited, interpreting the inefficiency of our combined drugs.

In addition to the ex vivo investigation, we conducted an in-silico analysis of all three ligands to obtain a better understanding of their mechanism of action in inhibiting cancer cells, utilizing resources such as the Berman database [**Berman, Helen et al. 2003**] and methods such as molecular docking and virtual screening [**Daina, Antoine, and Vincent Zoete. 2016**]. We utilized the combination of Kaempferol with Verapamil for this experiment at a concentration such that Verapamil alone did not exhibit any significant impact on cancer cells (i.e., IC-5), while its co-administration with Kaempferol led to a synergistic effect and potentiated the anticancer activity. The molecular docking study was conducted separately for each ligand (Kaempferol with Verapamil and Gemcitabine), revealing that the combination of these molecules exerts varying binding affinities, resulting in differential physiological effects. When present in an intracellular environment, these two substances exhibit a greater effect than when administered individually, and Gemcitabine does not cause direct cytotoxic effects on cancer cell lines when used as an adjunct or at very low concentrations. The in-silico experiment appropriately maintained the ex-vivo outcome and revealed that both ligands exhibit a pleiotropic effect on various receptor classes or targets in a biological system, as indicated by the Swiss-target database. Kaempferol exhibited numerous drug-like properties and physicochemical characteristics along with high absorption. Conversely, Verapamil exhibited high BBB penetration and efflux prediction utilizing the Pg-P receptor. It could be hypothesized that Kaempferol might be changed the specificity of the Pg-P receptor by utilizing Verapamil promoting the ant-cancer effect through induction of the synergistic mode or action. Kaempferol achieved every one of the drug-like limitations and computational screening displayed a close resemblance to numerous phytochemicals, whose efficacy as potent anti-cancer agents has been widely reported. Verapamil is also efficacious, and its existence, even in a negligible

quantity, exerts an additional effect on Kaempferol, and vice versa. The molecular docking results demonstrated that Kaempferol has the highest binding affinity compared to Verapamil. The combination of both Kaempferol and Verapamil in the cellular milieu may exert synergistic effects by targeting different signalling cascades and pathways, leading to the effective inhibition of various cancer cells. Our ex vivo study showed that the selected chemical combination efficiently inhibits cancerous cells by inhibiting different proteins. These results were corroborated by in silico studies, which showed that all proteins had negative binding energy or high binding affinity **[Berman, Helen et al. 2003]**. The precise mechanism of action by which the two compounds may combine within the cell to form a novel compound or whether their presence in the cellular microenvironment leads to an increase in efficacy of the other remains an active area of investigation due to the lack of certainty. Consequently, we distinctly examined the binding affinities independently in silico model that documented the anticarcinogenic effects or if both act in combination, it is anticipated to be significantly more effective than their counterparts. Moreover, we have tried to illuminate the mechanism of the anti-cancer effect of the candidate drug combination by ex-vivo and in-silico experiments model, more investigations are desirable to be completed that can reveal new mechanisms or pathways as well as comprehensive process and regulation of the suppression.

In Figure 40, we have demonstrated that there is an interconnection between markers that regulate tumour acidification, cancer stemness, drug resistance, and lysosomal upregulation, all of which contribute to the development of a chemoresistant phenotype in tumour s. Tumour s evade oxidative stress by inducing upregulation of Lysosomal $Ca2^+$, TFEB, and HIF1α, as well as several transporters such as Na+/K+ ATPase, NHE1, and GLUT2. The corelation of chemo-resistance with Lysosomal Ca+ was attenuated through KV drug combination in low glucose (LG) condition but not in high glucose conditions. Kaempferol treatment resulted in the overproduction of reactive oxygen species (ROS), causing a disturbance in lysosomal expression and perturbing the lysosomal calcium-based chemo-evasive mechanism. This was followed by ROS-mediated autophagy and cell death. Kaempferol was found to downregulate all the cognate markers responsible for chemoresistance and tumour aggressiveness, particularly under low glucose conditions. In contrast, Gemcitabine did not demonstrate similar robustness in downregulating these markers. In the corresponding figure, we demonstrated the distinctiveness of our potential drug combinations in disrupting chemoresistance pathways via the suppression of these
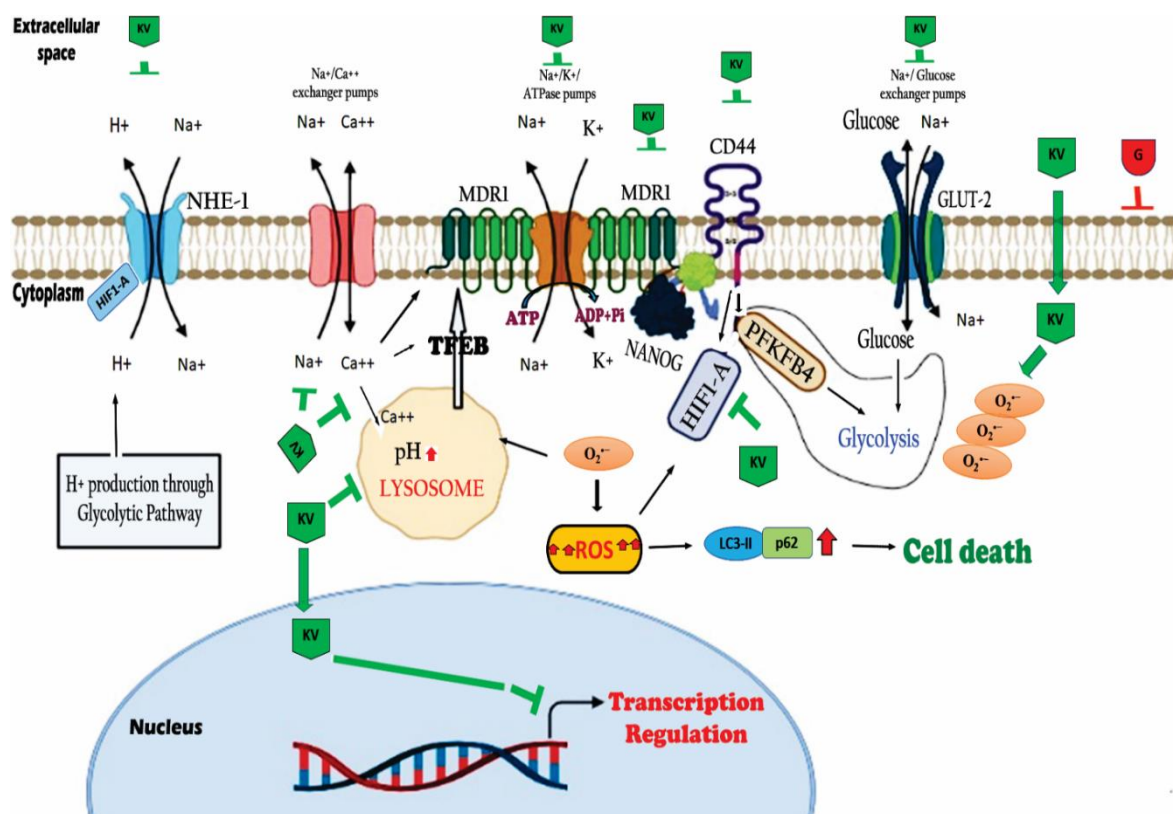
Figure 40: Disruption of lysosomal calcium homeostasis-based chemoresistance mechanism by Kaempferol and Verapamil (KV) with an emphasis on excessive generation of reactive oxygen species (ROS), followed by ROS-mediated autophagy and cell death. Tumours evade oxidative stress by upregulating lysosomal calcium, transcription factor EB (TFEB), hypoxia-inducible factor 1-alpha (HIF1α) along with inducing several transporters like sodium/potassium adenosine triphosphatase (Na+/K+ ATPase), sodium/hydrogen exchanger 1 (NHE1), and glucose transporter 2 (GLUT2). KV treatment inhibited the association of chemoresistance with lysosomal calcium in low glucose (LG) conditions. KV downregulated all these cognate markers responsible for chemoresistance and tumour aggressiveness, under low glucose condition, whereas Gemcitabine was ineffective.

markers. In summary, our study presents a novel and innovative approach for inhibiting breast cancer cells by using the KV combination, which leads to a significant increase in expression and inhibits the release of Ca2+ ions, resulting in the downregulation of chemoresistance, glucose metabolism, acidosis, and stemness markers. Our study demonstrates the multifaceted and promising anticancer mechanism of our candidate drugs, which may pave the way for new cancer therapeutics and prevention strategies. Furthermore, our findings may inspire further research into the detailed mechanisms and signalling pathways involved in this therapeutic phenomenon.

Conclusion

Aggressiveness and chemo evasion in breast cancer is conferred by Breast cancer stem cell (BCSC), a distinct niche of cancer cells in the tumours. Acquisition of chemo-evasive mechanisms has a close association with stem cell renewal, the complex mechanism of which is not fully unravelled. DNA-damaging drugs cannot target BCSC as the cells are mostly quiescent and have fully functional DNA repair genes. As replication inhibitors cannot efficiently target breast cancer stem cells, we wanted to look for plant-derived synthetic antimetabolites with less systemic toxicity, to target primary breast tumours. The outcome of our study would generate know-how regarding the application of Kaempferol as monotherapy or in combination with conventional drugs towards the management of treatment-resistant breast carcinoma and associated inflammation.

Herein, we wanted to check the efficacy of Kaempferol on tumour explants, obtained from NACT recipient TNBC patients. Our study revealed that Kaempferol attenuated the expression of induced pluripotent stem cell markers (NANOG, CD44, and ALDH1) as well as markers associated with chemo evasion, viz. MDR1, CD44+/ CD24- and CD44+/CD326+, downregulated the expression of pro-survival markers BCL-2, Ki-67, NF-kB and upregulated Caspase 3 expression. In another study setup, we cultured and enriched BCSC populations from freshly excised and ex-vivo cultured tumours and validated the data on BCSC-enriched breast cancer cell line MDA-MB-231. We observed that Kaempferol could attenuate the viability of BCSC and the effect of Kaempferol was even more robust when combined with Verapamil (50% inhibitory dosage for Kaempferol alone: 223.6µM; in combination with Verapamil: 40.714µM). Kaempferol alone or along with Verapamil could reduce tumorosphere formation, and reduce RNA and protein expression of iPSC markers (SOX2, OCT4, NANOG, MDR1, CD44) in breast cancer stem cells derived from primary breast tumour and breast cancer cell line MDA-MB-231. Kaempferol alone or along with Verapamil (KV) could also induce G2/M dependent cell cycle arrest in the MDA-MB-231 cell line. We conclude that Kaempferol alone or in combination with a micro-dosage of Verapamil could serve as an efficient candidate drug for the treatment of aggressive, drug-resistant breast cancers. The outcome of this study potentiated the role of Kaempferol as an ideal candidate for cancer chemotherapeutics, alone or in combination with Verapamil, an inhibitor of ATP-dependent proton pump.

In another part of the investigation, we studied the effectiveness of KV under differential glucose stress, on the expression pattern of genes that maintain tumour acidosis, hypoxia

and chemo-evasion markers and revealed that the following phenomenon and the targeted markers such as HIF1α, GLUT2, NANOG, MDR1, CD44, ATP1B1, NHE1 were downregulated upon the treatment of KV in low glucose condition in addition of interfering with lysosome-Ca2+-TFEB pathway-based chemoresistance through ROS overproduction and autophagy induced cell death. We also documented a molecular model of the interactome of these candidate genes that are expressed under glucose stress, in the presence of our candidate drug KV. The outcome of this study documented that KV had robust anti-proliferative efficacy through downregulation of the aforementioned candidate genes regulating tumour acidosis, hypoxia and chemoevasion, perturbation of lysosome-Ca2+-TFEB mediated autophagic survival and upregulation of cell death under low glucose condition, indicating the therapeutic potential of the candidate drug system under low glucose condition. Our candidate drugs, Kaempferol with Verapamil, disrupted several chemo evasion networks in breast cancer, unlike other classes of inhibitors which act by decreasing the ROS or overall oxidative stress of the cellular environment. The cumulative information on the chemo tolerance mechanisms and the improvement of therapeutic approaches will improvise clinical outcomes and endorse a novel therapeutic strategy for overcoming chemoresistance in breast tumours.

References

Al-Hajj, M., Wicha, M. S., Benito-Hernandez, A., Morrison, S. J., & Clarke, M. F. (2003). Prospective identification of tumorigenic breast cancer cells. *Proceedings of the National Academy of Sciences of the United States of America*, *100*(7), 3983–3988. https://doi.org/10.1073/pnas.0530291100

Altunok, İ., Aksel, G., & Eroğlu, S. E. (2019). Correlation between sodium, potassium, hemoglobin, hematocrit, and glucose values as measured by a laboratory autoanalyzer and a blood gas analyzer. *The American journal of emergency medicine*, *37*(6), 1048–1053. https://doi.org/10.1016/j.ajem.2018.08.045

Alvarado-Ortiz, E., de la Cruz-López, K. G., Becerril-Rico, J., Sarabia-Sánchez, M. A., Ortiz-Sánchez, E., & García-Carrancá, A. (2021). Mutant p53 Gain-of-Function: Role in Cancer Development, Progression, and Therapeutic Approaches. *Frontiers in cell and developmental biology*, *8*, 607670. https://doi.org/10.3389/fcell.2020.607670

Anders, C. K., & Carey, L. A. (2009). Biology, metastatic patterns, and treatment of patients with triple-negative breast cancer. *Clinical breast cancer*, *9 Suppl 2*(Suppl 2), S73–S81. https://doi.org/10.3816/CBC.2009.s.008

Arunasree K. M. (2010). Anti-proliferative effects of carvacrol on a human metastatic breast cancer cell line, MDA-MB 231. *Phytomedicine : international journal of phytotherapy and phytopharmacology*, *17*(8-9), 581–588. https://doi.org/10.1016/j.phymed.2009.12.008

Ashton J. C. (2015). Drug combination studies and their synergy quantification using the Chou-Talalay method--letter. *Cancer research*, *75*(11), 2400. https://doi.org/10.1158/0008-5472.CAN-14-3763

Ayob, A. Z., & Ramasamy, T. S. (2018). Cancer stem cells as key drivers of tumour progression. Journal of biomedical science, 25(1), 20. https://doi.org/10.1186/s12929-018-0426-4

Azad, M. B., Chen, Y., & Gibson, S. B. (2009). Regulation of autophagy by reactive oxygen species (ROS): implications for cancer progression and treatment. *Antioxidants & redox signaling*, *11*(4), 777–790. https://doi.org/10.1089/ars.2008.2270

Azevedo, C., Correia-Branco, A., Araújo, J. R., Guimarães, J. T., Keating, E., & Martel, F. (2015). The chemopreventive effect of the dietary compound kaempferol on the MCF-7 human breast cancer cell line is dependent on inhibition of glucose cellular uptake. *Nutrition and cancer*, *67*(3), 504–513. https://doi.org/10.1080/01635581.2015.1002625

Baelde, H. J., Cleton-Jansen, A. M., van Beerendonk, H., Namba, M., Bovée, J. V., & Hogendoorn, P. C. (2001). High quality RNA isolation from tumours with low cellularity and high extracellular matrix component for cDNA microarrays: application to chondrosarcoma. *Journal of clinical pathology*, *54*(10), 778–782. https://doi.org/10.1136/jcp.54.10.778

Baker, E. K., Johnstone, R. W., Zalcberg, J. R., & El-Osta, A. (2005). Epigenetic changes to the MDR1 locus in response to chemotherapeutic drugs. *Oncogene*, *24*(54), 8061–8075. https://doi.org/10.1038/sj.onc.1208955

Bane, A. L., Whelan, T. J., Pond, G. R., Parpia, S., Gohla, G., Fyles, A. W., Pignol, J. P., Pritchard, K. I., Chambers, S., & Levine, M. N. (2014). Tumor factors predictive of response to hypofractionated radiotherapy in a randomized trial following breast conserving therapy. *Annals of oncology : official journal of the European Society for Medical Oncology*, *25*(5), 992–998. https://doi.org/10.1093/annonc/mdu090

Barve, A., Chen, C., Hebbar, V., Desiderio, J., Saw, C. L., & Kong, A. N. (2009). Metabolism, oral bioavailability and pharmacokinetics of chemopreventive kaempferol in rats. *Biopharmaceutics & drug disposition*, *30*(7), 356–365. https://doi.org/10.1002/bdd.677

Beck, B., & Blanpain, C. (2013). Unravelling cancer stem cell potential. *Nature reviews. Cancer*, *13*(10), 727–738. https://doi.org/10.1038/nrc3597

Berman, H., Henrick, K., & Nakamura, H. (2003). Announcing the worldwide Protein Data Bank. *Nature structural biology*, *10*(12), 980. https://doi.org/10.1038/nsb1203-980

Bhattacharya, R., Banerjee, K., Mukherjee, N., Sen, M., & Mukhopadhyay, A. (2017). From molecular insight to therapeutic strategy: The holistic approach for treating triple negative breast cancer. *Pathology, research and practice*, *213*(3), 177–182. https://doi.org/10.1016/j.prp.2017.01.001

Bockhorn, J., Dalton, R., Nwachukwu, C., Huang, S., Prat, A., Yee, K., Chang, Y. F., Huo, D., Wen, Y., Swanson, K. E., Qiu, T., Lu, J., Park, S. Y., Dolan, M. E., Perou, C. M., Olopade, O. I., Clarke, M. F., Greene, G. L., & Liu, H. (2013). MicroRNA-30c inhibits human breast tumour chemotherapy resistance by regulating TWF1 and IL-11. *Nature communications*, *4*, 1393. https://doi.org/10.1038/ncomms2393

Bourguignon, L. Y., Singleton, P. A., Zhu, H., & Zhou, B. (2002). Hyaluronan promotes signaling interaction between CD44 and the transforming growth factor beta receptor I in metastatic breast tumor cells. The Journal of biological chemistry, 277(42), 39703–39712. https://doi.org/10.1074/jbc.M204320200

Bourguignon, L. Y., Peyrollier, K., Xia, W., & Gilad, E. (2008). Hyaluronan-CD44 interaction activates stem cell marker Nanog, Stat-3-mediated MDR1 gene expression, and ankyrin-regulated multidrug efflux in breast and ovarian tumor cells. *The Journal of biological chemistry*, *283*(25), 17635–17651. https://doi.org/10.1074/jbc.M800109200

Bourguignon, L. Y., Wong, G., Earle, C., & Chen, L. (2012). Hyaluronan-CD44v3 interaction with Oct4-Sox2-Nanog promotes miR-302 expression leading to self-renewal, clonal formation, and cisplatin resistance in cancer stem cells from head and neck squamous cell carcinoma. *The Journal of biological chemistry*, *287*(39), 32800–32824. https://doi.org/10.1074/jbc.M111.308528

Bourguignon, L. Y., Shiina, M., & Li, J. J. (2014). Hyaluronan-CD44 interaction promotes oncogenic signaling, microRNA functions, chemoresistance, and radiation resistance in cancer stem cells leading to tumor progression. *Advances in cancer research*, *123*, 255–275. https://doi.org/10.1016/B978-0-12-800092-2.00010-1

Boyer, M. J., Barnard, M., Hedley, D. W., & Tannock, I. F. (1993). Regulation of intracellular pH in subpopulations of cells derived from spheroids and solid tumours. *British journal of cancer*, *68*(5), 890–897. https://doi.org/10.1038/bjc.1993.451

Bradford M. M. (1976). A rapid and sensitive method for the quantitation of microgram quantities of protein utilizing the principle of protein-dye binding. *Analytical biochemistry*, *72*, 248–254. https://doi.org/10.1006/abio.1976.9999

Brandão, M., Caparica, R., Eiger, D., & de Azambuja, E. (2019). Biomarkers of response and resistance to PI3K inhibitors in estrogen receptor-positive breast cancer patients and combination therapies involving PI3K inhibitors. *Annals of oncology : official journal of the European Society for Medical Oncology*, *30*(Suppl_10), x27–x42. https://doi.org/10.1093/annonc/mdz280

Brasseur, K., Gévry, N., & Asselin, E. (2017). Chemoresistance and targeted therapies in ovarian and endometrial cancers. *Oncotarget*, *8*(3), 4008–4042. https://doi.org/10.18632/oncotarget.14021

Brentnall, M., Rodriguez-Menocal, L., De Guevara, R. L., Cepero, E., & Boise, L. H. (2013). Caspase-9, caspase-3 and caspase-7 have distinct roles during intrinsic apoptosis. *BMC cell biology*, *14*, 32. https://doi.org/10.1186/1471-2121-14-32

Cabarcas, S. M., Mathews, L. A., & Farrar, W. L. (2011). The cancer stem cell niche--there goes the neighborhood?. *International journal of cancer*, *129*(10), 2315–2327. https://doi.org/10.1002/ijc.26312

Callaghan, R., Luk, F., & Bebawy, M. (2014). Inhibition of the multidrug resistance P-glycoprotein: time for a change of strategy?. *Drug metabolism and disposition: the biological fate of chemicals*, *42*(4), 623–631. https://doi.org/10.1124/dmd.113.056176

Calvert, J. W., Cahill, J., Yamaguchi-Okada, M., & Zhang, J. H. (2006). Oxygen treatment after experimental hypoxia-ischemia in neonatal rats alters the expression of HIF-1alpha and its downstream target genes. *Journal of applied physiology (Bethesda, Md. : 1985)*, *101*(3), 853–865. https://doi.org/10.1152/japplphysiol.00268.2006

Campbell, E. J., Dachs, G. U., Morrin, H. R., Davey, V. C., Robinson, B. A., & Vissers, M. C. M. (2019). Activation of the hypoxia pathway in breast cancer tissue and patient survival are inversely associated with tumor ascorbate levels. *BMC cancer*, *19*(1), 307. https://doi.org/10.1186/s12885-019-5503-x

Cao, N., Cheng, D., Zou, S., Ai, H., Gao, J., & Shuai, X. (2011). The synergistic effect of hierarchical assemblies of siRNA and chemotherapeutic drugs co-delivered into hepatic cancer cells. *Biomaterials*, *32*(8), 2222–2232. https://doi.org/10.1016/j.biomaterials.2010.11.061

Cardoso, F., Kyriakides, S., Ohno, S., Penault-Llorca, F., Poortmans, P., Rubio, I. T., Zackrisson, S., Senkus, E., & ESMO Guidelines Committee. Electronic address: clinicalguidelines@esmo.org (2019). Early breast cancer: ESMO Clinical Practice Guidelines for diagnosis, treatment and follow-up†. *Annals of oncology : official journal of the European Society for Medical Oncology*, *30*(8), 1194–1220. https://doi.org/10.1093/annonc/mdz173

Chambers, I., Colby, D., Robertson, M., Nichols, J., Lee, S., Tweedie, S., & Smith, A. (2003). Functional expression cloning of Nanog, a pluripotency sustaining factor in embryonic stem cells. *Cell*, *113*(5), 643–655. https://doi.org/10.1016/s0092-8674(03)00392-1

Chang J. C. (2016). Cancer stem cells: Role in tumor growth, recurrence, metastasis, and treatment resistance. *Medicine*, *95*(1 Suppl 1), S20–S25. https://doi.org/10.1097/MD.0000000000004766

Chanmee, T., Ontong, P., Kimata, K., & Itano, N. (2015). Key Roles of Hyaluronan and Its CD44 Receptor in the Stemness and Survival of Cancer Stem Cells. *Frontiers in oncology*, *5*, 180. https://doi.org/10.3389/fonc.2015.00180

Chen J. (2016). The Cell-Cycle Arrest and Apoptotic Functions of p53 in Tumor Initiation and Progression. *Cold Spring Harbor perspectives in medicine*, *6*(3), a026104. https://doi.org/10.1101/cshperspect.a026104

Chen, J., Ding, Z., Peng, Y., Pan, F., Li, J., Zou, L., Zhang, Y., & Liang, H. (2014). HIF-1α inhibition reverses multidrug resistance in colon cancer cells via downregulation of MDR1/P-glycoprotein. *PloS one*, *9*(6), e98882. https://doi.org/10.1371/journal.pone.0098882

Chen, Q., Liu, Y., Zhu, X. L., Feng, F., Yang, H., & Xu, W. (2019). Increased NHE1 expression is targeted by specific inhibitor cariporide to sensitize resistant breast cancer cells to doxorubicin in vitro and in vivo. *BMC cancer*, *19*(1), 211. https://doi.org/10.1186/s12885-019-5397-7

Chen, Y. N., Mickley, L. A., Schwartz, A. M., Acton, E. M., Hwang, J. L., & Fojo, A. T. (1990). Characterization of adriamycin-resistant human breast cancer cells which display overexpression of a novel resistance-related membrane protein. *The Journal of biological chemistry*, *265*(17), 10073–10080.

Chen, Y., Azad, M. B., & Gibson, S. B. (2009). Superoxide is the major reactive oxygen species regulating autophagy. *Cell death and differentiation*, *16*(7), 1040–1052. https://doi.org/10.1038/cdd.2009.49

Cheung, S. M., Husain, E., Masannat, Y., Miller, I. D., Wahle, K., Heys, S. D., & He, J. (2020). Lactate concentration in breast cancer using advanced magnetic resonance spectroscopy. *British journal of cancer*, *123*(2), 261–267. https://doi.org/10.1038/s41416-020-0886-7

Choi, E. J., & Ahn, W. S. (2008). Kaempferol induced the apoptosis via cell cycle arrest in human breast cancer MDA-MB-453 cells. *Nutrition research and practice*, *2*(4), 322–325. https://doi.org/10.4162/nrp.2008.2.4.322

Choi, H. S., Kim, J. W., Cha, Y. N., & Kim, C. (2006). A quantitative nitroblue tetrazolium assay for determining intracellular superoxide anion production in phagocytic cells. *Journal of immunoassay & immunochemistry*, *27*(1), 31–44. https://doi.org/10.1080/15321810500403722

Chou T. C. (2010). Drug combination studies and their synergy quantification using the Chou-Talalay method. *Cancer research*, *70*(2), 440–446. https://doi.org/10.1158/0008-5472.CAN-09-1947

Chuthapisith, S., Eremin, J., El-Sheemey, M., & Eremin, O. (2010). Breast cancer chemoresistance: emerging importance of cancer stem cells. *Surgical oncology*, *19*(1), 27–32. https://doi.org/10.1016/j.suronc.2009.01.004

Cortes, J., & Baselga, J. (2007). Targeting the microtubules in breast cancer beyond taxanes: the epothilones. *The oncologist*, *12*(3), 271–280. https://doi.org/10.1634/theoncologist.12-3-271

Crespy, V., Morand, C., Besson, C., Cotelle, N., Vézin, H., Demigné, C., & Rémésy, C. (2003). The splanchnic metabolism of flavonoids highly differed according to the nature of the compound. *American journal of physiology. Gastrointestinal and liver physiology*, *284*(6), G980–G988. https://doi.org/10.1152/ajpgi.00223.2002

Critchfield, F.E., Johnson, J.B., 1959. Effect of neutral salts on pH of acid solutions. Anal. Chem. 570–572. https://doi.org/10.1021/ac50164a034. April 31.

Croker, A. K., & Allan, A. L. (2012). Inhibition of aldehyde dehydrogenase (ALDH) activity reduces chemotherapy and radiation resistance of stem-like ALDHhiCD44+ human breast cancer cells. *Breast cancer research and treatment*, *133*(1), 75–87. https://doi.org/10.1007/s10549-011-1692-y

Cui, Q., Wang, J. Q., Assaraf, Y. G., Ren, L., Gupta, P., Wei, L., Ashby, C. R., Jr, Yang, D. H., & Chen, Z. S. (2018). Modulating ROS to overcome multidrug resistance in cancer. *Drug resistance updates : reviews and commentaries in antimicrobial and anticancer chemotherapy*, *41*, 1–25. https://doi.org/10.1016/j.drup.2018.11.001

Daina, A., & Zoete, V. (2016). A BOILED-Egg To Predict Gastrointestinal Absorption and Brain Penetration of Small Molecules. *ChemMedChem*, *11*(11), 1117–1121. https://doi.org/10.1002/cmdc.201600182

Degardin, M., Bonneterre, J., Hecquet, B., Pion, J. M., Adenis, A., Horner, D., & Demaille, A. (1994). Vinorelbine (navelbine) as a salvage treatment for advanced breast cancer. *Annals of oncology : official journal of the European Society for Medical Oncology*, *5*(5), 423–426. https://doi.org/10.1093/oxfordjournals.annonc.a058873

Devarajan, E., Sahin, A. A., Chen, J. S., Krishnamurthy, R. R., Aggarwal, N., Brun, A. M., Sapino, A., Zhang, F., Sharma, D., Yang, X. H., Tora, A. D., & Mehta, K. (2002). Down-regulation of caspase 3 in breast cancer: a possible mechanism for chemoresistance. *Oncogene*, *21*(57), 8843–8851. https://doi.org/10.1038/sj.onc.1206044

Diantini, A., Subarnas, A., Lestari, K., Halimah, E., Susilawati, Y., Supriyatna, Julaeha, E., Achmad, T. H., Suradji, E. W., Yamazaki, C., Kobayashi, K., Koyama, H., & Abdulah, R. (2012). Kaempferol-3-O-rhamnoside isolated from the leaves of Schima wallichii Korth. inhibits MCF-7 breast cancer cell proliferation through activation of the caspase cascade pathway. *Oncology letters*, *3*(5), 1069–1072. https://doi.org/10.3892/ol.2012.596

Dielschneider, R. F., Henson, E. S., & Gibson, S. B. (2017). Lysosomes as Oxidative Targets for Cancer Therapy. *Oxidative medicine and cellular longevity*, *2017*, 3749157. https://doi.org/10.1155/2017/3749157

Ding, Z., Yang, L., Xie, X., Xie, F., Pan, F., Li, J., He, J., & Liang, H. (2010). Expression and significance of hypoxia-inducible factor-1 alpha and MDR1/P-glycoprotein in human colon carcinoma tissue and cells. *Journal of cancer research and clinical oncology*, *136*(11), 1697–1707. https://doi.org/10.1007/s00432-010-0828-5

Dorman, S. N., Baranova, K., Knoll, J. H., Urquhart, B. L., Mariani, G., Carcangiu, M. L., & Rogan, P. K. (2016). Genomic signatures for paclitaxel and gemcitabine resistance in

breast cancer derived by machine learning. *Molecular oncology*, *10*(1), 85–100. https://doi.org/10.1016/j.molonc.2015.07.006

Esfandiari, N., Sharma, R. K., Saleh, R. A., Thomas, A. J., Jr, & Agarwal, A. (2003). Utility of the nitroblue tetrazolium reduction test for assessment of reactive oxygen species production by seminal leukocytes and spermatozoa. *Journal of andrology*, *24*(6), 862–870. https://doi.org/10.1002/j.1939-4640.2003.tb03137.x

Finkel T. (2003). Oxidant signals and oxidative stress. *Current opinion in cell biology*, *15*(2), 247–254. https://doi.org/10.1016/s0955-0674(03)00002-4

Furuta, E., Okuda, H., Kobayashi, A., & Watabe, K. (2010). Metabolic genes in cancer: their roles in tumor progression and clinical implications. *Biochimica et biophysica acta*, *1805*(2), 141–152. https://doi.org/10.1016/j.bbcan.2010.01.005

Gao, L., Yang, Y., Song, S., Hong, H., Zhao, X., & Li, D. (2013). The association between genetic variant of MDR1 gene and breast cancer risk factors in Chinese women. *International immunopharmacology*, *17*(1), 88–91. https://doi.org/10.1016/j.intimp.2013.05.025

Gao, R., Li, D., Xun, J., Zhou, W., Li, J., Wang, J., Liu, C., Li, X., Shen, W., Qiao, H., Stupack, D. G., & Luo, N. (2018). CD44ICD promotes breast cancer stemness via PFKFB4-mediated glucose metabolism. *Theranostics*, *8*(22), 6248–6262. https://doi.org/10.7150/thno.28721

Gatenby, R. A., Smallbone, K., Maini, P. K., Rose, F., Averill, J., Nagle, R. B., Worrall, L., & Gillies, R. J. (2007). Cellular adaptations to hypoxia and acidosis during somatic evolution of breast cancer. *British journal of cancer*, *97*(5), 646–653. https://doi.org/10.1038/sj.bjc.6603922

Generali, D., Berruti, A., Brizzi, M. P., Campo, L., Bonardi, S., Wigfield, S., Bersiga, A., Allevi, G., Milani, M., Aguggini, S., Gandolfi, V., Dogliotti, L., Bottini, A., Harris, A. L., & Fox, S. B. (2006). Hypoxia-inducible factor-1alpha expression predicts a poor response to primary chemoendocrine therapy and disease-free survival in primary human breast cancer. *Clinical cancer research : an official journal of the American Association for Cancer Research*, *12*(15), 4562–4568. https://doi.org/10.1158/1078-0432.CCR-05-2690

Ghadimi, B. M., Grade, M., Difilippantonio, M. J., Varma, S., Simon, R., Montagna, C., Füzesi, L., Langer, C., Becker, H., Liersch, T., & Ried, T. (2005). Effectiveness of gene expression profiling for response prediction of rectal adenocarcinomas to preoperative chemoradiotherapy. *Journal of clinical oncology : official journal of the American Society of Clinical Oncology*, *23*(9), 1826–1838. https://doi.org/10.1200/JCO.2005.00.406

Gilkes, D. M., & Semenza, G. L. (2013). Role of hypoxia-inducible factors in breast cancer metastasis. *Future oncology (London, England)*, *9*(11), 1623–1636. https://doi.org/10.2217/fon.13.92

Gillies, R. J., Verduzco, D., & Gatenby, R. A. (2012). Evolutionary dynamics of carcinogenesis and why targeted therapy does not work. *Nature reviews. Cancer*, *12*(7), 487–493. https://doi.org/10.1038/nrc3298

Gradishar, W. J., Tjulandin, S., Davidson, N., Shaw, H., Desai, N., Bhar, P., Hawkins, M., & O'Shaughnessy, J. (2005). Phase III trial of nanoparticle albumin-bound paclitaxel

compared with polyethylated castor oil-based paclitaxel in women with breast cancer. *Journal of clinical oncology : official journal of the American Society of Clinical Oncology*, *23*(31), 7794–7803. https://doi.org/10.1200/JCO.2005.04.937

Granja, S., Tavares-Valente, D., Queirós, O., & Baltazar, F. (2017). Value of pH regulators in the diagnosis, prognosis and treatment of cancer. *Seminars in cancer biology*, *43*, 17–34. https://doi.org/10.1016/j.semcancer.2016.12.003

Grimshaw, M. J., Cooper, L., Papazisis, K., Coleman, J. A., Bohnenkamp, H. R., Chiapero-Stanke, L., Taylor-Papadimitriou, J., & Burchell, J. M. (2008). Mammosphere culture of metastatic breast cancer cells enriches for tumorigenic breast cancer cells. *Breast cancer research : BCR*, *10*(3), R52. https://doi.org/10.1186/bcr2106

Guttilla, I. K., Phoenix, K. N., Hong, X., Tirnauer, J. S., Claffey, K. P., & White, B. A. (2012). Prolonged mammosphere culture of MCF-7 cells induces an EMT and repression of the estrogen receptor by microRNAs. *Breast cancer research and treatment*, *132*(1), 75–85. https://doi.org/10.1007/s10549-011-1534-y

Haffty, B. G., Yang, Q., Reiss, M., Kearney, T., Higgins, S. A., Weidhaas, J., Harris, L., Hait, W., & Toppmeyer, D. (2006). Locoregional relapse and distant metastasis in conservatively managed triple negative early-stage breast cancer. *Journal of clinical oncology : official journal of the American Society of Clinical Oncology*, *24*(36), 5652–5657. https://doi.org/10.1200/JCO.2006.06.5664

Harbeck, N., Penault-Llorca, F., Cortes, J., Gnant, M., Houssami, N., Poortmans, P., Ruddy, K., Tsang, J., & Cardoso, F. (2019). Breast cancer. *Nature reviews. Disease primers*, *5*(1), 66. https://doi.org/10.1038/s41572-019-0111-2

Hatina J. (2012). The dynamics of cancer stem cells. Neoplasma, 59(6), 700–707. https://doi.org/10.4149/neo_2012_092

Herrero-Martínez, J. M., Sanmartin, M., Rosés, M., Bosch, E., & Ràfols, C. (2005). Determination of dissociation constants of flavonoids by capillary electrophoresis. *Electrophoresis*, *26*(10), 1886–1895. https://doi.org/10.1002/elps.200410258

Hjelmeland, A. B., Wu, Q., Heddleston, J. M., Choudhary, G. S., MacSwords, J., Lathia, J. D., McLendon, R., Lindner, D., Sloan, A., & Rich, J. N. (2011). Acidic stress promotes a glioma stem cell phenotype. *Cell death and differentiation*, *18*(5), 829–840. https://doi.org/10.1038/cdd.2010.150

Holthouser, K. A., Mandal, A., Merchant, M. L., Schelling, J. R., Delamere, N. A., Valdes, R. R., Jr, Tyagi, S. C., Lederer, E. D., & Khundmiri, S. J. (2010). Ouabain stimulates Na-K-ATPase through a sodium/hydrogen exchanger-1 (NHE-1)-dependent mechanism in human kidney proximal tubule cells. *American journal of physiology. Renal physiology*, *299*(1), F77–F90. https://doi.org/10.1152/ajprenal.00581.2009

Hong, S. P., Wen, J., Bang, S., Park, S., & Song, S. Y. (2009). CD44-positive cells are responsible for gemcitabine resistance in pancreatic cancer cells. *International journal of cancer*, *125*(10), 2323–2331. https://doi.org/10.1002/ijc.24573

Huang, J., Gao, L., Li, B., Liu, C., Hong, S., Min, J., & Hong, L. (2019). Knockdown of Hypoxia-Inducible Factor 1α (HIF-1α) Promotes Autophagy and Inhibits

Phosphatidylinositol 3-Kinase (PI3K)/AKT/Mammalian Target of Rapamycin (mTOR) Signaling Pathway in Ovarian Cancer Cells. *Medical science monitor : international medical journal of experimental and clinical research*, *25*, 4250–4263. https://doi.org/10.12659/MSM.915730

Huang, J., Li, H., & Ren, G. (2015). Epithelial-mesenchymal transition and drug resistance in breast cancer (Review). *International journal of oncology*, *47*(3), 840–848. https://doi.org/10.3892/ijo.2015.3084

Hung, T. W., Chen, P. N., Wu, H. C., Wu, S. W., Tsai, P. Y., Hsieh, Y. S., & Chang, H. R. (2017). Kaempferol Inhibits the Invasion and Migration of Renal Cancer Cells through the Downregulation of AKT and FAK Pathways. *International journal of medical sciences*, *14*(10), 984–993. https://doi.org/10.7150/ijms.20336

Hwang, I. T., Chung, Y. M., Kim, J. J., Chung, J. S., Kim, B. S., Kim, H. J., Kim, J. S., & Yoo, Y. D. (2007). Drug resistance to 5-FU linked to reactive oxygen species modulator 1. *Biochemical and biophysical research communications*, *359*(2), 304–310. https://doi.org/10.1016/j.bbrc.2007.05.088

Iida, N., & Bourguignon, L. Y. (1995). New CD44 splice variants associated with human breast cancers. *Journal of cellular physiology*, *162*(1), 127–133. https://doi.org/10.1002/jcp.1041620115

Iinuma, S., Farshi, S. S., Ortel, B., & Hasan, T. (1994). A mechanistic study of cellular photodestruction with 5-aminolaevulinic acid-induced porphyrin. *British journal of cancer*, *70*(1), 21–28. https://doi.org/10.1038/bjc.1994.244

Imran, M., Salehi, B., Sharifi-Rad, J., Aslam Gondal, T., Saeed, F., Imran, A., Shahbaz, M., Tsouh Fokou, P. V., Umair Arshad, M., Khan, H., Guerreiro, S. G., Martins, N., & Estevinho, L. M. (2019). Kaempferol: A Key Emphasis to Its Anticancer Potential. *Molecules (Basel, Switzerland)*, *24*(12), 2277. https://doi.org/10.3390/molecules24122277

Jackson, D. P., Lewis, F. A., Taylor, G. R., Boylston, A. W., & Quirke, P. (1990). Tissue extraction of DNA and RNA and analysis by the polymerase chain reaction. *Journal of clinical pathology*, *43*(6), 499–504. https://doi.org/10.1136/jcp.43.6.499

Javvaji, P. K., Dhali, A., Francis, J. R., Kolte, A. P., Mech, A., Roy, S. C., Mishra, A., & Bhatta, R. (2020). An Efficient Nitroblue Tetrazolium Staining and Bright-Field Microscopy Based Method for Detecting and Quantifying Intracellular Reactive Oxygen Species in Oocytes, Cumulus Cells and Embryos. *Frontiers in cell and developmental biology*, *8*, 764. https://doi.org/10.3389/fcell.2020.00764

Jeter, C. R., Yang, T., Wang, J., Chao, H. P., & Tang, D. G. (2015). Concise Review: NANOG in Cancer Stem Cells and Tumor Development: An Update and Outstanding Questions. *Stem cells (Dayton, Ohio)*, *33*(8), 2381–2390. https://doi.org/10.1002/stem.2007

Ji, X., Lu, Y., Tian, H., Meng, X., Wei, M., & Cho, W. C. (2019). Chemoresistance mechanisms of breast cancer and their countermeasures. Biomedicine & pharmacotherapy = Biomedecine&pharmacotherapie, 114, 108800. https://doi.org/10.1016/j.biopha.2019.108800

141

Jia, Y., & Xie, J. (2015). Promising molecular mechanisms responsible for gemcitabine resistance in cancer. *Genes & diseases*, *2*(4), 299–306. https://doi.org/10.1016/j.gendis.2015.07.003

Jiang, Y. Z., Ma, D., Suo, C., Shi, J., Xue, M., Hu, X., Xiao, Y., Yu, K. D., Liu, Y. R., Yu, Y., Zheng, Y., Li, X., Zhang, C., Hu, P., Zhang, J., Hua, Q., Zhang, J., Hou, W., Ren, L., Bao, D., … Shao, Z. M. (2019). Genomic and Transcriptomic Landscape of Triple-Negative Breast Cancers: Subtypes and Treatment Strategies. *Cancer cell*, *35*(3), 428–440.e5. https://doi.org/10.1016/j.ccell.2019.02.001

Jiao, X., Rizvanov, A. A., Cristofanilli, M., Miftakhova, R. R., & Pestell, R. G. (2016). Breast Cancer Stem Cell Isolation. *Methods in molecular biology (Clifton, N.J.)*, *1406*, 121–135. https://doi.org/10.1007/978-1-4939-3444-7_10

Jung, S. N., Yang, W. K., Kim, J., Kim, H. S., Kim, E. J., Yun, H., Park, H., Kim, S. S., Choe, W., Kang, I., & Ha, J. (2008). Reactive oxygen species stabilize hypoxia-inducible factor-1 alpha protein and stimulate transcriptional activity via AMP-activated protein kinase in DU145 human prostate cancer cells. *Carcinogenesis*, *29*(4), 713–721. https://doi.org/10.1093/carcin/bgn032

Kanagasabai, R., Krishnamurthy, K., Druhan, L. J., & Ilangovan, G. (2011). Forced expression of heat shock protein 27 (Hsp27) reverses P-glycoprotein (ABCB1)-mediated drug efflux and MDR1 gene expression in Adriamycin-resistant human breast cancer cells. *The Journal of biological chemistry*, *286*(38), 33289–33300. https://doi.org/10.1074/jbc.M111.249102

Karekla, E., Liao, W. J., Sharp, B., Pugh, J., Reid, H., Quesne, J. L., Moore, D., Pritchard, C., MacFarlane, M., & Pringle, J. H. (2017). *Ex Vivo* Explant Cultures of Non-Small Cell Lung Carcinoma Enable Evaluation of Primary Tumor Responses to Anticancer Therapy. *Cancer research*, *77*(8), 2029–2039. https://doi.org/10.1158/0008-5472.CAN-16-1121

Keith, B., Johnson, R. S., & Simon, M. C. (2011). HIF1α and HIF2α: sibling rivalry in hypoxic tumour growth and progression. *Nature reviews. Cancer*, *12*(1), 9–22. https://doi.org/10.1038/nrc3183

Khan, S. A., Tyagi, M., Sharma, A. K., Barreto, S. G., Sirohi, B., Ramadwar, M., Shrikhande, S. V., & Gupta, S. (2014). Cell-type specificity of β-actin expression and its clinicopathological correlation in gastric adenocarcinoma. *World journal of gastroenterology*, *20*(34), 12202–12211. https://doi.org/10.3748/wjg.v20.i34.12202

Kim, S. H., & Choi, K. C. (2013). Anti-cancer Effect and Underlying Mechanism(s) of Kaempferol, a Phytoestrogen, on the Regulation of Apoptosis in Diverse Cancer Cell Models. *Toxicological research*, *29*(4), 229–234. https://doi.org/10.5487/TR.2013.29.4.229

Kim, Y. M., Muthuramalingam, K., & Cho, M. (2020). Redox Regulation of NOX Isoforms on FAK[(Y397)]/SRC[(Y416)] Phosphorylation Driven Epithelial-to-Mesenchymal Transition in Malignant Cervical Epithelial Cells. *Cells*, *9*(6), 1555. https://doi.org/10.3390/cells9061555

Kooistra, A., Elissen, N. M., König, J. J., Vermey, M., van der Kwast, T. H., Romijn, J. C., & Schröder, F. H. (1995). Immunocytochemical characterization of explant cultures of human prostatic stromal cells. *The Prostate*, *27*(1), 42–49. https://doi.org/10.1002/pros.2990270108

Kuo, P. L., Hsu, Y. L., Chang, C. H., & Lin, C. C. (2005). The mechanism of ellipticine-induced apoptosis and cell cycle arrest in human breast MCF-7 cancer cells. *Cancer letters*, *223*(2), 293–301. https://doi.org/10.1016/j.canlet.2004.09.046

Larsen, K. B., Lamark, T., Øvervatn, A., Harneshaug, I., Johansen, T., & Bjørkøy, G. (2010). A reporter cell system to monitor autophagy based on p62/SQSTM1. *Autophagy*, *6*(6), 784–793. https://doi.org/10.4161/auto.6.6.12510

Leonessa, F., & Clarke, R. (2003). ATP binding cassette transporters and drug resistance in breast cancer. *Endocrine-related cancer*, *10*(1), 43–73. https://doi.org/10.1677/erc.0.0100043

Lerner-Marmarosh, N., Gimi, K., Urbatsch, I. L., Gros, P., & Senior, A. E. (1999). Large scale purification of detergent-soluble P-glycoprotein from Pichia pastoris cells and characterization of nucleotide binding properties of wild-type, Walker A, and Walker B mutant proteins. *The Journal of biological chemistry*, *274*(49), 34711–34718. https://doi.org/10.1074/jbc.274.49.34711

Li, C., Zhao, Y., Yang, D., Yu, Y., Guo, H., Zhao, Z., Zhang, B., & Yin, X. (2015). Inhibitory effects of kaempferol on the invasion of human breast carcinoma cells by downregulating the expression and activity of matrix metalloproteinase-9. *Biochemistry and cell biology = Biochimie et biologie cellulaire*, *93*(1), 16–27. https://doi.org/10.1139/bcb-2014-0067

Li, S., Yan, T., Deng, R., Jiang, X., Xiong, H., Wang, Y., Yu, Q., Wang, X., Chen, C., & Zhu, Y. (2017). Low dose of kaempferol suppresses the migration and invasion of triple-negative breast cancer cells by downregulating the activities of RhoA and Rac1. *OncoTargets and therapy*, *10*, 4809–4819. https://doi.org/10.2147/OTT.S140886

Li, W., Ma, H., Zhang, J., Zhu, L., Wang, C., & Yang, Y. (2018). Author Correction: Unraveling the roles of CD44/CD24 and ALDH1 as cancer stem cell markers in tumorigenesis and metastasis. *Scientific reports*, *8*(1), 4276. https://doi.org/10.1038/s41598-018-22220-0

Liang, S. Q., Marti, T. M., Dorn, P., Froment, L., Hall, S. R., Berezowska, S., Kocher, G., Schmid, R. A., & Peng, R. W. (2015). Blocking the epithelial-to-mesenchymal transition pathway abrogates resistance to anti-folate chemotherapy in lung cancer. *Cell death & disease*, *6*(7), e1824. https://doi.org/10.1038/cddis.2015.195

Linder, B., & Kögel, D. (2019). Autophagy in Cancer Cell Death. *Biology*, *8*(4), 82. https://doi.org/10.3390/biology8040082

Liou, G. Y., & Storz, P. (2010). Reactive oxygen species in cancer. *Free radical research*, *44*(5), 479–496. https://doi.org/10.3109/10715761003667554

Liu, Q., Yu, B., Tian, Y., Dan, J., Luo, Y., & Wu, X. (2020). P53 Mutant p53^{N236S} Regulates Cancer-Associated Fibroblasts Properties Through Stat3

Pathway. *OncoTargets and therapy*, *13*, 1355–1363. https://doi.org/10.2147/OTT.S229065

Livak, K. J., & Schmittgen, T. D. (2001). Analysis of relative gene expression data using real-time quantitative PCR and the 2(-Delta Delta C(T)) Method. *Methods (San Diego, Calif.)*, *25*(4), 402–408. https://doi.org/10.1006/meth.2001.1262

Lorendeau, D., Dury, L., Genoux-Bastide, E., Lecerf-Schmidt, F., Simões-Pires, C., Carrupt, P. A., Terreux, R., Magnard, S., Di Pietro, A., Boumendjel, A., & Baubichon-Cortay, H. (2014). Collateral sensitivity of resistant MRP1-overexpressing cells to flavonoids and derivatives through GSH efflux. *Biochemical pharmacology*, *90*(3), 235–245. https://doi.org/10.1016/j.bcp.2014.05.017

Lorendeau, D., Rinaldi, G., Boon, R., Spincemaille, P., Metzger, K., Jäger, C., Christen, S., Dong, X., Kuenen, S., Voordeckers, K., Verstreken, P., Cassiman, D., Vermeersch, P., Verfaillie, C., Hiller, K., & Fendt, S. M. (2017). Dual loss of succinate dehydrogenase (SDH) and complex I activity is necessary to recapitulate the metabolic phenotype of SDH mutant tumors. *Metabolic engineering*, *43*(Pt B), 187–197. https://doi.org/10.1016/j.ymben.2016.11.005

Lu, H., Tran, L., Park, Y., Chen, I., Lan, J., Xie, Y., & Semenza, G. L. (2018). Reciprocal Regulation of DUSP9 and DUSP16 Expression by HIF1 Controls ERK and p38 MAP Kinase Activity and Mediates Chemotherapy-Induced Breast Cancer Stem Cell Enrichment. *Cancer research*, *78*(15), 4191–4202. https://doi.org/10.1158/0008-5472.CAN-18-0270

Makki J. (2015). Diversity of Breast Carcinoma: Histological Subtypes and Clinical Relevance. *Clinical medicine insights. Pathology*, *8*, 23–31. https://doi.org/10.4137/CPath.S31563

Martinez-Outschoorn, U. E., Prisco, M., Ertel, A., Tsirigos, A., Lin, Z., Pavlides, S., Wang, C., Flomenberg, N., Knudsen, E. S., Howell, A., Pestell, R. G., Sotgia, F., & Lisanti, M. P. (2011). Ketones and lactate increase cancer cell "stemness," driving recurrence, metastasis and poor clinical outcome in breast cancer: achieving personalized medicine via Metabolo-Genomics. *Cell cycle (Georgetown, Tex.)*, *10*(8), 1271–1286. https://doi.org/10.4161/cc.10.8.15330

Massaro, M., Basta, G., Lazzerini, G., Carluccio, M. A., Bosetti, F., Solaini, G., Visioli, F., Paolicchi, A., & De Caterina, R. (2002). Quenching of intracellular ROS generation as a mechanism for oleate-induced reduction of endothelial activation and early atherogenesis. *Thrombosis and haemostasis*, *88*(2), 335–344.

McAleese, C. E., Choudhury, C., Butcher, N. J., & Minchin, R. F. (2021). Hypoxia-mediated drug resistance in breast cancers. *Cancer letters*, *502*, 189–199. https://doi.org/10.1016/j.canlet.2020.11.045

McDevitt, C. A., & Callaghan, R. (2007). How can we best use structural information on P-glycoprotein to design inhibitors?. *Pharmacology & therapeutics*, *113*(2), 429–441. https://doi.org/10.1016/j.pharmthera.2006.10.003

Michels, K. B., & Xue, F. (2006). Role of birthweight in the etiology of breast cancer. *International journal of cancer*, *119*(9), 2007–2025. https://doi.org/10.1002/ijc.22004

Miletti-González, K. E., Chen, S., Muthukumaran, N., Saglimbeni, G. N., Wu, X., Yang, J., Apolito, K., Shih, W. J., Hait, W. N., & Rodríguez-Rodríguez, L. (2005). The CD44 receptor interacts with P-glycoprotein to promote cell migration and invasion in cancer. *Cancer research*, *65*(15), 6660–6667. https://doi.org/10.1158/0008-5472.CAN-04-3478

Moitra K. (2015). Overcoming Multidrug Resistance in Cancer Stem Cells. *BioMed research international*, *2015*, 635745. https://doi.org/10.1155/2015/635745

Morten, B. C., Scott, R. J., & Avery-Kiejda, K. A. (2016). Comparison of Three Different Methods for Determining Cell Proliferation in Breast Cancer Cell Lines. *Journal of visualized experiments : JoVE*, (115), 54350. https://doi.org/10.3791/54350

Motoi F. (2021). Overcoming acquired chemo-resistance to gemcitabine: implications from the perspective of multi-modal therapy including surgery for pancreatic cancer. *Cancer drug resistance (Alhambra, Calif.)*, *4*(4), 881–884. https://doi.org/10.20517/cdr.2021.75

Muley, H., Fadó, R., Rodríguez-Rodríguez, R., & Casals, N. (2020). Drug uptake-based chemoresistance in breast cancer treatment. *Biochemical pharmacology*, *177*, 113959. https://doi.org/10.1016/j.bcp.2020.113959

Mutebi, M., Anderson, B. O., Duggan, C., Adebamowo, C., Agarwal, G., Ali, Z., Bird, P., Bourque, J. M., DeBoer, R., Gebrim, L. H., Masetti, R., Masood, S., Menon, M., Nakigudde, G., Ng'ang'a, A., Niyonzima, N., Rositch, A. F., Unger-Saldaña, K., Villarreal-Garza, C., Dvaladze, A., … Eniu, A. (2020). Breast cancer treatment: A phased approach to implementation. *Cancer*, *126 Suppl 10*, 2365–2378. https://doi.org/10.1002/cncr.32910

Nagao, A., Kobayashi, M., Koyasu, S., Chow, C. C. T., & Harada, H. (2019). HIF-1-Dependent Reprogramming of Glucose Metabolic Pathway of Cancer Cells and Its Therapeutic Significance. *International journal of molecular sciences*, *20*(2), 238. https://doi.org/10.3390/ijms20020238

Nandi, S. K., Bhattacharya, R., Roychowdhury, T., Roy, U. K., Chattopadhyay, S., Mukhopadhyay, A., Ex-vivo drug sensitivity of primary breast cancer stems cell populations to potentiate therapeutic strategy for treatment resistant breast cancer. *Ann. Oncol.* 29 (2018) ix18, https://doi.org/10.1093/annonc/mdy428.012

Nandi, S. K., Pradhan, A., Das, B., Das, B., Basu, S., Mallick, B., Dutta, A., Sarkar, D. K., Mukhopadhyay, A., Mukhopadhyay, S., & Bhattacharya, R. (2022). Kaempferol attenuates viability of ex-vivo cultured post-NACT breast tumor explants through downregulation of p53 induced stemness, inflammation and apoptosis evasion pathways. *Pathology, research and practice*, *237*, 154029. https://doi.org/10.1016/j.prp.2022.154029

Nandi, S. K., Roychowdhury, T., Chattopadhyay, S., Basu, S., Chatterjee, K., Choudhury, P., Banerjee, N., Saha, P., Mukhopadhyay, S., Mukhopadhyay, A., & Bhattacharya, R. (2022). Deregulation of the CD44-NANOG-MDR1 associated chemoresistance pathways of breast cancer stem cells potentiates the anti-cancer effect of Kaempferol in synergism

with Verapamil. Toxicology and applied pharmacology, 437, 115887. https://doi.org/10.1016/j.taap.2022.115887

Nedeljković, M., & Damjanović, A. (2019). Mechanisms of Chemotherapy Resistance in Triple-Negative Breast Cancer-How We Can Rise to the Challenge. *Cells*, *8*(9), 957. https://doi.org/10.3390/cells8090957

Nikolaou, M., Pavlopoulou, A., Georgakilas, A. G., &Kyrodimos, E. (2018). The challenge of drug resistance in cancer treatment: a current overview. Clinical & experimental metastasis, 35(4), 309–318. https://doi.org/10.1007/s10585-018-9903-0

Nishimoto, A., Kugimiya, N., Hosoyama, T., Enoki, T., Li, T. S., & Hamano, K. (2014). HIF-1α activation under glucose deprivation plays a central role in the acquisition of anti-apoptosis in human colon cancer cells. *International journal of oncology*, *44*(6), 2077–2084. https://doi.org/10.3892/ijo.2014.2367

Nygren, P., Larsson, R., Gruber, A., Peterson, C., & Bergh, J. (1991). Doxorubicin selected multidrug-resistant small cell lung cancer cell lines characterised by elevated cytoplasmic Ca2+ and resistance modulation by verapamil in absence of P-glycoprotein overexpression. *British journal of cancer*, *64*(6), 1011–1018. https://doi.org/10.1038/bjc.1991.456

Pavlopoulou, A., Oktay, Y., Vougas, K., Louka, M., Vorgias, C. E., &Georgakilas, A. G. (2016). Determinants of resistance to chemotherapy and ionizing radiation in breast cancer stem cells. *Cancer letters*, *380*(2), 485–493. https://doi.org/10.1016/j.canlet.2016.07.018

Perez E. A. (2009). Impact, mechanisms, and novel chemotherapy strategies for overcoming resistance to anthracyclines and taxanes in metastatic breast cancer. Breast cancer research and treatment, 114(2), 195–201. https://doi.org/10.1007/s10549-008-0005-6

Perez, E. A., Hillman, D. W., Stella, P. J., Krook, J. E., Hartmann, L. C., Fitch, T. R., Hatfield, A. K., Mailliard, J. A., Nair, S., Kardinal, C. G., & Ingle, J. N. (2000). A phase II study of paclitaxel plus carboplatin as first-line chemotherapy for women with metastatic breast carcinoma. *Cancer*, *88*(1), 124–131. https://doi.org/10.1002/(sici)1097-0142(20000101)88:1<124::aid-cncr17>3.3.co;2-6

Philip, B., Ito, K., Moreno-Sánchez, R., & Ralph, S. J. (2013). HIF expression and the role of hypoxic microenvironments within primary tumours as protective sites driving cancer stem cell renewal and metastatic progression. *Carcinogenesis*, *34*(8), 1699–1707. https://doi.org/10.1093/carcin/bgt209

Prescott, D. M., Charles, H. C., Sostman, H. D., Page, R. L., Thrall, D. E., Moore, D., Oleson, J. R., & Dewhirst, M. W. (1993). Manipulation of intra- and extracellular pH in spontaneous canine tumours by use of hyperglycaemia. *International journal of hyperthermia : the official journal of European Society for Hyperthermic Oncology, North American Hyperthermia Group*, *9*(5), 745–754. https://doi.org/10.3109/02656739309032061

Qiu, W., Lin, J., Zhu, Y., Zhang, J., Zeng, L., Su, M., & Tian, Y. (2017). Kaempferol Modulates DNA Methylation and Downregulates DNMT3B in Bladder Cancer. *Cellular*

physiology and biochemistry : international journal of experimental cellular physiology, biochemistry, and pharmacology, *41*(4), 1325–1335. https://doi.org/10.1159/000464435

Quint, K., Tonigold, M., Di Fazio, P., Montalbano, R., Lingelbach, S., Rückert, F., Alinger, B., Ocker, M., & Neureiter, D. (2012). Pancreatic cancer cells surviving gemcitabine treatment express markers of stem cell differentiation and epithelial-mesenchymal transition. *International journal of oncology*, *41*(6), 2093–2102. https://doi.org/10.3892/ijo.2012.1648

Rajaram, N., Frees, A. E., Fontanella, A. N., Zhong, J., Hansen, K., Dewhirst, M. W., & Ramanujam, N. (2013). Delivery rate affects uptake of a fluorescent glucose analog in murine metastatic breast cancer. *PloS one*, *8*(10), e76524. https://doi.org/10.1371/journal.pone.0076524

Rattigan, Y. I., Patel, B. B., Ackerstaff, E., Sukenick, G., Koutcher, J. A., Glod, J. W., & Banerjee, D. (2012). Lactate is a mediator of metabolic cooperation between stromal carcinoma associated fibroblasts and glycolytic tumor cells in the tumor microenvironment. *Experimental cell research*, *318*(4), 326–335. https://doi.org/10.1016/j.yexcr.2011.11.014

Ren, J., Lu, Y., Qian, Y., Chen, B., Wu, T., & Ji, G. (2019). Recent progress regarding kaempferol for the treatment of various diseases. *Experimental and therapeutic medicine*, *18*(4), 2759–2776. https://doi.org/10.3892/etm.2019.7886

Reynolds, C. P., & Maurer, B. J. (2005). Evaluating response to antineoplastic drug combinations in tissue culture models. *Methods in molecular medicine*, *110*, 173–183. https://doi.org/10.1385/1-59259-869-2:173

Riahi-Chebbi, I., Souid, S., Othman, H., Haoues, M., Karoui, H., Morel, A., Srairi-Abid, N., Essafi, M., & Essafi-Benkhadir, K. (2019). The Phenolic compound Kaempferol overcomes 5-fluorouracil resistance in human resistant LS174 colon cancer cells. *Scientific reports*, *9*(1), 195. https://doi.org/10.1038/s41598-018-36808-z

Rivera, E., & Gomez, H. (2010). Chemotherapy resistance in metastatic breast cancer: the evolving role of ixabepilone. *Breast cancer research : BCR*, *12 Suppl 2*(Suppl 2), S2. https://doi.org/10.1186/bcr2573

Rodda, D. J., Chew, J. L., Lim, L. H., Loh, Y. H., Wang, B., Ng, H. H., & Robson, P. (2005). Transcriptional regulation of nanog by OCT4 and SOX2. *The Journal of biological chemistry*, *280*(26), 24731–24737. https://doi.org/10.1074/jbc.M502573200

Rota, L. M., Lazzarino, D. A., Ziegler, A. N., LeRoith, D., & Wood, T. L. (2012). Determining mammosphere-forming potential: application of the limiting dilution analysis. *Journal of mammary gland biology and neoplasia*, *17*(2), 119–123. https://doi.org/10.1007/s10911-012-9258-0

Rust, S., Guillard, S., Sachsenmeier, K., Hay, C., Davidson, M., Karlsson, A., Karlsson, R., Brand, E., Lowne, D., Elvin, J., Flynn, M., Kurosawa, G., Hollingsworth, R., Jermutus, L., & Minter, R. (2013). Combining phenotypic and proteomic approaches to identify membrane targets in a 'triple negative' breast cancer cell type. *Molecular cancer*, *12*, 11. https://doi.org/10.1186/1476-4598-12-11

Samulitis, B. K., Pond, K. W., Pond, E., Cress, A. E., Patel, H., Wisner, L., Patel, C., Dorr, R. T., & Landowski, T. H. (2015). Gemcitabine resistant pancreatic cancer cell lines acquire an invasive phenotype with collateral hypersensitivity to histone deacetylase inhibitors. *Cancer biology & therapy*, *16*(1), 43–51. https://doi.org/10.4161/15384047.2014.986967

Schmid, T., Zhou, J., & Brüne, B. (2004). HIF-1 and p53: communication of transcription factors under hypoxia. *Journal of cellular and molecular medicine*, *8*(4), 423–431. https://doi.org/10.1111/j.1582-4934.2004.tb00467.x

Schmittgen, T. D., & Livak, K. J. (2008). Analyzing real-time PCR data by the comparative C(T) method. *Nature protocols*, *3*(6), 1101–1108. https://doi.org/10.1038/nprot.2008.73

Schneider, L. S., von Schwarzenberg, K., Lehr, T., Ulrich, M., Kubisch-Dohmen, R., Liebl, J., Trauner, D., Menche, D., & Vollmar, A. M. (2015). Vacuolar-ATPase Inhibition Blocks Iron Metabolism to Mediate Therapeutic Effects in Breast Cancer. *Cancer research*, *75*(14), 2863–2874. https://doi.org/10.1158/0008-5472.CAN-14-2097

Screaton, G. R., Bell, M. V., Jackson, D. G., Cornelis, F. B., Gerth, U., & Bell, J. I. (1992). Genomic structure of DNA encoding the lymphocyte homing receptor CD44 reveals at least 12 alternatively spliced exons. *Proceedings of the National Academy of Sciences of the United States of America*, *89*(24), 12160–12164. https://doi.org/10.1073/pnas.89.24.12160

Semenza G. L. (2013). Advances in cancer biology and therapy. *Journal of molecular medicine (Berlin, Germany)*, *91*(4), 409. https://doi.org/10.1007/s00109-013-1024-2

Senbanjo, L. T., & Chellaiah, M. A. (2017). CD44: A Multifunctional Cell Surface Adhesion Receptor Is a Regulator of Progression and Metastasis of Cancer Cells. *Frontiers in cell and developmental biology*, *5*, 18. https://doi.org/10.3389/fcell.2017.00018

Settembre, C., De Cegli, R., Mansueto, G., Saha, P. K., Vetrini, F., Visvikis, O., Huynh, T., Carissimo, A., Palmer, D., Klisch, T. J., Wollenberg, A. C., Di Bernardo, D., Chan, L., Irazoqui, J. E., & Ballabio, A. (2013). TFEB controls cellular lipid metabolism through a starvation-induced autoregulatory loop. *Nature cell biology*, *15*(6), 647–658. https://doi.org/10.1038/ncb2718

Sharma, V., Joseph, C., Ghosh, S., Agarwal, A., Mishra, M. K., & Sen, E. (2007). Kaempferol induces apoptosis in glioblastoma cells through oxidative stress. *Molecular cancer therapeutics*, *6*(9), 2544–2553. https://doi.org/10.1158/1535-7163.MCT-06-0788

Shaw, F. L., Harrison, H., Spence, K., Ablett, M. P., Simões, B. M., Farnie, G., & Clarke, R. B. (2012). A detailed mammosphere assay protocol for the quantification of breast stem cell activity. *Journal of mammary gland biology and neoplasia*, *17*(2), 111–117. https://doi.org/10.1007/s10911-012-9255-3

Shimoda, L. A., Fallon, M., Pisarcik, S., Wang, J., & Semenza, G. L. (2006). HIF-1 regulates hypoxic induction of NHE1 expression and alkalinization of intracellular pH in pulmonary arterial myocytes. *American journal of physiology. Lung cellular and molecular physiology*, *291*(5), L941–L949. https://doi.org/10.1152/ajplung.00528.2005

Silva, A. S., Yunes, J. A., Gillies, R. J., & Gatenby, R. A. (2009). The potential role of systemic buffers in reducing intratumoral extracellular pH and acid-mediated

invasion. *Cancer research*, *69*(6), 2677–2684. https://doi.org/10.1158/0008-5472.CAN-08-2394

Silver, N., Best, S., Jiang, J., & Thein, S. L. (2006). Selection of housekeeping genes for gene expression studies in human reticulocytes using real-time PCR. *BMC molecular biology*, *7*, 33. https://doi.org/10.1186/1471-2199-7-33

Spike, B. T., & Wahl, G. M. (2011). p53, Stem Cells, and Reprogramming: Tumor Suppression beyond Guarding the Genome. *Genes & cancer*, *2*(4), 404–419. https://doi.org/10.1177/1947601911410224

Stock, C., & Pedersen, S. F. (2017). Roles of pH and the Na^+/H^+ exchanger NHE1 in cancer: From cell biology and animal models to an emerging translational perspective?. *Seminars in cancer biology*, *43*, 5–16. https://doi.org/10.1016/j.semcancer.2016.12.001

Tanida, I., Minematsu-Ikeguchi, N., Ueno, T., & Kominami, E. (2005). Lysosomal turnover, but not a cellular level, of endogenous LC3 is a marker for autophagy. *Autophagy*, *1*(2), 84–91. https://doi.org/10.4161/auto.1.2.1697

Tanida, I., Ueno, T., & Kominami, E. (2008). LC3 and Autophagy. *Methods in molecular biology (Clifton, N.J.)*, *445*, 77–88. https://doi.org/10.1007/978-1-59745-157-4_4

Themistocleous, S. C., Yiallouris, A., Tsioutis, C., Zaravinos, A., Johnson, E. O., & Patrikios, I. (2021). Clinical significance of P-class pumps in cancer. *Oncology letters*, *22*(3), 658. https://doi.org/10.3892/ol.2021.12919

Thottassery, J. V., Zambetti, G. P., Arimori, K., Schuetz, E. G., & Schuetz, J. D. (1997). p53-dependent regulation of MDR1 gene expression causes selective resistance to chemotherapeutic agents. *Proceedings of the National Academy of Sciences of the United States of America*, *94*(20), 11037–11042. https://doi.org/10.1073/pnas.94.20.11037

Tièche, C. C., Gao, Y., Bührer, E. D., Hobi, N., Berezowska, S. A., Wyler, K., Froment, L., Weis, S., Peng, R. W., Bruggmann, R., Schär, P., Amrein, M. A., Hall, S. R. R., Dorn, P., Kocher, G., Riether, C., Ochsenbein, A., Schmid, R. A., & Marti, T. M. (2019). Tumor Initiation Capacity and Therapy Resistance Are Differential Features of EMT-Related Subpopulations in the NSCLC Cell Line A549. *Neoplasia (New York, N.Y.)*, *21*(2), 185–196. https://doi.org/10.1016/j.neo.2018.09.008

Tomita, H., Tanaka, K., Tanaka, T., & Hara, A. (2016). Aldehyde dehydrogenase 1A1 in stem cells and cancer. *Oncotarget*, *7*(10), 11018–11032. https://doi.org/10.18632/oncotarget.6920

Traverso, N., Ricciarelli, R., Nitti, M., Marengo, B., Furfaro, A. L., Pronzato, M. A., Marinari, U. M., & Domenicotti, C. (2013). Role of glutathione in cancer progression and chemoresistance. *Oxidative medicine and cellular longevity*, *2013*, 972913. https://doi.org/10.1155/2013/972913

Trock, B. J., Leonessa, F., & Clarke, R. (1997). Multidrug resistance in breast cancer: a meta-analysis of MDR1/gp170 expression and its possible functional significance. *Journal of the National Cancer Institute*, *89*(13), 917–931. https://doi.org/10.1093/jnci/89.13.917

van der Kuip, H., Mürdter, T. E., Sonnenberg, M., McClellan, M., Gutzeit, S., Gerteis, A., Simon, W., Fritz, P., & Aulitzky, W. E. (2006). Short term culture of breast cancer tissues to study the activity of the anticancer drug taxol in an intact tumor environment. *BMC cancer*, *6*, 86. https://doi.org/10.1186/1471-2407-6-86

Vaupel, P., Thews, O., &Hoeckel, M. (2001). Treatment resistance of solid tumors: role of hypoxia and anemia. *Medical oncology (Northwood, London, England)*, *18*(4), 243–259. https://doi.org/10.1385/MO:18:4:243

Verma, N., Pink, M., & Schmitz-Spanke, S. (2021). A new perspective on calmodulin-regulated calcium and ROS homeostasis upon carbon black nanoparticle exposure. *Archives of toxicology*, *95*(6), 2007–2018. https://doi.org/10.1007/s00204-021-03032-0

Vishvakarma, N. K., Kumar, A., Singh, V., & Singh, S. M. (2013). Hyperglycemia of tumor microenvironment modulates stage-dependent tumor progression and multidrug resistance: implication of cell survival regulatory molecules and altered glucose transport. *Molecular carcinogenesis*, *52*(12), 932–945. https://doi.org/10.1002/mc.21922

Wang, C., Gao, X., Wang, F., Guan, W., Dou, H., & Xu, G. (2020). Effect of Starvation in Reversing Cancer Chemoresistance Based on Drug-Resistance Detection by Dextran Nanoparticles. *International journal of nanomedicine*, *15*, 9255–9264. https://doi.org/10.2147/IJN.S283430

Wang, H., Li, X., Chen, T., Wang, W., Liu, Q., Li, H., Yi, J., & Wang, J. (2013). Mechanisms of verapamil-enhanced chemosensitivity of gallbladder cancer cells to platinum drugs: glutathione reduction and MRP1 downregulation. *Oncology reports*, *29*(2), 676–684. https://doi.org/10.3892/or.2012.2156

Wang, J., Wang, H., Zhao, L., Fan, S., Yang, Z., Gao, F., Chen, L., Xiao, G. G., Molnár, J., & Wang, Q. (2010). Down-regulation of P-glycoprotein is associated with resistance to cisplatin and VP-16 in human lung cancer cell lines. *Anticancer research*, *30*(9), 3593–3598.

Wang, R., Cheng, L., Xia, J., Wang, Z., Wu, Q., & Wang, Z. (2014). Gemcitabine resistance is associated with epithelial-mesenchymal transition and induction of HIF-1α in pancreatic cancer cells. *Current cancer drug targets*, *14*(4), 407–417. https://doi.org/10.2174/1568009614666140226114015

Wartenberg, M., Ling, F. C., Müschen, M., Klein, F., Acker, H., Gassmann, M., Petrat, K., Pütz, V., Hescheler, J., & Sauer, H. (2003). Regulation of the multidrug resistance transporter P-glycoprotein in multicellular tumor spheroids by hypoxia-inducible factor (HIF-1) and reactive oxygen species. *FASEB journal : official publication of the Federation of American Societies for Experimental Biology*, *17*(3), 503–505. https://doi.org/10.1096/fj.02-0358fje

Welker, E., Szabó, K., Holló, Z., Müller, M., Sarkadi, B., & Váradi, A. (1995). Drug-stimulated ATPase activity of a deletion mutant of the human multidrug-resistance protein (MDR1). *Biochemical and biophysical research communications*, *216*(2), 602–609. https://doi.org/10.1006/bbrc.1995.2665

Weng, X., Maxwell-Warburton, S., Hasib, A., Ma, L., & Kang, L. (2022). The membrane receptor CD44: novel insights into metabolism. *Trends in endocrinology and metabolism: TEM*, *33*(5), 318–332. https://doi.org/10.1016/j.tem.2022.02.002

Xi, Y., Yuan, P., Li, T., Zhang, M., Liu, M. F., & Li, B. (2020). hENT1 reverses chemoresistance by regulating glycolysis in pancreatic cancer. *Cancer letters*, *479*, 112–122. https://doi.org/10.1016/j.canlet.2020.03.015

Yang, F., Xu, J., Tang, L., & Guan, X. (2017). Breast cancer stem cell: the roles and therapeutic implications. Cellular and molecular life sciences : CMLS, 74(6), 951–966. https://doi.org/10.1007/s00018-016-2334-7

Yeo, S. K., & Guan, J. L. (2017). Breast Cancer: Multiple Subtypes within a Tumor?. Trends in cancer, 3(11), 753–760. https://doi.org/10.1016/j.trecan.2017.09.001

Yodogawa, S., Arakawa, T., Sugihara, N., & Furuno, K. (2003). Glucurono- and sulfo-conjugation of kaempferol in rat liver subcellular preparations and cultured hepatocytes. *Biological & pharmaceutical bulletin*, *26*(8), 1120–1124. https://doi.org/10.1248/bpb.26.1120

Zamora-León, S. P., Golde, D. W., Concha, I. I., Rivas, C. I., Delgado-López, F., Baselga, J., Nualart, F., & Vera, J. C. (1996). Expression of the fructose transporter GLUT5 in human breast cancer. *Proceedings of the National Academy of Sciences of the United States of America*, *93*(5), 1847–1852. https://doi.org/10.1073/pnas.93.5.1847

Zeino, M., Brenk, R., Gruber, L., Zehl, M., Urban, E., Kopp, B., &Efferth, T. (2015). Cytotoxicity of cardiotonic steroids in sensitive and multidrug-resistant leukemia cells and the link with Na(+)/K(+)-ATPase. *The Journal of steroid biochemistry and molecular biology*, *150*, 97–111. https://doi.org/10.1016/j.jsbmb.2015.03.008

Zhang, F., Song, C., Ma, Y., Tang, L., Xu, Y., & Wang, H. (2011). Effect of fibroblasts on breast cancer cell mammosphere formation and regulation of stem cell-related gene expression. *International journal of molecular medicine*, *28*(3), 365–371. https://doi.org/10.3892/ijmm.2011.700

Zhang, H., Qian, D. Z., Tan, Y. S., Lee, K., Gao, P., Ren, Y. R., Rey, S., Hammers, H., Chang, D., Pili, R., Dang, C. V., Liu, J. O., & Semenza, G. L. (2008). Digoxin and other cardiac glycosides inhibit HIF-1alpha synthesis and block tumor growth. *Proceedings of the National Academy of Sciences of the United States of America*, *105*(50), 19579–19586. https://doi.org/10.1073/pnas.0809763105

Zhang, S., Zhou, Z., Gong, Q., Makielski, J. C., & January, C. T. (1999). Mechanism of block and identification of the verapamil binding domain to HERG potassium channels. *Circulation research*, *84*(9), 989–998. https://doi.org/10.1161/01.res.84.9.989

Zhang, X., Yu, L., & Xu, H. (2016). Lysosome calcium in ROS regulation of autophagy. *Autophagy*, *12*(10), 1954–1955. https://doi.org/10.1080/15548627.2016.1212787

Zhao, L., Wientjes, M. G., & Au, J. L. (2004). Evaluation of combination chemotherapy: integration of nonlinear regression, curve shift, isobologram, and combination index analyses. *Clinical cancer research : an official journal of the American Association for Cancer Research*, *10*(23), 7994–8004. https://doi.org/10.1158/1078-0432.CCR-04-1087

Zheng H. C. (2017). The molecular mechanisms of chemoresistance in cancers. Oncotarget, 8(35), 59950–59964. https://doi.org/10.18632/oncotarget.19048

Zheng, C., Jiao, X., Jiang, Y., & Sun, S. (2013). ERK1/2 activity contributes to gemcitabine resistance in pancreatic cancer cells. *The Journal of international medical research*, *41*(2), 300–306. https://doi.org/10.1177/0300060512474128

Zheng, W., Li, M., Lin, Y., & Zhan, X. (2018). Encapsulation of verapamil and doxorubicin by MPEG-PLA to reverse drug resistance in ovarian cancer. *Biomedicine & pharmacotherapy = Biomedecine & pharmacotherapie*, *108*, 565–573.https://doi.org/10.1016/j.biopha.2018.09.039

Zhitomirsky, B., & Assaraf, Y. G. (2016). Lysosomes as mediators of drug resistance in cancer. *Drug resistance updates : reviews and commentaries in antimicrobial and anticancer chemotherapy*, *24*, 23–33. https://doi.org/10.1016/j.drup.2015.11.004

Zhitomirsky, B., Yunaev, A., Kreiserman, R., Kaplan, A., Stark, M., & Assaraf, Y. G. (2018). Lysosomotropic drugs activate TFEB via lysosomal membrane fluidization and consequent inhibition of mTORC1 activity. *Cell death & disease*, *9*(12), 1191. https://doi.org/10.1038/s41419-018-1227-0

Zhou, Q., Brown, J., Kanarek, A., Rajagopal, J., & Melton, D. A. (2008). In vivo reprogramming of adult pancreatic exocrine cells to beta-cells. *Nature*, *455*(7213), 627–632. https://doi.org/10.1038/nature07314

Zhou, Z. Y., Wan, L. L., Yang, Q. J., Han, Y. L., Li, D., Lu, J., & Guo, C. (2016). Nilotinib reverses ABCB1/P-glycoprotein-mediated multidrug resistance but increases cardiotoxicity of doxorubicin in a MDR xenograft model. *Toxicology letters*, *259*, 124–132. https://doi.org/10.1016/j.toxlet.2016.07.710

Zhu, L., & Xue, L. (2019). Kaempferol Suppresses Proliferation and Induces Cell Cycle Arrest, Apoptosis, and DNA Damage in Breast Cancer Cells. *Oncology research*, *27*(6), 629–634. https://doi.org/10.3727/096504018X15228018559434

Zhuang, Y., Chan, D. K., Haugrud, A. B., & Miskimins, W. K. (2014). Mechanisms by which low glucose enhances the cytotoxicity of metformin to cancer cells both in vitro and in vivo. *PloS one*, *9*(9), e108444. https://doi.org/10.1371/journal.pone.0108444

Zong, W. X., Edelstein, L. C., Chen, C., Bash, J., & Gélinas, C. (1999). The prosurvival Bcl-2 homolog Bfl-1/A1 is a direct transcriptional target of NF-kappaB that blocks TNFalpha-induced apoptosis. *Genes & development*, *13*(4), 382–387. https://doi.org/10.1101/gad.13.4.382

Zou, W., Yang, Y., Zheng, R., Wang, Z., Zeng, H., Chen, Z., Yang, F., & Wang, J. (2020). Association of CD44 and CD24 phenotype with lymph node metastasis and survival in triple-negative breast cancer. *International journal of clinical and experimental pathology*, *13*(5), 1008–1016.
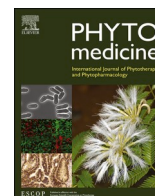
Original Article

Kaempferol with Verapamil impeded panoramic chemoevasion pathways in breast cancer through ROS overproduction and disruption of lysosomal biogenesis

Sourav Kumar Nandi [a], Niloy Chatterjee [b], Tanaya Roychowdhury [c], Ayan Pradhan [d], Sumaiya Moiz [a], Krishnendu Manna [e], Diptendra Kumar Sarkar [d], Pubali Dhar [f], Amitava Dutta [g], Soma Mukhopadhyay [a], Rittwika Bhattacharya [a,*]

[a] Department of Molecular Biology, Netaji Subhas Chandra Bose Cancer Research Institute, 3081 Nayabad, Kolkata-700094, India
[b] Centre for Research in Nanoscience & Nanotechnology, University of Calcutta, JD 2, Sector III, Salt Lake City, Kolkata 700 098, West Bengal, India
[c] Cancer Biology and Inflammatory Disorder Division, Indian Institute of Chemical Biology, 4, Raja S. C. Mullick Road, Kolkata-700032, India
[d] Department of General Surgery, Institute of Post graduate Medical Education &Research and SSKM Hospital, 244B AJC Bose Road Kolkata-700020, India
[e] Department of Food and Nutrition, University of Kalyani, Kalyani, West Bengal, 741235, India
[f] Laboratory of Food Science and Technology, Food and Nutrition division, University of Calcutta, 20B Judges Court Road. Kolkata 700027, West Bengal, India
[g] Department of Pathology, Netaji Subhas Chandra Bose Cancer Research Institute, 3081 Nayabad, Kolkata-700094

ARTICLE INFO

ABSTRACT

Background: Reactive oxygen species (ROS) at low level promotes cell survival through lysosome induced autophagy induction. Glucose stress induced acidosis, hypoxia, ROS, upregulates markers related to cancer stemness and multidrug resistance. Also, lysosomal upregulation is proposed to be one of the important indicators of cell survival under ROS induced stress. Studies supported that, stimulation of Lysosome-TFEB-Ca^{2+} cascade has important role in induction of chemoresistance and survival of cancerous cells.

Purpose: To observe the effect of synergistic drug combination, Kaempferol and Verapamil on markers regulating chemoevasion, tumor stemness & acidosis as well as lysosome upregulation pathways, under low as well as high glucose conditions.

Hypothesis: Based on our earlier observation as well as previous reports, we hypothesized, our drug combination Kaempferol with Verapamil could attenuate markers related to chemoevasion, tumor stemness & acidosis as well as lysosome-TFEB-Ca2+ pathway, all of which have indispensable association and role in chemoresistance.

Methods: RNA and protein expression of candidate genes, along with ROS production and Ca2+ concentrations were measured in ex vivo models in altered glucose conditions upon treatment with KV. Also, computational approaches were utilized to hypothesize the mechanism of action of the drug combination. PCR, IHC, western blotting and molecular docking approaches were used in this study.

Results: The overproduction of ROS by our candidate drugs KV, downregulated the chemoresistance and tumor acidosis markers along with ATP1B1 and resulted in lysosomal disruption with reduction of Ca^{2+} release, diminishing TFEB expression under low glucose condition. An anomalous outcome was observed in high glucose conditions. We also observed KV promoted the overproduction of ROS levels thereby inducing autophagy-mediated cell death through the upregulation of LC3-II and p62 in low glucose conditions. The ex vivo studies also corroborate with in silico study that exhibited the parallel outcome.

Conclusion: Our ex-vivo and in-silico studies revealed that our candidate drug combination KV, could effectively target several pathways regulating chemoresistance, that were not hitherto studied in the same experimental setup and thus may be endorsed for therapeutic purposes.

Introduction

ROS (Reactive oxygen species) is considered an important predictor of not only cancer commencement, but also progression and apoptosis, thus playing a dual role in survival of cancerous cells (Zhang et al., 2016). Early studies have identified that in response to oxidative stress, lysosomes, through stimulate and nuclear transcription of TFEB, and subsequent release of calcium ions (Ca^{2+}), induce autophagy which eventually promotes cellular survival through scavenging of extracellular ROS (Zhang et al., 2016). Many cancer therapeutics thereby target to promote ROS production, albeit their cellular fate and detailed mechanism of action is yet to be explored.

In our erstwhile study, we identified a drug combination Kaempferol and Verapamil (KV), which showed a robust anti-proliferative effect against breast cancer (BC) stem cells (Nandi et al., 2022). Based on early reports that affirmed Verapamil to be efficacious in depleting intracellular reduced Glutathione (Lorendeau et al., 2017), we hypothesized that KV drug combination could have interference with proliferative and chemoresistance signaling cascades that are induced through elevated ROS production in breast cancer.

Tumor cells can survive in moderate levels of ROS in comparison to their normal counterparts through upregulation of HIF1α (Hypoxia-inducible factor1-α) (Jung et al., 2008). HIF1α contributes to the upregulation of NHE1, a class of Na+/H+ exchanger membrane protein (Holthouser et al., 2010), which maintains extracellular acidosis in tumor microenvironment (Stock et al., 2017). NHE1 upregulation cooperatively upregulates Na+/K+ ATPase (Gene name, ATP1B1), the master regulator maintaining the overall cellular membrane potential (Holthouser et al., 2010). In normal tissues, HIF1α induces downregulation of sodium-/potassium-/-ATPase, by Von Hippel Lindau protein (pVHL) (Zhou et al., 2008), while in cancer cells, owing to stabilization of HIF1α, the process is perturbed leading to their survival. HIF1α also associates with other hypoxia associated transcription factors which consist of a few membrane protein that transport glucose (GLUTs) (Calvert et al.2006).Thus, a moderate level of ROS maintains an ambient intracellular milieu for promoting tumor growth and chemoevasion (Liou and Storz, 2010). This study also reported that a disproportionate overproduction of ROS can be detrimental to cancer cells and can lead to their mortality.

In the pathway to malignant transformation, cells upregulate their ordinary glucose uptake system to facilitate their invasive potential (Calvert et al., 2006). Role of glucose transporters in defining the efficacy of cytotoxic drug is poorly understood, as high glucose alone has the ability to activate proliferation pathways in a cancer cell (Nandi et al., 2022).

Overall, we pointed to study the effectiveness of KV under differential glucose stress, on the expression pattern of genes that maintain tumor acidosis, hypoxia and chemoevasion viz. *HIF1α, GLUT2, NANOG, MDR1, CD44, ATP1B1, NHE1*. We delineated that, our candidate drug KV interferes with lysosome-Ca^{2+}-TFEB pathway-based chemoresistance through autophagy induced cell death. We also simulated a molecular model of the interactome of these candidate genes that are expressed under glucose stress, in presence of our candidate drug KV. Our data showed that our candidate drug system KV had robust anti-proliferative efficacy through downregulation of the aforementioned candidate genes regulating tumor acidosis, hypoxia and chemoevasion, perturbation of lysosome-Ca^{2+}-TFEB mediated autophagic survival and upregulation of cell death under low glucose condition, indicating the therapeutic potential of the candidate drug combination under low glucose condition. The novelty of this unique study is the surprising result that a synergistic combination of Kaempferol (anti-cancerous concentration) and Verapamil (adjunct dosage) in the chosen concentration inhibits cancerous cells through a complex signaling pathway under low glucose, downregulating all these markers of chemoresistance and indirectly through increasing ROS production, finally leading to autophagy induced cell death, unlike several other inhibitors which act by decreasing the ROS level or reducing overall oxidative stress of the cellular environment.

Materials and methods

Reagents

All chemicals were collected from Sigma Aldrich (St. Louis, MO, USA) except tris-Cl, (Himedia) sodium dodecyl sulfate (Merck, India). All requirements of tumor cell culture and breast cancer cell line culture were obtained from Gibco, Thermo Fisher Scientific – US. For BC Cell Lines such as MDA-MB-231 and MCF-7 were obtained from NCCS, Pune with reported STR profile (ATCC).

Tumor specimens

Primary breast tumors of patients ($n = 38$) were collected from the hospital section of NCRI (Netaji Subhas Chandra Bose Cancer Research Institute) and their subtype was confirmed through immunohistochemistry (IHC) (Table S1). Also, the normal tissues of those respective patients were obtained for this study. Tumor limits were recognised by a Onco-pathologist and categorised according to international guide line such as UICC (International Union against Cancer) and AJCC (American Joint Committee on Cancer). BC patients with unknown types, male BC patients or clinical trial related BC were excluded from this study. All counted patients provided consent form with the conduct of tumor samples for investigate resolutions, and the proposal was acceptable by the Ethics Committee of Netaji Subhash Candra Bose Cancer Research Institutional Review Board (EC approval No. ECS/NCRI/08/2012, extended approval: EC/NSCBCRI/01/2021).

Cell culture

BC cell lines MDA-MB-231 (TNBC cell line), and MCF-7 were re-cultured in L-DMEM (Cat No: 11,054,001, Gibco) and h-DMEM, (Cat No: 11,960,592, Gibco) added with supplements in a 5% CO_2 humidified chamber. These cell lines were maintained in L-DMEM and h-DMEM until 80% confluence was achieved and treated with Kaempferol and Verapamil (KV) in combination, that induced 50% cell death (K: 104.81 μM; V: 5 μM for TNBC cell line and K: 103.15 μM, V: 5 μM in MCF-7 according to CI index) in both L-DMEM and h-DMEM panel, as per our previous study (Nandi et al., 2022) in cell line. In ex-vivo model (primary tumor drive cell culture) we used the synergistic conc. at IC$_{50}$ concentration of K (109.9 μM) and Verapamil at IC$_5$ value (5 μM) where previous studies showed the least survival (around 16%) (Nandi et al., 2022) and freshly documented the outcome of cytotoxicity assay through new TNBC patients (Fig. S1). Gemcitabine (G) as positive control was taken at a optimised concentration of 101 μM, as 50% cell inhibition was not achieved. In our experiment, the candidate drug treated panel in case of L-DMEM were labelled as LC: low glucose in control, LG: low glucose in Gemcitabine, LKV: low glucose in Kaempferol with Verapamil, and in case of h-DMEM such as HC: high glucose in control, HG: high glucose in Gemcitabine, HKV: high glucose in Kaempferol with Verapamil.

Explant culture

For immunohistochemistry study, the H&E staining (Fig. S2) was accomplished through previously established protocol (Nandi et al., 2022). A part of tumor and respective normal were taken for chemoresistance gene expression without candidate drug treatment. To identify the efficacy of candidate drug in both the type of culture condition (l-DMEM and h-DMEM) on candidate gene expression, the recently operated breast tumor ($n = 12$) tissue section were cut into ~2.3 × 2 0.1 × 2.5 mm^3 and were grown in L-DMEM and h-DMEM in similar treatment condition (Nandi et al., 2022). Following treatment, one part of the

tissue was in Trizol reagent for determination of the candidate gene expression and the rest part of the tissue was taken for paraffin block preparation for immunocytochemistry analysis. All tissues were obtained as explants within 12 h of receipt from the onco-pathological checkup.

Identification of candidate markers through RT-PCR analysis

Based on the previously established protocol, both cell lines and explants were cultured in complete L-DMEM and h-DMEM media as well as treated with the aforementioned established dose of KVfor 48 h (Nandi et al., 2022). RNA was isolated from untreated tissue ($n = 21$) through previous protocol (Nandi et al., 2022) and evaluated spectrophotometrically. The primers for each specific targeted gene, as well as for reference genes were designed in oligo analyzer tools from IDT (Table S2). For q-RT-PCR, fold change of RNA expression was estimated after normalization with Ct value of β-Actin, as per our standardized protocol (Nandi et al., 2022). All experiments were performed in triplicates.

Auto-analyser based ion measurement

We analyzed Ca^{2+} ion, in both L-DMEM/h-DMEM in all treated samples and without KV treated sample including normal through autoanalyzer (Roch Cobas C 311) through the slight modification of previous protocol (Altunok et al., 2019). A total of 12 consecutive tissue samples were cultured and treated with candidate drugs in the study. Cells were harvested and pelleted through 2000 rpm for 10 min spin and the remain was collected. As a reaction control, we used blank complete media. For the experiment, the auto-analyzer were calibrated at 24-hour intermissions according to the constructers' directions.

Detection of ROS: TNBC cells (2.23×10^5) were cultured in L-DMEM and h-DMEM media and permitted for adherence to gelatin-coated cover-slips, positioned in a non-adherent six-well cell culture plate. After 48 h of candidate drug treatment (IC-50 concentration) in different glucose media panels, the cells were treated with 0.1% NBT (Nitroblue-Tetrazolium) with PMA (-phorbol-12-myristate-13-acetate) with a few modifications of the previously established protocol (Esfandiari et al., 2003). Cover-slips along with cells were placed in an NBT with PMA for negative control. After few mins. cells were washed with warm 1X PBS and fixed with paraformaldehyde (4%) for 10 – 15 mins or counter-stained with 1% safranin O solution (Javvaji et al., 2020). After mounting the cover slips with Dibutylphthalate Polystyrene Xylene (DPX), randomly ROS-positive cells (blue color) along with ROS-negative cells (red color) were counted in at least three microscopic fields under a bright-field microscope.

For colorimetric NBT Assay, the primary tumor ($n = 8$) isolated cells were cultured with the previously established protocol (Choi et al., 2006). Cells (1×10^3) were cultured and candidate drugs were used with IC50 concentration. In this assay, we follow the above-described procedure without fixation and counter staining. For extracellular Y-NBT complete removal, the cells were resuspended with methanol. To assess the NBT deposits in cells, 120 ml of 2 M KOH was used degrade cell membrane and 140 ml of DMSO was added to dissolve blue color formazan through shaking for 10 min. The solution was transported to another plate respectively and absorbance was measured at 620 nm.

Western blot analysis: To confirm all the targeted gene products upon the candidate drugs treatment under low and high glucose condition, the expression of those proteins (SOX2, OCT4, NANOG, MDR1, CD44, GLUT2, HIIF1-α) was verified through immunoblotting technique using a previously modified protocol (Nandi et al., 2022). The protein expressions under different treatment groups were normalized with respect to β-Actin expression in corresponding sets (Nandi et al., 2022).

Immunofluorescence and confocal microscopy of candidate proteins

TNBC cells (1×10^6) were culture in L-DMEM and h-DMEM and allowable to grow in cover slips, as previously described (Nandi et al., 2022). After 48 h of candidate drug treatment with their IC50 concentration in different glucose media panels, the expression and the sub-cellular localization of the gene-targeted proteins such as SOX2, OCT4, NANOG, MDR1, CD44, GLUT2, TFEB, HIIF1-α, NHE1, Na+/K+/ATPase, LC3-II and p62 in the cultured cells were analyzed by the established protocol of immunocytochemistry (ICC) (Nandi et al., 2022). Cells were fixed with 4% paraformaldehyde, permeabilized with 0.025% Triton-X-100 in PBS for 10 mins. After blocking with 3% BSA, cells were incubated overnight with respective primary antibody anti-SOX2 antibody (Abcam Cat # ab79351), anti-OCT4 antibody (Thermo Fisher Scientific Cat# MA5–31,458), anti-NANOG antibody (Abcam Ca # ab109250), anti-MDR1 antibody (Santa Cruz Ca # sc-13, 131) anti-CD44 antibody (Abcam Cat# ab51037), anti-GLUT2 antibody (Abcam Cat# ab54460), anti-TFEB antibody (Abcam Cat# ab267351), anti-HIIF1-α antibody (Cell Signaling Technology #79,233), anti-NHE1 antibody (Abcam Cat#ab67314), anti-Na+/K+/ATPase antibody (Cell Signaling Technology #23,565), anti-LC3-II antibody (Abcam Cat# ab192890) anti-p-62 antibody (Cell Signaling Technology # 88,588), in 1:200 dilution, washed and incubated with fluorescent conjugated secondary antibodies (Alexa Fluor 488 conjugated Goat Anti-Rabbit IgG; Abcam Cat# ab97048, and Alexa Fluor 647 conjugated Goat Anti-Mouse IgG; Abcam Cat# ab150115,) in 1:500 dilution, the experimental slides were mounted with ProlongGold antifade reagent containing DAPI (Abcam Cat# ab104139).

To study the expression of the candidate proteins in the explant cultures in the above-described glucose media, the human breast tissue embedded in paraffin sections were deparaffinized and subjected to gradual rehydration as per our earlier protocol (Nandi et al., 2022). After antigen retrieval with Tris-EDTA buffer (pH 9), as described in the previously established protocol (Nandi et al., 2022), the tissue was prepared for ICC and incubated with primary and secondary (fluorescence conjugated) antibodies. All experimental slides were mounted with DAPI (ProlongGold antifade encompassing). All reactions were completed in triplicate.

For both cell line and explant culture, LysoTracker red (l 7528, Thermo Fisher) was used to identify intact lysosomes in viable cells. To estimate the expression of the lysosome, the Mean Fluorescence Intensity (MFI) of LysoTracker™ probes were estimated from all tumor samples ($n = 38$). Olympus Fluo-view confocal microscope was used with 60X objective. The images were extracted through Image J software.

Determination of glucose uptake

Confocal microscopy imaging sessions were carried out in the experimental set that tested 2-NBDG (2-(N-(7-nitrobenz-2-oxa-1,3-diazol-4-yl)amino)-2-deoxyglucose) (Cayman Chemical Company; Cat No: 11,046) uptake through GLUT2 receptor in MDA-MB-231cell lines, after the treatment condition (U: Untreated, G: Gemcitabine, KV: Kaempferol + Verapamil) according to previously established IC50 concentration. The assay was completed through previous modified methods (Rajaram et al., 2013). Cells were incubated with 2-NBDG for 20 min and its uptake in presence of GLUT2 protein (Abcam Cat# ab234440) was determined through the above maintain immunocytochemistry protocol. The colocalization of 2-NBDG and GLUT2 were analysed with statistical parameter such as Pearson correlation coefficient.

In silico study

We performed an *in-silico* study of the two compounds besides *ex vivo* anti-cancerous studies on breast cancer cell lines to know the effectiveness on the malignant cells and unravel how these compounds inhibit cancer, which pathways they may regulate, physico-chemical and drug-like properties, pharmacokinetic parameters, toxicity, biological activities and gene expression changes induced by them were studied using computational approaches. Gemcitabine was chosen as the

reference drug. All these *in silico* studies were performed by using a set of free databases, web resources and software. We have also assessed the interaction of these compounds with targets of our *ex vivo* experiments using the Molecular docking as they offer heavily supported data for any compound to be used as a drug in physiological systems.

Ligand and receptor structure retrieval: ligands were taken from pubchem (https://pubchem.ncbi.nlm.nih.gov/) and receptors from RCSB PDB (www.wwpdb.org) (Berman et al., 2003).

Physico-chemical, Drug-likeness and Basic pharmacokinetic parameters of ligand: Using Swiss-Adme server, an online portal for such evaluations freely distributed by Swiss Institute of Bioinformatics (SIB) (Daina and Zoete, 2016).

Target prediction: using Swiss Target server, distributed by Swiss Institute of Bioinformatics (SIB) (www.swisstargetprediction.ch) (Daina and Zoete, 2016).

Molecular docking: Molecular interaction in silico or computationally was evaluated using the PyRx software. The ligand and receptor macromolecular structures were processed accordingly and prepared for docking.

Statistical analysis

One-way ANOVA (GraphPad Prism 8, RRID: SCR_002798) was used to calculated the MFI. The student's *t*-test was performed in the implication of gene and protein experimental outcome in the six treatment groups through the software. For statistical parameter such as 95% confidence, a *p*-value of ≤ 0.05 were measured statistically. All the study were finished deprived of significant damage of statistical power.

Results

ROS detection and associated signaling cascade of NANOG-CD44-

MDR1-ATPase: High level of ROS production is a key precursor of cancer hallmark. However, overexpression of ROS promotes tumor progression and proliferation and result in cancer cell apoptosis or senescence though oxidative stress induced by ROS. ROS can signal both autophagy induction and lysosome biogenesis. Through confocal microscopy, tumor cells showed increased fluorescence of LysoTracker red (Fig. 1A), indicating an intact lysosomal biogenesis mechanism for their survival before our candidate drug treatment. The average MFI value of Lyso-Tracker™ of all patient's tumor ($n = 38$) were (54.9008 ± 1.215) (Fig. 1B). To understand the correlation between chemoresistance marker and lysosomal Ca^{2+}-based ROS signalling, a heatmap was generated to compare the expression of *NANOG, CD44, MDR1* and *ATPase* genes in 38 breast tumor samples and assorted normal tissues (Fig. 1C). The lysosome also interacts with other organelles by the release and uptake of Ca^{2+}. The amount of intracellular Ca^{2+} from the harvested tumor tissue were found to be 3.231% (± 0.785%) in contrast to normal tissues with 1.1% (± 0.101%) (Fig. 1D). Here we find the cycle threshold (dCt) values of these candidate genes were highly upregulated in tumor samples, compared to their normal counterparts with concomitant upregulation of lysosomes. Overall, we conclude that the upregulation of genes responsible for chemoresistance might be involved in lysosomal Ca^{2+}-based ROS signaling which in turn promoted lysosomal upregulation and tumor cell survival (Fig. 1).

ROS estimation and analysis of candidate genes expression upon treatment with Kaempferol in combination with Verapamil in breast cancer: The detection and quantification of intracellular ROS production based on NBT staining was correlated with the former results of the lysosomal expression analysis. After 48 h of treatment on TNBC cell line, the intracellular ROS was detected in L-DMEM / h-DMEM media panels. No formazan precipitate was identified in the control set whereas Gemcitabine treated panel showed few reddish blue cells (low

Fig. 1. Hypothesis on the upregulation of chemoresistance gene might be contributed by lysosomal Ca^{2+} based ROS signaling in primary tumor. (A) Fluorescence-based immunohistochemical localization of Lysosome. (B) Index of Mean Fluorescence Intensity (MFI) of LysoTracker™ probes in tumor samples ($n = 38$). (C) Expression of chemoresistance marker in tumor ($n = 38$) and respective normal ($n = 38$) samples. (D) Estimation of Calcium ion in normal and tumor sample. Student's *t*-test was used to correlate the significance where *$p < 0.0332$ **$p < 0.0021$ ***$p < 0.0002$ **** < 0.0001.

formazan precipitate) in L-DMEM / h-DMEM media panels (Fig. 2A). In this figure, NBT staining characterized purple and blue formazan precipitates (represent overproduction of ROS) in KV treated group in both glucose panels whereas KV group in L-DMEM panel produced more ROS than KV group in h-DMEM panel in MDA-MB-231 cell line. No such significant difference in Gemcitabine and KV treated a panel of h-DMEM was observed. In this assay, NBT reaction exhibited oxidative action in cell cytoplasm as a basis of free radicals' formation and coloured cells dark blue as an indicator of profuse free radical formation" in MDA-MB-231 cell line. The quantity of intracellular ROS (% of NBT marked area) in MDA-MB-231 did not differ significantly between LC (11.91 ± 0.351%) and LG (13.32 ± 2.17%) (Fig. 2B). However, significantly (p < 0.0001) higher level of intracellular ROS (96.51 ± 2.571%) was noticed in LKV group whereas in h-DMEM panel, the ROS production of HC (18.6 ± 0.26%), HG (10.35 ± 0.42%) and HKV (21.38 ± 0.33%) were not significant (Fig. 2B). For confirming the assay, colorimetric NBT assay was also performed that demonstrated the OD value of dissolved NBT of LKV group in MDA-MB-231 (Fig. S3A) and primary tumor cell (Fig. 2C) were significantly increased from LG and HG treatment panel. In this treatment, we also observed that intracellular Ca^{2+} ion was significantly reduced (1.92 ± 0.24) (Fig. S3B) in LKV treatment.

In L-DMEM and h-DMEM panels, the RNA quantification of *SOX-2, OCT-4, NANOG, MDR-1, CD44, ATP1B1, NHE1, HIF1-α, GLUT2* and gene *β-Actin* (housekeeping) were determined by semi-qRT-PCR and q-RT-PCR, upon treatment with candidate drugs, in both MDA-MB-231, MCF-7 and primary breast tumor cells. For MDA-MB-231(Fig. 2D and F) and primary BC tumor cells (Fig. 2E and G), KV diminished the expression of candidate genes in L-DMEM panel whereas, in h-DMEM panel, there was no significant difference across different treatment groups. In MCF-7, KV

treatment showed aberrant outcomes (Fig. S3C, S3D). In this cell line, KV treated L-DMEM panel of *SOX2* and *MDR1* (Fig. 2D and F) expression was not significantly reduced. No substantial alteration in expression of *HIF1-α* gene was observed in MCF-7 of L-DMEM panel and KV showed inefficiency in attenuating *HIF1-α* gene for both L-DMEM and h-DMEM panels. It was interesting to find that KV induced downregulation of chemoresistance genes such as *CD44, NANOG, MDR1, ATP1B1* alongwith other markers in concordance with upregulated ROS production in cell line and in patient tumors (in comparision to the observation in Fig. 1)

Immunoblotting to determine candidate protein expression under experimental drug conditions: After finding the gene expression and their role in ROS production, we confirmed the candidate protein expression. KV resulted in significant alteration of the key chemo resistance protein such as CD44, NANOG, and MDR1, alongwith other related proteins like SOX2, OCT4, HIF1-α, and GLUT2 as distinguished from specific western blot (Fig. 2H) and from densitometric analysis of the relative fold change of candidate proteins were normalized to β-Actin (Fig. 2I–O). Interestingly, Gemcitabine treatment (LG/HG) in both L-DMEM and h-DMEM panels did not result in any significant downregulation in fold change of expression of the candidate proteins compared to control (LC/HC) in Fig. 2. This specified that KV promoted a significant diminishment of candidate proteins that were excessively upregulated as chemoresistance factors in breast cancer. In this analysis, KV was significantly working in L-DMEM panel whereas, in h-DMEM panel, the results were anomalous and inconclusive. It was observed that SOX2 (Fig. 2I), MDR1 (Fig. 2l), GLUT2 (Fig. 2N) and HIF1-α (Fig. 2O) were upregulated and OCT4 (Fig. 2J), NANOG (Fig. 2K) and CD44 (Fig. 2M) were downregulated in KV treatment in h-DMEM panel (HKV) compared to the
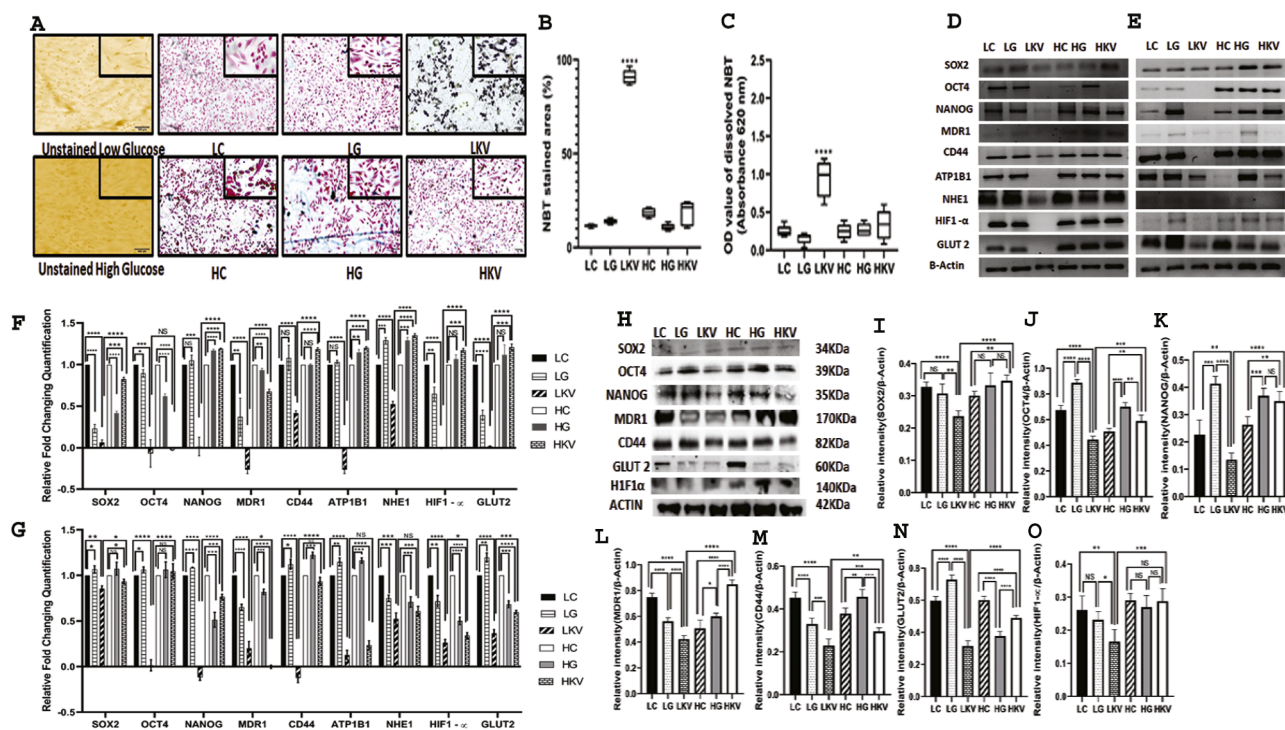
Fig. 2. Effect of Kaempferol with Verapamil on ROS production and chemo-evasion mechanisms. (A) ROS production in MDA-MB-231 cells, upper panel low glucose treated set and lower panel high glucose treated set. (B) Estimated the NBT stained area in MDA-MB-231 cells under various treatment conditions (48 h). (C) Estimated of ROS production in primary tumor cellsunder similar treatment conditions (48 h). (D, E) Semiquantitative and (F, G) quantitative RT-PCR to determine the expression status of candidate genes viz. *SOX2, OCT4, NANOG1, MDR1, CD44, ATP1B1, NHE1, HIF1-α, GLUT2,* upregulated in (D, F) MDA-MB-231 and (E, G) primary tumor respectively; *β-Actin* gene was used as endogenous control for both semiquantitative and quantitative RT-PCR under identical treatment group (48 h). (H) Western blot analysis to investigate the fold change of expression of candidate markers in MDA-MB-231 cell line under various treatment conditions (48 h) . Fold change of expression of candidate genes were normalized to the expression of (I–O) β-Actin. Student's *t*-test and Two-way ANOVA were used to correlate the significance where *$p < 0.0332$ **$p < 0.0021$ ***$p < 0.0002$ **** < 0.0001. Different treatment groups indicated in above following experiment includeLow glucose control (LC), Low glucose Gemcitabine (LG), Low glucose Kaempferol with verapamil (LKV), High glucose control (HC), High glucose Gemcitabine (HG),and High glucose Kaempferol with verapamil (HKV).

Gemcitabine treated set (HG). In contrast, LKV treatment set showed a significant reduction of candidate gene expressions with respect to HKV treatment set.

Immunocytochemical analysis of candidate chemoresistance proteins: Compared to LC treatment set, it was observed that LKV inhibited tumor cell growth and reduced the expression of candidate markers CD44 (Fig. 3A,and E), NANOG (Fig. 3B and F), MDR1 (Fig. 3C and G), and Na+/K+/ATPase (Fig. 3D and H) although treatment with LG did not have any significant effect on the expression status of candidate markers in tumor sample and MDA-MB-231 (Fig. S4A, S4B, S4C and S4D). In h-DMEM panel we found HKV upregulated the expression of candidate proteins. MFI value of tumor sample (Fig. 3E-H) and MDA-MB-231 (Fig. S4E, S4F, S4G and S4H) exhibited significant downregulation of expression of targeted proteins LKV treatment conditions. In HG treatment all four markers were significantly upregulated. Except for NANOG protein, the significant fold change in the other candidate proteins did not change in Gemcitabine group (Fig. 3B and S4B). Fluorescence intensity (FI) was estimated through the ImageJ software as the previous study (S.K. Nandi et al., 2022). MFI values of each cell were calculated from five different areas and the background FI of the cell-free area was subtracted. Statistical significance of MFI values in different treatment groups were calculated.

Synergistic Effect of Kaempferol and Verapamil on glucose transport: In primary tumor, both HIF-1α (Fig. 4A, D) and NHE1(Fig. 4C, F) were downregulated in LKV treatment panel which showed high level of ROS production (Fig. 2). In MDA-MB-231 the HIF-1α (Fig. S5A, S5D) dependent NHE1 activation (Fig. S5C, S5F) showed a similar kind of outcome. It was observed that LKV was more effective than HKV set (Fig. 4D and F) in both primary tumor (Fig. 4) and MDA-MB-231 (Fig. S5). Moreover, we also observed that a reduction of GLUT2 markers in the primary tumor (Fig. 4B and E) and MDA-MB-231 (Fig. S5B, 5E) resulted in less cellular proliferation in LKV treatment set. Here, we wanted to confirm the experiment in MDA-MB-231 by 2-

NBDG uptake and then determine the effect of glucose uptake through GLUT2 receptor. Confocal microscopy imaging with MFI sessions was carried out after 48 h candidate drug treatment in MDA-MB-231 (Fig. 5A and B). Here, in control or Gemcitabine treatment both MDA-MB-231 and tumor samples showed more glucose uptake than KV treatment. In respect of control, Gemcitabine has no significant role in glucose uptake system. In addition, the HIF-1α and NHE1 were downregulated in this treatment condition (LKV).

ROS-associated fate of lysosome in the treatment of Kaempferol with Verapamil: In continuation with our former study, we aimed to find a significant change in lysosomal expression in both treatment panels in tumor sample (Fig. 6A) and MDA-MB-231 (Fig. S6A). Compared to control (LC) in L-DMEM panel of both samples, it was observed that LKV downregulate the lysosomal expression, although treatment with Gemcitabine in L-DMEM and h-DMEM panels did not have any significant influence on the expression status. MFI value in tumor sample (Fig. 6E) and MDA-MB-231 (Fig. S6E) showed significant downregulation of lysosome in LKV treatment conditions whereas no significant changes were observed in h-DMEM panel in both samples. In this LKV treatment condition, we also found that TFEB was also downregulated in tumor samples (Fig. 6B and F) as well as MDA-MB-231 (Fig. S6B, S6F). In Fig. 6 and figure S5, we found that the KV drug recycled lysosomal Ca^{2+}expression that promotes ROS production whereas chemotherapeutics Gemcitabine (G) could not play the role. In LKV treatment, we detected autophagy-mediated cell death through the upregulation of central autophagy-associated proteins such as LC3II (Protein-light-chain-3) (Fig. 6C and G) and p62 (sequestosome1) (Fig. 6D and H) in primary tumor and MDA-MB-231 (Fig. S5C, S5G) and (Fig. S6D, S6H) respectively. Morphologically, autophagic cell death was reliant on the autophagic elements with extensive cytoplasmic vacuolization of LKV treated tumor tissue (Fig. 6) or MDA-MB-231 (Fig. S6) and lysosomal degradation whereas no significant upregulation was observed in HKV
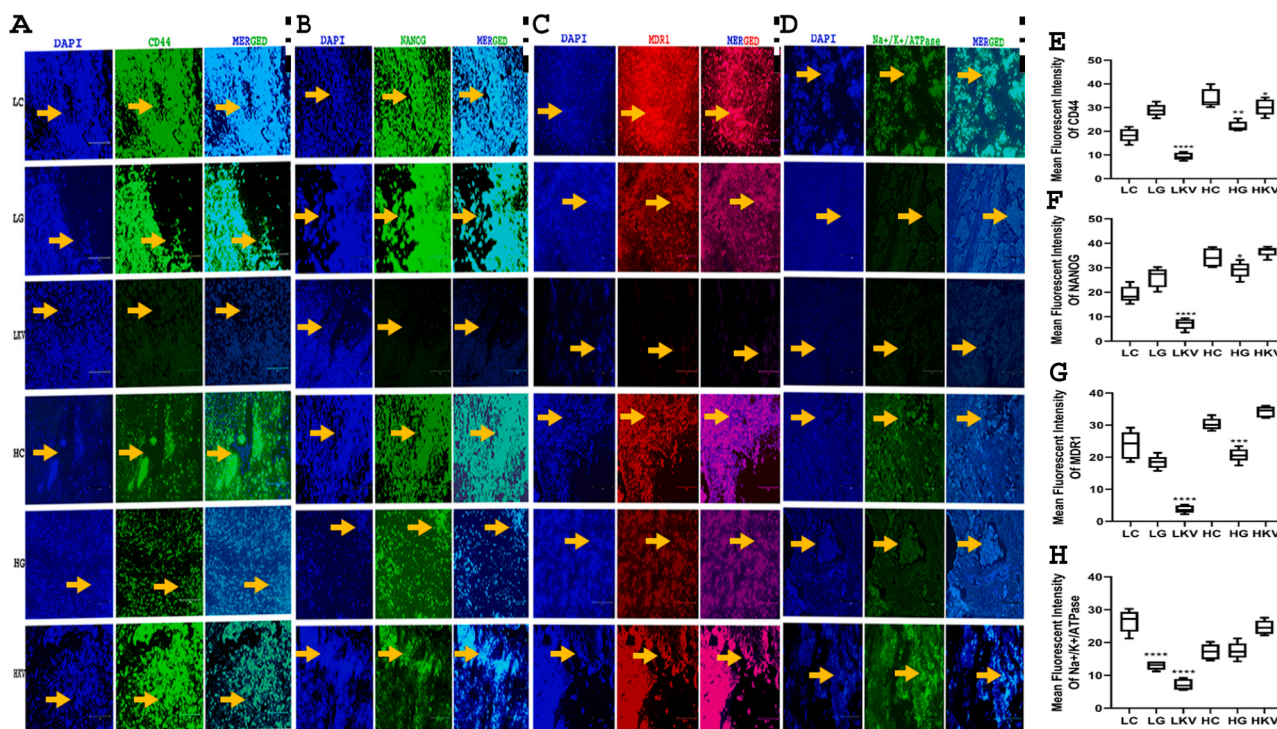
Fig. 3. Immunofluorescence microscopy exploring the expression of chemoresistance marker following drug treatment exposure. Fluorescence-based immunohistochemical localization of (A) CD44, (B) NANOG, (C) MDR1 and (D)Na+/K+/ATPase protein in primary tumorupon different treatment (48 h.) conditions. Scale bar: 150 μM. Mean fluorescent intensity of (E) CD44, (F) NANOG, (G), MDR1 and (H) Na+/K+/ATPase. The different treatment groups included: Low glucose control (LC), Low glucose Gemcitabine (LG), Low glucose Kaempferol with Verapamil (LKV), High glucose control (HC), High glucose Gemcitabine (HG),and High glucose Kaempferol with Verapamil (HKV). One way ANOVA is used for statistical significance ***p < 0.0002, **** p < 0.0001.
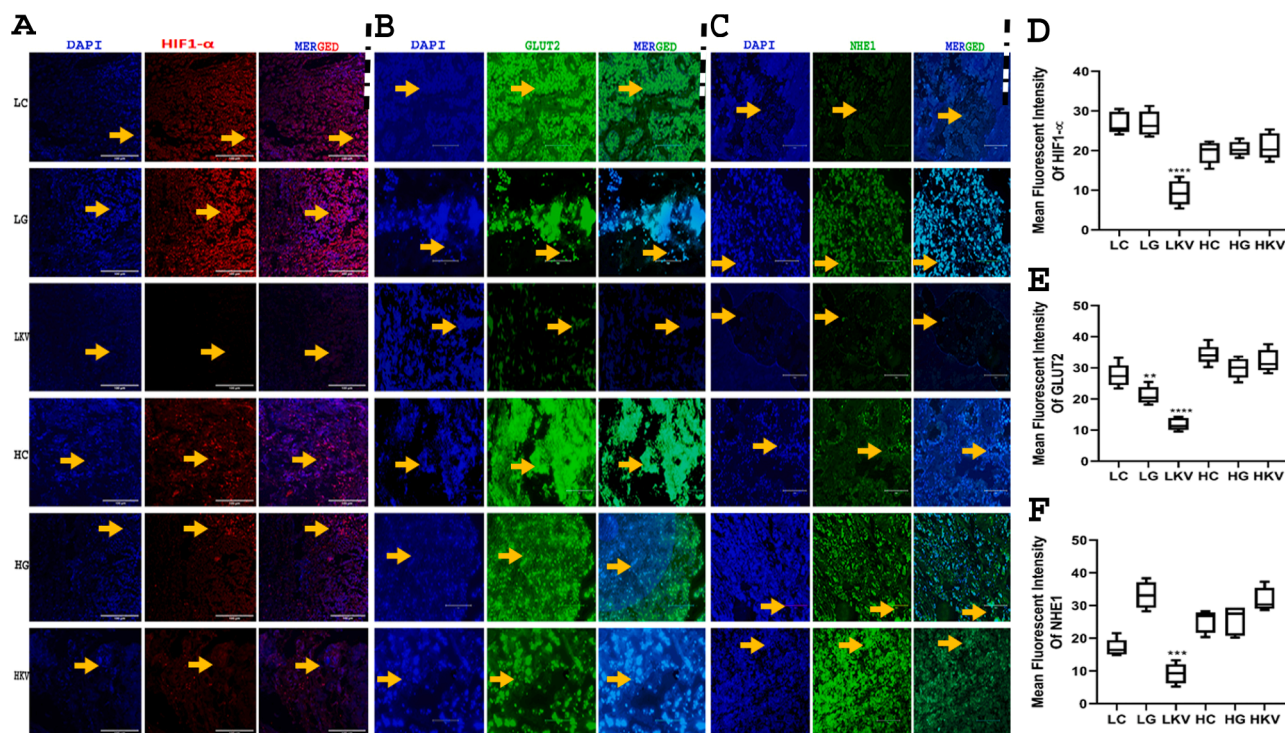
Fig. 4. Hypoxia and glucose transporter-based acidosis marker expression upon treatment with Kaempferol and Verapamil under low and high glucose. Fluorescence-based immunohistochemical localization of (A)HIF1-α, (B) GLUT2, (C) NHE1 and protein in primary tumorwith candidate drugs treatment (48 h.) conditions. Scale bar: 150 μM. Mean fluorescent intensity of (D) HIF1-α, (E) GLUT2, and (F)NHE1. The different treatment groups included: Low glucose control (LC), Low glucose Gemcitabine (LG), Low glucose Kaempferol with Verapamil (LKV), High glucose control (HC), High glucose Gemcitabine (HG),and High glucose Kaempferol with Verapamil (HKV). One way ANOVA is used for statistical significance ***$p < 0.0002$, **** $p < 0.0001$.
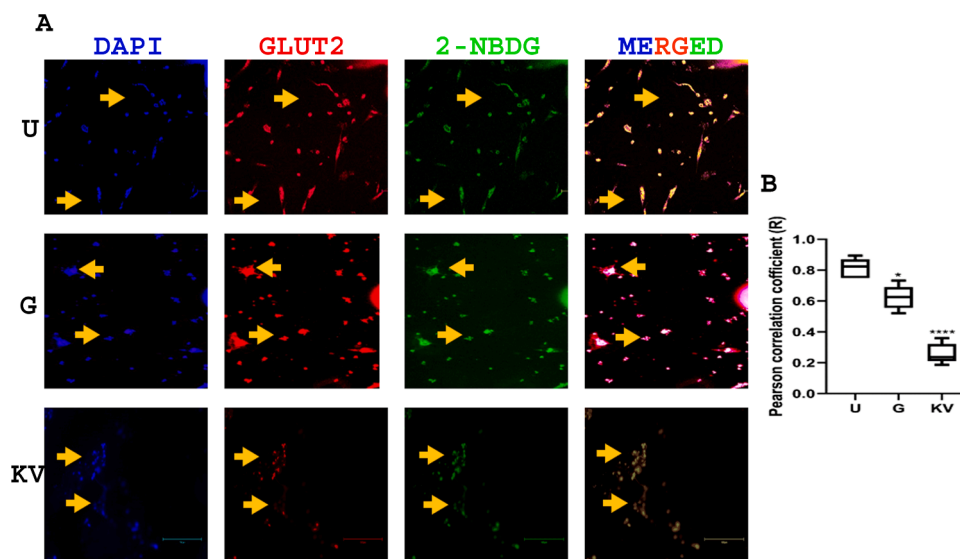
Fig. 5. Effect of KV on glucose uptake through GLUT2 transporter. Colocalization of (A) GLUT2, and 2-NBDG in primary tumorwith different treatment (48 h.) conditions. Scale bar: 150μM. (B) Pearson correlation coefficient (R) of co-localization of GLUT2 and 2-NBDG was analysed.The treatment groups included: control (C), Gemcitabine (G), Kaempferol with verapamil (KV). One way ANOVA is used for statistical significance ***$p < 0.0002$, **** $p < 0.0001$.

treatment. In both L-DMEM and h-DMEM panels, the G treated (LG/HG) had no significance in respect of control (LC/HC).

The outcome of in silico study

Structure retrieval of ligands and receptors: Our previous work had shown the combinatorial enhancement of Kaempferol and Verapamil combination than when used singly against cancerous cell lines. The structure of the flavonoid, drug and Gemcitabine (control) are illustrated respectively in Fig. 7 (Fig. 7A-C). The structure of receptors is given in the supplementary section (Fig. S7).

Drug-likeness, Physico-chemical property and pharmacokinetics of Ligands: The physicochemical properties and drug-like properties of the three chosen ligands are depicted by the biological radar of the SWISS-ADME webserver. The results show that Kaempferol cannot be fully treated as a drug molecule as it has too much unsaturation in the
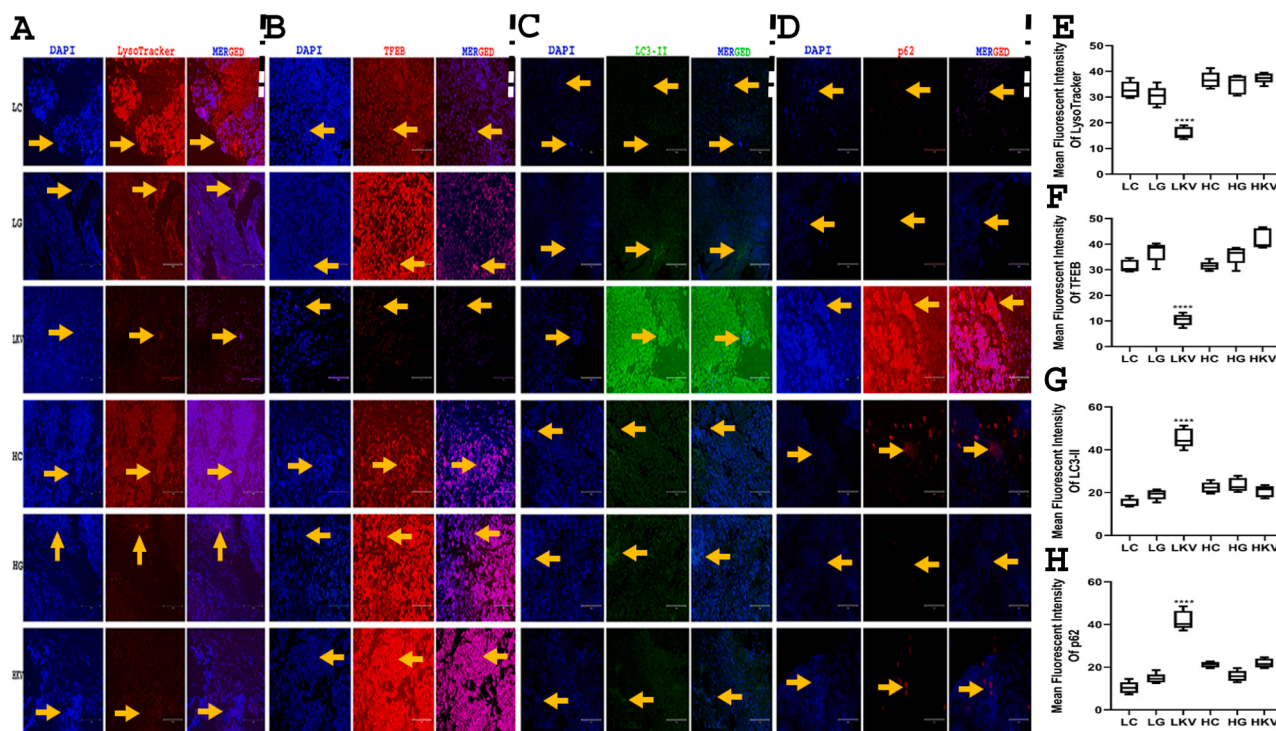
Fig. 6. Effect of KV on lysosome, TFEB and autophagic cell death marker expression under low and high glucose condition. Fluorescence-based immunohisto-chemical localization of (A) Lysosome, (B) TFEB, (C) LC3-II, and (D) p62 protein in primary tumor upon different treatment (48 h.) conditions. Scale bar: 150μM. Mean fluorescent intensity of (E) LysoTracker™ probes, (F) TFEB,(G) LC3-II, and (H) p62. The treatment groups included: Low glucose control (LC), Low glucose Gemcitabine (LG), Low glucose Kaempferol with Verapamil (LKV), High glucose control (HC), High glucose Gemcitabine (HG),and High glucose Kaempferol with Verapamil (HKV). One way ANOVA is used for statistical significance ***$p < 0.0002$, **** $p < 0.0001$.
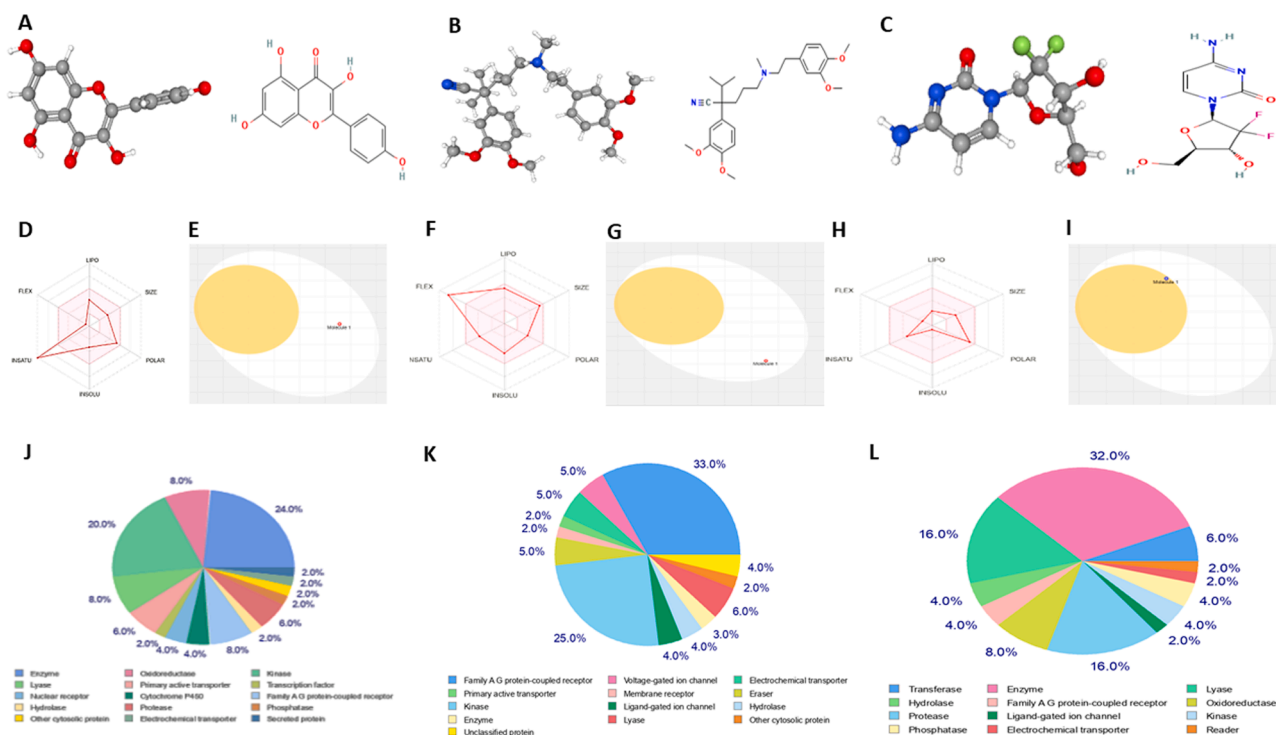
Fig. 7. A, B, and C. Ligand structures: Kaempferol, Verapamil and Gemcitabine respectively. D, F, and H. Physico-chemical properties of Kaempferol, Verapamil and Gemcitabine respectively. E, G, and I. Boiled egg representation of Kaempferol, Verapamil and Gemcitabine respectively. J, K, and l. predicted cellular targets of Kaempferol, Verapamil and Gemcitabine respectively.

molecule (Fig. 7D.) i.e. the fraction of carbons in the sp3 hybridized state (Fraction Csp3)) is less than 0.25 (0.00). The drug Verapamil was also shown to be not fully drug-like molecule as evident from the radar, the flexibility of the molecule is outside the range (Fig. 7F.) i.e. 13. The effective range is 1 – 9. On the other hand, the drug Gemcitabine, fully remained on the biological radar (Fig. 7H.) suggesting it to be a full drug which can be easily made bioavailable, in respect of the previous two ligands. However, the combination of ligands may exert a different effect when in the biological system. Despite not having optimal drug-likeness properties, they are still effective as anti-cancerous agents. All of them follow Lipinski's rule efficiently. All other physicochemical properties, solubility and drug-likeness parameters are provided in Table S3.

The BOILED-Egg, predicts concurrently dual key ADME parameters, i.e., the passive gastrointestinal absorption (HIA) and brain access (BBB) of the ligands along with active efflux from the CNS or to the gastrointestinal lumen. The consequence depends on dual physicochemical descriptors only (WLOGP and TPSA, for lipophilicity and deceptive polarity respectively). Kaempferol lies in the white portion having highly probable HIA absorption and least probable BBB permeation along with being a non-substrate of P-gp receptor (Fig. 7E.), almost similar to Gemcitabine (Fig. 7I.), while Verapamil lies in the inner yolk portion with a high probability of BBB permeation and also actively effluxes by P-gp (Fig. 7G).

Target prediction: To predict the most probable targets of our ligands or bioactive molecules, we have used the Swiss-Target. It predicts the macromolecular targets (proteins from humans) of our ligands. Kaempferol is seen to be the most active against enzyme targets being followed by kinase receptors. Oxidoreductase, G-protein coupled receptors and Lyase class of receptors are the next class of putative targets. The least affected group of proteins includes protease, Phosphatase, Transcription factors and transporter proteins (Fig. 7J). In contrast, Verapamil drug has the most targets in G-Protein coupled receptors and then kinase class of receptors. Lyase proteins, voltage-gated ion channels and transporter proteins are also putative targets and can be targeted for biological activities. Cytosolic proteins, active transporters and membrane receptors are the least possible targets of this ligand (Fig. 7K). Gemcitabine shows that their most proficient targets include enzymatic receptors being followed by the Lyase and Protease group of proteins. Oxidoreductase and Transferase class of enzymes are their next group of putative receptors with GPCR receptors, Ligand-gated ion channels and electrochemical receptors as the least affected ones (Fig. 7l).

Molecular docking studies: Molecular docking was performed to see the interactions between our chosen ligands and other receptor protein targets which we have worked with during our *ex vivo* experiments. Kaempferol showed the highest binding to NHE1, a plasma membrane ion antiport transporter with a binding affinity of -8.2 kcal/mol. This protein plays role in maintaining an acidic cell microenvironment and thereby upregulation of Lysosomes promoting ROS scavenging activity finally leading to autophagy-induced cell death. TFEB, LC3-II, NANOG and CD44 also showed high binding affinity each of them having a high affinity above -7.0 kcal/mol. TFEB is a recognized transcription factor involved in the biogenesis of lysosomes as well as autophagy, and LC3-II induces starvation-induced autophagy but Kaempferol impeded lysosomal biogenesis thus inducing autophagy in an irreversible manner. The other two chemoresistance markers are also positively correlated, the former playing an important role for stem cells and the latter being responsible for maintaining the acidic environment along with an immunological role in this case. MDR1 showed the least binding with a score of about -4.7 kcal/mol which may infer that Kaempferol alone may not efficiently regulate Pg-P receptor. Verapamil also showed the highest binding to NHE1 (-7.6 kcal/mol), followed by TFEB (-7.6 kcal/mol) almost similar to the former ligand. NANOG and LC3-II, showed lower binding to this drug having docking scores of -6.1 and -5.6 kcal/mol respectively. SOX2 and OCT4 transcription which play important roles in development and self-renewal, stem cell plasticity is at the lower
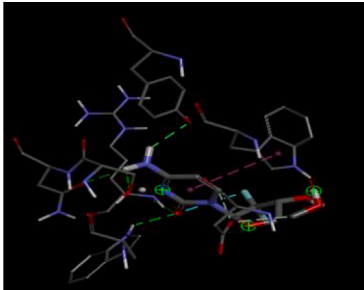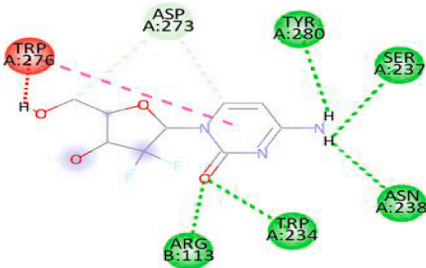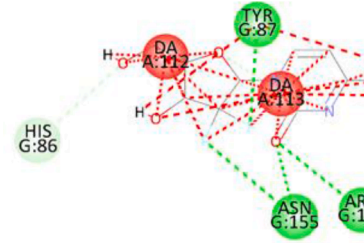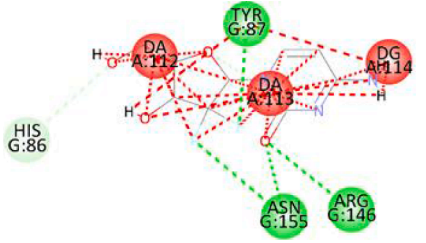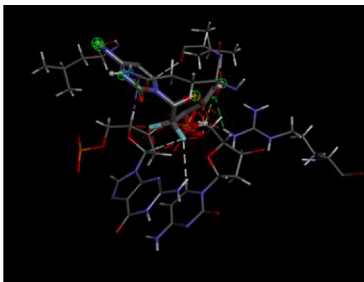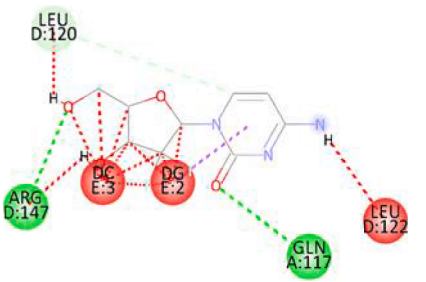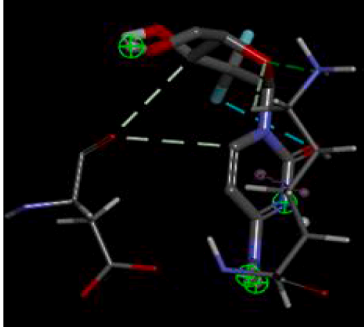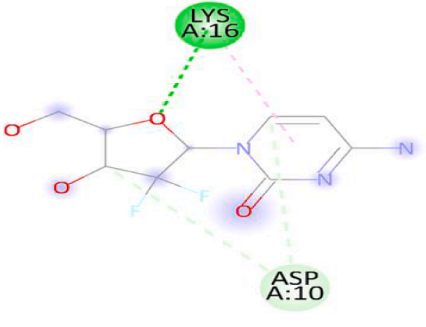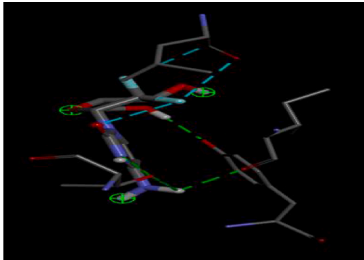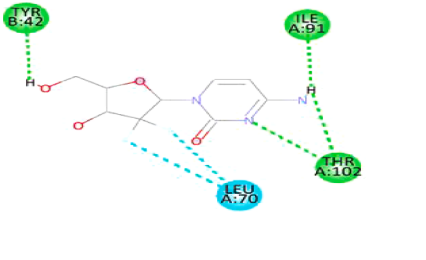
ends with binding around -5.0 kcal/mol. The combination of KV may downregulate the function of MDR1 thereby decreasing Ca2+ions as well as lysosome biogenesis, increasing the anti-cancerous activity of the ligand combination manifold. Gemcitabine showed bindings in an almost similar range with LC3-II showing the highest (-6.9) which is much lower than the top-most receptor binders of previous ligands and then NHE1 (-6.8 kcal/mol) (Table 1).

Similarly, the binding affinity can be again compared in terms of Inhibition constant (Ki). The lesser the Ki, more the binding affinity between the ligand and receptor. Although numerically, the values did not expand or varied much but in terms of enzyme chemistry it is well noticeable. The Ki varied between 0.998267 (G-MDR1) and 0.9966797 (K-NHE1). In the range of good binding affinity based on *in silico* study, we found three complexes (i.e. around 0.996) and they are- K-NHE1, K-TFEB and K-LC3-II. Based on these outcomes it can be well determined that Kaempferol is the most active drug amongst all used in this study. Again, when comparing the binding amino acid residues of the receptor or active residues of binding pocket there has been huge disparity among, the ligands. In SOX-2 G and K seemed to be bound to same pocket but not V. although all of them bounded to a single common amino acids-LYS B113. This receptor showed many hydrogen bonds in their association. OCT4 also showed the similar trend and in this case ARG G146 was found to be the similar amino acids. In NANOG, no such similar amino acids are seen and even binding pockets. The MDR1 receptor showed a different trend from the before ones, as this receptor showed binding to all the ligands in same binding pocket. The amino acids also show huge similarity and almost all coincided in terms of bonds also. CD44 showed no similar residues however G and K showed similarity in binding pocket. TFEB also showed no similar amino acids in binding pockets and they all bind to different pockets. For NHE1 it can be said that G and K binds almost to the similar active site of the receptor as evident from amino acids residues but not V. the amino acid Proline (B167) is common in all the complexes and all the three ligands seem to interact in vicinity for this target. The HIFIA receptor interactions with G as well as K showed several binding residues similarity suggesting that they bind to the same binding pocket. Several amino acids are common while in case of V it's just the opposite and none of the residue are similar. In accordance with the previous receptors LCS-II also showed similar trends showing that G and K binds to same residues and all residues are similar. While the other one is much different having no parity in binding amino acids. Overall, it can be concluded that Gemcitabine and Kaempferol are very much similar in respect of binding to receptors and hence it can be inferred that they exert the same effect or act via similar mechanisms in biological systems. Verapamil on the other hand is radically different and enhances the mode of action of Kaempferol.

Discussion

ROS and autophagy regulation acts as two-faced swords in cancer initiation and uncontrolled proliferation and are promising targets for novel anticancerous therapy. ROS plays vital roles in malignancy and survival of ROS-induced cellular stress is maintained by lysosomes in cancer cells (Zhang et al., 2016). Prior reports demonstrated that, upon cellular stress, lysosomes induced autophagy-associated cell death more robustly as compared to mitochondria (Zhang et al., 2016). Oncogenic transformation generates an increased number and volume of lysosomes that up-regulates lysosomal enzymes which plays a critical role in cancer growth, metastasis, and multidrug resistance (MDR) (a product of P-glycoprotein (Pgp) that is expressed in intracellular organelles to confer drug resistance) (Schneider et al., 2015). Moreover, limited study shows that the increased level of Ca2+ ion was responsible for PgP overexpression in tumor cells (Nygren et al., 1991). Ca2+ signaling is controlled through extracellular Ca2+ entry and Ca2+ discharge from intracellular stores. Lysosome has been recognized as a significant intracellular Ca2+ store that is responsible for Ca2+ to regulate many
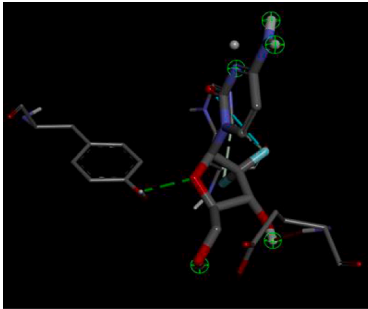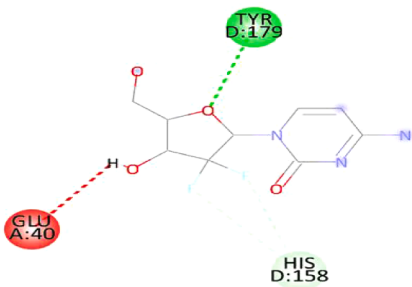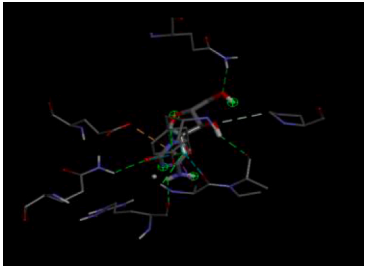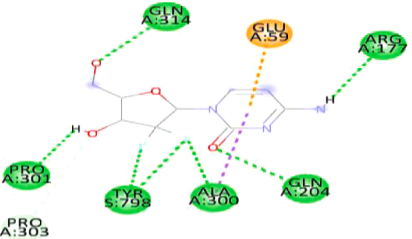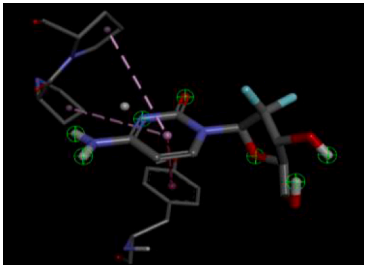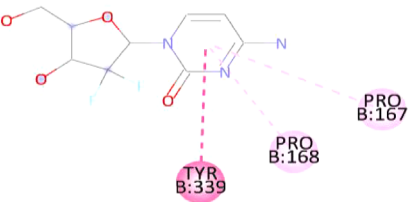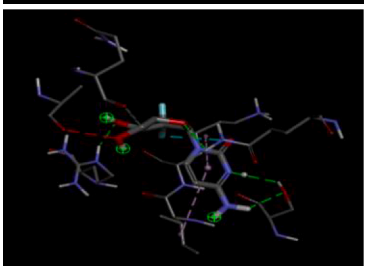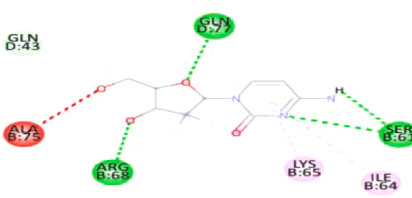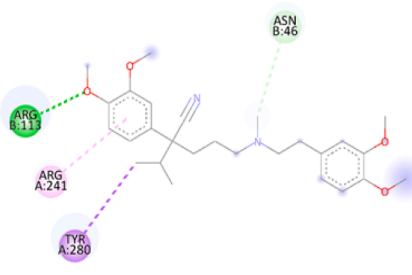
Table 1

computational interaction analysis through Molecular Docking of individual ligands and control with receptors. The table shows 3D as well as 2D interaction map of the receptor ligand complexes with interacted residues involved and binding affinity. The highest interaction scores are indicated in red.

Ligand	Receptor	3D interaction	2D interaction	Binding energy	Inhibition/ dissociation constant (Ki)
Gemcitabine	SOX2 (6WX9)			-5.6 ± 0.05	0.997743
	OCT4 (5KRB)			-6.1 ± 0.06	0.997543
	NANOG (4RBO)			-6.1 ± 0.063	0.997543
	MDR1 (6COV)			-4.3 ± 0.052	0.998267
	CD44 (1UUH)			-6.6 ± 0.083	0.997341
					0.997421
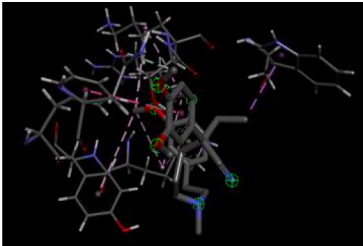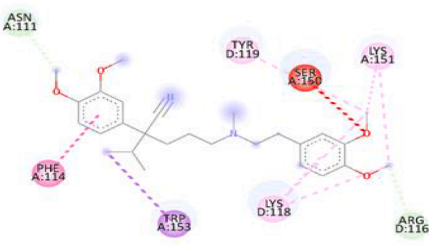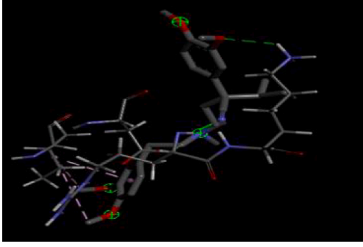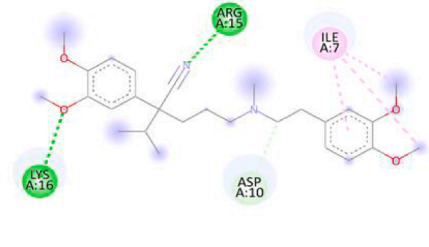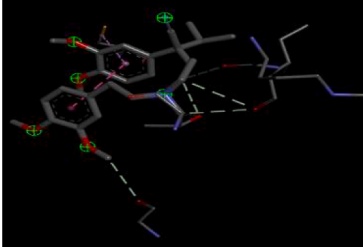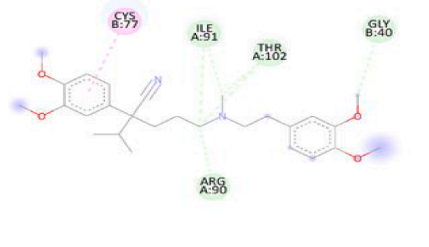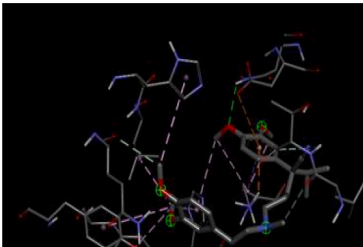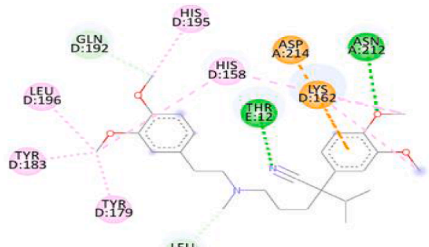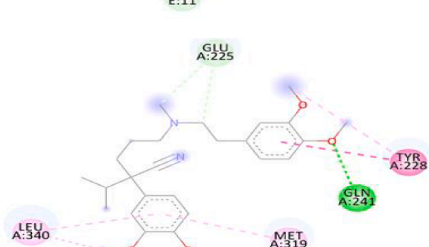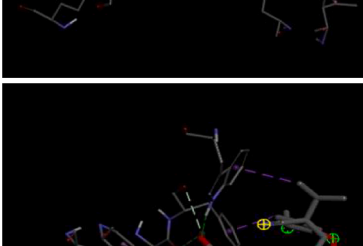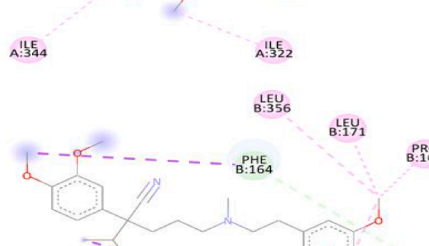
Table 1 (*continued*)

Ligand	Receptor	3D interaction	2D interaction	Binding energy	Inhibition/ dissociation constant (Ki)
	TFEB (6A5S)			-6.4 ± 0.072	
	HIF1A (1H2K)			-5.4 ± 0.061	0.997823
	NHE1 (7DSW)			-6.8 ± 0.052	0.997260
	LC3-II (5XAC)			-6.9 ± 0.068	0.997220
Verapamil	SOX2 (6WX9)			-4.8 ± 0.052	0.998065
	OCT4 (5KRB)			-4.9 ± 0.059	0.998025
					0.997543
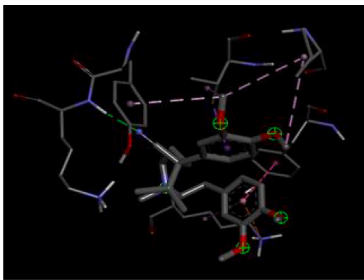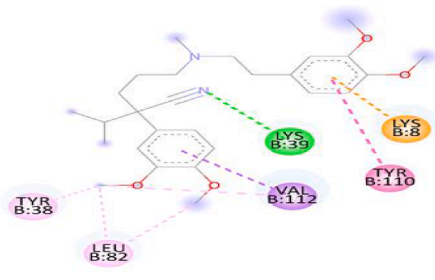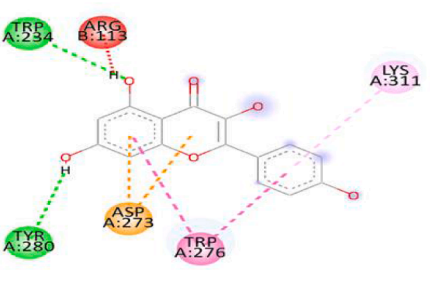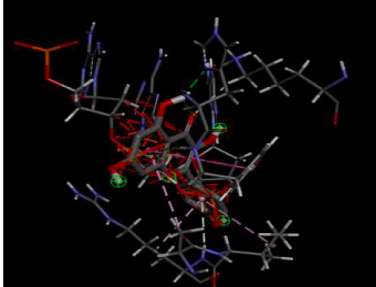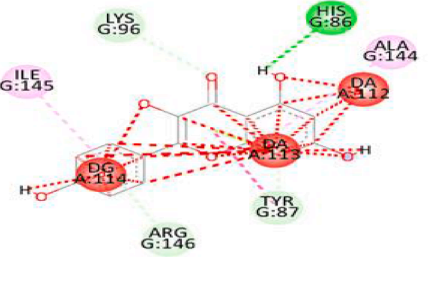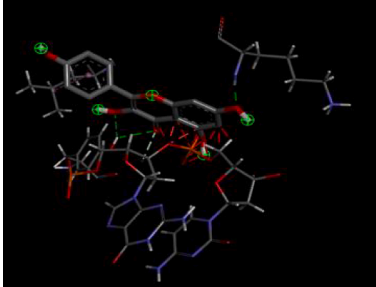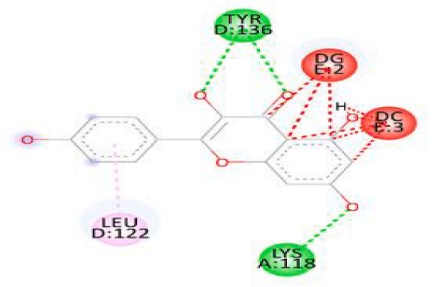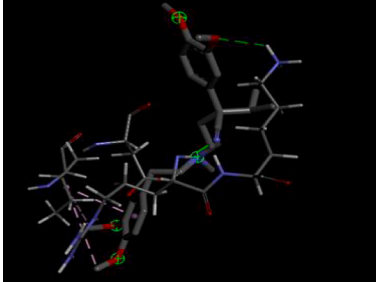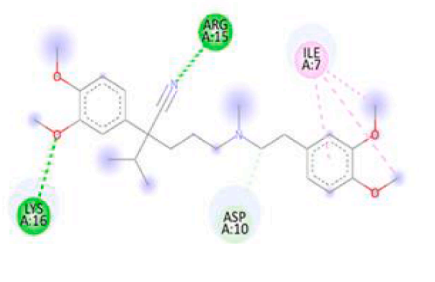
Table 1 (*continued*)

Ligand	Receptor	3D interaction	2D interaction	Binding energy	Inhibition/ dissociation constant (Ki)
	NANOG (4RBO)			**-6.1 ± 0.066**	
	MDR1 (6COV)			**-5.2 ± 0.058**	**0.997907**
	CD44 (1UUH)			**-5.7 ± 0.044**	**0.997703**
	TFEB (6A5S)			**-7.4 ± 0.051**	**0.997019**
	HIF1A (1H2K)			**-5.5 ± 0.056**	**0.997836**
	NHE1 (7DSW)			**-7.6 ± 0.069**	**0.996938**
					0.997666
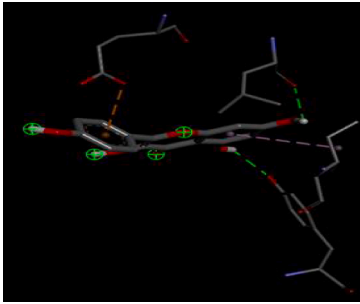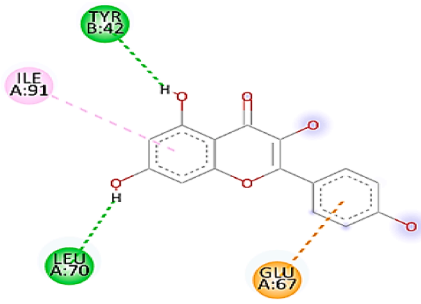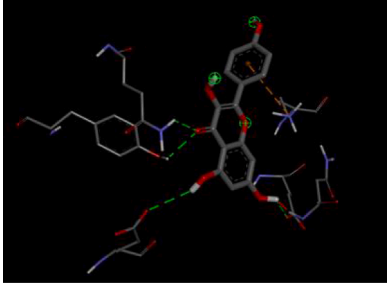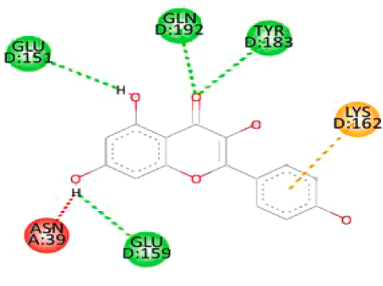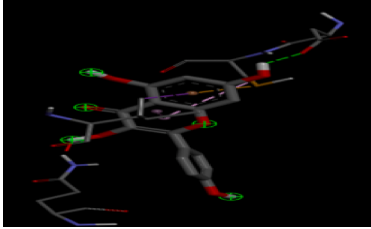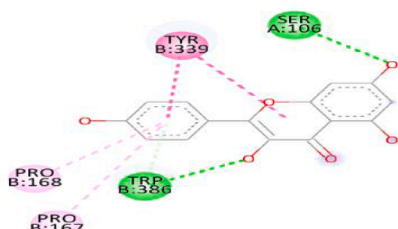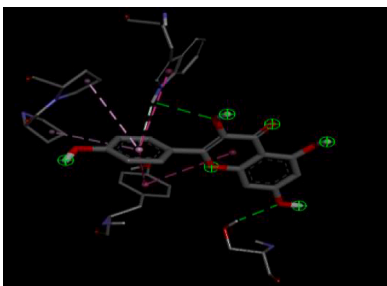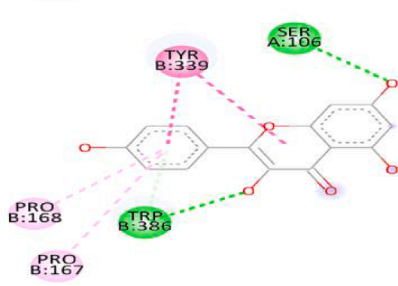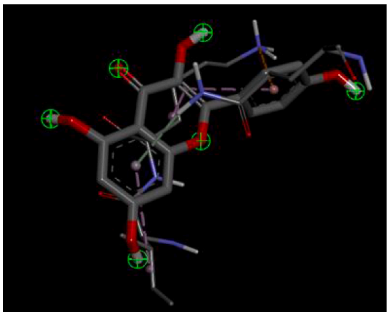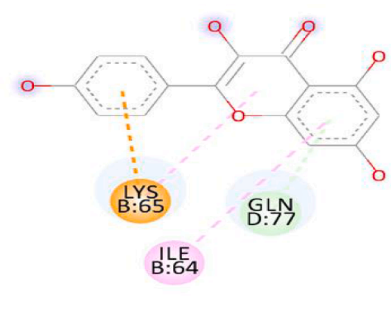
Table 1 (*continued*)

Ligand	Receptor	3D interaction	2D interaction	Binding energy	Inhibition/ dissociation constant (Ki)
	LC3-II (5XAC)			**-5.8 ± 0.086**	
Kaempferol	SOX2 (6WX9)			**-6.4 ± 0.091**	0.997421
	OCT4 (5KRB)			**-7.0 ± 0.11**	0.997180
	NANOG (4RBO)			**-7.3 ± 0.096**	0.997060
	MDR1 (6COV)			**-4.7 ± 0.075**	0.998105

Table 1 (*continued*)

Ligand	Receptor	3D interaction	2D interaction	Binding energy	Inhibition/ dissociation constant (Ki)
	CD44 (1UUH)			**-6.9 ± 0.095**	**0.997220**
	TFEB (6A5S)			**-7.5 ± 0.078**	**0.996979**
	HIF1A (1H2K)			**-6.5 ± 0.097**	**0.997381**
	NHE1 (7DSW)			**-8.2 ± 0.099**	**0.9966797**
	LC3-II (5XAC)			**-7.8 ± 0.11**	**0.996858**

cellular processes (Settembre et al., 2013). In Fig. 1, we observed concomitant upregulation of lysosomal Ca^{2+} in tumors with upregulation of markers contributing to chemo resistance such as CD44, NANOG, MDR1 and ATP1B1.

Several previous reported suggested that chemoresistance develops after long time treatment of chemotherapy (Liou and Storz, 2010). Other reports of different type of cancer, documented the expression of few markers such as CD44, NF-KB, PI3K/AKT, MAPK, HIF1A, ABC

transporter family proteins and NANOG that are directly or indirectly related Gemcitabine resistance phenomenon (Jia and Xie, 2015). Previous reports also documented that tumors with overexpression of CD44s are more invasive and rapidly become resistant to Gemcitabine and ABC transporter inhibitor Verapamil resensitizes the resistant cells to Gemcitabine and RNAi of CD44 repressed the clonogenic properties of the resistant cells (Jia and Xie, 2015). The CD44 associates with P-gp to induced cell migration or the invasion of BC tumor cells and

CD44-NANOG complex formation with the help of SOX2 and OCT4, leads to NANOG stimulation and expression of embryonic stem cell marker in chemotherapeutic drug resistance (Bourguignon et al., 2008). Also, downregulation of HIF-1α in Gemcitabine-treatment resistant cells triggered a part of reverse phenomenon of EMT phenotype (Jia and Xie, 2015). Reflexively, HIF-1α contributes to Warberg's effect which has association with increased glucose transporter expression and lactate accumulation (Jia and Xie, 2015). The Na+/H+ pump (NHE1) plays a vital role in the survival of cancer cell. Earlier reports showed that resistance to doxorubicin (DOX) occurs through NHE1 upregulation (Chen et al., 2019). Besides, Na/K-ATPase is an important marker in cancer treatment that induced the activation of numerous molecular oncogenic signal pathways, and elevation of autophagy or apoptosis (Themistocleous et al., 2021) but an intrinsic understanding with other chemoresistance markers has not been reported.

The signature of chemoresistance markers in different cell line and mice model is well documented but none of the earlier studies showed these gene signatures in ex-vivo model in breast cancer. No prior studies compared all these chemoresistance genes expression under low and high glucose conditions. The uniqueness of our study is, we observed a uniqueness of our drug combination KV on markers that regulate chemoevasion, tumor stemness & acidosis as well as lysosome upregulation, all of which have indispensable association and role in chemoresistance (Fig. 8). We had taken Gemcitabine as our standard positive control drug, on the logic, that, Gemcitabine is used as a mainstream drug for metastatic breast cancer and patients develop early resistance to that after a brief period of time.

Based on previous reports on antagonizing effect of Verapamil on multidrug efflux transporters, we had chosen it as an adjunct drug in our earlier study and found that combining Verapamil with Kaempferol increases its effectiveness as an anticancer drug. Another important role of Verapamil lies in its ability to export reduced Glutathione through multidrug efflux transporters (Settembre et al., 2013), so it may be concluded that adding Verapamil to Kaempferol produces more oxidative stress to the tumor cells. Kaempferol alone can also promote ROS production (superoxide anion (O2•-)) in cancers (Sharma et al., 2007), though its anti-inflammatory effect has also been reported in tumors (Sharma et al., 2007). In our study, a synergistic combination of KV, on one hand, halted cellular antioxidant scavenging properties, as observed in our NBT assay, and on other hand, attenuated the expression of key regulators like HIF1α, NHE1, MDR1 etc. which play important role in chemoevasion following oxidative stress.

Autophagy is regulated by ROS including superoxide ($O_2^{\bullet-}$) and hydrogen peroxide (H_2O_2). In our study, KV under low glucose condition induced autophagy-mediated cell death and simultaneous overproduction of ROS. By employing NBT assay we found that $O_2^{\bullet-}$ was selectively induced by low glucose. Additionally, with autophagy inhibitor such as 3-methyladenine, Zhang group detected extreme viability of cells in Verapamil treatment, and suggested that Verapamil-promoted autophagy might contribute to its cytotoxicity (Zhang et al., 2016). In our study, KV treatment also induced ROS generation, leading to oxidative stress that was also indicated to autophagy initiation.

It has been hypothesized that high glucose transporter expression might have a vital role for maintaining the growth of cancer cells (Vishvakarma et al., 2013). Numerous medical circumstances can intensify glucose level in blood that contribute to reduced efficacy of chemotherapeutics and confer resistance to tumors (Vishvakarma et al., 2013). In laboratory studies, glucose concentration of around 17.5 mM in cell culture growth media and extracellular levels at 10 mM (Zhang et al., 2016) are maintained. In our experiment, we observed the outcome of our experimental drug system KV in low (5.55 mM) and high extracellular glucose (25 mM) concentrations. The results from this study showed that KV worked efficiently under low glucose concentration. In our previous study, we have documented that KV-induced strong γH2AX expression in tumor cell but not in normal breast tissue (Nandi et al., 2022). In our present study, LKV treatment conditions showed
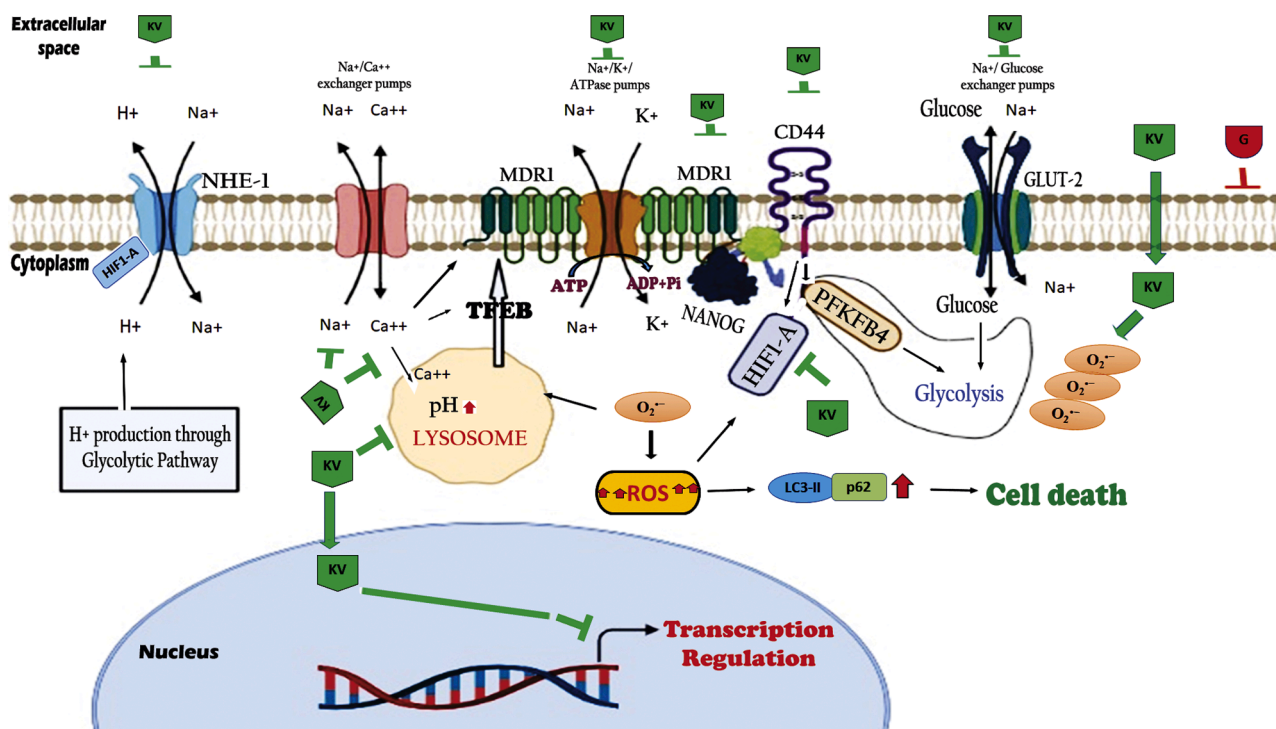
Fig. 8. Perturbation of lysosomal Ca$^+$ based chemo-evasive mechanism by Kaempferol+ Verapamil (KV) with an emphasis on overproduction of ROS, followed by ROS mediated autophagy and cell death. Tumors obviate oxidative stress through upregulation of Lysosomal Ca^{2+}, TFEB, HIF1α along with induction of several transporters like Na+/K+ ATPase, NHE1, GLUT2. The association of chemoresistance with Lysosomal Ca$^+$ was inhibited by KV in low glucose (LG) condition. KV downregulated all these cognate markers responsible for chemoresistance and tumor aggressiveness, under low glucose condition whereas Gemcitabine was ineffective.

higher efficacy than Gemcitabine treatment in attenuating the stemness and chemoevasion associated candidate markers (NANOG, SOX2, OCT4, MDR-1, CD44, Na+-K+ ATPase), while in high glucose KV displayed aberrant results.

In lysosomal Ca^{2+}-dependent processes, autophagy plays an important role in cancer. Other reports documented that lysosomotropic drug sequestration reassures Ca^{2+} release into the cytoplasm, simplifying calcineurin stimulation, chelation of cytosolic Ca^{2+} with translocation of TFEB into the nucleus (Zhitomirsky et al., 2018). In our study, LKV treatment showed reduced expression of lysosome and intracellular Ca^{2+}levels, in comparison to untreated. From our study, we conclude that reduction of TFEB, following treatment with KV in low glucose panel downregulates the lysosomal Ca^{2+}associated chemoresistance.

Significant work documented blockage of ion channel upregulation can vitiate tumor proliferation and metastatic phenomenon in numerous cancer cell lines (Holthouser et al., 2010). Previous studies described about 35% raised in BC incidence with the use of cardiac glycosides, but it is undistinguishable whether Na/K-ATPase and GLUTs have a direct underlying association with it (Holthouser et al., 2010). Remarkably, the normal cell and tumor cells show differential manner for uptake of glucose through GLUTs that are associated with Na/K-ATPase pump, in presence of ATP and Ca^{2+} ion. Other studies suggested a role of ion channels with Warburg outcome and hypoxia, and focus on the role of Na^+ and K^+ pump in hypoxia that is generated by acidic pH mechanisms of tumor. The damaging consequences of Na+/K+ATPase and overproduction of ROS may describe the phenomenon of oncogene-induced cellular senescence (Holthouser et al., 2010). In our earlier work (Nandi et al., 2022) we discussed the effect of KV to alter the acidic pH environment of tumor cells. Here, we find, Na+/K+ATPase and Ca^{2+} were decreased following KV treatment in low glucose conditions where ROS in the similar conditions were overproduced.

The Na+/K+/-ATPase is defined as an active Na+/K+ antiporter that maintain the Na+ gradient across the membrane, effectively as a driving force for Na+ and glucose reabsorption (Holthouser et al., 2010). Again, Na+/K+ exchangers like NHE1 maintain tumor acidosis through H+ exclusion in exchange of Na+ ions. A previous study also demonstrated that Hypoxia promotes acidosis through HIF-1α-induced upregulation of NHE1. Tumor acidosis has a close association with hypoxia (Calvert et al., 1985) and the hypoxia induced acidosis increases the expression of proteases that remodel extracellular matrix. In the present study, the expression of NHE1 was also downregulated in LKV treatment in both MDA-MB-231 cell line and primary tumor tissue. In LKV treatment conditions, protein expression of Na+/K+/-ATPase was also reduced apart from its inhibitory effect on lysosomal Ca^{2+}-associated chemoresistance through TFEB. However, in HKV treatment, all of these pathways were aberrantly regulated and KV treatment did not affect these cognate markers of chemoresistance. Hence it may be hypothesized that extracellular glucose significantly interferes with the antiproliferative efficacy of KV treatment.

Overexpression of GLUTs has been reported to induce carcinogenesis, and aggressiveness of tumors (Holthouser et al., 2010). A group of researchers showed that in hexose uptake assays, MCF-7 and MDA-468 cells regulates the glucose ion channel GLUT2 in both normal and overexpressed in breast tumor tissue (Zamora-León et al., 1996). Previous reports suggested that CD44 is involved in the regulation of glucose metabolism in metabolic tissues (Weng et al., 2022). Numerous studies have focused on CD44 affecting stem cell self-proliferation and differentiation while its role in glucose metabolism is poorly understood. Moreover, Ca2+ influx regulated the proteolytic character of the CD44 ectodomain from the membrane. CD44 overexpression also increased the Lactate dehydrogenase that promoted lactate glycolysis through HIF-1α in breast cancer cells (Gao et al., 2018). Previous studies reported that 6-Phosphofructo-2-kinase/fructose-2,6-biphosphatase 4 (PFKFB4) is alternative bi-functional enzyme that catalyses 6-phosphofructose (F6P) to fructose-2, 6-biphosphate (F-2,6-BP) during glycolysis. Studies reported that CD44 promoted glycolysis via upregulation of

PFKFB4 expression (Gao et al., 2018). Previous reports explored that HIF-1α regulates the activity of GLUTs (Calvert et al., 1985). In our study, the gene expression of both HIF-1α and GLUT2 were downregulated in LKV conditions. Protein expression showed that HIF1α expression was low in L-DMEM but increased in h-DMEM. In our study, glucose uptake through GLUT2 was reduced in LKV treatment as observed through an immunocytochemical co-localization study of 2-NBDG, a fluorescent glucose analogue, with GLUT2, in MDA-MB-231 cell line.

Previous results documented that in cancer cells, high glucose stress (Holthouser et al., 2010) and ROS leads to stabilization of HIF-1α (Jung et al., 2008), which contributes to their aggressive phenotype. In our experiment we find that HIF-1α was downregulated upon KV treatment, also ensuing overproduction of ROS level resulting in cell death, under low glucose conditions. An early study showed that in HIF-1α knockdown cells, lysosomal degradation and autophagosome development was induced and the expression of autophagy-related proteins LC3-II and p62 was also promoted (Huang et al., 2019). Damaged lysosomes result in the release of proteolytic enzymes into the cytosol and introduce apoptosis. Long-period stimulation of the autophagosomal/lysosomal network can result in autophagic cell death (Linder and Kögel, 2019). In our study, LC3-II and p62 were upregulated in low glucose conditions for KV treatment conditions. From our experimental data, we hypothesized that in tumors where Na+/K+ ATPase is upregulated, high extracellular Na+ coupled with high extracellular glucose co-operatively activates glucose transporters like GLUT2 and the Na+/H+ antiport NHE1, both of which are dependent on extracellular Na+, thus maintaining extracellular acidosis. Our western blot data also showed that in high glucose conditions, HIF1α expression is also upregulated and thus, several oncogenic pathways are unleashed, rendering the inefficiency of our candidate drugs.

Besides *ex vivo* study we have carried out *in silico* study of all three ligands to gain insights into the mechanism of inhibition of cancer cells inhibition (Berman et al., 2003; Daina and Zoete, 2016). We have used a combination of Kaempferol and Verapamil for this study at doses such that Verapamil does not cause any direct effect on cancer cells (i.e., IC5) whereas its addition to Kaempferol resulted in a synergistic effect and increased the anti-carcinogenic effect. The docking study of the two ligands as well as Gemcitabine was carried out separately showing each molecule in the combination exerts different binding affinities and therefore physiological effects up to different degrees. When inside a cellular milieu, both these compounds act more profoundly than when used singly and Verapamil when being given just as an adjunct compound or very low concentration has no direct mortal effect on cancer lines. Our *in-silico* study aptly supported the *ex vivo* data showing that both the ligands in biological system affect a variety of targets or receptor classes as evident from the Swiss-target. Kaempferol possessed various drug-like characteristics as well as physico-chemical properties with high absorption. Verapamil on the other hand showed high BBB penetration as well as efflux prediction through Pg-P receptor. It may be hypothesized that Kaempferol may change the Pg-P receptor specificity of Verapamil leading to its retention in cancer cells and finally increasing the synergistic mode of action. Kaempferol fulfilled all the drug-like parameters and virtual screening showed high similarity to several phytochemicals whose studies found them to be highly potent anti-cancerous agents. Verapamil is also effective and it may be its presence even in a minimal dose exerts an additive effect on Kaempferol and vice versa. Docking studies revealed that Kaempferol is the most efficient ligand of all followed by Verapamil. The presence of both compounds in the cellular microenvironment may synergistically inhibit different cancer cells via various pathways and signaling cascades. Different proteins are shown to be inhibited *ex vivo* in this study confirming that our chosen chemical combination efficiently inhibits cancerous cells. The *in-silico* study, further supported this observation as all proteins showed negative binding energy or high binding affinity (Berman et al., 2003). As we are not sure whether these two compounds

after cell uptake combine to form a novel compound and act as a single large macromolecule or the presence of one in the cellular microenvironment leads to an increase in efficacy of the other may be an active area of study. Therefore, we separately studied their properties and studied binding affinities individually *in silico* which corroborates with their anti-carcinogenic effects and if both act in a combined manner it is expected to be far more efficient than their individual counterparts. Although we have tried to elucidate the mechanism of anti-carcinogenicity of the combination of compounds through *ex vivo* and *in silico* studies, more studies are needed to be done which can unravel new mechanisms, pathways and detailed process and regulation of the inhibition.

In Fig. 8, we showed that there is an interdependence of markers regulating tumor acidosis, cancer stemness, drug efflux and lysosome upregulation, that promote chemo evasive phenotype to the tumors. Tumors obviate oxidative stress through upregulation of Lysosomal Ca2+, TFEB, HIF1α along with induction of several transporters like Na+/K+ ATPase, NHE1, GLUT2. The association of chemoresistance with Lysosomal Ca+ was inhibited by KV in low glucose (LG) condition but not in high glucose condition. KV induced the ROS overpoduction, disrupted lysosomal expression, thus perturbating the lysosomal Ca+ based chemo-evasive mechanism, followed by ROS mediated autophagy and cell death. KV downregulated all these cognate markers responsible for chemoresistance and tumor aggressiveness, under low glucose condition whereas Gemcitabine did not show similar robustness. In the same figure, we showed the uniqueness of our candidate drug combinations in perturbating chemoevasion pathways through downregulation of these markers.

Overall, our study showed a pioneering and trailblazing pathway of inhibition of cancerous cells on breast cancer cell lines, via a radically different approach showing that KV combination increases the overproduction of ROS in cellular milieu, resulting in breakdown of Lysosomes, loss of Ca^{2+} ions release, downregulation of chemoresistance, glucose metabolism, acidosis and stemness markers. This anticancer mechanism of our candidate drugs is promising and multifaceted. Our study may pave new ways for cancer therapeutics and prevention as well as be the forerunner for various research about the detailed mechanism and signaling pathways involved in this curative phenomenon.

Author contributions

Sourav Kumar Nandi[1]* - Designed of work, write the manuscript, methodology, data analysis, software handling, writing main draft, correction and discussion, and Validation; Niloy Chatterjee[2] - methodology, data analysis, software handling, writing main draft; Tanaya Roychowdhury[3]- methodology, data analysis; Ayan Pradhan[4], - methodology, data analysis; Sumaiya Moiz[1] - methodology; Krishnendu Manna[5] - methodology, data analysis; Diptendra Kumar Sarkar[4] - data analysis; Pubali Dhar[6] - data analysis; Amitava Dutta[7] - data analysis; Soma Mukhopadhyay[1] - Administrative support; Rittwika Bhattacharya[1]**-Investigation, data analysis, Supervision, Writing - review & editing, Validation; Visualization. All data were generated in-house, and no paper mill was used. All authors agree to be accountable for all aspects of work ensuring integrity and accuracy.

Funding

Declaration of Competing Interest

The authors declare no conflict of interest.

Supplementary materials

Supplementary material associated with this article can be found, in the online version, at doi:10.1016/j.phymed.2023.154689.

References

Altunok, İ., Aksel, G., Eroğlu, S.E., 2019. Correlation between sodium, potassium, hemoglobin, hematocrit, and glucose values as measured by a laboratory autoanalyzer and a blood gas analyzer. Am. J. Emerg. Med. 37 (6), 1048–1053.

Bourguignon, L.Y., Peyrollier, K., Xia, W., Gilad, E., 2008. Hyaluronan-CD44 interaction activates stem cell marker Nanog, Stat-3-mediated MDR1 gene expression, and ankyrin-regulated multidrug efflux in breast and ovarian tumor cells. J. Biol. Chem. 283 (25), 17635–17651.

Berman, H., Henrick, K., Nakamura, H., 2003. Announcing the worldwide Protein Data Bank. Nat. Struct. Biol. 10 (12), 980.

Calvert, J.W., Cahill, J., Yamaguchi-Okada, M., Zhang, J.H., 2006. Oxygen treatment after experimental hypoxia-ischemia in neonatal rats alters the expression of HIF-1alpha and its downstream target genes. J. Appl. Physiol. 101 (3), 853–865, 1985.

Chen, Q., Liu, Y., Zhu, X.L., Feng, F., Yang, H., Xu, W., 2019. Increased NHE1 expression is targeted by specific inhibitor cariporide to sensitize resistant breast cancer cells to doxorubicin in vitro and in vivo. BMC Cancer 19 (1), 211.

Choi, H.S., Kim, J.W., Cha, Y.N., Kim, C., 2006. A quantitative nitroblue tetrazolium assay for determining intracellular superoxide anion production in phagocytic cells. J. Immunoassay Immunochem. 27 (1), 31–44.

Daina, A., Zoete, V., 2016. A BOILED-Egg to predict gastrointestinal absorption and brain penetration of small molecules. ChemMedChem 11 (11), 1117–1121.

Esfandiari, N., Sharma, R.K., Saleh, R.A., Thomas Jr, A.J., Agarwal, A., 2003. Utility of the nitroblue tetrazolium reduction test for assessment of reactive oxygen species production by seminal leukocytes and spermatozoa. J. Androl. 24 (6), 862–870.

Gao, R., Li, D., Xun, J., Zhou, W., Li, J., Wang, J., Liu, C., Li, X., Shen, W., Qiao, H., Stupack, D.G., Luo, N., 2018. CD44ICD promotes breast cancer stemness via PFKFB4-mediated glucose metabolism. Theranostics 8 (22), 6248–6262.

Holthouser, K.A., Mandal, A., Merchant, M.L., Schelling, J.R., Delamere, N.A., Valdes Jr, R.R., Tyagi, S.C., Lederer, E.D., Khundmiri, S.J., 2010. Ouabain stimulates Na-K-ATPase through a sodium/hydrogen exchanger-1 (NHE-1)-dependent mechanism in human kidney proximal tubule cells. Am. J. Physiol. Renal. Physiol. 299 (1), F77–F90.

Huang, J., Gao, L., Li, B., Liu, C., Hong, S., Min, J., Hong, L., 2019. Knockdown of hypoxia-inducible factor 1α (HIF-1α) promotes autophagy and inhibits phosphatidylinositol 3-Kinase (PI3K)/AKT/Mammalian Target of rapamycin (mTOR) signaling pathway in ovarian cancer cells. Med. Sci. Monit. 25, 4250–4263.

Javvaji, P.K., Dhali, A., Francis, J.R., Kolte, A.P., Mech, A., Roy, S.C., Mishra, A., Bhatta, R., 2020. An efficient nitroblue tetrazolium staining and bright-field microscopy based method for detecting and quantifying intracellular reactive oxygen species in oocytes, Cumulus cells and embryos. Front. Cell Dev. Biol. 8, 764.

Jia, Y., Xie, J., 2015. Promising molecular mechanisms responsible for gemcitabine resistance in cancer. Genes Dis 2 (4), 299–306.

Jung, S.N., Yang, W.K., Kim, J., Kim, H.S., Kim, E.J., Yun, H., Park, H., Kim, S.S., Choe, W., Kang, I., Ha, J., 2008. Reactive oxygen species stabilize hypoxia-inducible factor-1 alpha protein and stimulate transcriptional activity via AMP-activated protein kinase in DU145 human prostate cancer cells. Carcinogenesis 29 (4), 713–721.

Linder, B., Kögel, D., 2019. Autophagy in cancer cell death. Biology (Basel). 8 (4), 82.

Liou, G.Y., Storz, P., 2010. Reactive oxygen species in cancer. Free Radic Res 44 (5), 479–496.

Lorendeau, D., Rinaldi, G., Boon, R., Spincemaille, P., Metzger, K., Jäger, C., Christen, S., Dong, X., Kuenen, S., Voordeckers, K., Verstreken, P., Cassiman, D., Vermeersch, P., Verfaillie, C., Hiller, K., Fendt, S.M., 2017. Dual loss of succinate dehydrogenase (SDH) and complex I activity is necessary to recapitulate the metabolic phenotype of SDH mutant tumors. Metab. Eng. 43 (Pt B), 187–197.

Nandi, S.K., Roychowdhury, T., Chattopadhyay, S., Basu, S., Chatterjee, K., Choudhury, P., Banerjee, N., Saha, P., Mukhopadhyay, S., Mukhopadhyay, A., Bhattacharya, R., 2022. Deregulation of the CD44-NANOG-MDR1 associated chemoresistance pathways of breast cancer stem cells potentiates the anti-cancer effect of Kaempferol in synergism with Verapamil. Toxicol. Appl. Pharmacol. 437, 115887.

Nygren, P., Larsson, R., Gruber, A., Peterson, C., Bergh, J., 1991. Doxorubicin selected multidrug-resistant small cell lung cancer cell lines characterised by elevated cytoplasmic Ca2+ and resistance modulation by verapamil in absence of P-glycoprotein overexpression. Br. J. Cancer 64 (6), 1011–1018.

Rajaram, N., Frees, A.E., Fontanella, A.N., Zhong, J., Hansen, K., Dewhirst, M.W., Ramanujam, N., 2013. Delivery rate affects uptake of a fluorescent glucose analog in murine metastatic breast cancer. PLoS ONE 8 (10), e76524.

Schneider, L.S., von Schwarzenberg, K., Lehr, T., Ulrich, M., Kubisch-Dohmen, R., Liebl, J., Trauner, D., Menche, D., Vollmar, A.M., 2015. Vacuolar-ATPase inhibition blocks iron metabolism to mediate therapeutic effects in breast cancer. Cancer Res. 75 (14), 2863–2874.

Settembre, C., De Cegli, R., Mansueto, G., Saha, P.K., Vetrini, F., Visvikis, O., Huynh, T., Carissimo, A., Palmer, D., Klisch, T.J., Wollenberg, A.C., Di Bernardo, D., Chan, L., Irazoqui, J.E., Ballabio, A., 2013. TFEB controls cellular lipid metabolism through a starvation-induced autoregulatory loop. Nat. Cell Biol. 15 (6), 647–658.

Sharma, V., Joseph, C., Ghosh, S., Agarwal, A., Mishra, M.K., Sen, E., 2007. Kaempferol induces apoptosis in glioblastoma cells through oxidative stress. Mol. Cancer Ther. 6 (9), 2544–2553.

Stock, C., Pedersen, S.F., 2017. Roles of pH and the Na+/H+ exchanger NHE1 in cancer: from cell biology and animal models to an emerging translational perspective? Semin. Cancer Biol. 43, 5–16.

Themistocleous, S.C., Yiallouris, A., Tsioutis, C., Zaravinos, A., Johnson, E.O., Patrikios, I., 2021. Clinical significance of P-class pumps in cancer. Oncol Lett 22 (3), 658.

Vishvakarma, N.K., Kumar, A., Singh, V., Singh, S.M., 2013. Hyperglycemia of tumor microenvironment modulates stage-dependent tumor progression and multidrug resistance: implication of cell survival regulatory molecules and altered glucose transport. Mol. Carcinog. 52 (12), 932–945.

Weng, X., Maxwell-Warburton, S., Hasib, A., Ma, L., Kang, L., 2022. The membrane receptor CD44: novel insights into metabolism. Rends Endocrinol. Metab. 33 (5), 318–332.

Zamora-León, S.P., Golde, D.W., Concha, I.I., Rivas, C.I., Delgado-López, F., Baselga, J., Nualart, F., Vera, J.C., 1996. Expression of the fructose transporter GLUT5 in human breast cancer. Proc. Natl. Acad. Sci. U.S.A. 93 (5), 1847–1852.

Zhang, X., Yu, L., Xu, H., 2016. Lysosome calcium in ROS regulation of autophagy. Autophagy 12 (10), 1954–1955.

Zhou, Q., Brown, J., Kanarek, A., Rajagopal, J., Melton, D.A., 2008. In vivo reprogramming of adult pancreatic exocrine cells to beta-cells. Nature 455 (7213), 627–632.

Zhitomirsky, B., Yunaev, A., Kreiserman, R., Kaplan, A., Stark, M., Assaraf, Y.G., 2018. Lysosomotropic drugs activate TFEB via lysosomal membrane fluidization and consequent inhibition of mTORC1 activity. Cell Death. Dis. 9 (12), 1191.
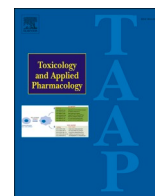
Deregulation of the CD44-NANOG-MDR1 associated chemoresistance pathways of breast cancer stem cells potentiates the anti-cancer effect of Kaempferol in synergism with Verapamil

Sourav Kumar Nandi [a], Tanaya Roychowdhury [b], Samit Chattopadhyay [b,c], Sudarshana Basu [a], Krishti Chatterjee [d], Pritha Choudhury [e], Nirmalya Banerjee [d], Prosenjit Saha [e], Soma Mukhopadhyay [a,*], Ashis Mukhopadhyay [f], Rittwika Bhattacharya [a,*]

[a] Department of Molecular Biology, Netaji Subhas Chandra Bose Cancer Research Institute, 3081 Nayabad, Kolkata 700094, India
[b] Cancer Biology and Inflammatory Disorder Division, Indian Institute of Chemical Biology, 4, Raja S. C. Mullick Road, Kolkata 700032, India
[c] Department of Biological Sciences, BITS Pilani, K K Birla Goa Campus, India
[d] Department of Pathology, Netaji Subhas Chandra Bose Cancer Research Institute, 3081 Nayabad, Kolkata 700094, India
[e] Department of Cancer Chemoprevention, Chittaranjan National Cancer Institute, 37, Shyamaprasad Mukherjee Rd, Kolkata, West Bengal 700026, India
[f] Department of Haematooncology, Netaji Subhas Chandra Bose Cancer Research Institute, 3081 Nayabad, Kolkata 700094, India

ARTICLE INFO

ABSTRACT

Chemoresistance is an imminent therapeutic challenge for breast cancer. Previous evidence suggests that breast cancer stem cells (BCSC) develop resistance through upregulation of stemness and chemo-evasion markers viz. SOX2, OCT4, NANOG, MDR1 and CD44, following anticancer chemotherapeutic treatments. Early studies suggest an inhibitory role of Kaempferol in BCSC propagation through downregulation of epithelial to mesenchymal transition. We hypothesized that the pathway involved in chemoresistance could be effectively addressed through Kaempferol (K), alone or in combination with Verapamil (V), which is an inhibitor of MDR1. We used K in combination with V, in multiple assays to determine if there was an inhibitory effect on BCSC. Both K and KV attenuated pH-dependent mammosphere formation in primary BCSC and MDA-MB-231 cells. RNA and protein (immunocytochemistry, western blot) expression of candidate markers viz. SOX2, OCT4, NANOG, MDR1 and CD44 were carried out in the presence or absence of candidate drugs in ex-vivo grown primary BCSC and MDA-MB-231 cell line. Immunoprecipitation assay, cell cycle analysis was carried out in MDA-MB-231. Our candidate drugs were not only anti-proliferative, but also downregulated candidate genes expression at RNA and protein level in both settings, with more robust efficacy in KV treatment than K; induced G2/M dependent cell cycle arrest, and interrupted physical association of CD44 with NANOG as well as MDR1 in MDA-MB-231. In primary tumor explant but not in adjacent normal tissue, our candidate drugs K and KV induced robust γH2AX expression. Thus, our candidate drugs are effective in attenuating BCSC survival.

1. Introduction

Acquisition of chemoresistance has a close association with stem cell renewal, the complex mechanism of which is not fully unravelled. The phenomena of the early development of chemoresistance are characteristically observed in triple negative breast cancers (TNBCs), the most heterogeneous subtype of breast cancer, with characteristic lack of expression of estrogen receptor (ER), the progesterone receptor (PgR) and deficiency of overexpression/gene amplification of human epidermal growth factor receptor 2 (HER2). Therefore, the therapeutic options targeting these hormone receptors are not available for TNBC patients (Anders and Carey, 2009). However, chemoresistance is not only the prerogative of TNBC, as hormone receptor-positive breast tumors also acquire chemoresistance with time (Brandão et al., 2019).

In aggressive breast tumours, some of the pluripotent stem cell markers viz. NANOG, SOX2, OCT4 are reportedly upregulated (thus termed as induced pluripotent stem cell markers/iPSC), to facilitate the process of perpetual maintenance of stemness and induction of drug resistance, through a feedback loop mechanism (Jeter et al., 2015). One important attributor of chemoresistance is P-glycoprotein (P-gp) protein, belonging to the ATP dependent proton pump family, the product of the *MDR1* gene (Miletti-González et al., 2005), that corroborates with stem cell markers to maintain chemoresistance networking. Earlier reports (Chen et al., 1990) in human breast cancer cell line, suggested that Verapamil, a calcium channel inhibitor, could be effective in blocking P-gp function (McDevitt and Callaghan, 2007).

BCSC are the distinct niche of cancer stem cells in tumours that confer aggressiveness and chemoresistance phenotype to the resident tumour. Accumulated shreds of evidence suggested that apart from iPSC markers, MDR1 and CD44 are also upregulated in breast cancer stem cells (Bourguignon et al., 2002). In the present study, we wanted to explore the ability of our phytoflavenoid based drug system in attenuating survival of BCSCs and their effect on the candidate genes regulating chemoresistance and maintenance of stemness.

Kaempferol, a bioflavonoid, is endowed with several pharmacological, including anticancer properties (Kim and Choi, 2013). Previous evidence suggested that Kaempferol, abundant in tea, grapes, berries, and cruciferous vegetables, acts as a potent antitumor growth agent of BCSC propagation through downregulation of EMT (Liang et al., 2015). Here, we hypothesized that Kaempferol alone or in combination with Verapamil (Callaghan et al., 2014) could probably attenuate breast cancer stem cell progression.

To address the issue of chemoresistance network in ex-vivo / in vitro model of BCSC, it was imperative to study the role of our candidate drugs on survival of BCSC. Our present study revealed that Kaempferol alone or with Verapamil attenuated RNA and protein expression of iPSC markers (NANOG, SOX2, and OCT4) as well as MDR1 and CD44 and the candidate drug combinations disrupted the CD44-NANOG-MDR1 feedback loop activation network, depicting the probable mechanism of the drug combination in attenuating viability and acquisition of chemoresistance in BCSCs line MDA-MB-231 and primary breast tumour derived cells, implicating their immense pharmacological importance.

2. Methods

2.1. In-vitro cell culture

Stem cell enriched breast cancer cell line MDA-MB-231 (AddexBio; ATCC; Cat# CRL-12532, RRID: CVCL_0062) was purchased from National Centre for Cell Science (NCCS, Pune) Maharashtra, India. MDA-MB-231 (Holliday and Speirs, 2011) cells were cultured at $37°C$ in a humidified atmosphere of 5% CO_2 in DMEM/F-12 (Gibco) medium with supplements (10% fetal bovine serum (FBS, Thermo Fisher Scientific, India), 5 µg/ml insulin (Himedia), 500 ng/ml hydrocortisone (Sigma-Aldrich) 10 ng/ml EGF (Sigma, St. Louis, MO) (Baker et al., 2005). The viability of cultured cells was examined through the Trypan Blue dye exclusion method using a conventional hemocytometer counting chamber, as described previously (Morten et al., 2016).

2.2. Primary tumour cell isolation and stem cell-enriched ex-vivo culture

Patients with histopathologically confirmed primary breast tumours, recipients of Neoadjuvant chemotherapy treatment (NACT) (Table S1) were chosen for this study. A total of 34 primary tumor samples from female patients were involved. Breast cancer patients with unidentified subtypes, male breast cancer and patients included in clinical trials were left out. All included patients conveyed written consent with the handling of tumour samples for research purposes, and the study was approved by the Ethics Committee Netaji Subhash Candra Bose Cancer Research Institutional Review Board (approval No. ECS/NCRI/08/

2012). Freshly operated female primary tumour samples ($n = 34$) were obtained randomly from the hospital section of Netaji Subhas Chandra Bose Cancer Research Institute, tumour margins were identified by a clinical pathologist as designated previously and tumours were also classified according to International Union against Cancer (UICC) and American Joint Committee on Cancer (AJCC). Tumour-node-metastasis (TNM) staging, as well as tumor subtype data, were obtained from the pathologist (Table S1). The clinicopathological history of the patients is represented in Table S2. All patient samples were collected in a sterile container with $1\times$ Phosphate-buffered saline (PBS). The tumour was chopped into 1 mm pieces with a scalpel. The chopped pieces were further treated collagenase type IV and hyaluronidase solution (Sigma-Aldrich), incubated at $37°C$ in 5% CO_2 incubator, to obtain a single-cell suspension. The digested tissue slurry was filtered through a 40 µm sterile cell strainer, transferred to sterile conical tubes, filled with PBS, and centrifuged at 700 $\times$g for 5 min. The supernatant was discarded and the pellet was resuspended with 0.25% trypsin/ EDTA solution (Sigma-Aldrich), and Dispase/DNase solution (Himedia) in DMEM/F-12 medium with supplements and kept at $37°C$. After centrifugation at 700 $\times$g for 5 min, the pellet was resuspended in haemolysis buffer solution and incubated at $37°C$ for 5 min; centrifuged at 700 $\times$g for 5 min and washed with PBS twice. The pellet was resuspended appropriately in DMEM/F-12 complete medium (DMEM/F-12 with 10% FBS, 5 µg/ml insulin, 500 ng/ml hydrocortisone, 10 ng/ml EGF, 1% penicillin/streptomycin (Sigma-Aldrich), 50 µg/ml Gentamicin (Sigma-Aldrich), 2.5 µg/ml Amphotericin B (Sigma-Aldrich) antibiotics) and cells were allowed to grow (Jiao et al., 2016).

2.3. Single/combination drug effect in Ex-vivo/in-vitro cell survival model

To study the effect of a set of the drug combinations in both ex-vivo culture from tumor-derived cells and in-vitro culture with MDA-MB-231 cell line, combination index (CI) calculation is an appropriate technique to determine the optimum quantity of every single drug, to get a synergistic effect, as described previously (Zhao et al., 2004; Cao et al., 2011).

The effective concentration (*e.g.,* IC-50) of drug positive control Gemcitabine (G) as well as candidate drugs viz. Kaempferol (K) and Verapamil (V) were estimated following the established protocol of MTT (ABCAM) (Arunasree, 2010) and XTT (ABCAM) (Kuo et al., 2005) assay in MDA-MB-231 cell line and ex-vivo grown primary breast tumour cells respectively. XTT assay was carried out for ex-vivo primary tumour derived cells ($n = 12$). The mean value of a single drug i.e. G, K and V was plotted in a two coordination plot, and drug concentration that induced 50% cell death (IC-50) was identified.

For the combinational system, MTT/XTT assay was carried out with different concentrations of Kaempferol with a fixed concentration of Verapamil (5 µM). The nature of the interaction of two drugs, i.e., Kaempferol and drug Verapamil, were evaluated with CI analysis calculation, as described previously (Ashton, 2015, Chou, 2010).

Based on CI index calculations, for subsequent studies with drug combination of Kaempferol and Verapamil, both Kaempferol and Verapamil were taken at a low concentration (Kaempferol (104.8 µM, corresponding to its IC-15 value) and Verapamil (5 µM, corresponding to its IC-5 value), to induce synergism. Also, for the Verapamil alone treatment, Verapamil dosage was kept as 5 µM.

2.4. Effect of drug-induced pH alteration on tumorsphere formation assay

MDA-MB-231 cell line and primary breast tumour cells (1000 cells/cm^2) were seeded in 6 well ultra-low attachment plates in serum-free non-adherent mammosphere culture media with the supplement of B27 (Invitrogen) and allowed to grow following reported protocol (Reynolds and Maurer, 2005; Shaw et al., 2012; Grimshaw et al., 2008). Secondary mammospheres (2°) (Rota et al., 2012) were formed by disaggregating the primary mammospheres and culturing the same number

of cells, in a new 6 well plates. For primary breast tumour ($n = 6$) cells were allowed to grow for 14 days till visible mammosphere are formed. For both cell lines as well as ex vivo grown primary tumours, five sets of treatment groups were prepared, viz. untreated (U), Gemcitabine (G) treated, Kaempferol (K) treated, Verapamil (V) treated, and Kaempferol with Verapamil (KV) treated. For each group, experiments were done in triplicates so that the statistical power analysis calculation under different treatment conditions could be performed, with a statistical significance value of $p \leq 0.05$. Drug treatments were carried out in 2° mammospheres with the appropriate concentration i.e. IC-20 for G (100 μM; as 50% cell death was not attained), IC-50 for K (224.51 μM), IC-5 for V (5 μM) and IC-50 for KV (K: 104.8 μM; V: 5 μM) as per CI index. The number of mammospheres was counted by two independent researchers blinded to the treatment conditions. The efficacy of mammosphere formation under different treatment conditions (Mammosphere Forming Effect) was plotted.

Drug resistance, metastasis and cell to cell adherence depends on the tumour cell pH alteration which performs a key role to regulate the tumorsphere development (Silva et al., 2009).

2.4.1. Equation 1

After drug treatment in 2° Mammospheres, the pH*e* was measured (Prescott et al., 1993) and calculated consuming this equitation 2 (Boyer et al., 1993).

$$pHe = pKa + log\{(C_B - C_A)/(C_T - C_B)\}$$

where C_B is the pH of the drug; C_A is the mean value of pH before drug treatment at acidic endpoint observation; C_T is the mean value of pH after drug treatment at the alkaline endpoint observation. The dissociation constant (pKa) value of G (http://www.drugbank.ca/drugs/DB00441), K, V, were 1.89 (Drug Bank), 7.96 (Herrero-Martínez et al., 2005) and 8.92 (Zhang et al., 1999) respectively. pKa value of KV was calculated based on a previous method (Critchfield and Johnson, 1959). Before each study, the electrodes were calibrated expending buffered solutions of pH 6.0, 7.0, 8.0, and 11.0.

2.5. Flow cytometry analysis

Cell cycle analysis, based on the incorporation of Propidium Iodide into DNA was carried out using BD Cycletest™ Plus DNA Kit, following the manufacturer's instruction. MDA-MB-231 cell line, at a concentration of 1×10^5 cells per ml seeded overnight in 25 cm² flask was treated with candidate drug concentrations as described before. Cell cycle distribution of nuclear DNA was carried out by flow cytometry (BD Biosciences) using the analyser and BD FACS Diva v8.0.1 software (Choi and Ahn, 2008).

2.6. Reverse transcription, PCR and RT-qPCR level gene expression

RNA extraction of candidate drug-treated cells in both cell line and ex-vivo cultured primary breast tumour cells ($n = 12$) was carried out using TRI Reagent® (Sigma-Aldrich) reagent following the manufacturer's protocol. cDNA was obtained from total RNA through Verso cDNA synthesis Kit (Thermo Fisher), according to manufacturer's instruction. Semi-quantitative real-time PCR and Power SYBR Green master mix (Thermo Fisher) based RT-qPCR was carried out with gene-specific primers (Table S3). PCR products were checked using a 2.0% agarose gel electrophoresis. RT-qPCR amplifications were done in triplicates for each gene and the Ct values were calculated (Ghadimi et al., 2005). Fold change in expression of candidate genes were calculated after normalization with the corresponding Ct values of β-*Actin*, following established protocol (Silver et al., 2006).

2.7. Immunofluorescence staining and confocal microscopic analyses of candidate proteins in tumour explant culture under treatment conditions

To study the effect of drug treatment on candidate gene expression and their co-localization, freshly operated primary breast tumour ($n = 8$) tissue explants were cut into ~2.5 × 2.5 × 2.5 mm³ and were cultured for 48 h in DMEM/F-12 complete medium (DMEM/F-12 medium with 10% FBS, 1% penicillin/streptomycin (Sigma-Aldrich), 50 μg/ml Gentamicin (Sigma-Aldrich), 2.5 μg/ml Amphotericin B (Sigma-Aldrich)) in a 6-well dish, (Karekla et al., 2017) under different experimental drug treatment mentioned above. After 48 h treatment, the explant specimens were embedded into paraffin blocks from which 5 μm sections were collected for immunofluorescence detection of candidate proteins following established protocol (ABCAM).

Validation of the expression as well as the subcellular localization of the protein (SOX2, OCT4, NANOG, CD44, & MDR1) were carried out by immunofluorescence staining and confocal microscopy in MDA-MB-231 cells, at a concentration of 1×10^4 per well. Cells were seeded in 6 well plates, and drugs were treated at 60% confluence. After drug treatment (48 h) immunocytochemistry was carried out with established protocol (ABCAM) (Bockhorn et al., 2013).

For all immunofluorescence experiments with cell line, briefly, after fixation with 4% paraformaldehyde, cells were permeabilized and blocked and then incubated with primary antibody ((anti-SOX2 antibody; Abcam Ca # ab79351, RRID:AB_10710406, anti-OCT4 antibody; Thermo Fisher Scientific Cat# MA5-31458, RRID:AB_2787090, anti-NANOG antibody; Abcam Ca # ab109250, RRID:AB_10863442 and Santa Cruz Ca # sc-293121, RRID:AB_2665475, anti-CD44 antibody; Abcam Cat# ab51037, RRID:AB_868936 and anti-MDR1 antibody Santa Cruz Ca # sc-13131, RRID:AB_626990), anti-Phospho-Histone H2AX (Ser139) or γH2AX; Cell Signaling Technology Ca#9718) in 1: 200 dilution overnight, washed and treated with fluorescent conjugated secondary antibodies (Alexa Fluor 488 conjugated Goat Anti-Rabbit IgG; Abcam Cat# ab97048, and Alexa Fluor 647 conjugated Goat Anti-Mouse IgG; Abcam Cat# ab150115,) and mounted on a slide with ProlongGold antifade reagent containing DAPI (Invitrogen). The slides were visualized using an Olympus Fluoview confocal microscope using the 60× objective.

For immunofluorescence experiments with explant cultures, gradual hydration of paraffin sections, followed by antigen retrieval was carried out following our established protocol on immunohistochemistry (Ghosh et al., 2021). The tissue sections were then blocked, followed by incubation with primary and fluorescence conjugated secondary antibodies.

2.8. Immunoblotting and immunoprecipitation to determine expression and association of candidate proteins under experimental drug conditions

MDA-MB-231 cells at a seeding concentration of 1×10^5 cells/flask, upon treatment with different drugs in the aforementioned concentrations for 48 h, were homogenised and protein concentrations of the different drug-treated cells were estimated using Bradford protein assay (Bradford, 1976). 30 μg of protein of each treatment group was loaded in each lane of a 12% SDS-PAGE gel and transferred to nitrocellulose membranes. The membranes were washed with TBS-T (5% milk in Tris-buffered saline-Tween 20), blocked with 5% skimmed milk and treated with specific primary antibodies (1:1000 dilution). TBS-T washed membranes were incubated with horseradish peroxidase-conjugated monoclonal secondary antibody (dilution: 1: 10,000; GeneTex Cat# GTX14122, RRID: AB_373069). The membranes were washed and after incubation with chemiluminescence substrate, were visualized by *ChemiDoc* Imaging System.

For immunoprecipitation, MDA-MB-231 cells were plated in 100 mm dishes and grown in DMEM media with 1% antibiotic-antimycotic in a 37°C incubator with 5% CO₂ supply. At 70% confluency cells were subjected to overnight serum starvation. The next day, fresh media was

added with 2% FBS and 1 mg/ml of hyaluronic acid and the following treatment were done, viz. DMSO control, only Kaempferol, and Kaempferol with Verapamil. After 48 h, cells were harvested for IP. Briefly, cells were lysed using RIPA lysis buffer $+1\times$ PIC cocktail and centrifuged at 12,000 rpm for 20 min at 4°C. The supernatant was collected in a fresh tube and pre-clearing was done using 20 μl of BSA blocked protein A/G beads for 1 h at 4°C in a 6 rpm rotation platform. After centrifugation at 1500 rpm for 5 min, the supernatant was collected in fresh 1.5 ml Eppendorf tubes. Protein was estimated using Bradford assay and 500 μg of lysate was used for each IP and Isotype control IgG pair. 5% input samples were prepared for each experiment, boiled with $5\times$ SDS loading dye and stored at -20 degree till use. For each IP and isotype control, 3 μg of rabbit anti-CD44 antibody (Abcam Cat# ab51037) and 3 μg normal rabbit IgG were added to the lysates respectively. Tubes were kept in rotation overnight at 6 r.p.m. at 4°C. The next day, 30 μl of blocked protein A/G beads were added to each tube and rotated for 4 h at 4°C. After centrifugation supernatant was discarded and beads washed in RIPA lysis buffer $+1$ X PIC thrice. 40 μl of $2\times$ SDS dye was added to each tube and vortexed for 5 min at RT. Samples were then heated at 95°C for 5 min followed by centrifugation at 12,000 rpm for 20 min at 4°C. Supernatants were collected in fresh tubes and western blotting was performed using 4% stacking and 10% resolving gel. Blots were probed using anti-mouse NANOG and mouse anti-MDR1 antibodies (Santa Cruz Ca # sc-13131) followed by incubation with goat anti-mouse HRP (GeneTex Cat# GTX14122) conjugated secondary antibody (Sigma). Images were captured using the Biorad Chemidoc system (Rust et al., 2013).

2.9. Comparison of the genotoxic effect of candidate drug systems in primary breast tumor and adjacent normal tissue explants

To study the genotoxic effect of our candidate drug systems in primary breast tumor and adjacent normal breast tissue, explant ($n = 4$) cultures of breast tumor and adjacent normal tissues were treated with our candidate drug systems as described above, for 48 h. Expression of phosphorylated H2AX on serine 139 (gamma-H2AX) expression was measured by immunocytochemistry following the protocol mentioned before.

2.10. Statistical analysis

One way ANOVA using GraphPad Prism version 8, (GraphPad Prism, RRID:SCR_002798) was used to determine to mean fluorescent intensity and Pearson correlation coefficient of immunofluorescence staining and confocal microscopic analyses and two way ANOVA using the software, was used to evaluate the percentage distribution of cells in the cell cycle. Student's *t*-test was used to determine the effect of treatment on mammosphere formation (diameter of mammospheres), the significance of RNA and protein expressions in the five treatment groups through GraphPad Prism. Fisher's exact test with 2 tailed statistics was used to correlate different clinicopathological parameters with tumours subtypes. Two way ANOVA was also used to quantify the normalized fold change of expression of candidate proteins with respect to untreated controls in immunoprecipitation analysis. For 95% confidence in all statistics, a *p*-value of ≤ 0.05 was considered statistically significant. All above the experiments were completed without important loss of statistical power.
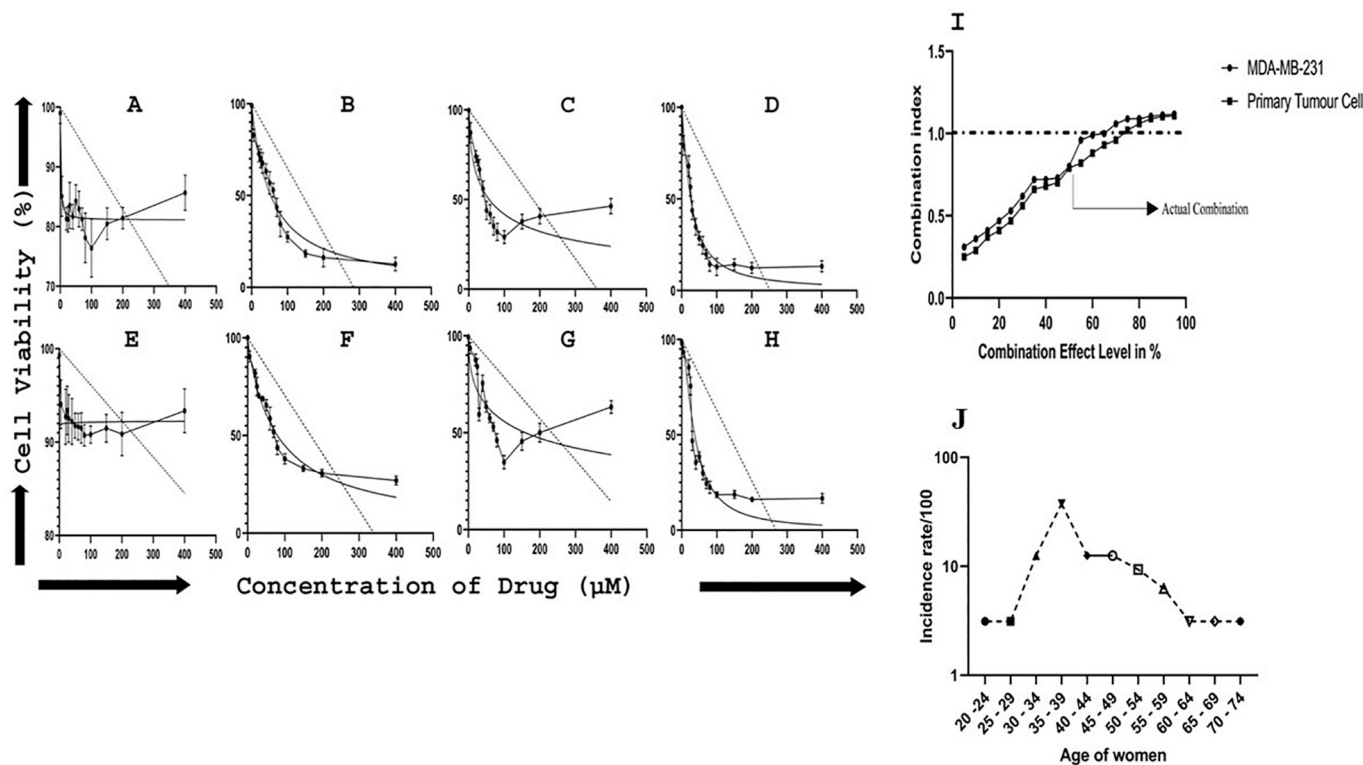
Fig. 1. Cell viability assay in MDA-MB-231 and ex-vivo grown culture of primary breast tumour. A nonlinear regression-based drugs effect were plotted where A & E: Gemcitabine, B & F: Kaempferol, C & G: Verapamil and D & H: the combination of Kaempferol with Verapamil. For different treatment conditions, the IC-50 dosage was calculated in MDA-MB-231 (A–D) and in primary tumour derived cells (E–H). Data were analysed with nonlinear (bar line) and linear (dotes line) regressions. The dots and bars are mean values and $\pm$ SD. The nonlinear plots are the best-fitted regressed lines. I: Combination index of Kaempferol with Verapamil drugs as analysed in MDA-MB-231 and primary tumour derived cells. CI values less than, equal to, or greater than 1 represents synergy, additivity, or antagonism, accordingly. The CI values were calculated and for KV treatment, dosages corresponding to CI index 0.7 were chosen for subsequent studies. The Age-incidence curve of breast cancer in Fig. 1J; log-log plot (data of NCRI hospital) according to the supplementary Table S1.

3. Results

3.1. Antiproliferative effect of Kaempferol alone or in combination with Verapamil on cultured breast tumour cells

3.1.1. Cell survival assay

The cell survival data was plotted as nonlinear regression, which provided better-fitted curves (Fig. 1). We performed MTT and XTT cell survival assay for single drug K and V in MDA-MB-231 cell and primary breast tumour derived cells of BCSC respectively. The nonlinear survival curve in MDA-MB-231 (upper panel of Fig. 1A–D) cells and primary tumour cells (lower panel of Fig. 1E–H) showed, for single drug K and V, IC-50 mean value was approximately 224.51 μM, 170.6 μM respectively. Verapamil was included only to inhibit the drug efflux pumps and not as an antiproliferative drug. 5 μM of V (IC-5) was taken for single as well as for combination treatment. (Fig. 1C and G). G treatment did not achieve 50% inhibitory effect and so for entirely comparisons in our study, the quantity of G was taken as 100 μM (approximately 20% inhibitory effect) (Fig. 1A and E).

For combinational system, Kaempferol, at a much lower dosage (104.8 μM in MDA-MB-231 and 109.9 μM in primary BCSC, approximately corresponding to its IC-15 value) showed robust efficacy in combination with Verapamil (5 μM, IC-5 value). The CI index value of KV combination was calculated and the CI index value of the combination that showed 50% inhibitory effect, was 0.7 (Fig. 1I) in both cell line and ex-vivo grown primary breast tumour cells.

3.1.2. Baseline characteristics and clinical response of patients

This reflective study of BC patients ($n = 34$) with a median follow-up of 36 months was taken for evaluation of adding gemcitabine into standard chemotherapy. In Fig. 1J, the incidence of breast cancer increased with age throughout the reproductive with a median age of 37.5 years and then increased at a slower rate after about age 50 years ($n = 34$). According to history, maximum patients had invasive breast carcinoma of no special type inflammatory breast cancer with a predomination of grade 3/4 tumours (77%). From supplementary Table S2, the clinicopathological correlations data showed early age of onset has a significant association with triple-negative breast cancer (TNBC) but had no significance with grade and stages.

3.2. Drug induced pH dependent mammosphere assay

Mammosphere formation from MDA-MB-231 (Fig. 2A) cell line as well as primary breast tumour (Fig. 2D) was done followed by quantification of Mammosphere Forming Efficacy (MFE) (Fig. 2B, C, E, and F). For both *in-vitro* grown MDA-MB-231 and *ex-vivo grown primary tumours*, the external acidic pH neutralized and probably prohibited the uptake of weak base chemotherapeutic drugs viz. Gemcitabine, with consequential physiological drug resistance. The mean effective pHe of MDA-MB-231 and primary tumour cells were calculated from eq. 1 and the value were, U: 6.7 ± 0.01, and 6.2 ± 0.01; G: 6.82 ± 0.01 and 6.5 ± 0.01; K: 11.8 ± 0.01 and 9.6 ± 0.01; V: 7.1 ± 0.01 and 5.3 ± 0.01; KV: 11.3 ± 0.01 and 10.62 ± 0.01 respectively (Fig. 2G) Thus, the pHe was suggested to be one compounding factor for diminished efficacy of Gemcitabine whereas Kaempferol alone or along with Verapamil treatment had a profound effect in attenuating tumorsphere formation. Verapamil treatment alone however had no significant effect on the reduction of tumorsphere formation.

3.3. Cell cycle analysis

Cell cycle analysis in a typical asynchronous culture of MDA-MB-231 cell line exhibited that although Gemcitabine treatment resulted in increased apoptosis (approximately 5%) compared to untreated cells, it
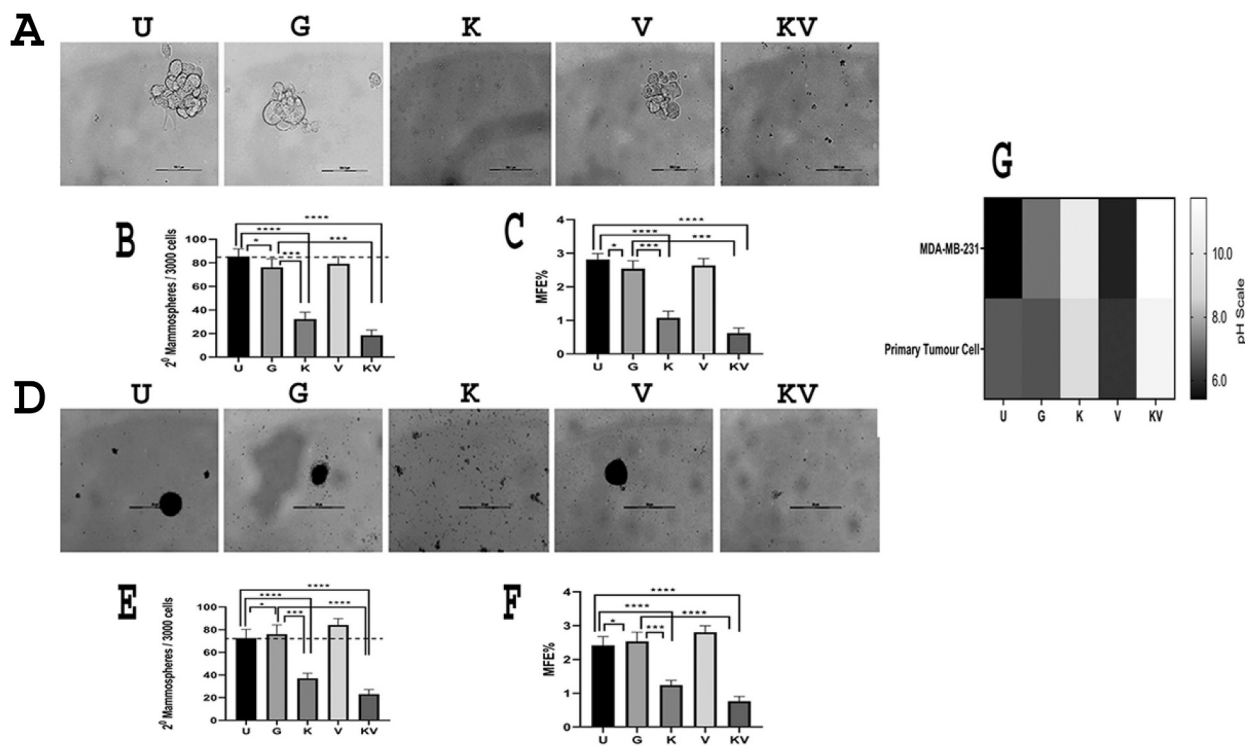
Fig. 2. Mammosphere formation in MDA-MB-231 cells (A) / primary tumour cells (D). U: untreated (Control in both upper [A] and lower panel [D]) G: Gemcitabine (panel A, D); K: Kaempferol (panel A, D) V: Verapamil (panel A, D); KV: Kaempferol with Verapamil (panel A, D). Cells were treated with our candidate drugs at their calculated dosage that resulted in 50% inhibitory effect. Quantification of mammosphere and MFE in percentage were analysed concerning inoculum of 3000 cells in MDA-MB-231 cell line (B, C) and Primary tumour derived cells (E, F). Student's *t*-test is used to correlate the significance where ***$p < 0.01$ **** < 0.0001. Heat map of extracellular pH change in 2° mammosphere after drug treatment (48 h.) in Fig. 2G. Upper panel MDA-MB-231 and lower panel primary tumour derived cells. U: untreated (Control) G: Gemcitabine; K: Kaempferol; V: Verapamil; KV: Kaempferol with Verapamil.

did not have any significant effect on G0/G1, S or G2/M phase compared to control (Fig. 3A–F). Kaempferol resulted in approximately 4% increment in S phase and approximately 5% increment of G2/M phase with concomitant reduction of G0/G1 phase population, indicating that K interferes with both DNA replication as well as entry into mitosis, leading to cell cycle arrest (Fig. 3C). Kaempferol with Verapamil also showed synergism in incrementing the S phase and G2/M phase (Fig. 3E). Gemcitabine and Verapamil alone however did not affect cell cycle progression (Fig. 3B and D). Cell cycle distribution showed a significant reduction of fold change in Kaempferol alone or combination with Verapamil treatment group.

3.4. Kaempferol alone and in combination with Verapamil, attenuated RNA expression of candidate genes in cultured breast tumour cells

RNA expression of *SOX2, OCT4, NANOG, MDR1, CD44* and housekeeping control gene *β-Actin* (Livak and Schmittgen, 2001; Schmittgen and Livak, 2008); were examined by RT-PCR and q-RT-PCR, upon treatment with different drugs in both MDA-MB-231 and primary breast tumour cells. For MDA-MB-231 and primary tumour cells, K and KV attenuated expression of *CD44, OCT4, NANOG* and *MDR1* although alteration of *SOX2* expression was nominal for MDA-MB-231 (Fig. 4A and C). In ex-vivo cultured primary tumor cells, KV treatment showed robust efficacy than K in attenuating expression of *SOX2, OCT4, NANOG, MDR1* and *CD44* expression (Fig. 4B and D). It was interesting to find that the expression of *CD44* was high (in case of gemcitabine treatment panel) in ex-vivo grown primary tumors (Fig. 4B and D). The fold change of expression of candidate genes showed a significant difference in K and KV treatment groups in both MDA-MB-231 and ex-vivo grown primary breast tumor cells (Fig. 4B and D). The Independent *t*-test was used to calculate the statistical difference in fold change of different treatment groups and significant differences, as observed with candidate drugs, are indicated in the corresponding figures (Fig. 4A–D).

3.5. Kaempferol alone and in combination attenuated protein expression of iPSC markers, CD44 and MDR1 in cultured breast tumour cells and disrupted the physical association of CD44 with NANOG and MDR

3.5.1. Immunofluorescence analysis of primary explant cultures

In primary explant culture, expression and MFI of SOX2 (Fig. 5A and B) and OCT4 (Fig. 5C and D) were attenuated under K and KV treatment conditions. Co-localizations of CD44-NANOG (Fig. 6A), as well as CD44-MDR (Fig. 6C) were reduced in K and KV treatment groups, indicating a probable role of these treatments in disrupting the CD44-NANOG-MDR1 network. Pearson's correlation coefficient showed a significant reduction of co-localization of CD44 with NANOG as well as CD44 with MDR1 respectively (Fig. 6B and D).

3.5.2. Immunocytochemical analysis in MDA-MB-231 cell line

Compared to control, it was observed that Kaempferol alone or along with Verapamil inhibited tumour cell proliferation and attenuated the expression of breast cancer stem cell markers SOX2, OCT4, NANOG, MDR1 and CD44, although treatment with Gemcitabine or with Verapamil alone did not have any significant influence on the expression status of these markers in MDA-MB-231 (Figs. S1A, S2A, S3A, S4A, and S5A). Mean fluorescence intensity (MFI) value (Figs. S1B, S2B, S3B, S4B, and S5B) showed significant downregulation of expression of candidate proteins in K and KV treatment conditions. In the control panel as well as in Gemcitabine and Verapamil treatment groups, expression of the candidate cancer stem cell markers were both nuclear and cytoplasmic whereas in Kaempferol mono treatment group as well as in Kaempferol with Verapamil treatment, expression of the candidate proteins were scanty, punctate and diffusely cytoplasmic. Except for NANOG protein, Gemcitabine treatment did not cause any significant fold change of the other candidate proteins (Fig. S3B).

Fluorescence intensity (FI) was evaluated through the ImageJ software as an established method, described by Iinuma S, et al. (Iinuma et al., 1994). The mean FI (MFI) values of each cell were estimated from five different areas and the background FI of the cell-free area was subtracted. MFI value and statistical significance in different treatment groups.
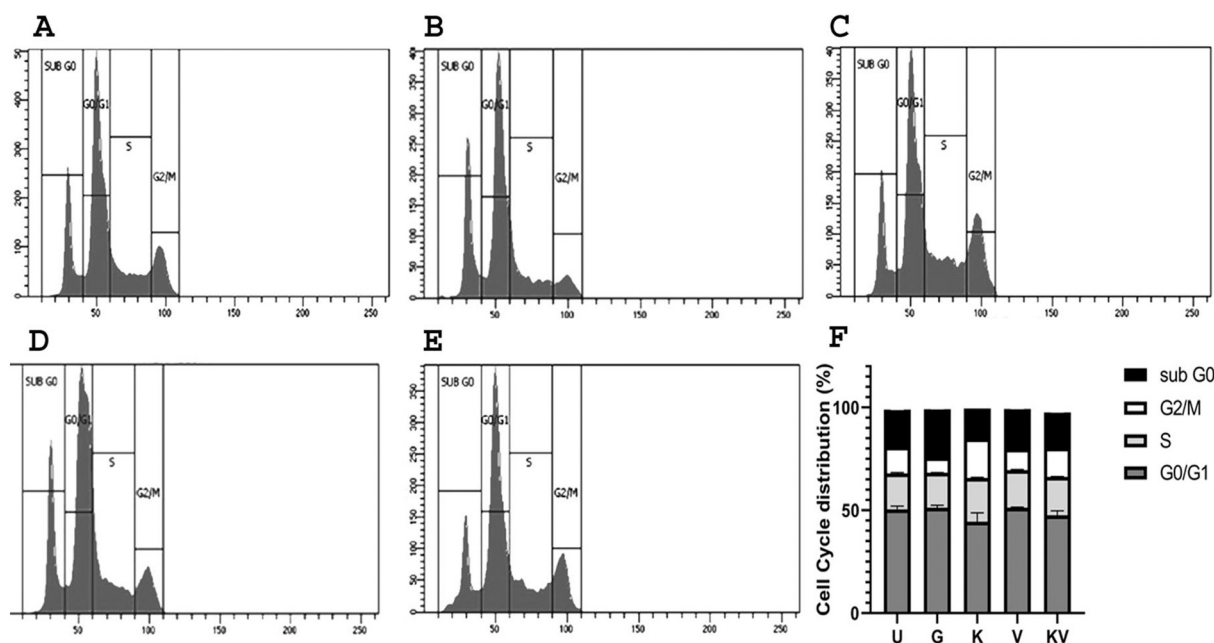
Fig. 3. Cell cycle analysis through PI staining followed by flow cytometry for the cells of a typical asynchronized culture of MDA-MB-231 under different treatment conditions (48 h): A: Untreated; B: Gemcitabine; C: Kaempferol, D: Verapamil, E: Kaempferol with Verapamil. The relative distribution of total DNA in different phases of the cell cycle under different treatment conditions is indicated. F: The quantitative measurement of cell cycle phase. Statistical analysis through two way ANOVA showed G2/M dependent cell cycle arrest to be significant under K and KV treatment. (*p*-value ≤0.05).
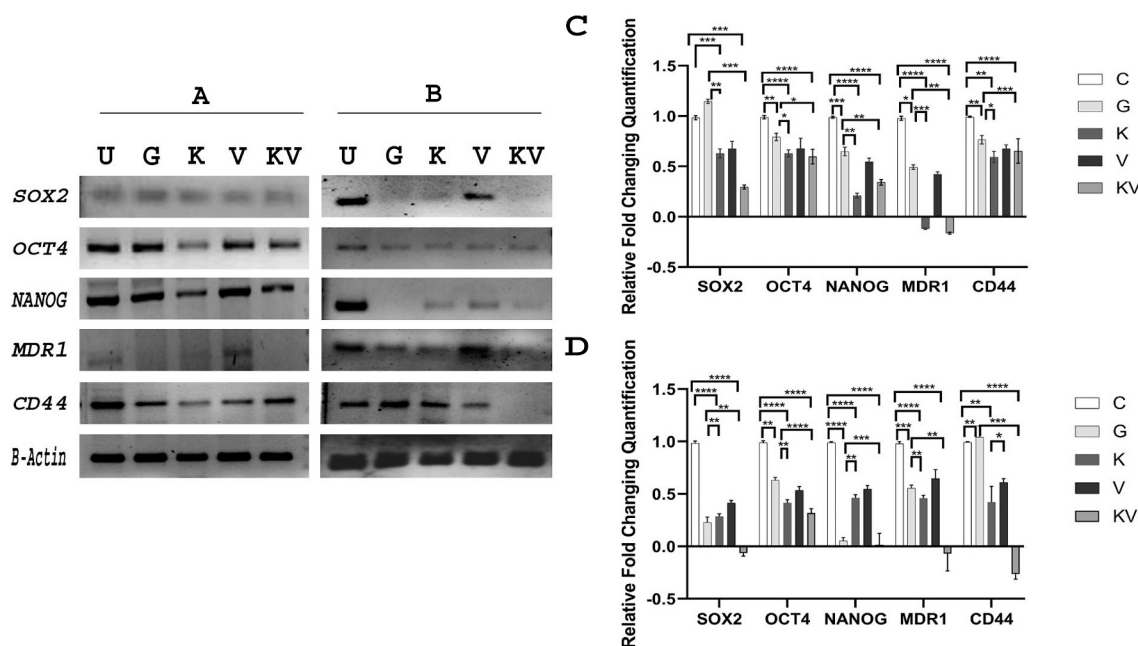
Fig. 4. Semiquantitative (A, B) and quantitative RT-PCR (C, D) to determine the expression status of candidate genes viz. *SOX2, NANOG1, OCT4, MDR1, CD44,* upregulated in breast cancer stem cell line MDA-MB-231 (A, C) and cultured primary BC (B, D) respectively; *β-Actin* gene was used as endogenous control for both semiquantitative and quantitative RT-PCR. Different treatment groups indicated in semiquantitative RT-PCR include U: Control; G: Gemcitabine; K: Kaempferol; V: Verapamil; KV: Kaempferol with Verapamil; In quantitative RT-PCR, Bars represent the relative fold changing gene expression normalized to *β-Actin* gene and relative to the corresponding untreated cells. Student's t-test is used to correlate the significance where $*p < 0.0332$ $**p < 0.0021$ $***p < 0.0002$ $**** p < 0.0001$.
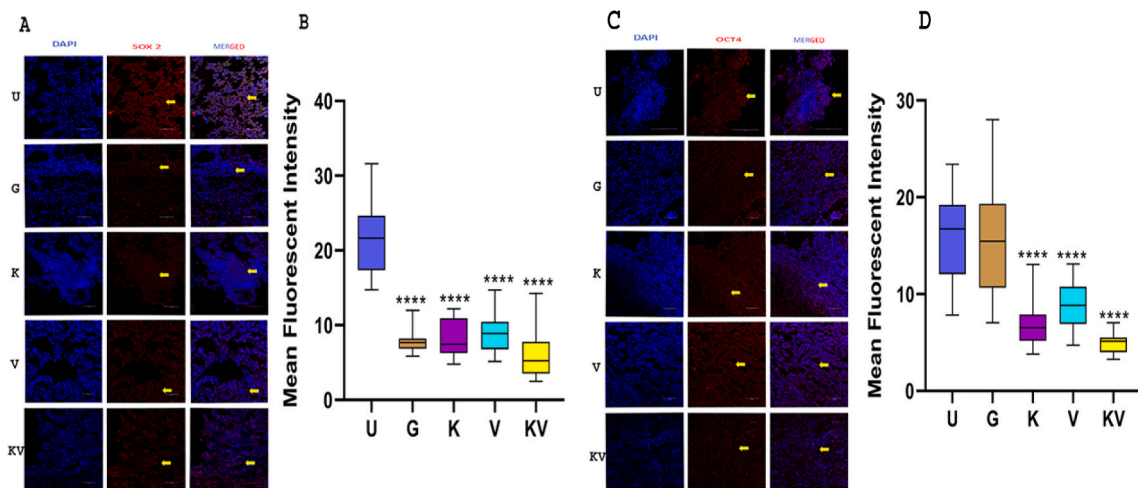

Fig. 5. Fluorescence-based immunohistochemical localization of SOX 2 (A), OCT4 (C), (D), protein in primary breast tumour in different treatment (48 h.) conditions. Scale bar: 10 μM. The different treatment groups included: U: Control; G: Gemcitabine; K: Kaempferol; V: Verapamil; KV: Kaempferol with Verapamil. Mean fluorescent intensity of SOX2 (B), OCT4 (D), One way ANOVA is used for statistical significant $***p < 0.0002$, $**** p < 0.0001$..

3.5.3. Immunoblotting and immunoprecipitation

Kaempferol alone and in combination with Verapamil resulted in significant downregulation of the candidate iPSC protein viz. SOX2, OCT4, NANOG, MDR1 and CD44 as detected from individual western blot (Fig. 7A) as well as from densitometric analysis of the relative fold change of expression of candidate proteins normalized to the expression of β-Actin (Khan et al., 2014) (Fig. 7B–F). Interestingly, Gemcitabine treatment did not result in any reduction in fold change of expression of the candidate proteins compared to control (Fig. 7B–F). This indicated that Kaempferol alone or along with Verapamil induced a significant reduction of candidate proteins redundantly upregulated in breast cancer stem cells. To identify the interaction of NANOG, CD44 and MDR1 marker, the immunoprecipitations was completed with the

candidate drugs in BCSC. To recognize how our candidate drug system reprograms CD44-NANOG-MDR1 network in chemoresistance breast cancer, immunoprecipation was carried out using CD44 primary antibody as bait, for three treatment groups, viz. U, K and KV. The co-immunoprecipitation of NANOG with CD44 and MDR1 with CD44 was disrupted in K and KV treatment groups (Fig. 7G), indicating interruption of the CD44-NANOG and CD44-MDR1 (Fig. 7G) network. Two way ANOVA data showed a significant reduction of fold change in Kaempferol alone or combination with Verapamil treatment group (Fig. 7H).
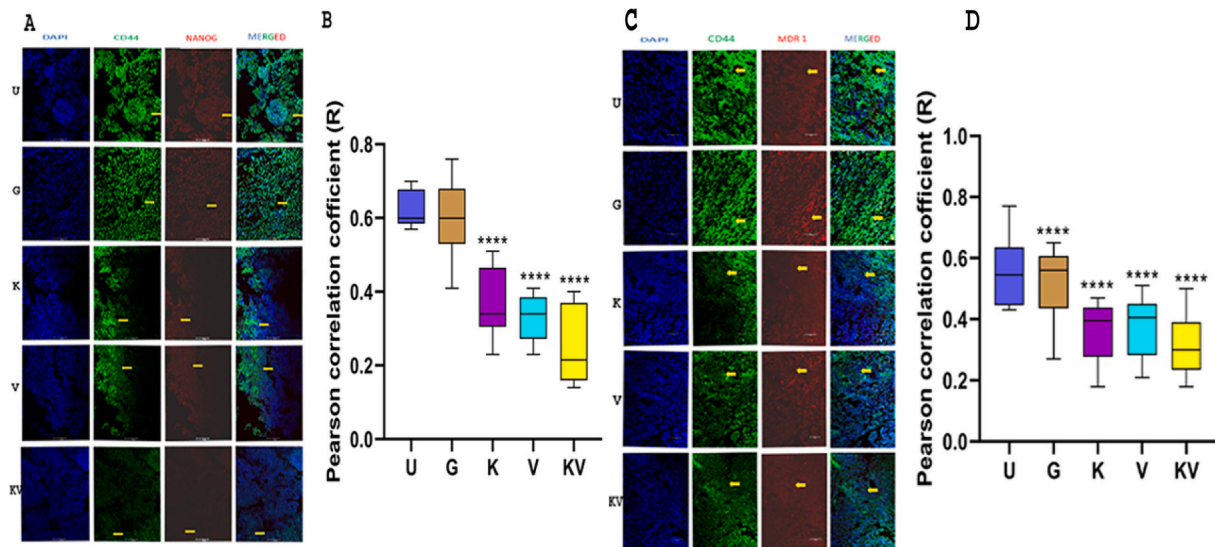
Fig. 6. Colocalization of CD44-NANOG (A) and CD44 and MDR1 (C) were also attenuated under K and KV treatment. Magnification: 20× for explant culture. Scale bar: 100 μM. The different treatment groups included: U: Control; G: Gemcitabine; K: Kaempferol; V: Verapamil; KV: Kaempferol with Verapamil. Pearson correlation coefficient (R) of colocalization of CD44 and NANOG were analysed in Fig. B and D respectively. Magnification: 20× for explant culture. One way ANOVA is used for statistical significant ***$p < 0.0002$, **** $p < 0.0001$.
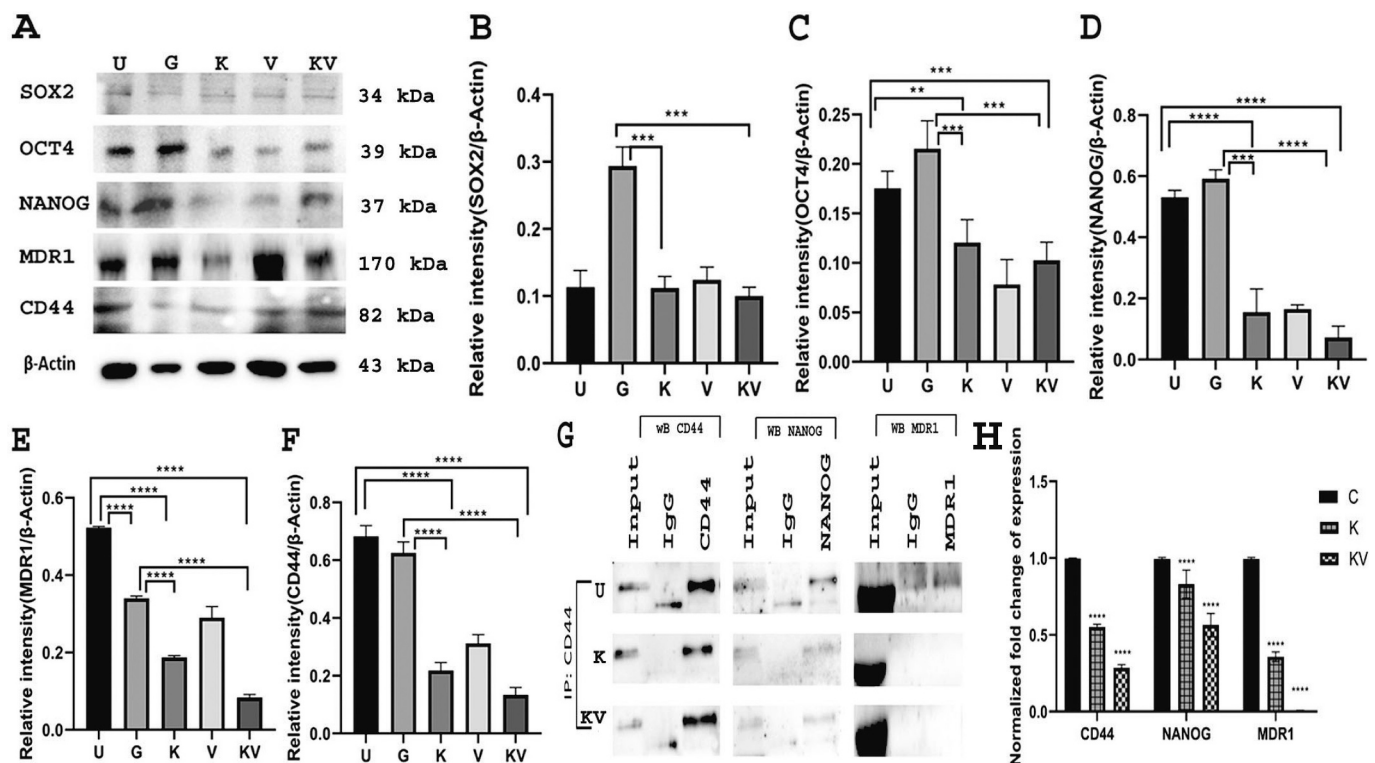
Fig. 7. Western blot analysis to check the fold change of expression of candidate iPSC markers in MDA-MB-231 cell line under various treatment conditions (48 h) (A). U: Control; G: Gemcitabine; K: Kaempferol, V: Verapamil: KV: Kaempferol and Verapamil. Fold change of expression of candidate genes were normalized to the expression of β-Actin (B–F). Co-immunoprecipitation analysis in an MDA-MB-231 cell line (G), under various treatment conditions viz. untreated, K and KV treatment, with CD44 as bait, showed that in both K and KV treatment, co-localization of NANOG with CD44 as well as MDR1 with CD44 is attenuated. U: Control; K: Kaempferol, KV: Kaempferol and Verapamil. Quantification of co-immunoprecipitation data for each candidate protein was plotted after normalization with their corresponding untreated controls (Fig. 7H). Student's t-test and Two way ANOVA were used to correlate the significance where *$p < 0.0332$ **$p < 0.0021$ ***$p < 0.0002$ **** < 0.0001.

3.6. Genotoxic effect of candidate drug systems in primary breast tumor and adjacent normal tissue explants

K induced robust expression of γH2AX (Ser-139 phosphorylated H2AX) in primary tumor explants, followed by KV and G treatment. However none of these treatments induced significant upregulation of the γH2AX expression in ex-vivo cultured adjacent breast normal tissues (Fig. 8). This indicated that the experimental dosage of our candidate
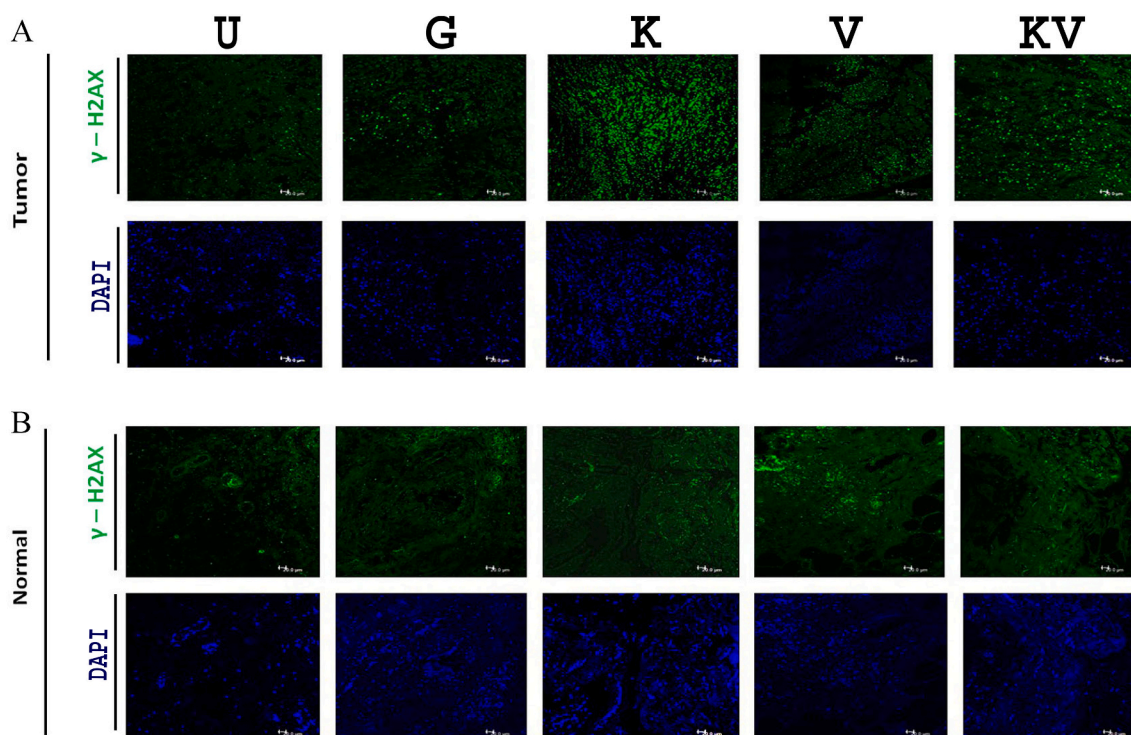
Fig. 8. Measurement of genotoxicity of our candidate drug systems in breast tumors and their paired normal tissues ($n = 4$), based on immunofluorescence based estimation of phosphorylated H2AX on serine 139 (gamma-H2AX) expression. Panel A: gamma-H2AX expression in tumor explant culture under the different treatment conditions. Panel B: Expression of gamma-H2AX in adjacent normal tissue explants grown under similar treatment conditions. Treatment conditions include U: Untreated; G: Gemcitabine treated; K: Kaempferol treated; V: Verapamil treated; KV: Kaempferol and Verapamil treated. Magnification: 20×; Scale Bar: 20 μM.

drugs system has no potent genotoxic effect in normal breast tissues.

4. Discussions

Chemoresistance an attribute of cancer stem cells, is an intrinsically complex process, involving pathways that are hitherto less characterized. Earlier reports showed that induced pluripotent stem cells (iPSC), a subset of the pluripotent stem cell population, to be redundantly expressed in aggressive and metastatic tumours (Cabarcas et al., 2011). Based on several shreds of evidence, we hypothesized that the iPSC markers could upregulate chemoresistance network through a mechanism involving MDR1, CD44, NANOG, SOX2 and OCT4.

Earlier reports showed that P-gp, an ATP dependent transmembrane protein and the product of the *MDR1* gene, expressed highly on cancer stem cells, play important role in the efflux of chemotherapeutics (Moitra, 2015). An earlier report also showed a clear association between CD44 and NANOG on upregulation of the *MDR1* gene (Bourgui-gnon et al., 2008). Early studies suggested a probable implication of Kaempferol, a bioflavonoid, in CSC propagation through downregulation of EMT (Tièche et al., 2019). A robust anticancer potential of Kaempferol, with minimal toxicity to healthy cells, endorses its application for therapeutic purposes (Imran et al., 2019; Ren et al., 2019).

In the present study, we aimed to study the effect of Kaempferol, on the expression of the aforementioned candidate genes conferring perpetual stemness and chemoresistance. As Verapamil, an inhibitor of ATP dependent proton pump was reported to inhibit P-gp (Lerner-Marmar-osh et al., 1999; Welker et al., 1995), an adjunct low dosage (5 μM) of Verapamil was also added with Kaempferol, to determine their effect on chemoresistance networking, stemness and survival of breast cancer.

Development of mammospheres culture from breast cancer cell lines as well as primary breast tumors (NACT) is still a challenge to numerous investigators (Zhang et al., 2011) but is an appropriate system to analyse the anticancer effect and chemoresistance network of the candidate

drugs. Tumour acidosis signifies a key selective force developing cancer progression and therapeutic resistance (Gillies et al., 2012). Acidic pHe encourages migration, invasion and metastasis of cancer cells through varied mechanisms (Gatenby et al., 2007), and stimulate the development of a cancer stem cell phenotype (Martinez-Outschoorn et al., 2011).The acidic pHe enriched cell malignancy through stimulating expression of stem cell markers such as OCT4, CD44 and NANOG (Hjelmeland et al., 2011) and attract human mesenchymal stem cells to tumour cells (Rattigan et al., 2012). In our study, the effect of the candidate drug system was significantly associated with pHe dependent disruption of tumorsphere formation in vitro/ex vivo, irrespective of tumour grade or tumour volume and pHe.

To develop the molecular mechanism of Kaempferol sensitization, the mRNA expression of *SOX2, OCT4, NANOG, MDR1, CD44* markers was carried out in MDA-MB-231 cell line and primary tumor-derived mammosphere. Kaempferol alone or in combination was effective in attenuating the expression of the candidate proteins both ex-vivo and in-vitro model, Gemcitabine to which showed minimal effect on BCSC.

Our study revealed that the iPSC markers (NANOG, SOX2, OCT4) are differentially upregulated in primary BCSC cells. Expression of NANOG, CD44 and MDR1 were consistently high in both tumour derived cells as well as in MDA-MB-231 cell line. In MDA-MB-231, western blot data showed SOX2 expression was low while expression of NANOG, MDR1, and CD44, as well as OCT4 were highly conspicuous and the effect of the drug combination was effective in attenuating their expression. In presence of Verapamil, the efficacy of Kaempferol was even more robust as its IC-50 dosage was attained at a much lower concentration. Owing to the inclusion of Verapamil, in our study, KV combination was found to be more robust than K, as revealed by mammosphere formation, relative fold change of candidate gene (RNA, protein) expression.

NANOG, a transcription factor, with its role in self-regeneration and maintenance of pluripotency in embryonic stem cells, has been reported in several tumour cells (Chambers et al., 2003). The activation of

NANOG occurs in a feedback loop mechanism in BCSC. As OCT4 partner, NANOG regulates the transcription factor SOX2 for maintaining the pluripotency of BC. NANOG induced transcriptional upregulation of SOX2 and OCT4, in turn, depends on upregulated CD44-MDR1 network. The intrinsic mechanism of chemo-evasiveness through these factors is complex. Our candidate drug system showed that the combined effect of the drugs was more effective than Kaempferol alone, in attenuating the expression of the candidate proteins, as substantiated by the immunoblotting and immunoprecipitation. Our RT-PCR data showed that the anti-stem cell effect of KV combination treatment was robust, with attenuation of expression of *SOX2, OCT4, NANOG, MDR1, CD44.*

Bourguignon and associates group exhibited that interaction of CD44 with extracellular Hyaluronic acid initiates CD44 and NANOG association and correspondingly leads to activation of multidrug-resistant genes, tumour development, and chemoresistance in several carcinoma cells (Bourguignon et al., 2002). It was affirmed earlier that hyaluronic acid and CD44 promote the association of NANOG with CD44, followed by activation of stem cell regulator proteins (Chanmee et al., 2015). For the first time, data from our immunoprecipitation study using CD44 as bait showed that Kaempferol alone or with Verapamil attenuated Hyaluronic acid-induced CD44 upregulation and also CD44 induced transactivation and membrane translocation of NANOG as well as MDR. This was validated in an observational study of co-localization of CD44 and NANOG as well as CD44 and MDR1 in primary breast tumour explant culture system under our experimental treatment conditions.

Immunocytochemical data that showed in Kaempferol combination with Verapamil resulted in disruption of cellular cytoskeleton, enlargement of the cell and low punctate expression of the candidate proteins (SOX2, OCT4, NANOG, MDR1 and CD44) with our candidate drugs.

Additionally, we also confirmed that both K and KV induced G2/M dependent cell cycle arrest in MDA-MB-231 cell line, indicating the efficacy of our drug system through probable induction of DNA damage which resulted in upregulation of G2/M checkpoints. This was also validated in our study where we found that both K and KV induced robust expression of γH2AX in primary breast tumor explant cultures but not in adjacent normal breast tissues. This indicated that both K and KV could be endorsed as safe drugs at their experimental dosage.

Gemcitabine-Carboplatin combination is widely used in NACT regimen for breast cancer patients in India and thus we included Gemcitabine as our control drug system. An earlier study indicated development of resistance networking to Gemcitabine therapy occurs almost in all patients (Dorman et al., 2016) and probably through upregulation of CD44 (Gillies et al., 2012). Based on our data, we hypothesized, Gemcitabine had an insignificant effect on did not show any efficacy as an anticancer drug. Our investigation evidenced that targeting the CD44-MDR1-NANOG network with our candidate drug system could mitigate Gemcitabine treatment failure breast tumour progression.

A previous report of Barve et al. (2009) showed that after IV administration of Kaempferol, the plasma concentration time was consistently high with a terminal half-life value of 3–4 h while the oral administration showed poor bioavailability (2%) owing to their extensive and rapid glucuronidation and other modifications in the gut and the liver. Through intestinal conjugation enzymes, the incorporated Kaempferol undergoes metabolic alteration to produce the glucuronides and sulfoconjugates forms in the liver (Yodogawa et al., 2003) and small intestine (Crespy et al., 2003). Previous reports showed that derivatization of Kaempferol could enhance its efficacy, where Kaempferol-3-O-α-arabinofuranoside was reported to be more robust than Kaempferol-3-O-rhamnoside in attenuating viability of different cancer cell lines (Diantini et al., 2012). In our study, we used HPLC purified Kaempferol (Sigma-Aldrich) and hypothesize that derivatization of our candidate drugs for future therapeutic application through intravenous route would not only enhance their bioavailability but enhance their therapeutic potential for aggressive breast cancers. Pharmacodynamically,

Kaempferol imparts antiproliferative effect through diverse mechanisms viz. interference with TNF-α-induced mitogen-activated protein kinase (MAPK) activation (Ren et al., 2019), activation of JAK/STAT3, PI3K/AKT and NF-κB etc. (Riahi-Chebbi et al., 2019). Kaempferol was also reported to downregulate DNMT3B expression, thus affecting DNA methylation patterns in bladder cancer (Qiu et al., 2017).

Pharmacokinetics of Verapamil showed that the drug is almost 90% absorbed when given orally, although its bioavailability is much lower (10–35%) owing to its rapid metabolism.

Intriguingly, apart from its inhibitory effect on PgP (Welker et al., 1995), Verapamil also depletes intracellular GSH in cells overexpressing MRP1, thereby imparting an antiproliferative effect on tumor cells (Lorendeau et al., 2014). Thus, both of our candidate drugs can attenuate the proliferation of aggressive tumors and our study revealed their synergistic effect in inhibiting BCSC cell viability, and their inhibition on cell viabilities was induced through inhibiting transcription. We recommend that to overcome the drug resistance to Gemcitabine in BCSC, our drug system is the best way to control the process through their interference with CD44-NANOG-MDR network.

Funding

Declaration of Competing Interest

The authors declare that there is no potential conflict of interest.

Acknowledgement

References

Anders, C.K., Carey, L.A., 2009. Biology, metastatic patterns, and treatment of patients with triple-negative breast cancer. Clin. Breast Cancer 9 (Suppl. 2), S73–S81. https://doi.org/10.3816/CBC.2009.s.008.

Arunasree, K.M., 2010. Anti-proliferative effects of carvacrol on a human metastatic breast cancer cell line, MDA-MB 231. Phytomed. Int. J. Phytother. Phytopharmacol. 17, 581–588. https://doi.org/10.1016/j.phymed.2009.12.008.

Ashton, J.C., 2015. Drug combination studies and their synergy quantification using the Chou-Talalay method–letter. Cancer Res. 75, 2400. https://doi.org/10.1158/0008-5472.CAN-14-3763.

Baker, E.K., Johnstone, R.W., Zalcberg, J.R., El-Osta, A., 2005. Epigenetic changes to the MDR1 locus in response to chemotherapeutic drugs. Oncogene 24, 8061–8075. https://doi.org/10.1038/sj.onc.1208955.

Barve, A., Chen, C., Hebbar, V., Desiderio, J., Saw, C.L., Kong, A.N., 2009. Metabolism, oral bioavailability and pharmacokinetics of chemopreventive kaempferol in rats. Biopharm. Drug Dispos. 30, 356–365. https://doi.org/10.1002/bdd.677.

Bockhorn, J., Dalton, R., Nwachukwu, C., Huang, S., Prat, A., Yee, K., Chang, Y.F., Huo, D., Wen, Y., Swanson, K.E., Qiu, T., Lu, J., Park, S.Y., Dolan, M.E., Perou, C.M., Olopade, O.I., Clarke, M.F., Greene, G.L., Liu, H., 2013. MicroRNA-30c inhibits

human breast tumour chemotherapy resistance by regulating TWF1 and IL-11. Nat. Commun. 4, 1393. https://doi.org/10.1038/ncomms2393.

Bourguignon, L.Y., Singleton, P.A., Zhu, H., Zhou, B., 2002. Hyaluronan promotes signaling interaction between CD44 and the transforming growth factor beta receptor I in metastatic breast tumor cells. J. Biol. Chem. 277, 39703–39712. https://doi.org/10.1074/jbc.M204320200.

Bourguignon, L.Y., Peyrollier, K., Xia, W., Gilad, E., 2008. Hyaluronan-CD44 interaction activates stem cell marker Nanog, Stat-3-mediated MDR1 gene expression, and ankyrin-regulated multidrug efflux in breast and ovarian tumor cells. J. Biol. Chem. 283, 17635–17651. https://doi.org/10.1074/jbc.M800109200.

Boyer, M.J., Barnard, M., Hedley, D.W., Tannock, I.F., 1993. Regulation of intracellular pH in subpopulations of cells derived from spheroids and solid tumours. Br. J. Cancer 68, 890–897. https://doi.org/10.1038/bjc.1993.451.

Bradford, M.M., 1976. A rapid and sensitive method for the quantitation of microgram quantities of protein utilizing the principle of protein-dye binding. Anal. Biochem. 72, 248–254. https://doi.org/10.1006/abio.1976.9999.

Brandão, M., Caparica, R., Eiger, D., de Azambuja, E., 2019. Biomarkers of response and resistance to PI3K inhibitors in estrogen receptor-positive breast cancer patients and combination therapies involving PI3K inhibitors. Ann. Oncol. Off. J. Eur. Soc. Med. Oncol. 30, x27–x42. https://doi.org/10.1093/annonc/mdz280.

Cabarcas, S.M., Mathews, L.A., Farrar, W.L., 2011. The cancer stem cell niche–there goes the neighborhood? Int. J. Cancer 129, 2315–2327. https://doi.org/10.1002/ijc.26312.

Callaghan, R., Luk, F., Bebawy, M., 2014. Inhibition of the multidrug resistance P-glycoprotein: time for a change of strategy? Drug Metab. Dispos. Biol. Fate Chem. 42, 623–631. https://doi.org/10.1124/dmd.113.056176.

Cao, N., Cheng, D., Zou, S., Ai, H., Gao, J., Shuai, X., 2011. The synergistic effect of hierarchical assemblies of siRNA and chemotherapeutic drugs co-delivered into hepatic cancer cells. Biomaterials 32, 2222–2232. https://doi.org/10.1016/j.biomaterials.2010.11.061.

Chambers, I., Colby, D., Robertson, M., Nichols, J., Lee, S., Tweedie, S., Smith, A., 2003. Functional expression cloning of Nanog, a pluripotency sustaining factor in embryonic stem cells. Cell 113, 643–655. https://doi.org/10.1016/s0092-8674(03)00392-1.

Chanmee, T., Ontong, P., Kimata, K., Itano, N., 2015. Key roles of hyaluronan and its CD44 receptor in the stemness and survival of cancer stem cells. Front. Oncol. 5, 180. https://doi.org/10.3389/fonc.2015.00180.

Chen, Y.N., Mickley, L.A., Schwartz, A.M., Acton, E.M., Hwang, J.L., Fojo, A.T., 1990. Characterization of adriamycin-resistant human breast cancer cells which display overexpression of a novel resistance-related membrane protein. J. Biol. Chem. 265, 10073–10080. 1972154.

Choi, E.J., Ahn, W.S., 2008. Kaempferol induced the apoptosis via cell cycle arrest in human breast cancer MDA-MB-453 cells. Nutr. Res. Pract. 2, 322–325. https://doi.org/10.4162/nrp.2008.2.4.322.

Chou, T.C., 2010. Drug combination studies and their synergy quantification using the Chou-Talalay method. Cancer Res. 70, 440–446. https://doi.org/10.1158/0008-5472.CAN-09-1947.

Crespy, V., Morand, C., Besson, C., Cotelle, N., Vézin, H., Demigné, C., Rémésy, C., 2003. The splanchnic metabolism of flavonoids highly differed according to the nature of the compound. Am. J. Physiol. Gastrointest. Liver Physiol. 284, G980–G988.

Critchfield, F.E., Johnson, J.B., 1959. Effect of neutral salts on pH of acid solutions. Anal. Chem. 159, 570. https://doi.org/10.1021/ac50164a034. April 31.

Diantini, A., Subarnas, A., Lestari, K., Halimah, E., Susilawati, Y., Supriyatna, Julaeha, E., Achmad, T.H., Suradji, E.W., Yamazaki, C., Kobayashi, K., Koyama, H., Abdulah, R., 2012. Kaempferol-3-O-rhamnoside isolated from the leaves of *Schima wallichii* Korth. inhibits MCF-7 breast cancer cell proliferation through activation of the caspase cascade pathway. Oncol. Lett. 3, 1069–1072. https://doi.org/10.3892/ol.2012.596.

Dorman, S.N., Baranova, K., Knoll, J.H., Urquhart, B.L., Mariani, G., Carcangiu, M.L., Rogan, P.K., 2016. Genomic signatures for paclitaxel and gemcitabine resistance in breast cancer derived by machine learning. Mol. Oncol. 10, 85–100. https://doi.org/10.1016/j.molonc.2015.07.006.

Gatenby, R.A., Smallbone, K., Maini, P.K., Rose, F., Averill, J., Nagle, R.B., Worrall, L., Gillies, R.J., 2007. Cellular adaptations to hypoxia and acidosis during somatic evolution of breast cancer. Br. J. Cancer 97, 646–653. https://doi.org/10.1038/sj.bjc.6603922.

Ghadimi, B.M., Grade, M., Difilippantonio, M.J., Varma, S., Simon, R., Montagna, C., Füzesi, L., Langer, C., Becker, H., Liersch, T., Ried, T., 2005. Effectiveness of gene expression profiling for response prediction of rectal adenocarcinomas to preoperative chemoradiotherapy. J. Clin. Oncol. Off. J. Am. Soc. Clin. Oncol. 23, 1826–1838. https://doi.org/10.1200/JCO.2005.00.406.

Ghosh, A., Roychowdhury, T., Nandi, R., Maiti, R., Ghosh, N.N., Molla, S.A., Mukhopadhyay, S., Prodhan, C., Chaudhury, K., Das, P., Sarkar, N.K., Chattopadhyay, S., Bhattacharya, R., Bose, C.K., Maiti, D.K., 2021. Inhibitory role of a smart nano-trifattyglyceride of Moringa oleifera root in epithelial ovarian cancer, through attenuation of FSHR - c-Myc axis. J. Tradit. Complement. Med. 11, 481–492. https://doi.org/10.1016/j.jtcme.2021.03.005.

Gillies, R.J., Verduzco, D., Gatenby, R.A., 2012. Evolutionary dynamics of carcinogenesis and why targeted therapy does not work. Nat. Rev. Cancer 12, 487–493. https://doi.org/10.1038/nrc3298.

Grimshaw, M.J., Cooper, L., Papazisis, K., Coleman, J.A., Bohnenkamp, H.R., Chiapero-Stanke, L., Taylor-Papadimitriou, J., Burchell, J.M., 2008. Mammosphere culture of metastatic breast cancer cells enriches for tumorigenic breast cancer cells. Breast Cancer Res. BCR 10, R52. https://doi.org/10.1186/bcr2106.

Herrero-Martínez, J.M., Sanmartin, M., Rosés, M., Bosch, E., Ràfols, C., 2005. Determination of dissociation constants of flavonoids by capillary electrophoresis. Electrophoresis 26, 1886–1895. https://doi.org/10.1002/elps.200410258.

Hjelmeland, A.B., Wu, Q., Heddleston, J.M., Choudhary, G.S., MacSwords, J., Lathia, J. D., McLendon, R., Lindner, D., Sloan, A., Rich, J.N., 2011. Acidic stress promotes a glioma stem cell phenotype. Cell Death Differ. 18, 829–840. https://doi.org/10.1038/cdd.2010.150.

Holliday, D.L., Speirs, V., 2011. Choosing the right cell line for breast cancer research. Breast Cancer Res. BCR 13, 215. https://doi.org/10.1186/bcr2889.

Iinuma, S., Farshi, S.S., Ortel, B., Hasan, T., 1994. A mechanistic study of cellular photodestruction with 5-aminolaevulinic acid-induced porphyrin. Br. J. Cancer 70, 21–28. https://doi.org/10.1038/bjc.1994.244.

Imran, M., Salehi, B., Sharifi-Rad, J., Aslam Gondal, T., Saeed, F., Imran, A., Shahbaz, M., Tsouh Fokou, P.V., Umair Arshad, M., Khan, H., Guerreiro, S.G., Martins, N., Estevinho, L.M., 2019. Kaempferol: a key emphasis to its anticancer potential. Molecules (Basel, Switzerland) 24, 2277. https://doi.org/10.3390/molecules24122277.

Jeter, C.R., Yang, T., Wang, J., Chao, H.P., Tang, D.G., 2015. Concise review: NANOG in cancer stem cells and tumor development: an update and outstanding questions. Stem Cells (Dayton, Ohio) 33, 2381–2390. https://doi.org/10.1002/stem.2007.

Jiao, X., Rizvanov, A.A., Cristofanilli, M., Miftakhova, R.R., Pestell, R.G., 2016. Breast cancer stem cell isolation. Methods in Mol. Biol. (Clifton, N.J.) 1406, 121–135. https://doi.org/10.1007/978-1-4939-3444-7_10.

Karekla, E., Liao, W.J., Sharp, B., Pugh, J., Reid, H., Quesne, J.L., Moore, D., Pritchard, C., MacFarlane, M., Pringle, J.H., 2017. *Ex vivo* explant cultures of non-small cell lung carcinoma enable evaluation of primary tumor responses to anticancer therapy. Cancer Res. 77, 2029–2039. https://doi.org/10.1158/0008-5472.CAN-16-1121.

Khan, S.A., Tyagi, M., Sharma, A.K., Barreto, S.G., Sirohi, B., Ramadwar, M., Shrikhande, S.V., Gupta, S., 2014. Cell-type specificity of β-actin expression and its clinicopathological correlation in gastric adenocarcinoma. World J. Gastroenterol. 20, 12202–12211. https://doi.org/10.3748/wjg.v20.i34.12202.

Kim, S.H., Choi, K.C., 2013. Anti-cancer effect and underlying mechanism(s) of kaempferol, a phytoestrogen, on the regulation of apoptosis in diverse cancer cell models. Toxicol. Res. 29, 229–234. https://doi.org/10.5487/TR.2013.29.4.229.

Kuo, P.L., Hsu, Y.L., Chang, C.H., Lin, C.C., 2005. The mechanism of ellipticine-induced apoptosis and cell cycle arrest in human breast MCF-7 cancer cells. Cancer Lett. 223, 293–301. https://doi.org/10.1016/j.canlet.2004.09.046.

Lerner-Marmarosh, N., Gimi, K., Urbatsch, I.L., Gros, P., Senior, A.E., 1999. Large scale purification of detergent-soluble P-glycoprotein from Pichia pastoris cells and characterization of nucleotide binding properties of wild-type, Walker A, and Walker B mutant proteins. J. Biol. Chem. 274, 34711–34718. https://doi.org/10.1074/jbc.274.49.34711.

Liang, S.Q., Marti, T.M., Dorn, P., Froment, L., Hall, S.R., Berezowska, S., Kocher, G., Schmid, R.A., Peng, R.W., 2015. Blocking the epithelial-to-mesenchymal transition pathway abrogates resistance to anti-folate chemotherapy in lung cancer. Cell Death Dis. 6 https://doi.org/10.1038/cddis.2015.195 e1824.

Livak, K.J., Schmittgen, T.D., 2001. Analysis of relative gene expression data using real-time quantitative PCR and the 2(-Delta Delta C(T)) method. Methods (San Diego, Calif.) 25, 402–408. https://doi.org/10.1006/meth.2001.1262.

Lorendeau, D., Dury, L., Genoux-Bastide, E., Lecerf-Schmidt, F., Simões-Pires, C., Carrupt, P.A., Terreux, R., Magnard, S., Di Pietro, A., Boumendjel, A., Baubichon-Cortay, H., 2014. Collateral sensitivity of resistant MRP1-overexpressing cells to flavonoids and derivatives through GSH efflux. Biochem. Pharmacol. 90 (3), 235–245. https://doi.org/10.1016/j.bcp.2014.05.017.

Martinez-Outschoorn, U.E., Prisco, M., Ertel, A., Tsirigos, A., Lin, Z., Pavlides, S., Wang, C., Flomenberg, N., Knudsen, E.S., Howell, A., Pestell, R.G., Sotgia, F., Lisanti, M.P., 2011. Ketones and lactate increase cancer cell "stemness," driving recurrence, metastasis and poor clinical outcome in breast cancer: achieving personalized medicine via metabolo-genomics. Cell Cycle (Georgetown, Tex.) 10, 1271–1286. https://doi.org/10.4161/cc.10.8.15330.

McDevitt, C.A., Callaghan, R., 2007. How can we best use structural information on P-glycoprotein to design inhibitors? Pharmacol. Ther. 113, 429–441. https://doi.org/10.1016/j.pharmthera.2006.10.003.

Miletti-González, K.E., Chen, S., Muthukumaran, N., Saglimbeni, G.N., Wu, X., Yang, J., Apolito, K., Shih, W.J., Hait, W.N., Rodríguez-Rodríguez, L., 2005. The CD44 receptor interacts with P-glycoprotein to promote cell migration and invasion in cancer. Cancer Res. 65, 6660–6667. https://doi.org/10.1158/0008-5472.CAN-04-3478.

Moitra, K., 2015. Overcoming multidrug resistance in cancer stem cells. Biomed. Res. Int. 2015, 635745. https://doi.org/10.1155/2015/635745.

Morten, B.C., Scott, R.J., Avery-Kiejda, K.A., 2016. Comparison of three different methods for determining cell proliferation in breast cancer cell lines. J. Visualized Exp. JoVE 115, 54350. https://doi.org/10.3791/54350.

Prescott, D.M., Charles, H.C., Sostman, H.D., Page, R.L., Thrall, D.E., Moore, D., Oleson, J.R., Dewhirst, M.W., 1993. Manipulation of intra- and extracellular pH in spontaneous canine tumours by use of hyperglycaemia. Int. J. Hyperthermia Off. J. Eur. Soc. Hyperthermic Oncol. N. Am. Hyperthermia Group 9, 745–754. https://doi.org/10.3109/02656739309032061.

Qiu, W., Lin, J., Zhu, Y., Zhang, J., Zeng, L., Su, M., Tian, Y., 2017. Kaempferol modulates DNA methylation and downregulates DNMT3B in bladder cancer. Cell. Physiol. Biochem. Int. J. Exp. Cell. Physiol. Biochem. Pharmacol. 41, 1325–1335. https://doi.org/10.1159/000464435.

Rattigan, Y.I., Patel, B.B., Ackerstaff, E., Sukenick, G., Koutcher, J.A., Glod, J.W., Banerjee, D., 2012. Lactate is a mediator of metabolic cooperation between stromal carcinoma associated fibroblasts and glycolytic tumor cells in the tumor microenvironment. Exp. Cell Res. 318, 326–335. https://doi.org/10.1016/j.yexcr.2011.11.014.

Ren, J., Lu, Y., Qian, Y., Chen, B., Wu, T., Ji, G., 2019. Recent progress regarding Kaempferol for the treatment of various diseases. Exp. Ther. Med. 18, 2759–2776. https://doi.org/10.3892/etm.2019.7886.

Reynolds, C.P., Maurer, B.J., 2005. Evaluating response to antineoplastic drug combinations in tissue culture models. Methods Mol. Med. 110, 173–183. https://doi.org/10.1385/1-59259-869-2:173.

Riahi-Chebbi, I., Souid, S., Othman, H., Haoues, M., Karoui, H., Morel, A., Srairi-Abid, N., Essafi, M., Essafi-Benkhadir, K., 2019. The phenolic compound Kaempferol overcomes 5-fluorouracil resistance in human resistant LS174 colon cancer cells. Sci. Rep. 9, 195. https://doi.org/10.1038/s41598-018-36808-z.

Rota, L.M., Lazzarino, D.A., Ziegler, A.N., LeRoith, D., Wood, T.L., 2012. Determining mammosphere-forming potential: application of the limiting dilution analysis. J. Mammary Gland Biol. Neoplasia 17, 119–123. https://doi.org/10.1007/s10911-012-9258-0.

Rust, S., Guillard, S., Sachsenmeier, K., Hay, C., Davidson, M., Karlsson, A., Karlsson, R., Brand, E., Lowne, D., Elvin, J., Flynn, M., Kurosawa, G., Hollingsworth, R., Jermutus, L., Minter, R., 2013. Combining phenotypic and proteomic approaches to identify membrane targets in a 'triple negative' breast cancer cell type. Mol. Cancer 12, 11. https://doi.org/10.1186/1476-4598-12-11.

Schmittgen, T.D., Livak, K.J., 2008. Analyzing real-time PCR data by the comparative C(T) method. Nat. Protoc. 3, 1101–1108. https://doi.org/10.1038/nprot.2008.73.

Shaw, F.L., Harrison, H., Spence, K., Ablett, M.P., Simões, B.M., Farnie, G., Clarke, R.B., 2012. A detailed mammosphere assay protocol for the quantification of breast stem cell activity. J. Mammary Gland Biol. Neoplasia 17, 111–117. https://doi.org/10.1007/s10911-012-9255-3.

Silva, A.S., Yunes, J.A., Gillies, R.J., Gatenby, R.A., 2009. The potential role of systemic buffers in reducing intratumoral extracellular pH and acid-mediated invasion. Cancer Res. 69, 2677–2684. https://doi.org/10.1158/0008-5472.CAN-08-2394.

Silver, N., Best, S., Jiang, J., Thein, S.L., 2006. Selection of housekeeping genes for gene expression studies in human reticulocytes using real-time PCR. BMC Mol. Biol. 7, 33. https://doi.org/10.1186/1471-2199-7-33.

Tièche, C.C., Gao, Y., Bührer, E.D., Hobi, N., Berezowska, S.A., Wyler, K., Froment, L., Weis, S., Peng, R.W., Bruggmann, R., Schär, P., Amrein, M.A., Hall, S., Dorn, P., Kocher, G., Riether, C., Ochsenbein, A., Schmid, R.A., Marti, T.M., 2019. Tumor initiation capacity and therapy resistance are differential features of EMT-related subpopulations in the NSCLC cell line A549. Neoplasia (New York, N.Y.) 21, 185–196. https://doi.org/10.1016/j.neo.2018.09.008.

Welker, E., Szabó, K., Holló, Z., Müller, M., Sarkadi, B., Váradi, A., 1995. Drug-stimulated ATPase activity of a deletion mutant of the human multidrug-resistance protein (MDR1). Biochem. Biophys. Res. Commun. 216, 602–609. https://doi.org/10.1006/bbrc.1995.2665.

Yodogawa, S., Arakawa, T., Sugihara, N., Furuno, K., 2003. Glucurono- and sulfo-conjugation of Kaempferol in rat liver subcellular preparations and cultured hepatocytes. Biol. Pharm. Bull. 26, 1120–1124. https://doi.org/10.1248/bpb.26.1120.

Zhang, S., Zhou, Z., Gong, Q., Makielski, J.C., January, C.T., 1999. Mechanism of block and identification of the verapamil binding domain to HERG potassium channels. Circ. Res. 84, 989–998. https://doi.org/10.1161/01.res.84.9.989.

Zhang, F., Song, C., Ma, Y., Tang, L., Xu, Y., Wang, H., 2011. Effect of fibroblasts on breast cancer cell mammosphere formation and regulation of stem cell-related gene expression. Int. J. Mol. Med. 28, 365–371. https://doi.org/10.3892/ijmm.2011.700.

Zhao, L., Wientjes, M.G., Au, J.L., 2004. Evaluation of combination chemotherapy: integration of nonlinear regression, curve shift, isobologram, and combination index analyses. Clin. Cancer Res. Off. J. Am. Assoc. Cancer Res. 10, 7994–8004. https://doi.org/10.1158/1078-0432.CCR-04-1087.

Kaempferol attenuates viability of ex-vivo cultured post-NACT breast tumor explants through downregulation of p53 induced stemness, inflammation and apoptosis evasion pathways

Sourav Kumar Nandi [a], Ayan Pradhan [b], Basudeb Das [c], Biswajit Das [d], Sudarshana Basu [a], Bibekanand Mallick [c], Amitava Dutta [d], Diptendra Kumar Sarkar [b], Ashis Mukhopadhyay [e], Soma Mukhopadhyay [a,*], Rittwika Bhattacharya [a,*]

[a] *Department of Molecular Biology, Netaji Subhas Chandra Bose Cancer Research Institute, 3081 Nayabad, Kolkata 700094, India*
[b] *Department of General Surgery, Institute of Post graduate Medical Education & Research and SSKM Hospital, 244B AJC Bose Road, Kolkata 700020, India*
[c] *Department of Life Science, National Institute of Technology, Rourkela, Odisha, 769008, India*
[d] *Department of Pathology, Netaji Subhas Chandra Bose Cancer Research Institute, 3081 Nayabad, Kolkata 700094, India*
[e] *Department of Haematooncology, Netaji Subhas Chandra Bose Cancer Research Institute, 3081 Nayabad, Kolkata 700094, India*

ARTICLE INFO

ABSTRACT

Early onset of chemotherapy evasion is a therapeutic challenge. Chemotherapy-induced upregulation of stem cell markers imparts invasiveness and metastatic property to the resident tumor. The efficacy of Kaempferol in attenuating epithelial to mesenchymal transition has earlier been established in the breast cancer cell. In our study population, progression-free survival was observed to be statistically more significant in post-NACT low-grade tumors than the high-grade tumors. Further, in post-NACT TNBCs, high-grade tumors showed a preponderance of strong nuclear p53 expression and very low expression of Caspase 3, indicating that, altered p53 expression predisposes these tumors to apoptosis escape and up-regulation of stemness markers. Herein, we report the robust efficacy of Kaempferol on ex-vivo grown breast tumors, derived from post-NACT TNBC patients, through downregulation of nuclear p53, CD44, ALDH1, NANOG, MDR1, Ki67, BCL2 and upregulation of Caspase 3. Such tumors also showed concurrent deregulated RNA and protein expression of CD44, NANOG, ALDH1 and MDR1 with upregulation of Caspase 3 and cleaved Caspase 3, upon Kaempferol treatment. Validation of efficacy of the treatment dosage of Kaempferol through immunophenotyping on MDA-MB-231, suggested that Kaempferol at its IC-50 dosage was effective against CD44 and CD326 positive breast cancer through deregulating their expression. Protein-protein interaction network through STRING pathway analysis and co-expression study of candidate proteins showed the highest degree of co-expression of *p53* and *KI-67, CD44, NF-kappaB, ALDH1, NANOG, MDR1*, and *BCL2*. Thus, potentially targetable oncogenic protein markers, that are susceptible to downregulation by Kaempferol, provides insight into biomarker-driven therapeutic approaches with it.

1. Introduction

Chemoevasion is an ominous challenge in treating aggressive breast tumors. Irrespective of subtypes, chemoevasion is initiated with upregulation of stem cell renewal and a diverse array of networks that results in disease progression. Triple negative breast cancer (TNBC), which comprise hormone receptor-negative undifferentiated subpopulations of breast cancer, are more amenable to develop early resistance to

chemotherapy, involving various signalling networks [1]. Early reports suggested that molecular profiling of TNBC would provide therapeutic benefit from neoadjuvant chemotherapy (NACT) [2]. The tumor suppressor, p53 is considered one important gatekeeper that regulates cell cycle progression, decides cell fate through the initiation of DNA damage repair or induction of apoptosis. The homeostasis of cellular plasticity, the balance between stem cell renewal and differentiation is disrupted when p53 is functionally mutated [3]. It was also revealed that

---

TP53 mutation also induces dedifferentiation of adult cells, through upregulation of several pluripotent stem cell markers [3]. Apart from the canonical pathways leading to cancer stem cell renewal, several other less characterized pathways concurrently maintain cancer stemness and chemoevasive phenotype. Aldehyde dehydrogenase 1 (ALDH1), that oxidises intracellular aldehydes with the aim of cellular detoxification, has been reported to be upregulated in CSCs in many kinds of cancers including breast cancer and thus accounts for the development of therapeutic resistance [4]. CD44, a cell surface glycoprotein adhesive molecule is highly expressed in the cell surface of breast cancer stem cells [5].

The residual cancer burden is considered an indispensable qualifier of residual disease [6]. In our study cohort, a significant percentage of patients with high grade and high residual cancer burden (RCB) scores, showed upregulated nuclear p53 expression with downregulated expression of Caspase 3. Altered p53 expression could unleash stem cell renewal, proliferation and apoptosis evasion and we found robust expression of several candidate proteins regulating these processes in such tumor explants.

In our erstwhile study we had observed robust antiproliferative efficacy of Kaempferol on breast cancer stem cell populations, through downregulation of pluripotent stem cell markers(SOX2, OCT4, NANOG), MDR1 and CD44 [7]. Herein, we wanted to check the efficacy of Kaempferol on tumor explants, obtained from NACT recipient TNBC patients. Our present study revealed that, Kaempferol attenuated the expression of induced pluripotent stem cell markers (NANOG, CD44, and ALDH1) as well as MDR1, CD44 + / CD24- and CD44 + /CD326 + , downregulated the expression of pro-survival markers BCL-2, Ki-67, NF-kB and upregulated Caspase 3 and cleaved Caspase 3 expression in patient tumor derived explants. STRING pathway analysis and co-expression analysis revealed the mutual association of these candidate proteins and suggested the probable antiproliferative mechanism of Kaempferol in such p-NACT-TNBC. The cumulative information of the prognostic markers upregulated in chemotolerant TNBC and their attenuation upon Kaempferol treatment could provide insights on developing treatment strategies.

2. Materials and methods

2.1. Reagents

All reagents and chemicals were acquired from Sigma Aldrich (St. Louis, MO, USA) except boric acid (Sisco Research Laboratories, Mumbai, and Maharashtra, India), Disodium phosphate (Na_2HPO_4), ethanol, Potassium dihydrogen phosphate (KH_2PO_4), sodium dodecyl sulphate (Merck, India), C44, CD24, CD326 and BD Cycletest™ Plus DNA Kit (BD Biosciences, San Jose, CA, USA). All ingredients of primary cell culture and cell line culture were purchased from Gibco, Thermo Fisher Scientific – US. For RNA isolation Diethyl pyrocarbonate (DEPC) was acquired from Invitrogen, Carlsbad, CA, USA.All antibodies were obtained from Abcam,Cambridge, United Kingdom.

2.2. Tumour specimens

Altogether, 271 female breast cancer patients, who were diagnosed with p-NACT-TNBC and received curative surgery for the treatment of breast cancer at Netaji Subhas Chandra Bose Cancer Hospital and IPGME&R and SSKM Hospital, during the period 2016–2021, were enrolled for the study. The patients were further characterized into different TNBC subtypes (basal like 1, basal like 2, immunomodulatory and mesenchymal like) (Table 1). A random set of 67 tumor specimens were chosen from this pool, to check for expression of p53 and Caspase-3. From this second cohort, another set of samples (n = 38) were taken for explants culture, drug treatment and RNA expression analysis. From the pool of 38 samples, a small subset of 17 specimens were taken for immunohistochemistry to check the efficacy of Kaempferol on tumor cell viability. Protein expression of few candidate proteins regulating chemoresistance and stemness (MDR1,NANOG, Caspase 3, Cleaved Caspase 3) alongwith p53 expression was analyzed in a smaller cohort of patients (n = 5).

Written informed consent was provided by the pathologist of the hospital section. The histology of tumours was analyzed by a clinical pathologist as entitled previously [8]. ER, PR, as well as HER2, were also classified through International Union against Cancer (UICC) and American Joint Committee on Cancer (AJCC) tumour-node-metastasis (TNM) staging, and the up-to-date informed consents were achieved from all patients. The clinicopathological parameter of the patients were represented in Table 1. The response to chemotherapy was confirmed through an oncologist and morphologically confirmed by a clinical pathologist. In our experiment, all cases represented p-NACT-TNBC patients, and none of the patients participated in the clinical trial.

2.3. Immunohistochemical analysis of p53 and Caspase 3 in different grades of p-NACT-TNBC

Immunohistochemical analysis of p53 and Caspase 3 expression was carried out in low grade (I/II) and high grade (III/IV) tumour in breast cancer, following our established protocol [7]. For histological analysis, the H&E [1% alcoholic] staining was completed as previously described method [7]. Immunohistochemical analysis of ER (1:200), PR (1:200),

Table 1
The clinicopathological antiquity of the post NACT breast cancer patients (n = 271).

Age	Basal Like − 1 (n = 69)	Basal Like − 2 (n = 66)	Immunomodulatory (n = 64)	Mesenchymal-like (n = 72)	p- values
Median	39	42	47	52.5	0.006
Stage					
1	38%	33.26%	15.33%	42%	0.005
2	31%	27.8%	34.3%	27.5%	0.0001
3	21%	26.2%	47.9%	18%	0.0001
4	5.8%	10.5%	42. 6%	6%	0.0001
Bilateral Carcinoma	1.9%	1.2%	1.4%	1.3%	0.05
Nuclear Grade					
1	6.3%	1.3%	3.1%	3.6%	0.0001
2	57%	42.9%	28.5%	18%	0.0001
3	11.5%	53.3%	66.6%	26%	0.0001
Ki-67 Mean Range	38%	46.7%	59%	36%	0.0023
Histological grade					
1	7.5%	3.6%	2.5%	4.1%	0.0001
2	52.3%	33.8%	26.5%	39%	0.0001
3	14.4%	57.5%	63.5%	43%	0.0001
Adjuvant Chemotherapy	78.8%	82.5%	92%	71%	0.0017
Adjuvant Radiation therapy	48.5%	58%	72%	63%	0.0001
Histology	DC, IDC	DC, IDC, INFDC	DC	IDC, AC	

HER2 (1:200) were performed following previously described method [9].

2.4. Databases and bioinformatics tools

The expression status of Caspase3 and p53 alongwith the iPSC (NANOG, ALDH1, CD44) and EMT(MDR1, NF-kappaB, BCL2) marker were obtained from TCGA-TNBC database, (http://ualcan.path.uab.edu/). The protein-protein interactions (PPI) were analyzed via the online STRING database (version 11.0). First, we input the targeted oncogenes obtained and the minimum interaction score was fixed to the highest confidence (score 0.900). The retrieval of Interacting Genes (STRING, http://string.embl.de/) was carried out, analyzed and exportedas the TSV file and employed to analyse the PPI networks. Moreover, we used DGIdb (http://www.dgidb.org), a valuable database that runs free services for searching the evidence on drug-gene interactions, to explore the potential targets of Kaempferol.

2.5. Tumor explants culture and drug treatment

For explants culture, all tumour specimens (n = 38) were obtained in a sterile container with 1X Phosphate-buffered saline (PBS) and dis-aggregated mechanically into- 10 mm pieces with a penknife. Tumour cells were propagated explants were cultured in DMEM/F-12 complete medium supplemented with 10% FBS, 5 μg/ml insulin, 500 ng/ml hydrocortisone, 10 ng/ml EGF, 1% penicillin/streptomycin,50 μg/ml Gentamicin, 2.5 μg/ml Amphotericin B antibiotics in at 37 °C in 5% CO_2/air.

Based on our previous established data [7], IC-50 dosage of Kaempferol in ex-vivo and in-vitro for breast tumor explant cultures were kept at 224.51 μM. The IC50 concentration of Carboplatin was determined in ex-vivo and in-vitro models from a concentration dependent viability of cells to Carboplatin (23.74 ± 4.67 μM) (Fig. 3 A). Cytotoxic activity was confirmed with IC50, which is the concentration necessary to reduce the absorbance of treated cells by 50% compared to the control (untreated cells). Tumor explants were cultured for 48 hrs with the following conditions, viz. untreated, with Kaempferol, with Carboplatin, both at their IC-50 concentration i.e 224.51 μM and 23.74 μM respectively.

2.6. RNA extraction, semiquantitative and quantitative RT-PCR

RNA extraction from the together drugs treated p-NACT-TNBC tumour (n = 38) explants was carried out using Trizol reagent and finally dissolved in DEPC treated water [10]. cDNA was synthesized from 10 μg of total RNA following our previously established protocol [7]. cDNAs were reverse transcribed with 10 picomolar each of the designed primers in Table S1. Semiquantitative and SYBR Green-based quantitative RT-PCR was carried out in triplicates in 96-well plates in StepOne™ Real-Time PCR System (Applied Biosystems). A fold change in the relative expression of the gene was calculated depending on the comparative Ct (2 −ΔΔCt) process [11].

2.6.1. Hematoxylin and Eosin (H&E) staining followed by Immunohistochemical analysis to identify stemness, proliferation and apoptosis evasion

Hematoxylin and Eosin (H&E) staining (Fig. S1) was carried out through a previously established protocol for p-NACT-TNBC (n = 17) after candidate drug treatment for 48 h. After the end of treatment, paraffin-embedded tissues blocks were prepared and 3 μM sections were cut for histological and immunohistochemical analysis. For histological analysis, the H&E [1% alcoholic] staining was completed as previously described method [9]. Through immunohistochemistry analysis, the expression of candidate proteins regulatingstemness, proliferation and apoptosis escape (p53, KI-67, CD44, NF-kappaB, ALDH1, NANOG, MDR1, BCL2) were performed following our established protocol [7].

Caspase 3 expression was also carried out to detect apoptosis.

2.6.2. Immunoblotting assay to determine expression of few proteins regulating stemness and chemoresistance, under experimental conditions

After explant culture (n = 5), upon treatment with different drugs in the aforementioned concentrations for 48 h, tissue explants were sonicated for cell lysis and protein concentrations of the study groups (untreated, Carboplatin treated, Kaempferol treated) were estimated using Bradford protein assay [7]. 30 μg of protein of each treatment group was loaded in each lane of a 10% SDS-PAGE gel and transferred to nitrocellulose membranes. The membranes were washed twice time with TBS-T (5% milk in Tris-buffered saline-Tween 20), blocked with 5% skimmed milk and treated with specific primary antibodies such as Anti-NANOG (Abcam Ca # ab109250, RRID:AB_10863442), Anti-MDR1 (Santa Cruz Ca # sc-13131, RRID:AB_626990), Anti-p53 (Cell Signaling Technology#2527), Anti-Caspase3(Cell Signaling Technology #9662), Anti-Cleaved-Caspase3(Cell Signaling Technology#9664)(1:1000 dilution). TBS-T washed membranes were incubated with horseradish peroxidase-conjugated monoclonal secondary antibody (dilution: 1: 10, 000; GeneTex Cat# GTX14122, RRID: AB_373069). The membranes were washed and after incubation with chemiluminescence substrate, were pictured by ChemiDoc Imaging System,Bio-Rad.

2.7. Expression of CD44 and CD326 as cancer stem cell markers for chemo tolerance TNBC

The expression profiles of CD44 (FITC- conjugated), CD24 (PE-conjugated), CD326 (APC-conjugated) in Kaempferol (224.51 μM and) and Carboplatin (23.74 μM) treated MDA-MB-231 cells, were analyzed by flow cytometry [12]. Briefly, 1×10^6 cells were grown and after treatment with candidate drugs for 48hrs, were incubated with CD44, CD24, CD326 antibodies inappropriate dilution for 1 h. Cells were washed and re-suspended in sheath solution and analyzed by flow cytometer. Untreated cells were treated with proper isotype PE-, FITC- and APC-conjugated antibodies. Cellular debris was left out from the investigation based on low forward light scatter.

2.8. Statistics

The ideal IC-50 (experiment data were revealed as means and SD from three individual judgements) values of both drugs were analyzed from the cell viability curve through GraphPad Prism® 8 software. All samples were run in three replicates. For RNA expression analysis, Student's Z test is used to correlate the significance. Student's t-test and two way ANOVA were used to correlate the significance of protein expression. Statistical tests were considered significant at probability value, $p \leq 0.05$. For 95% confidence in all statistics, a p-value of ≤ 0.05 was considered statistically significant. All above the experiments were completed without important loss of statistical power.

2.9. Ethics approval and informed consent

Fresh human p-NACT-TNBC tumours were collected from patients with signed informed consent that underwent surgery at Netaji Subhas Chandra Bose Cancer Hospital (NSCBCRI). Methods were carried out following the relevant guidelines and regulations Ethics Committee. The project was approved by the ICMR and by the Ethics Committee of NSCBCRI (EC/ NSCBCRI/01/2021).

3. Result

3.1. Clinicopathological characteristics of patients based on TNBC subtype

It was observed patients with immunomodulatory (n = 64) or Mesenchymal-like(n = 72) displayed a significantly worse survival than

patients with basal like-1 (n = 69)or basal like-2 (n = 66)TNBC tumors. The H&E Histopathology data of p-NACT-TNBC tumour samples (Fig. S1A – S1C), with immunohistochemically confirmed ER/PR/ HER2 negative (Fig. S1D – S1F) expression status of the patients are shown in Fig. S1A-C; S1D-F. The correlation between survival of low grade (I/II) (Fig. 1A) and high grade (III/IV) (Fig. 1B) was established through Kaplan–Meier survival curves (Fig. 1). Progression-free survival for the p-NACT-TNBC group was significantly higher in low grade (I/II) tumors than in high grade (III/IV), when compared with pre-therapeutic samples. The outcome of disease-free (Fig. 1C) and overall survival curve (Fig. 1D) were plotted. The 5-year survival disease-free survival and overall survival possibility were analyzed respectively for the whole experimental group of patients. In the group of pre-therapeutic patients there was a relapse earlier than the p-NACT-TNBC group. In the overall survival analysis, no significant change was observed.

3.2. Expression analysis of p53 and Caspase 3 and correlation

The analysis of TCGA data (primary breast tumor tissue, n = 1097 vs normal tissue, n = 114) showed that the expression of p53 (Fig. 2 A) and Caspase 3 (figure2 B) were higher in breast tumors compared to normal. Naturally, activation of caspase3 leads to initiation of apoptosis and resultant cell death. However, when the p53 is mutated then activation of caspase3 does not initiate apoptosis resulting in ineffectiveness of chemotherapeutic drugs which exerts its antitumor effects through the p53 pathway [13]. In our study cohort, a pattern of low p53 expression with high Caspase 3 expression in low-grade tumors and high nuclear p53 expression with low Caspase 3 expression was observed in high-grade tumors (Fig. 2C-D, Table 2). It has been previously demonstrated that the high expression of p53 and low expression of Caspase3 is closely correlated with cancer progression. The TCGA data of expression of p53 and Caspase 3 in different stages (Fig. S2A, S2B) and different nodal metastatic status (Fig. S2C, S2D) showed that expression of p53 was increased in higher stages (III/IV) (Fig. 2D) and high nodal metastatic status, in contrast, the expression of Caspase 3 was increased in lower stage (I/II) (Fig. 2C) and low nodal metastatic status. Further, the correlation of Caspase 3 expressions with p53 mutation status was validated in breast cancer through the TCGA-BRCA database. We found that Caspase 3 expression was higher in p53 mutant compared to non-mutant (Fig. S2E). As our first step in determining the expression levels of p53 and Caspase-3 in breast cancer, we performed IHC analysis (n = 62) (Table 2) on a panel of p-NACT-TNBC patients to validate the TCGA data. In this study, we found upregulation of p53 was observed in high grade(III/IV) tumour sample than the low grade (I/II) (Fig. 2C) and upregulation of Caspase-3 was observed in the low grade (I/II) tumors

than the high grade(III/IV) (Fig. 2D). All statistical analyses were done in Table 2.

3.3. Kaempferol effect in Proliferation kinetics and Gene expression profile analysis of p-NACT-TNBC patients

In corroboration with our earlier observation [14], a significant reduction of cell viability was observed in a dose-dependent manner in p-NACT-TNBC patients'tumour cells after treatment with various concentrations of Kaempferol (Fig. 3B) for 48 hrs and Carboplatin(Fig. 3 A). The IC50 values of the Kaempferol treatment group in p-NACT-TNBC patients'tumour cells was 205.7 ± 6.67 µM and Carboplatin was 23.74 ± 4.67 µM.

3.4. Kaempferol on RNA expression of candidate markers regulating cellular plasticity

Expression of EMT markers such as CD44, *NANOG, MDR1*, and *ALDH1* were quantitated in between different treatment groups (untreated, Carboplatin treated, Kaempferol treated) and normalized with respect to *β- ACTIN* (Fig. 3C-D). We found a lower expression of NANOG in the Kaempferol treated sample (Fig. 3 C). qRT-PCR data showed Kaempferol was more robust than Carboplatin in downregulating the expression of CD44,*NANOG, ALDH1, MDR1* (Fig. 3D). In *ALDH1* panel we find the Kaempferol treatment was more significant in respect of carboplatin whereas in *MDR1* panel the carboplatin treatment group was not significant (NS). Best significant changes in both drugs treatment sets were observed in *CD44* and *NANOG*.

3.4.1. Immunoblot analysis

Immunoblot data showed, compared to the untreated, Kaempferol resulted in significant downregulation of the candidate iPSC and chemoresistance markers such as NANOG and MDR1, downregulated p53 and upregulated expression of cleaved caspase3 (Fig. 3E). Densitometric analysis of the relative fold change of expression of candidate proteins were normalized to the expression of β-Actin (Fig. 3F–I). Interestingly, Carboplatin treatment did not result in any significant change in fold change of expression of MDR1 and p53, compared to control (Fig. 3F–I), while Kaempferol attenuated the expression of all these oncogenic markers. This indicated that Kaempferol induced a significant reduction of candidate proteins redundantly upregulated in p-NACT TNBC.
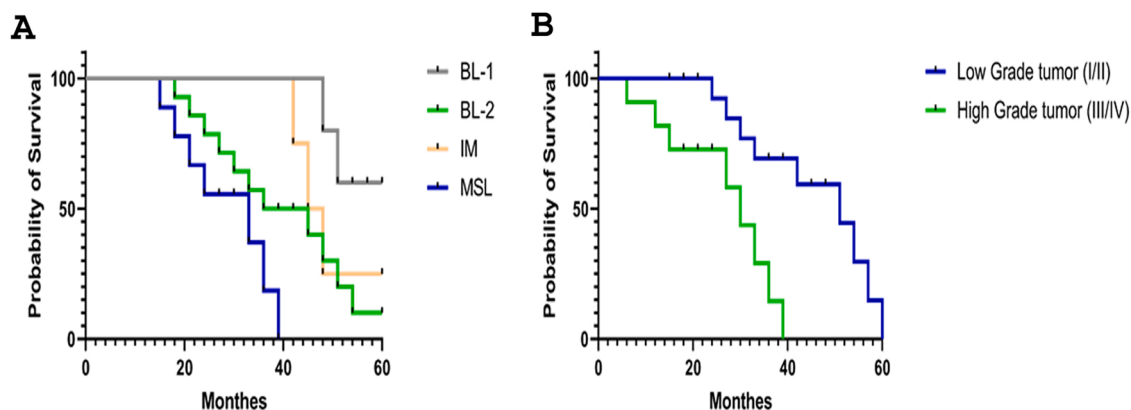
Fig. 1. Relapse-free survivals (RFS) of Random breast cancer and TNBC in with pre therapeutic vs post-NACT treated patients according to each TNM (tumour–node–metastasis) stage before and after chemo therapy. (A) RFS of the patients with grade I/II, (**** p < 0.0001), (B) RFS of the patients with grade III/IV, (*** p < 0.01), (C) RFS (**** p < 0.0001), (D) overall survival of the patients(**** p < 0.0001), (E)progression free survival of BL-1, BL-2, IM, and ml (**** p < 0.0001), Abbreviation Basal Like − 1:(BL-1), Basal Like − 2:(BL-2), Immunomodulatory: (IM), and Mesenchymal-like (ml).
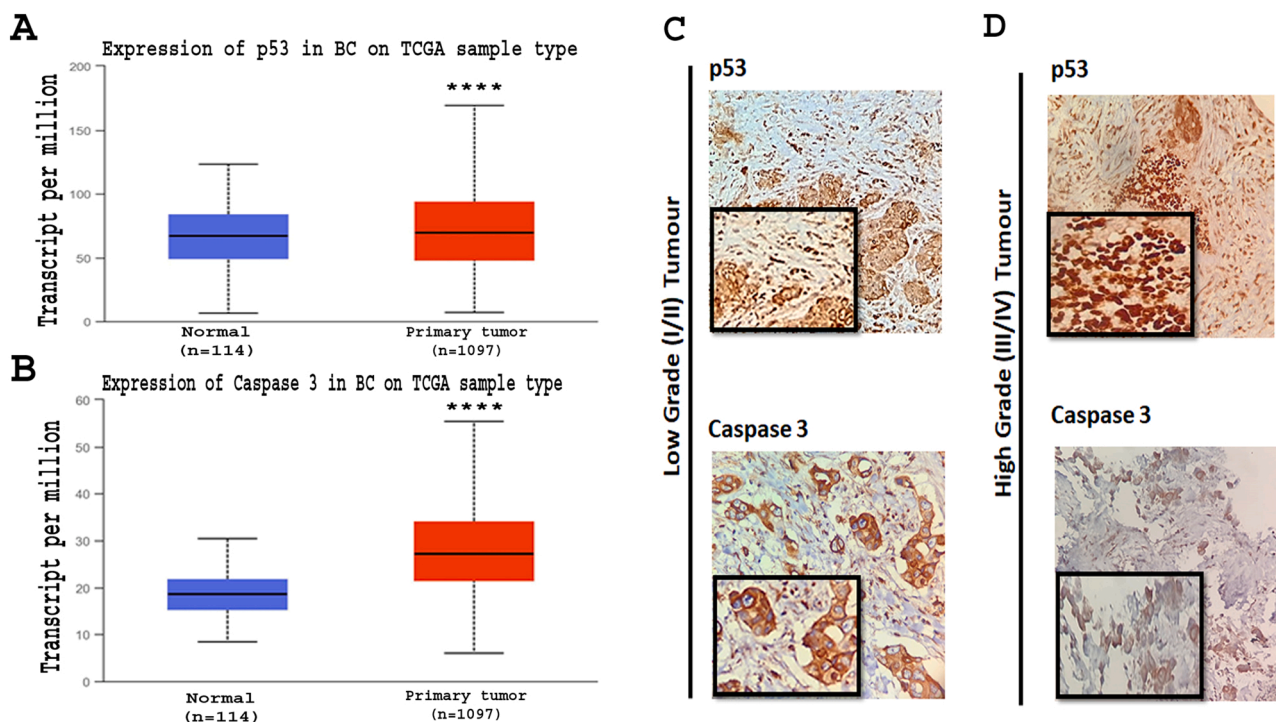
Fig. 2. Association between p53 and caspase 3 in different grades of post-NCT-TNBC tumor. (A) expression of p53 in normal and tumor from TCGA samples (B) expression of caspase 3 in normal and tumor from TCGA samples (C) expression of p53 and caspase 3 in low grade tumor (I/II) and expression of p53 and caspase 3 in high grade tumor (III/IV).

Table2
Relationship between caspase 3 protein expression and p53 for breast cancer.

|	Total Number (n)	Caspase 3 (%)	P-53 (%)	p-value
Tumour Size (cm)				
≤ 2	28	26.58 (± 0.16)	89.2	0.001
> 2	34	17.84 (± 0.12)	76.43	0.0001
Histological grade				
1	17	58.9	6.33	0.005
2	21	43.4	17.8	0.0001
3	24	31.6	52.33	0.0001
Histological type				
Ductal	56	36.9	48.29	0.0001
Lobular	6	24.33	81.37	0.0001
Nodes				
Positive	48	57.46	16.29	0.0001
Negative	14	23.11	67.77	0.0001
Adjuvant Chemotherapy	36	26.38 (± 4.28)	81.24	0.0017
Adjuvant Radiation therapy	62	42.35 (± 3.10)	61.41	0.0001

3.5. Protein-protein interaction and Co-expression of chemo tolerance Markers

It was reported that inactivation of p53 through mutations, unleashes stemness and upregulates MDR1 as well as expression of other anti-apoptotic genes such as *KI-67, CD44, NF- kappaB, ALDH1, NANOG,* and *BCL2,* leading to cell cycle arrest and thereby ensuring chemo tolerance in cancer patients through NF- kappaB mediated p53 related pathway [13,15–17]. Here, we obtained the expression (transcript per million) of various oncogenic markers responsible for bypassing chemotherapeutic agents in p53 mutant patients from the TCGA database, such as p53/p53mutant (Fig. S3A), KI—67/p53mutant (Fig. S3B), CD44/p53mutant (Fig. S3C), NF- kappaB/p53mutant (Fig. S3D),

ALDH1/p53mutant(Fig. S3E), NANOG/p53mutant(Fig. S3F), MDR1/p53mutant (Fig. S3G), BCL2/p53mutant(figure 3SH) and Caspase 3/p53mutant(Fig. 2E). The occurrence of p53 mutation is frequent in an assortment of tumors that suggests the p53 mutant induced malignant development of tumors. The data also represented that the mutant p53 is over-activated in aggressive tumors but was unable to induce apoptosis in such tumors. However, the molecular mechanism of these correlations is not well understood. In this study, using STRING analysis, we identified protein-protein interactions of genes regulated by mutant p53. Identified interactomes were then analyzed for predictions of the potential function and metabolic pathways involved (Fig. 4A). Identified interactions showed the correlation of metastatic and anti-apoptotic pathways with mutant p53. Co-expression of targeted oncogenes (Fig. 4B) were observed. Maximum co-expression was observed between KI67 and *p53,* which is consistent with our previous findings where we found KI67 is upregulated in p53 mutant breast cancer tissue with respect to normal tissue and p53 nonmutant tissue (figure. 3SB). Co-expression was also observed between *p53* and *KI-67, CD44, NF- kappaB, ALDH1, NANOG, MDR1,* and *BCL2.* Several other interactions between *CD44* and *NF- kappaB, NANOG, MDR1,* and *ALDH1* were observed. In Fig. 4B, the square point represented the interaction.

3.6. Immunohistochemistry analysis of mutant p53 associated candidate proteins identified from TCGA database

To determine the effect of various chemotherapeutic drugs on ex vivo primary human breast tissue, we focused on the p-NACT-TNBC tumour in breast cancer. The regulation of metastasis-related markers in mice, with 48 h treatment with Kaempferol were confirmed previously [18,19]. The histopathology of p-NACT-TNBC tumour upon Kaempferol treatment was studied and revealed cell death (H&E) (Fig. S4A – S4C). Treatment with Kaempferol revealed highly profound suppression of p53 (Fig. 5A), KI—67 (Fig. 5B), CD44 (Fig. 5C), NF- kappaB(Fig. 5D), ALDH1 (Fig. 5E), NANOG (Fig. 5F), MDR1 (Fig. 5G), and BCL2 (Fig. 5H), whereas Caspase 3(Fig. 5H) was found to be upregulated in that groups.
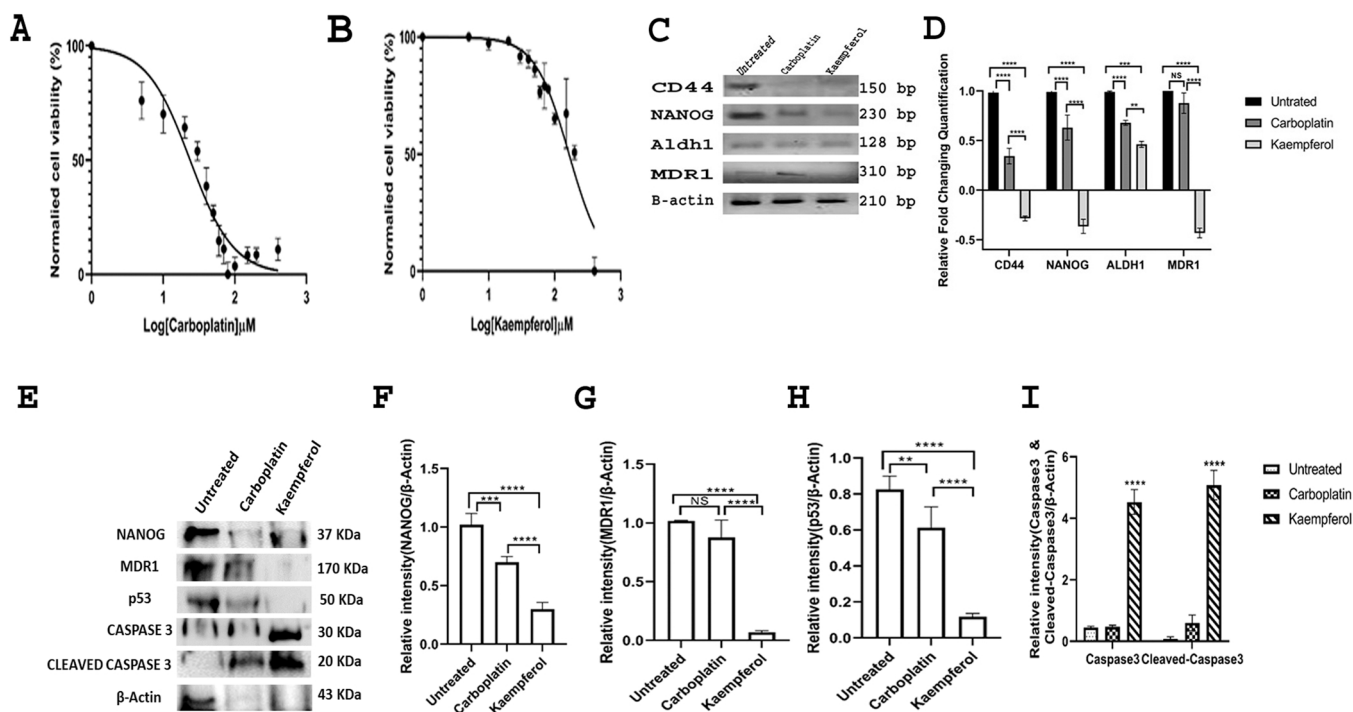
Fig. 3. Cell viability assay in ex-vivo grown culture of primary post-NCT-TNBC tumor. A log based drugs effect were plotted where (A): Carboplatin, (B): Kaempferol, IC-50 dosage was calculated. The dots and bars are mean values and ± SD.Semiquantitative (C) and quantitative RT-PCR (D) to determine the expression status of candidate genes viz. CD44, NANOG1, ALDH1, MDR1, and upregulated in post-NCT-TNBC tumor. Bars represent the relative fold changing gene expression normalized to β-Actin gene and relative to the corresponding untreated cells. For RNA expression analysis, Student's Z test is used to correlate the significance where *p < 0.0332 * *p < 0.0021 * **p < 0.0002 * ** * p < 0.0001. The different treatment groups included: U: Control; C: carboplatin; K: Kaempferol. Immunoblot analysis to check the fold change of expression of few candidate iPSC, chemoresistance and apoptosis markers in p-NACT-TNBC patients under various treatment conditions (48 h) (A). U: Control; C: Carboplatin; and K: Kaempferol. Fold change of expression of candidate genes were normalized to the expression of β-Actin (E–I). Student's t-test and Two way ANOVA were used to correlate the significance where *p < 0.0332 * *p < 0.0021 * **p < 0.0002 * ** * < 0.0001.
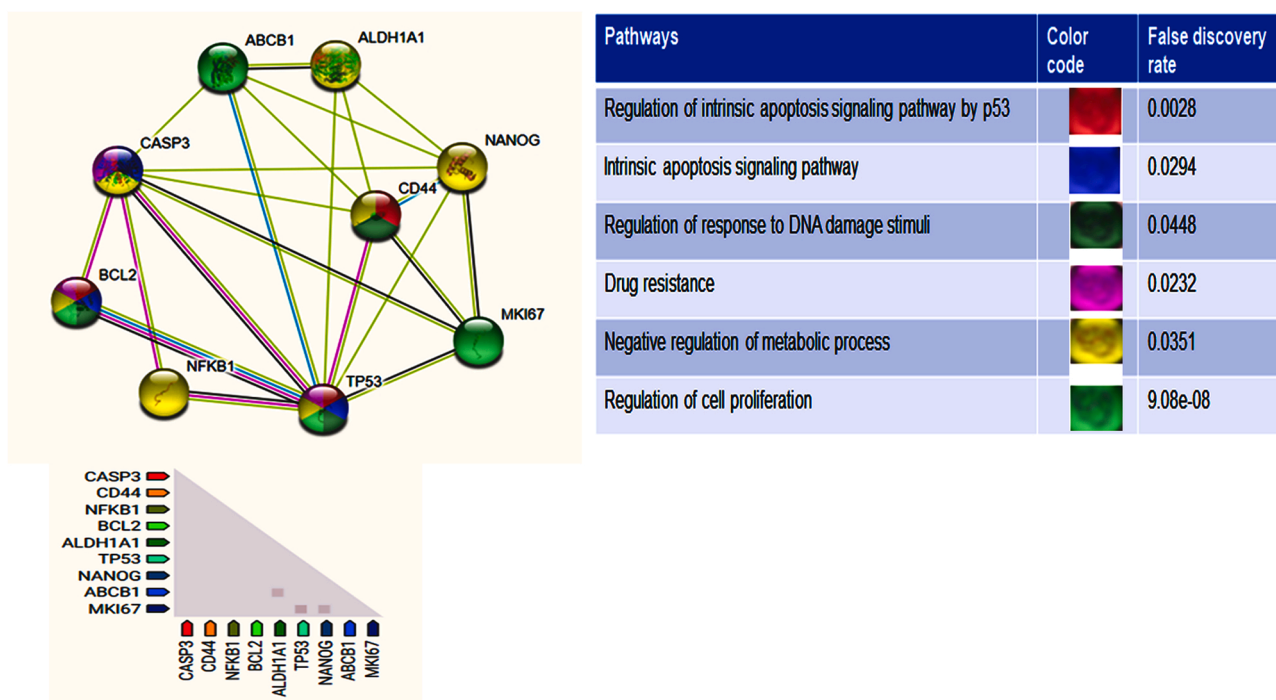
Fig. 4. PPI network and pathway analysis of using STRING. The colour codes showed the pathways regulated by p53 in association with the genes, including MDR1, ALDH1, NANOG, CD44, MKI67, TP53, NFKB1, BCL2 and CASP3. Coexpression analysis showed TP53 coexpressed with MKI67.
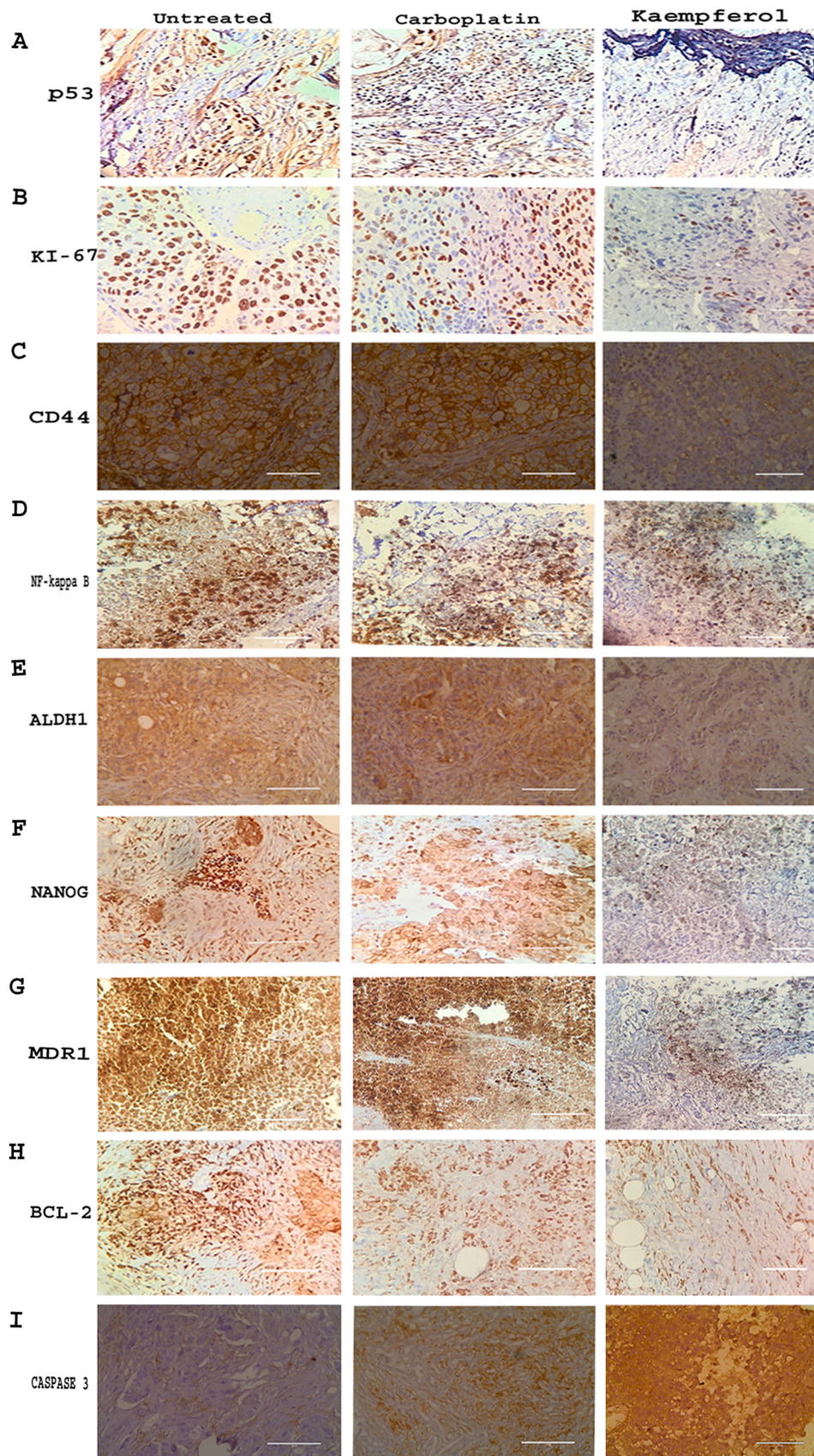
Fig. 5. Immunohistochemical analysis of tumor proliferation markers. Treatment with candidate drug for suppression of p53 (A), KI—67 (B), CD44 (C), NF- kappaB (D), ALDH1 (E), NANOG (F), MDR1 (G), and BCL2 (H) in explant culture. Data are shown as mean ± SEM. Values are statistically significant at *P < 0.05. Magnification: 40X.

In the Carboplatin treatment panels, protein markers did not show any significant change compared to the untreated group, except for NANOG, p53 and Caspase 3 panels. In the Fig. 5F panel, we observed that the expression of NANOG decreased in both drugs treatments conditions while Kaempferol was more robust than Carboplatin. In Caspase 3 panels, Kaempferol showed robust upregulation of Caspase 3 expression compared to Carboplatin. These studies indicate that the analysis of those molecular markers status can be used prospectively to evaluate the response of chemo tolerant breast tumors and suggest an innovative approach for developing markers for targeted therapies in advance of clinical trials.

3.7. Experimental validation of Kaempferol and the Evaluation of CD44 and CD326 as cancer stem cell markers in cell line

The effects of Carboplatin (Fig. S5A) Kaempferol (Fig. S5B) and treatment after 48 hrs on MDA-MB-231 cell line were studied to assay for the CD44/CD24 (Fig. 6A) and CD326/CD24 (Fig. 6B). The data showed that, the population of CD44 + ,CD24- cells and CD326 + , CD24- cells decrease by 18.33% (Fig. 6 A3)and 50.57% (Fig. 6 B3) in the treatment of Kaempferol in respect to the untreated panel whereas in Carboplatin treated cells, the same populations decreased approximately by 17% (Fig. 6 A2) and 38.67% (Fig. 6 B2) respectively. The effect of candidate drugs were also studied for the both CD326/CD44 population (Fig. S5C) where as Kaempferol reduced 40.2% cells in respect of control group.

4. Discussion

The mechanism of chemotolerance and eventual therapeutic escape mechanism is intrinsically complex. With the increased duration of therapeutic status, it becomes more important to classify patients according to the status of expression of markers that regulate cancer stemness, proliferation, chemoevasion, proliferation and apoptosis escape. Mutation of p53, the guardian of the genome, results in its upregulated nuclear expression, which contributes to upregulated stem cell renewal, uncontrolled proliferation and chemotolerance mechanisms in breast cancer progression [13]. Wild-type p53, an important gatekeeper of the cell cycle, determines cell fate, as to whether it should undergo apoptosis or DNA damage repair [21] following a cell cycle arrest. Therefore, p53 mutation is associated with the upregulation of all oncogenic markers [22] that contribute to chemo-tolerance. A lack of p53 in fibroblasts from the p53 nullizygous xenograft model is also related to the upregulation of bypass networks to chemotherapeutic agents [23]. RCB score, which integrates residual tumor diameter, percentage of cellularity, lymph node positivity, tumor histology and grade is an important predictor of progression-free survival, to the pathologist's eye. However, apart from these parameters, identification of prognostic markers predicting overall disease prognosis is considered important at the molecular level. We hypothesized that the inverse association of p53 and Caspase 3 activation in high-grade tumors with high RCB scores might be explained by tissue-specific effects of p53 on markers regulating stem cell renewal, proliferation, chemoresistance and apoptosis evasion. Overexpression of MDR1, an ATP-dependent efflux pump could result in the tolerance to drugs by pumping out the drugs from cells. Transient transfection analysis showed that like NF-kappaB, MDR1 promoters are also affected by mutant p53 [3]. Moreover, the deactivation of NF-κB was informed to be linked with reduction of *BCL-2*, resulting in Caspase-3 activation, which induces apoptosis activity [24]. This study also suggested the associations among Ki-67 expression, histopathological grading and BCL-2 expression have been defined through several molecular markers that are linked with high/low p53 status, high levels of BCL-2 expression [24]. Hereafter, BC patients with high Ki-67/BCL2 and altered p53 are expected to be at high risk of having a poor prognosis compared with the patients with low BCL2 in this study [24]. Several mechanisms in the breast cancer cell line are responsible to develop chemo tolerance among which the overexpression of ALDH1, the cellular detoxification
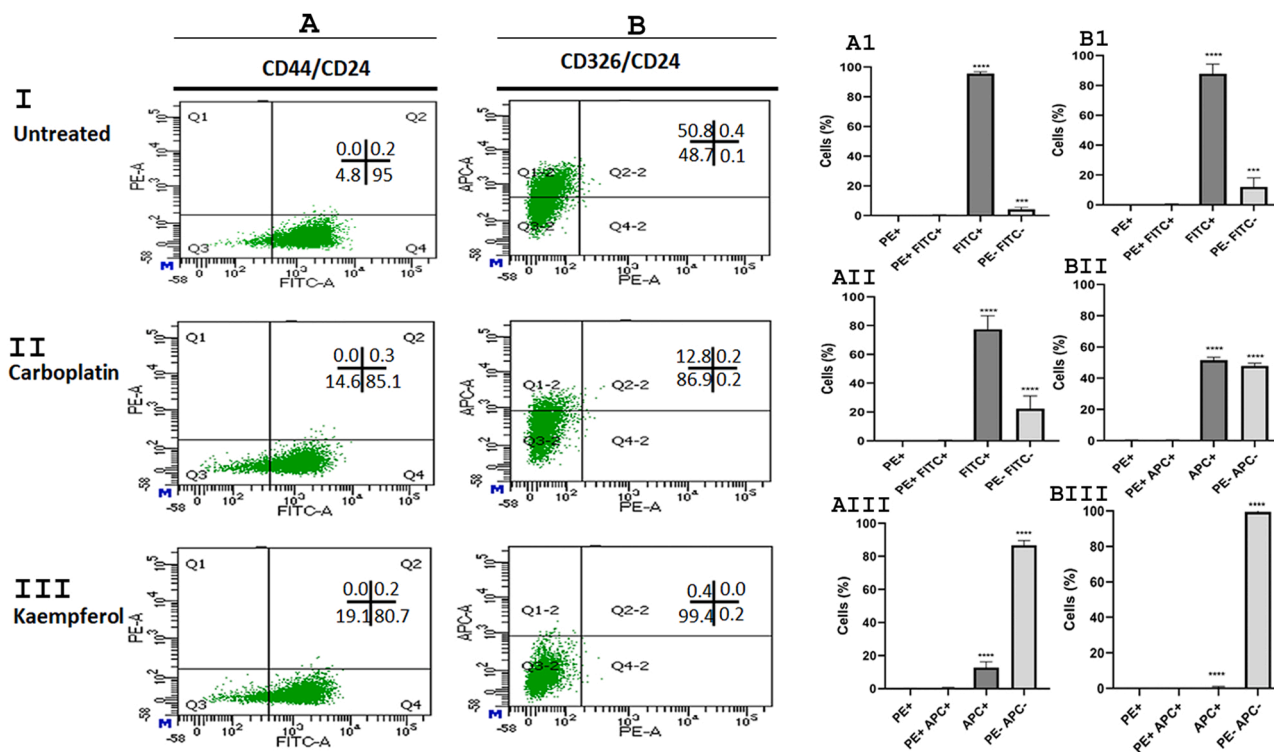

Fig. 6. Cell viability assay (48 h) in MDA-MB-231 in the treatment of (A) Carboplatin (B)Kaempferol.Fate of (C) CD44 (FICT conjugated) / CD24 (PE conjugated) and EpCAM (APC conjugated) / CD24 (PE conjugated) in MDA-MB-231 under the treatment of candidate drug. (C1, C2, C3) and (D1, D2, D3) plot represented the treatment condition such as untreated, carboplatin, Kaempferol respectively.

protein, CD44, the transducer of microenvironmental signals, are reported earlier [12,25]. Moreover, earlier reports demonstrated that Hyaluronan (HA)- CD44 interaction induces its binding to MDR1, resulting in the bypass mechanisms of chemotherapeutic agents [25]. Trock and co-workers established that breast tumors expressing MDR1 were three times more probable to chemotherapy failure than patients whose tumors were MDR1 negative [26]. In our study, we also observed upregulated RNA expression of induced pluripotent stem cell markers viz. *NANOG, ALDH1, CD44, MDR1* in ex-vivo cultured breast tumor explants, which got attenuated upon treatment with Kaempferol.

Previous evidence suggested that the mutant p53, which is more commonly observed in aggressive and chemotolerant tumors, may inhibit the ability of pro-Caspase-3 to become proteolytically activated by Caspase-9, leading to loss of activation of Apaf-1, the cell-death effector and downstream target of caspase-9, as observed in metastatic melanomas [27]. Moreover, resistance to apoptotic stimuli has been reported in MCF-7 human breast carcinoma cells that lack expression of Caspase-3 as a result of a 47 bp deletion in exon 3 of the *CASP3* gene [28]. In this study, we correlated that the high nuclear expression of mutant p53 in pretreated high-grade tumors, was unable to activate Caspase 3, thus promoting apoptosis escape which also contributed to chemo tolerance networking (Fig. 3, Fig. 5). These observations imply that loss of Caspase-3 expression may render breast cancer cells unaffected to chemotherapy and radiation therapy. Nevertheless, drug-tolerance of breast cancer cells could be rendered sensitive to chemotherapeutic agents simply by overexpressing the caspase-3 protein [28]. The ability of p53 to associate with the anti- and pro-apoptotic members of the Bcl-2 family at the mitochondria has been well characterized. It is also probable that p53 modulation of MDR1 depends on the addition of p53 signals with other signals acknowledged to affect MDR1 gene expression. Upregulation of another oncogenic protein NANOG that is also co-linked with NF kappaB, participated in a NANOG-CD44-MDR1 network, to promote chemo evasion and perpetual stemness [24]. We hypothesized that wild-type p53 represses endogenous MDR1 gene expression and that the effect of loss of functional p53 on the spectrum of drug sensitivity is, in part, determined by its selective tissue-specific effects on MDR1.

The role of flavonoids in the prevention and treatment of breast cancer have previously been reported [7,29]. Kaempferol, an aglycone flavonoids in the form of glycoside yellow colour compound, is a tetrahydroxyflavone in that the four hydroxy groups are found at positions 3, 5, 7, and 4. Previously, Kaempferol and its glycosylated derivatives have been reported as anticancer compounds and the mechanistic oncogenic pathway could not be well understood. In this perspective, Kaempferol consumption and associated application in cancer therapy are obtaining vast attention in the scientific community. In our prior report, we demonstrated the amount of Kaempferol (14.97 mg) consumption in a day and ensued in a plasma concentration of 16.69 ng/ml [7]. The earlier report demonstrated, Kaempferol inhibits several types of cancer cells through cell cycle arrest at G2/M phase, downregulation of signalling such as phosphoinositide 3-kinase (PI3K)/protein kinase B (AKT) pathways and evading the proliferation of reactive oxygen species (ROS) through its groups at C3, C5, and C4, an oxo group at C4, and a double bond at C2-C3 involved in cancer progressions.ROS are aerobic metabolism results that can upregulate malignant cell proliferation [7]. In our previous study, we reported a robust γH2AX expression in breast tumor explants and not in adjacent normal tissues, treated with Kaempferol [7]. Our study revealed that Kaempferol showed its effectiveness in p-NACT-TNBC tumour, through downregulation of mutant p53 dependent expression of candidate markers associated with stemness, proliferation and apoptosis escape. From our data, we can conclude that the downregulation of stemness, proliferative and apoptosis evasion markers and upregulation of Caspase-3 in p-NACT-TNBC upon the treatment of Kaempferol, is likely to indicate its apoptotic potential. This robustness was not observed in Carboplatin treatment groups. Earlier reports show that ALDH1 and CD44 positive patients had a worse

prognosis, which was associated with poorer tumour differentiation, lymph node metastasis, decreased overall and disease-free survival and increased tumorigenesis [4]. Moreover, Ki-67, a non-histone nuclear protein, is one of the most commonly used IHC proliferation antigens and has been defined as an independent predictive and prognostic factor in breast cancer. Upregulation of Ki-67 has been demonstrated to be correlated with larger tumor size, higher histological grade, lymph node involvement, shorter DFS and OS in breast cancer. A previous study also suggested that the rates of Ki67 with p53 mutation were higher, and it is revealed to be suggestive of a more invasive tumor and a higher frequency of metastasis. In our study, we also observed that upon the treatment of Kaempferol the expression of Ki-67 was reduced.

In MCF- 7 cell line CD44 + /CD24- and Epithelial-mesenchymal transition (EMT) marker i.e. ALDH1 has played a critical role in chemo tolerance and malignancy [12,30]. Additionally, in CD44 + high and ALDH1 high cell-induced mouse tumours and human cancer patients, the high expression of NANOG is recognized [24]. The outcomes point out that both CD44 and ALDH1 provide tumours survival advantages through self-renewal of the stem cell. Ample evidence in cell lines suggested that cell surface markers such as CD44 + /CD24 − and CD44 + /CD326 in TNBC are associated with increased expression of EMT markers required for metastasis [20]. Understanding the action of chemo tolerance in preclinical representations poses challenges as a result of the complex nature of chemo tolerance and compensatory passageways, as well as the use of heterogeneity cell of chemo tolerance primary breast tumour models with different chromosomal backgrounds.

To ensure the actual effect of Kaempferol, the evaluation of cancer stem cell markers (CD44 and CD326) in MDA-MB-231 cell line, as well as gene expression profile in tumour analysis were completed in the presence of positive control drug, Carboplatin in this study. In a previous study, it has been revealed that MCF-7 cells undergo EMT, generating a sub-population with CD44 + /CD24 − mesenchymal phenotype [30]. To address this possibility, we employed FACS to identify the percentage of CD44 + /CD24- and CD326 + /CD24- cells for additional analysis to confirm the only low CD24 population. Our experiments revealed that Kaempferol reduced EMT marker, CD44 + / CD326 + marker in the tumour cells (p < 0.05) more efficiently than the Carboplatin treated cells. Early report showed that Kaempferol arrests cell cycle at G2/M stage through downregulation of CDK1 in triple negative breast cancer cells [31]. Similar findings were obtained by our team in chemo tolerance primary breast tumour cells which are collected after chemotherapeutics treatments [7]. EMT and iPSC markers are reflected to play a key role in the progress of breast cancer. Replenishment of EMT markers in breast cancer cells will counterpoise chemotherapy, leading to treatment failure [32]. We found that low doses of Kaempferol (IC- 50) reduced ALDH1, and NANOG gene activation in the tumour cells via blocking MDR1 gene. Our western blot analysis revealed a concomitant upregulation of NANOG, MDR1 in tumors with upregulation of p53 and downregulation of Caspase 3 and cleaved Caspase 3. Kaempferol treatment reduced the expression of stemness and chemoresistance markers (NANOG, MDR1) with concomitant upregulation of Caspase 3 and cleaved Caspase 3, indicating its ability to initiate apoptosis in the cultured tumor explants.

The DGIdb (http://www.dgidb.org) data conferred NF-kappa B and NANOG to be targets of Kaempferol. The oncogenic marker of p-NACT-TNBC tumour cells achieved was additionally validated by TCGA database and STRING analysis and checked with immunohistochemistry staining which indicated that Kaempferol decrease the p53, NF-kappaB, ALDH1, CD44, NANOG, MDR1, KI-67 and BCL2 expression. Further, we constructed a PPI network using these in the STRING database, which revealed that all the genes are correlated with TP53. Higher correlation and coexpression of TP53 is observed with MKI67 which is consistent with our experimental data. TP53 is mainly regulating the following functions with these genes: intrinsic apoptosis signalling pathway, regulation of DNA damage response, drug resistance, metabolic process,

and cell proliferation.

In this study, we demonstrate one such problem in breast cancer cells that can attenuate drug-induced apoptosis through Kaempferol. The pharmacokinetics and pharmacodynamics of Kaempferol were reported in our previous study [7]. In observance with additional parallel approaches, [33] the cultured tissue explants retained the associated with MDR1 gene that is known to play important roles in the therapeutic sensitivities of chemo tolerance breast cancer. Herein, we also establish how the explant platform can be used to report the role of drug action by biomarker monitoring. Carboplatin was robust in attenuating viability of tumor cells but has very little effects on markers conferring cancer stemness.Earlier clinical reports demonstrated, the toxicity to Carboplatin was moderate, signifying that higher dosages of carboplatin could be used in first-line chemotherapy of patients with metastatic breast cancer [34]. Till today, carboplatin is still extensively applied in the treatment of cancer. Carboplatin interferes with DNA repair, so as to suppress and eventually kill cancer cells. The increased DNA repair process is considered the most significant characteristic in platinum-resistance cells. Amongst TNBC subtypes, only BL1 subtype with BRCA1 mutation is susceptible to Carboplatin therapy and can acquire resistance through diverse mechanisms [35]. Carboplatin was robust in attenuating viability of tumor cells but has very little effects on markers conferring cancer stemness. Our study revealed a p53 independent Caspase 3 activation with our candidate drug system. Caspase 3 activation can also occur in p53 independent way as observed earlier [36,37].

To sum up, a large number of preclinical experimental studies have definite the mechanisms of Kaempferol in the prevention and treatment of chemo tolerancebreast cancer. But there is a lack of in-depth understanding about Kaempferol. Collectively, the deliverables within this paper indicate that ex vivo chemo tolerant tumour explant culture could provide insights similar to clinical trials. Additionally, the explants are representatives of the unique tumor microenvironment and an ideal system to check the therapeutic efficacy of a drug. The technology is low-cost, rapid, and achievable within an integrated cancer translational research setting. The insights from these data would help in the improvisation of therapeutic strategies for p-NACT breast tumors.

Credit authorship contribution statement

Sourav Kumar Nandi: Conceptualization, Data curation, Methodology, Formal analysis, Writing – original draft. **Ayan Pradhan:** Data curation, Formal analysis, Methodology. **Basudeb Das:** Formal analysis, Methodology, Software. **Biswajit Das:** Methodology. **Sudarshana Basu:** Formal analysis, Methodology. **Bibekanand Mallick:** Data analysis. **Amitava Dutta:** Methodology. **Diptendra Kumar Sarkar:** Investigation, Methodology. **Ashis Mukhopadhyay:** Funding acquisition. **Soma Mukhopadhyay:** Project administration, Resources. **Rittwika Bhattacharya:** Investigation, Methodology, Supervision, Writing – review & editing, Formal analysis, Validation, Visualization.

Conflict of interest

The authors declare that there is no potential conflict of interest.

Appendix A. Supporting information

Supplementary data associated with this article can be found in the online version at doi:10.1016/j.prp.2022.154029.

References

[1] M. Nedeljković, A. Damjanović, Mechanisms of chemotherapy resistance in triple negative breast cancer-how we can rise to the challenge, Cells 8 (9) (2019) 957, https://doi.org/10.3390/cells8090957.

[2] Y.Z. Jiang, D. Ma, C. Suo, J. Shi, M. Xue, X. Hu, Y. Xiao, K.D. Yu, Y.R. Liu, Y. Yu, Y. Zheng, X. Li, C. Zhang, P. Hu, J. Zhang, Q. Hua, J. Zhang, W. Hou, L. Ren, D. Bao, Z.M. Shao, Genomic and transcriptomic landscape of triple-negative breast cancers: subtypes and treatment strategies, 428–440.e5, Cancer Cell 35 (3) (2019), https://doi.org/10.1016/j.ccell.2019.02.001.

[3] B.T. Spike, G.M. Wahl, p53, stem cells, and reprogramming: tumor suppression beyond guarding the genome, Genes Cancer 2 (4) (2011) 404–419, https://doi.org/10.1177/1947601911410224.

[4] H. Tomita, K. Tanaka, T. Tanaka, A. Hara, Aldehyde dehydrogenase 1A1 in stem cells and cancer, Oncotarget 7 (10) (2016) 11018–11032, https://doi.org/10.18632/oncotarget.6920.

[5] L.T. Senbanjo, M.A. Chellaiah, CD44: a multifunctional cell surface adhesion receptor is a regulator of progression and metastasis of cancer cells, Front. Cell Dev. Biol. 5 (2017) 18, https://doi.org/10.3389/fcell.2017.00018.

[6] A.S. Hamy, L. Darrigues, E. Laas, D. De Croze, L. Topciu, G.T. Lam, C. Evrevin, S. Rozette, L. Laot, F. Lerebours, J.Y. Pierga, M. Osdoit, M. Faron, J.G. Feron, M. Laé, F. Reyal, Prognostic value of the Residual Cancer Burden index according to breast cancer subtype: Validation on a cohort of BC patients treated by neoadjuvant chemotherapy, PloS One 15 (6) (2020), e0234191, https://doi.org/10.1371/journal.pone.0234191.

[7] S.K. Nandi, T. Roychowdhury, S. Chattopadhyay, S. Basu, K. Chatterjee, P. Choudhury, N. Banerjee, P. Saha, S. Mukhopadhyay, A. Mukhopadhyay, R. Bhattacharya, Deregulation of the CD44-NANOG-MDR1 associated chemoresistance pathways of breast cancer stem cells potentiates the anti-cancer effect of Kaempferol in synergism with Verapamil, Toxicol. Appl. Pharmacol. 437 (2022), 115887, https://doi.org/10.1016/j.taap.2022.115887.

[8] J. Makki, Diversity of breast carcinoma: histological subtypes and clinical relevance, Clin. Med. Insights Pathol. 8 (2015) 23–31, https://doi.org/10.4137/CPath.S31563.

[9] A. Kooistra, N.M. Elissen, J.J. König, M. Vermey, T.H. van der Kwast, J.C. Romijn, F.H. Schröder, Immunocytochemical characterization of explant cultures of human prostatic stromal cells, Prostate 27 (1) (1995) 42–49, https://doi.org/10.1002/pros.2990270108.

[10] H.J. Baelde, A.M. Cleton-Jansen, H. van Beerendonk, M. Namba, J.V. Bovée, P.C. Hogendoorn, High quality RNA isolation from tumours with low cellularity and high extracellular matrix component for cDNA microarrays: application to chondrosarcoma, J. Clin. Pathol. 54 (10) (2001) 778–782, https://doi.org/10.1136/jcp.54.10.778.

[11] D.P. Jackson, F.A. Lewis, G.R. Taylor, A.W. Boylston, P. Quirke, Tissue extraction of DNA and RNA and analysis by the polymerase chain reaction, J. Clin. Pathol. 43 (6) (1990) 499–504, https://doi.org/10.1136/jcp.43.6.499.

[12] W. Li, H. Ma, J. Zhang, L. Zhu, C. Wang, Y. Yang, Unraveling the roles of CD44/CD24 and ALDH1 as cancer stem cell markers in tumorigenesis and metastasis, Sci. Rep. 7 (1) (2017) 13856, https://doi.org/10.1038/s41598-017-14364-2.

[13] J.V. Thottassery, G.P. Zambetti, K. Arimori, E.G. Schuetz, J.D. Schuetz, p53-dependent regulation of MDR1 gene expression causes selective resistance to chemotherapeutic agents, Proc. Natl. Acad. Sci. USA 94 (20) (1997) 11037–11042, https://doi.org/10.1073/pnas.94.20.11037.

[14] S.K. Nandi, R. Bhattacharya, T. Roychowdhury, U.K. Roy, S. Chattopadhyay, A. Mukhopadhyay, Ex-vivo drug sensitivity of primary breast cancer stems cell populations to potentiate therapeutic strategy for treatment resistant breast cancer, Ann. Oncol. 29 (2018) ix18, https://doi.org/10.1093/annonc/mdy428.012.

[15] T. Cooks, I.S. Pateras, O. Tarcic, H. Solomon, A.J. Schetter, S. Wilder, G. Lozano, E. Pikarsky, T. Forshew, N. Rosenfeld, N. Harpaz, S. Itzkowitz, C.C. Harris, V. Rotter, V.G. Gorgoulis, M. Oren, Mutant p53 prolongs NF-κB activation and

promotes chronic inflammation and inflammation-associated colorectal cancer, Cancer Cell 23 (5) (2013) 634–646, https://doi.org/10.1016/j.ccr.2013.03.022.

[16] K.S. Putt, G.W. Chen, J.M. Pearson, J.S. Sandhorst, M.S. Hoagland, J.T. Kwon, S. K. Hwang, H. Jin, M.I. Churchwell, M.H. Cho, D.R. Doerge, W.G. Helferich, P. J. Hergenrother, Small-molecule activation of procaspase-3 to caspase-3 as a personalized anticancer strategy, Nat. Chem. Biol. 2 (10) (2006) 543–550, https://doi.org/10.1038/nchembio814.

[17] V.L. Grandage, R.E. Gale, D.C. Linch, A. Khwaja, PI3-kinase/Akt is constitutively active in primary acute myeloid leukaemia cells and regulates survival and chemoresistance via NF-kappaB, Mapkinase and p53 pathways, Leukemia 19 (4) (2005) 586–594, https://doi.org/10.1038/sj.leu.2403653.

[18] S.H. Kim, K.A. Hwang, K.C. Choi, Treatment with kaempferol suppresses breast cancer cell growth caused by estrogen and triclosan in cellular and xenograft breast cancer models, J. Nutr. Biochem. 28 (2016) 70–82, https://doi.org/10.1016/j.jnutbio.2015.09.027.

[19] L. Zhu, L. Xue, Kaempferol suppresses proliferation and induces cell cycle arrest, apoptosis, and DNA damage in breast cancer cells, Oncol. Res. 27 (6) (2019) 629–634, https://doi.org/10.3727/096504018×15228018559434.

[20] W. Zou, Y. Yang, R. Zheng, Z. Wang, H. Zeng, Z. Chen, F. Yang, J. Wang, Association of CD44 and CD24 phenotype with lymph node metastasis and survival in triple-negative breast cancer, Int. J. Clin. Exp. Pathol. 13 (5) (2020) 1008–1016.

[21] J. Chen, The cell-cycle arrest and apoptotic functions of p53 in tumor initiation and progression, Cold Spring Harb. Perspect. Med. 6 (3) (2016), a026104, https://doi.org/10.1101/cshperspect.a026104.

[22] E. Alvarado-Ortiz, K.G. de la Cruz-López, J. Becerril-Rico, M.A. Sarabia-Sánchez, E. Ortiz-Sánchez, A. García-Carrancá, Mutant p53 gain-of-function: role in cancer development, progression, and therapeutic approaches, Front. Cell Dev. Biol. 8 (2021), 607670, https://doi.org/10.3389/fcell.2020.607670.

[23] Q. Liu, B. Yu, Y. Tian, J. Dan, Y. Luo, X. Wu, P53 Mutant p53N236S regulates cancer-associated fibroblasts properties through stat3 pathway, Onco Targets Ther. 13 (2020) 1355–1363, https://doi.org/10.2147/OTT.S229065.

[24] S. Chuthapisith, J. Eremin, M. El-Sheemey, O. Eremin, Breast cancer chemoresistance: emerging importance of cancer stem cells, Surg. Oncol. 19 (1) (2010) 27–32, https://doi.org/10.1016/j.suronc.2009.01.004.

[25] L.Y. Bourguignon, G. Wong, C. Earle, L. Chen, Hyaluronan-CD44v3 interaction with Oct4-Sox2-Nanog promotes miR-302 expression leading to self-renewal, clonal formation, and cisplatin resistance in cancer stem cells from head and neck squamous cell carcinoma, J. Biol. Chem. 287 (39) (2012) 32800–32824, https://doi.org/10.1074/jbc.M111.308528.

[26] B.J. Trock, F. Leonessa, R. Clarke, Multidrug resistance in breast cancer: a meta-analysis of MDR1/gp170 expression and its possible functional significance, J. Natl. Cancer Inst. 89 (13) (1997) 917–931, https://doi.org/10.1093/jnci/89.13.917.

[27] M. Brentnall, L. Rodriguez-Menocal, R.L. De Guevara, E. Cepero, L.H. Boise, Caspase-9, caspase-3 and caspase-7 have distinct roles during intrinsic apoptosis, BMC Cell Biol. 14 (2013) 32, https://doi.org/10.1186/1471-2121-14-32.

[28] E. Devarajan, A.A. Sahin, J.S. Chen, R.R. Krishnamurthy, N. Aggarwal, A.M. Brun, A. Sapino, F. Zhang, D. Sharma, X.H. Yang, A.D. Tora, K. Mehta, Down-regulation of caspase 3 in breast cancer: a possible mechanism for chemoresistance, Oncogene 21 (57) (2002) 8843–8851, https://doi.org/10.1038/sj.onc.1206044.

[29] M. Imran, B. Salehi, J. Sharifi-Rad, T. Aslam Gondal, F. Saeed, A. Imran, M. Shahbaz, P.V. TsouhFokou, M. Umair Arshad, H. Khan, S.G. Guerreiro, N. Martins, L.M. Estevinho, Kaempferol: a key emphasis to its anticancer potential, Mol. (Basel, Switz.) 24 (12) (2019) 2277, https://doi.org/10.3390/molecules24122277.

[30] I.K. Guttilla, K.N. Phoenix, X. Hong, J.S. Tirnauer, K.P. Claffey, B.A. White, Prolonged mammosphere culture of MCF-7 cells induces an EMT and repression of the estrogen receptor by microRNAs, Breast Cancer Res. Treat. 132 (1) (2012) 75–85, https://doi.org/10.1007/s10549-011-1534-y.

[31] L. Zhu, L. Xue, Kaempferol suppresses proliferation and induces cell cycle arrest, apoptosis, and DNA damage in breast cancer cells, Oncol. Res. 27 (6) (2019) 629–634, https://doi.org/10.3727/096504018×15228018559434.

[32] J. Huang, H. Li, G. Ren, Epithelial-mesenchymal transition and drug resistance in breast cancer (Review), Int. J. Oncol. 47 (3) (2015) 840–848, https://doi.org/10.3892/ijo.2015.3084.

[33] H. van der Kuip, T.E. Mürdter, M. Sonnenberg, M. McClellan, S. Gutzeit, A. Gerteis, W. Simon, P. Fritz, W.E. Aulitzky, Short term culture of breast cancer tissues to study the activity of the anticancer drug taxol in an intact tumor environment, BMC Cancer 6 (2006) 86, https://doi.org/10.1186/1471-2407-6-86.

[34] E.A. Perez, D.W. Hillman, P.J. Stella, J.E. Krook, L.C. Hartmann, T.R. Fitch, A. K. Hatfield, J.A. Mailliard, S. Nair, C.G. Kardinal, J.N. Ingle, A phase II study of paclitaxel plus carboplatin as first-line chemotherapy for women with metastatic breast carcinoma, Cancer 88 (1) (2000) 124–131, https://doi.org/10.1002/(sici)1097-0142(20000101)88:1.

[35] R. Bhattacharya, K. Banerjee, N. Mukherjee, M. Sen, A. Mukhopadhyay, From molecular insight to therapeutic strategy: The holistic approach for treating triple negative breast cancer, Pathol., Res. Pract. 213 (3) (2017) 177–182, https://doi.org/10.1016/j.prp.2017.01.001.

[36] W. Guo, Y. Zhang, Z. Ling, X. Liu, X. Zhao, Z. Yuan, C. Nie, Y. Wei, Caspase-3 feedback loop enhances Bid-induced AIF/endoG and Bak activation in Bax and p53-independent manner, Cell death Dis. 6 (10) (2015), e1919, https://doi.org/10.1038/cddis.2015.276.

[37] S. Marchini, M. Ciro', Broggini, p53-Independent caspase-mediated apoptosis in human leukaemic cells is induced by a DNA minor groove binder with antineoplastic activity, Apoptosis 4 (1999) 39–45, https://doi.org/10.1023/A:1009630132087.

EC/NSCBCRI/01/2021

Date: 09th July, 2021

To
Dr. Rittwika Bhattacharya
Scientist, Dept. of Molecular Biology
Netaji Subhas Chandra Bose Cancer Institute
Supervisor of Sourav Kumar Nandi (As accepted by Jadavpur University)
&
Mr. Sourav Kumar Nandi
Ph.D., Research Fellow,
Registered to Jadavpur University

Sub: Title: "Perturbation of chemo evasive mechanism of ex-vivo and in vitro model of breast cancer stem cells with plant derived synthetic compound: A molecular understanding for treatment failure cases of breast cancer",

Subject: Ethics Committee Approval.

Dear Dr. Bhattacharya & Mr. Nandi,
With regards to your submission letter dated on 21st June, 2021, The **Ethics Committee N.S.C.B.C Research Institute** reviewed and discussed your application *entitled "Perturbation of chemo evasive mechanism of ex-vivo and in vitro model of breast cancer stem cells with plant derived synthetic compound: A molecular understanding for treatment failure cases of breast cancer."* EC meeting held on dated 03rd July, 2021 at hospital premises.

The following documents were reviewed:

1. ICMR appointment letter dated 26th Sep 2017.
2. Ph.D. registration and Supervision approved letter of Jadavpur University.
3. Synopsis of "Perturbation of chemo evasive mechanism of ex-vivo and in vitro model of breast cancer stem cells with plant derived synthetic compound: A molecular understanding for treatment failure cases of breast cancer".
4. Declaration letter of ICMR
5. CV of Mr. Sourav Kumar Nandi

The following are members who were participated in EC meeting held on 03rd July, 2021, at 18:30 hrs onwards, organized in Netaji Subhas Chandra Bose Cancer Hospital premises, Kolkata, WB, and India.

Sl. No.	Name	Designation	Position in IEC
01	Dr. Sanjay Sen	Doctor	Acting Chairperson

02	Dr. Jayasri Basak	Scientist	Member Secretary
03	Dr. Subhashree Bandyopadhyay	Pharmacologist	Member
04	Dr. Krishnendu Mukherjee	Doctor	Member
05	Mr. Raju Ray	Legal Expert	Member
06	Mrs. Shyamali Ganguly	Representative of non governmental agency.	Member
07	Mr. Malay Chatterjee	Lay person from the community	Member

- This is also for your information that the EC members were present and participated during decision making process for approval of the study proposal.

- We hereby confirm that neither you nor any of your study team members have participated in the voting/ decision making procedure of the committee. The members of the committee who have participated in the voting/ decision making procedure of the committee do not have any conflict of interest in the referenced study and have signed a declaration on conflict of interest.

- **The Ethics Committee N.S.C.B.C Research Institute** expects to be informed about the progress of the study, any SAE occurring in the course of the study, any changes in the synopsis and patient medical history and asks to be provided a copy of the final status report.

- **The Ethics Committee N.S.C.B.C Research Institute** is organized and operates according to Good Clinical Practice and New Drugs and Clinical trial Rules 2019.

Yours sincerely,

Jayasri Basak

Dr. Jayasri Basak
Member Secretary,
Ethics Committee N.S.C.B.C. Research Institute
(Netaji Subhas Chandra Bose Cancer Hospital)
3081, Nayabad, Kolkata-700094,
West Bengal, India.
Reg. No.: ECR/286/INST/WB/2013/RR-19

ETHICS COMMITTEE N.S.C.B.C RESEARCH INSTITUTE
Netaji Subhash Chandra Bose Cancer Hospital
3081 Nayabad, New Garia, Kolkata-700094
West Bengal, India
Reg. No:- ECR/286/Inst/WB/2013/RR-19